Synthesis of Novel Surface Active Agents via Copper Mediated Living Radical Polymerisation: Synthetic and Mechanistic Study.

By

Sébastien Perrier

A thesis submitted for the degree of Doctor in Philosophy

University of Warwick, Department of Chemistry

October 2001

'Dear Colleague, leave the concept of large molecules well alone... there can be no such thing as a macromolecule.'

Advice given to Herman Staudinger after one of his lecture introducing his revolutionary concept of polymers.

"I have never let my schooling interfere with my education."

Mark Twain

"Imagination is more important than knowledge. Knowledge is limited. Imagination encircles the world."

Albert Einstein

"Des idées, tout le monde en a. Souvent les mêmes. Ce qu'il faut, c'est savoir s'en servir."

Coluche

Table of contents

Table of figures

Table of tables

Acknowledgements

Three years ago, I arrived in England to undertake my PhD, feeling quite excited, but not knowing what kind of people I was going to meet and how on earth I would manage to communicate in English!

Three years later, after many football matches, pints (too many of those!), kebabs, two or three choreographed dances, a lot of broken glassware, many short nights and difficult mornings, and plenty of other things I don't really dare to write here, I am almost done and feel that it all went so fast...

I would like to thank few people, the first being my academic supervisor Professor David Haddleton. Thanks Dave for your welcome, your confidence and support over the past three years, and for giving me the freedom in my work which has helped me to work to my full potential. It is encouraging to find that success is possible while keeping a very good human relationship!

I would also like to thank Derek Irvine, my industrial supervisor, for the freedom he gave me whilst undertaking this work and ICI for their financial support.

Thank you to all members of the Warwick polymer group, both past and present, for their welcome when I first came to England, their patience in teaching me English and for all the fun we have had throughout my PhD studies. Thanks especially to Dr. Ir.

Stefan Bon for his constant advice and help on this project. Further special thanks should go to Dr. Adam Clarke for letting me play around with the NMR machine.

May Professor Bernard Boutevin be recognised for his influence during my studies in Ecole Nationale Supèrieure de Chimie de Montpellier, and for his advice in helping me to find a PhD in the first place.

I would also like to use this special space to acknowledge all the help and support my family has provided during all my years of study. 'Merci à vous, maman, papa et Laurent pour m'avoir toujours soutenu et encouragé dans mes choix, tout au long de ces années, et permis d'arriver là où j'en suis aujourd'hui!'

Finally, all of this would have been far more difficult to achieve without the help of a very special person to me, who have been here and helped me during all this time, especially in the few last months of writing up, thanks to you Rachel.

Declaration

All experimental work reported within this thesis is original research work performed by the author in the Department of Chemistry, University of Warwick, between October 1998 and October 2001. No material contained herein has been submitted for any other degree to this, or any other institution. Where collaboration has been necessary, the Collaborators have been named and the extent of the collaboration made clear.

Results from other authors are referenced in the usual manner throughout the text.

Date: 11/09/01

Sébastien Perrier

Abstract

The synthesis of poly(ethylene glycol)-based surface active agents was undertaken via copper mediated living radical polymrisation.

In a first approach, poly(ethylene glycol) was used as macroinitiator for the synthesis of poly(ethylene glycol) methyl ether-b-poly(methyl methacrylate) (MeOPEG-b-PMMA) block copolymers. The living character of the polymerisation was demonstrated, but MeOPEG was found to be a slow initiator.

In a second approach, MeOPEG was used as a methacrylate macromonomer (MeOPEG-MA). Graft polymers were obtained by polymerisation in toluene and water, and various block copolymers, aiming to increase the hydrophobicity character of the final molecules, were also synthesised.

The kinetics of the polymerisation was then studied, and various oxygen containing molecules were found to influence the polymerisation by polarity effect on the solution and potential competitive coordination with the ligands on the copper catalyst.

Finally, the physical properties of the block and graft copolymers synthesised were tested. Thermal analyses, surface properties of the PMMA block copolymers and aggregates formation in aqueous solution were investigated.

Abbreviations

%v/v	% volume
%wt/wt	% weight
$[M]_0$	initial monomer concentration
[M]	monomer concentration at time t
[X]	Concentration of X
2EIBr	Ethyl-2-bromoisobutryrate
AIBN	2,2'-azobis-iso-butylnitrile
Alk.	Alkyl
Ar.	Aromatic
ATP	Atom transfer polymerisation
ATRA	Atom transfer radical addition
ATRC	Atom transfer radical cyclisation
ATRP	Atom transfer radical polymerisation
BA	Butyl acrylate
bipy	2,2'- dipyridyl
BzMA	Benzyl methacrylate
c	Particle speed
CAC	Crtical aggregate concentration
CAC_{fluo}	Crtical aggregate concentration determined by fluorescence
CAC_{tensio}	Crtical aggregate concentration determined by tensiometry
CCl_4	Chlorophorm
CCTP	Catalyst chain transfer polymerisation
CMC	Critical micelle concentration
Conv.	Conversion
DCM	Dichloromethane
DMF	Dimethyl formamide

DMSO	Dimethyl sulfoxide
DNA	Deoxyribose nucleic acid
DP	Kinetic chain length / degree of polymerisation
DRI	Differential refractive index
DSC	Differential scanning calorimetry
$\mathbf{D_t}$	Translational diffusion coefficient
$\mathbf{E_{NR}}$	Energy for the maximum absorption wavelength of Nile Red
$\mathbf{(EtO)_2EG}$	Ethylene glycol diethyl ether
f	Initiator efficiency
FW(M)	Monomer molecular weight
$\mathbf{g_{lv}}$	Surface tension between liquid and vapour / Liquid surface tension
$\mathbf{g_{sl}}$	Surface tension between liquid and solid
$\mathbf{g_{sv}}$	Surface tension between solid and vapour
GPC	Gel permeation chromatography
GPEC	Gradient polymer elution chromatography
h	Solvent viscosity
h	Planck constant
I	Initiator
IR	Infra red
$\mathbf{k_a}$	Rate constant of activation
$\mathbf{k_d}$	Rate constant of deactivation
$\mathbf{k_{dec}}$	Rate constant of decomposition
$\mathbf{k_p}$	Rate constant of polymerisation
$\mathbf{k_t}$	Rate constant of termination
$\mathbf{k_{tc}}$	Rate constant of termination by combination
$\mathbf{k_{td}}$	Rate constant of termination by disproportionation
$\mathbf{k_{tr}}$	Rate constant of chain transfer
LRP	Living radical polymerisation

M	Monomer
MA	Methyl acrylate
$MeOPEG_X$	Poly(ethylene glycol) methyl ether with X repeating unit(s)
$MeOPEG\text{-}I_X$	Poly(ethylene glycol) methyl ether esterified with X repeating unit(s)
MeOPEG-MA	Poly(ethylene glycol) methyl ether methacrylate
MHz	Mega Herz
min	Minutes
MMA	Methyl methacrylate
M_n	Number average molecular weight
$M_{n,exp}$	Experimental number average molecular weight
M_n^{NMR}	Number average molecular weight by nuclear magnetic resonnance
M_n^{SEC}	Number average molecular weight by size exclusion chromatography
$M_{n,th}$	Theoretical number average molecular weight
MSC	p-methoxybenzenesulohonyl chloride
M_v	Viscosity average molecular weight
M_w	Weight average molecular weight
MWD	Molecular weight distributuion
Mwt	Molecular weight
^{n}BMA	Butyl methacrylate
Na	Avogadro number
NMP	Nitroxyde mediated polymerisation
NMR	Nuclear magnetic resonance
NNLS	Nonnegative least square
P	Wilhelmy probe diameter
P*	Active species
P_n*	Active species after n monomer addition
PDI	Polydispersity index
PDMS	Poly(dimethyl siloxane)

PECl	2-phenethyl chloride
PEG	Poly(ethylene glycol)
PEG-MA	Poly (ethylene glycol) methacrylate
PIBUE-MA	Poly(isobutyl vinyl ether methacrylate)
$PMMA_X$	Poly(methyl methacrylate) with X repeating unit(s)
PEO	Poly(ethylene oxide)
PS	Poly(styrene)
ppm	Parts per million
R_H	Hydrodynamic radius
R_i	Rate of initiation
R_p	Rate of propagation
R_t	Rate of termination
RAFT	Reversible addition fragmentation transfer
SEC	Size exclusion chromatography
STY	Styrene
TEMPO	1-oxy-2,2,6,6-tetramethylpiperidine
t	Time
T_g	Glass transition temperature
TGA	Thermo gravimetric analysis
THF	Tetrahydrofuran
UV	Ultraviolet
VAc	Vinyl acetate
VDF	Vinylidene fluoride
V_h	Hydrodynamic volume
λ	Wave length (nm)
ν	Frequency (Hz)
θ	Contact angle
τ_m	Life time for a defined moment

Chapter 1

Introduction

Radical polymerisation is to date a major method to synthesise high molecular weight polymers. Its success among industrial and academic laboratories comes from its apparent simplicity to undertake, the wide range of vinyl monomers that can be used and the mild reaction conditions necessary. Indeed, among the other chain growth polymerisation technique like ionic or coordination polymerisation, radical polymerisation does not need expensive catalysts, is tolerant to various monomer functional groups, to a large temperature range (-20 to 200°C) and does not need drastic purification and preparation methods (products can be obtained without removal of the stabilisers present in the commercial monomers, in presence of traces of oxygen and polymerisation can even occur in aqueous solution). In addition, many monomers can easily copolymerise by radical process, leading to an almost infinite number of copolymers with properties depending on the proportion of the comonomers. Such properties make of radical polymerisation the process of choice for industry, undertaken in bulk, solution or suspension/emulsion reactions.[1]

1.1. History of Living radical Polymerisation.

In 1920, Staudinger[2] was the first to come with the idea of macromolecules, and proposed the principle of chain polymerisation, initially thinking that monomers were connected head to tail by covalent bonding in large cyclic structures. Thirty years later the basic mechanism of free-radical polymerisation was set, and remains almost unchanged nowadays. The essential steps are the initiation and propagation which involves radical adding to the less substituted end of the double bond. The termination step occurs when two radicals react together, either by combination or by disproportionation (transfer of hydrogen leading to unsaturated end group).[1] Other

reactions resulting in dead chains are transfer reactions. As free radicals are very reactive, they can attract hydrogen from many molecules present in solution (solvent, impurities, monomer, etc.). In the case of a growing polymer chain, this would terminate its progression, but create a new radical that can initiate a new polymer chain. Therefore, the number of propagating species is kept constant, but the average molecular weight of the polymer produced is reduced. This process has been exploited for the synthesis of low molecular weight polymers, by deliberate addition of *chain transfer agents*, which present a labile X-H bond and therefore promote the chain transfer reactions. Example of such processes can be found in telomerisation,[3] mercaptans based polymerisation[4] or organo-cobalt complexes based polymerisation.[5]

The major problem encountered by free radical polymerisation is the lack of control over the macromolecular architecture: Reactions of termination and transfer lead to broad molecular weight distributions and make impossible to target a pre-defined architecture. With the growing of speciality industries over bulk production, one is yet more attracted to well-defined architecture polymers than bulk products. This involves polymers with well-known degree of polymerisation, molecular weight distributions, end functionalities, chain architectures and compositions.

The first system elaborated to answer this demand was an ionic polymerisation presented by Szwarc in 1956.[6,7] In two publications, Szwarc described the homogeneous electron-transfer-initiated polymerisation of styrene and isoprene and conclusively demonstrated the lack of termination and chain transfer in this process (figure 1.1), mainly due to the charge repulsion of the active chain ends.

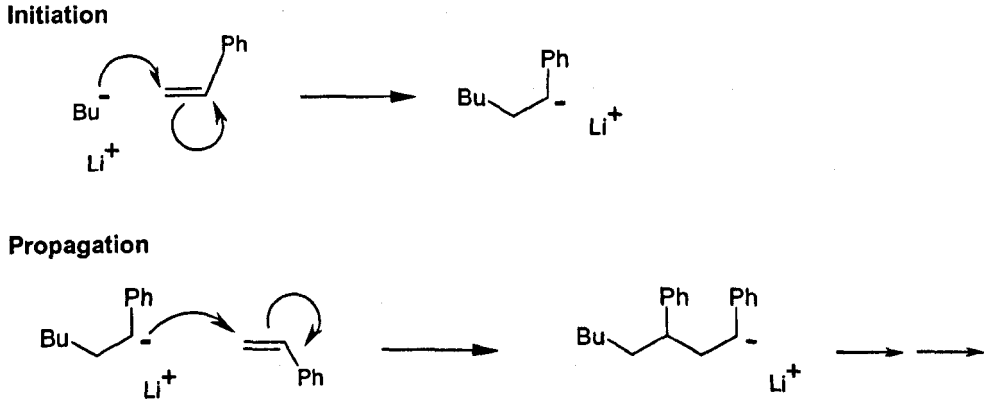

Figure 1.1: Anionic polymerisation of Styrene in presence of BuLi.

Therefore, the polymer chains retain their capacity to add monomer and continue their growth, increasing their molecular weight linearly with the monomer conversion, until all the monomers present are consumed. An addition of a new batch of monomer would make the chain carry on growing. As these growing polymer chains could virtually never die, Szwarc named this process *living polymerisation*. This was of primary importance to synthesise more elaborate architectures, like block copolymers by sequential addition of different monomers, or end-group control. However molecular weight control and narrow molecular weight distribution were not necessarily obtained. To do so, fast initiation by comparison to propagation would be necessary, in order to avoid production of new chains while those previously formed still continue their growth and exchange between species would need to be fast by comparison to propagation. More work was since then undertaken in order to improve this system, and well controlled polymer structures were successfully achieved.[8-12]

During the last 50 years, many new systems have been proposed for living polymerisation. The first system in which dormant and active species were both

clearly observed and the kinetics and thermodynamics of the exchange reactions were determined was the cationic ring-opening polymerisation of tetrahydrofuran.[13-15] This concept of equilibrium between a non active (dormant) polymer chain and a growing (active) one was utilised in anionic polymerisation to develop the group transfer polymerisation.[16] Since then, many research groups reported various systems showing a living process, as in anionic polymerisation, cationic polymerisation,[17-21] or coordination polymerisation.[22-24] Unfortunately, most of these systems suffer of numerous limits, economical (drastic experimental procedures) or technical (limited polymerisable monomers) which restrict their industrial use.[25]

These numerous disadvantages promoted the interest in the control over the architecture of polymers synthesised via radical process, and led to two different approaches of the problem. Up to the 1980's, researches were based on systems in which bimolecular terminations were rare or even non-existing, due to the physical nature of the reaction, or the direct environment of the end chain. Among these methods one can find the precipitation polymerisation,[26,27] some of the template polymerisations[28] and the polymerisation in clathrates.[29] In this case, control is generally obtained by physical stabilisation of the growing chains. However, such systems are very specific, and can not synthesised block copolymers.[30] From the end of the 1980's, a new system based on the formation of radical active species from dormant species was adopted, leading to the appearance of new radical techniques offering a better control on molecular architecture, functionalities, molecular weight control, etc. This new area extended so fast that soon the literature was scattered by various terms aiming to describe this process: controlled polymerisation, living, living/controlled, pseudo-living, living polymerisation with reversible deactivation are

few examples of what can be found in the literature. For better reading, the terminology '*living radical polymerisation*' (LRP) will be adopted through this work.[31]

Otsu *et al.*[32] used the term living radical polymerisation for the first time in 1982 to describe a polymerisation in the presence of dithiocarbamates. The term iniferters (figure 1.2) was adopted to describe such compounds that could *ini*tiate, trans*fer* and *ter*minate a radical polymerisation by analogy to the inifers used by Kennedy *et al.* in cationic polymerisation.[33] Numerous studies led to the synthesis of efficient iniferters, among which the one based on organosulphur radicals such as symmetrical dithiuram sulphides are the most successful (Figure 1.2).[34,35] However, because of slow initiation, these systems lead to high polydispersity and poor control over the molecular weight of the products.

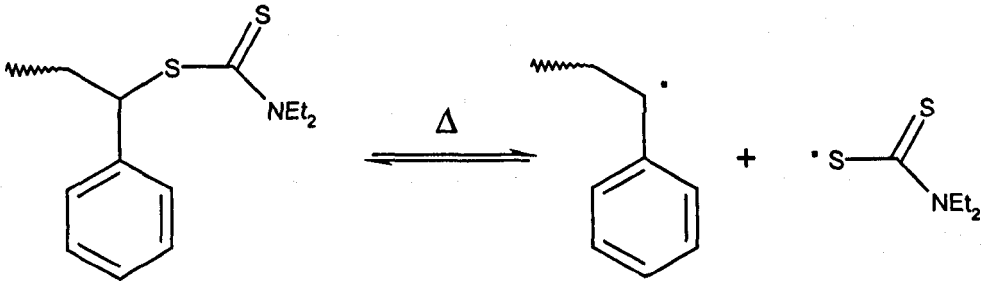

Figure 1.2: Iniferter equilibrium in the polymerisation of styrene.[32,34,35]

A new system describing the control of radical polymerisations by a stable free radical based on a nitroxide was patented in 1985 by Solomon and Rizzardo.[36] It took however eight years until Georges and coworkers showed the importance of such system by reporting the control bulk radical polymerisation of styrene in the presence of 2,2,6,6-tetramethylpiperidinyl-1-oxyl (TEMPO).[37] This opened the way to the

nitroxide mediated polymerisation (NMP), still investigated nowadays. In 1995, two group reported the use of transition metal complexes, $RuCl_2(PPh_3)_2$[38] and CuCl/2bipy[39], to undertake control polymerisation of respectively methyl methacrylate and styrene. Both systems were later proved to be successful for various monomers, and led to an important increase of research in the *transition metal mediated living radical polymerisation* field involving various metals: Cu(I),[40,41] Ni(II),[42,43] Fe(II),[44] Pd(II)[45] and Rh(III).[46]

Finally, the most recent development in LRP techniques was presented in 1998 by Rizzardo and coworkers who used the degenerative transfer process to lead to the *radical addition-fragmentation chain transfer* (RAFT).[47] RAFT has yet been demonstrated to be applicable to a wide range of monomers.[48,49]

1.2. Classification of Living radical polymerisation techniques.

One of the most important difference between free radical polymerisation and LRP is the life time of a polymer chain. In the case of conventional radical polymerisation, a chain is created, grows and dies in about 1 sec. On the other hand, in the case of LRP, it takes several hours for the polymer chains to grow, allowing any modification on the structure (e.g. end-functionalisation, variation of monomer, etc.). The keys to obtain LRP and well-defined structure polymers relies on (i) a rapid exchange between the dormant species and the growing chains, by comparison to the propagation or termination reactions (which means that the number of monomers added to the active chain before it comes back to the dormant state needs to be as low as possible), (ii) a low concentration in species involved in chain breaking reactions and (iii) a fast and quantitative initiation.

As the number of techniques following those keys keeps increasing, many ways of classified LRP methods have been proposed.[50-56]

Matyjaszewski has defined four different cases, classified according to the mechanistic of the process.[56] In the four groups, the dormant species is activated with the rate constant of activation (k_a) to form the active species P_n^*. P_n^* undergoes propagation and reacts with the monomer M with a propagation rate constant k_p. The propagating species can be deactivated back to a dormant species (k_d) or reacts irreversibly with other radicals with the termination rate constant k_t. In all living radical polymerisations, as the concentration of radicals is kept low, termination reactions can sometimes be neglected.

1.2.1. Spontaneous equilibrium between dormant and active species – Dissociation / Combination.

This kind of equilibrium is the most encountered (Figure 1.3). It corresponds to the homolytic break of a weak covalent bond at a high enough temperature. Good examples are the nitroxide mediated polymerisations, with TEMPO[36,57] or bulky acyclic nitroxides,[58,59] or iniferters polymerisation.[32,34,35] Other species corresponding to this scheme are triazolinyl radicals,[60] bulky organic radical like trityl,[61] photolabile C-S bonds,[32] organoborates[62] and even organometallic species with an odd number of electron as Cobalt(II).[63,64]

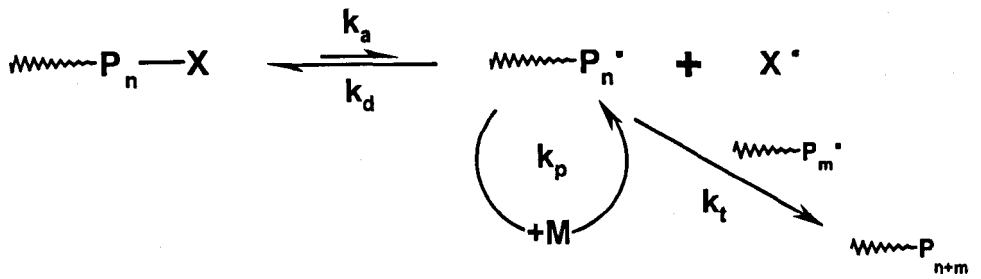

Figure 1.3: Spontaneous equilibrium between dormant and active species.

Figure 1.4 shows the typical example of TEMPO. Nitroxyde has been shown to be efficient with styrene and derivatives,[36,57] acrylates and acrylamides monomers.[58,59] To date, the synthesis of nitroxides able to polymerise methacrylate is still a challenge.

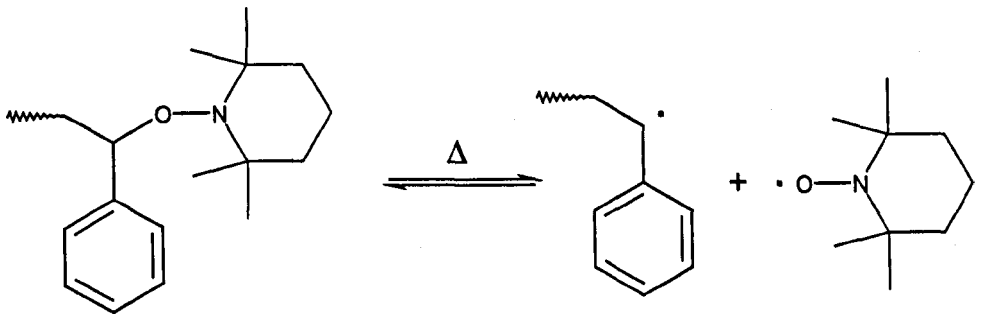

Figure 1.4: TEMPO LRP equilibrium in the polymerisation of styrene.[36,57]

1.2.2. Catalysed equilibrium between dormant and active species – Atom transfer.

This case is close to the previous one, the difference coming from the need of a catalyst to break the covalent bond (Figure 1.5). This reaction is close to the organic Kharasch reaction[65] or atom transfer radical addition in the case of a selective monaddition. X is generally a halogen atom (Cl or Br) and Y a transition metal

(Ru(II),[38] Cu(I),[39-41] Ni(II),[42,43] Fe(II),[44] Pd(II)[45] and Rh(III).[46]) complexed by various ligands. This complex is implicated in a redox process (pair $Metal^{(n)}$ / $Metal^{(n+1)}$) where the halogen atom is transferred from the dormant species to the reduced transition metal to form the oxydated transition metal and the growing chain. Hence the name transition metal mediated living radical polymerisation. Because of the presence of a catalyst, the mechanism is more complicated than seen in case 1.2.1. It is not yet well understood if the propagation takes place from a growing radical species or by coordination of the active species to the transition metal.

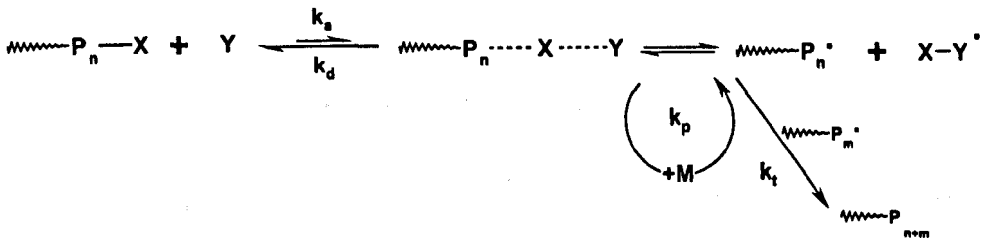

Figure 1.5: Catalysed equilibrium between dormant and active species.

By choosing the right transition metals or ligand, transition metal mediated LRP has been shown to polymerise any monomer with activated double bonds, but not yet the vinyl acetate. Copper mediated LRP (Figure 1.6) will be more specifically discussed in the following section.

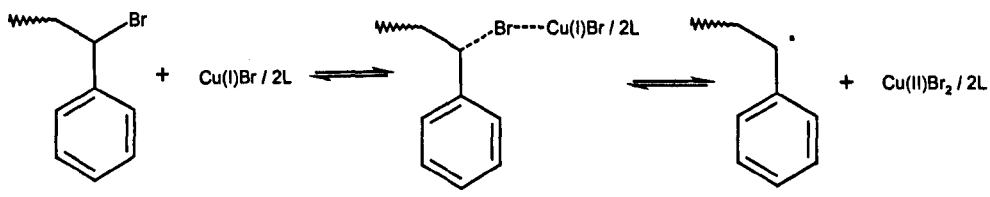

Figure 1.6: Copper mediated LRP equilibrium in the polymerisation of styrene.[39-41]

1.2.3. Degenerative chain transfer.

This case relies on the transfer of species between growing radical chains present at very low concentration and dormant species (Figure 1.7), present at higher concentration (three or four orders of magnitude). This system was described for the first time by Tatemoto *et al.*[66] using alkyl iodides (X = I) and reutilised by Matyjaszewski *et al.* who introduced the name of *degenerative transfer.*[67] It is however only recently that this system has shown is strength with the introduction of thioesters, leading to the RAFT process.[47-49] It is noted that in this case, the equilibrium is not shifted toward the dormant species but the activation and deactivation process are equivalent, $k_a = k_d = k_{exchange}$.

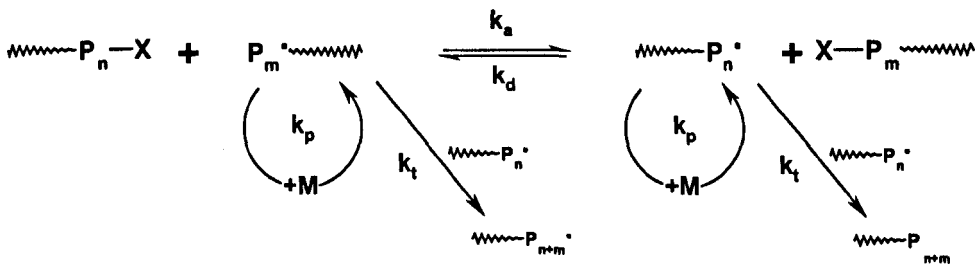

Figure 1.7: Degenerative chain transfer.

The RAFT process (Figure 1.8) seems to date the most powerful LRP. Nearly any monomers can be polymerised to give well-controlled molecular weight polymers with narrow polydispersity.

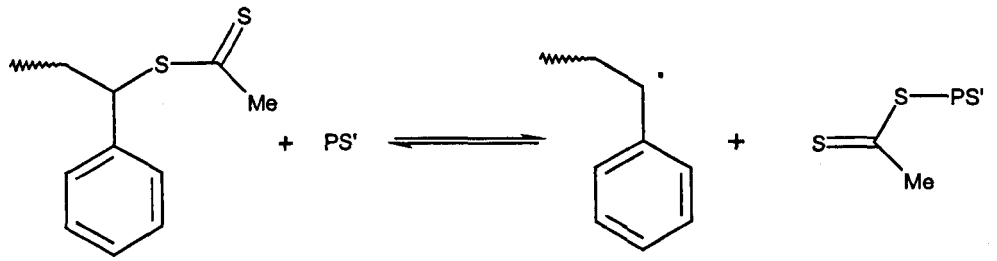

Figure 1.8: RAFT equilibrium in the polymerisation of styrene.[47-49]

1.2.4. Equilibrium between a non-radical species and a growing macroradical.

More rare encountered than the previous ones (Figure 1.9), this case as been described in the litterature for metallic or organometallic systems showing an even number of electrons (Cr(II),[51,53] Al(III)[53,68] or for non-metallic species like some phosphorus derivated.[69,70] The growing radical reacts with a species containing an even number of electron, forming a persistent radical that does not react with each other or with the monomer.

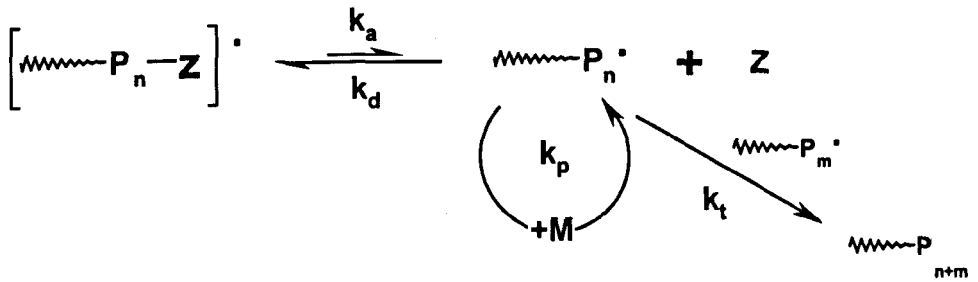

Figure 1.9: Equilibrium between a non-radical species and a growing macroradical.

1.2.5. Difference between living radical polymerisation and controlled radical polymerisation.

A polymerisation is 'living' if the termination and transfer reactions are neglectable by comparison to the propagation and activation/deactivation steps, but can have a slow initiation leading to a bad control over the molecular weight distribution (iniferters polymerisation[32,34,35] for instance). However, a polymerisation is 'controlled' if it can synthesised well-defined architectures, introduce chain end functionalities (Catalyst Chain Transfer Polymerisation (CCTP)[63,64] for instance), control the composition of copolymer (block, graft, etc.) and have a molecular weight targeted by the ratio [Monomer] / [Initiator] and a narrow polydispersity index (PDI).

1.3. Kinetics of LRP.

The basic reactions involved in a free radical polymerisation are *initiation*, divided in decomposition of the initiator (k_{dec}) and initiation of the first monomer (k_i), *propagation* where the radicals formed react with the monomer (k_p) and *termination* which can be either by disproportionation (k_{td}) or combination (k_{tc}) (figure 1.10).

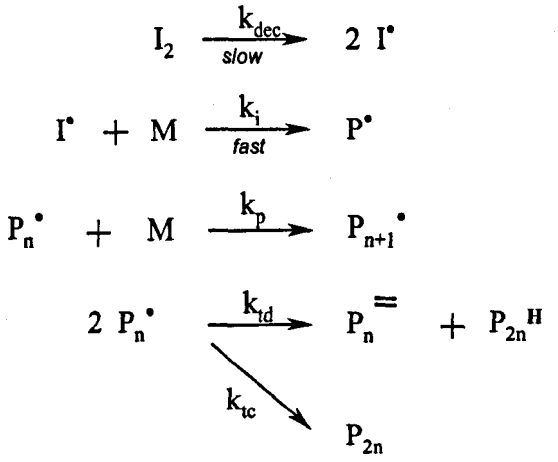

Figure 1.10: Basic reactions involved in a free radical polymerisation.

Since the decomposition of the initiator is far slower than the reaction of $I^{\cdot}$ with the monomer, the decomposition step controls the rate of initiation, R_i, which is defined by:

$$R_i = \frac{d[I^{\cdot}]}{dt} = 2 f k_{dec} [I_2] \qquad \textbf{eq.1.1}$$

where f, the initiator efficiency, is the fraction of primary free radicals $I^{\cdot}$ That successfully initiate polymerisation.

Assuming that the rate of propagation, R_p is independent of the length of the chain,

$$R_p = -\frac{d[M]}{dt} = k_p [M][P_n^{\cdot}] \qquad \textbf{eq.1.2}$$

Finally the termination rate can be represented by:

$$R_t = -\frac{d[P_n^{\cdot}]}{dt} = 2k_{tc} [P_n^{\cdot}]^2 + 2k_{td} [P_n^{\cdot}]^2 = 2k_t [P_n^{\cdot}]^2 \qquad \textbf{eq.1.3}$$

with k_t the overall rate constant of termination, $k_t = k_{tc} + k_{td}$

At the start of the reaction, the rate of formation of radicals greatly exceeds the rate at which they are lost by termination. However, $[P_n^{\cdot}]$ increases rapidly and so does the rate of termination. A value of $[P_n^{\cdot}]$ is soon attained at which the termination rate exactly equals the rate of radical formation, the reaction is said to be under steady-state condition. Therefore,

$$R_i = R_t = \frac{d[I^{\cdot}]}{dt} = -\frac{d[P_n^{\cdot}]}{dt} \qquad \textbf{eq.1.4}$$

and so,

$$2 f k_{dec} [I_2] = 2k_t [P_n^{\cdot}]^2$$

which, rearranged, gives:

$$[P_n^{\cdot}] = \sqrt{\frac{f\,k_{dec}\,[I_2]}{k_t}} \qquad \textbf{eq.1.5}$$

This equation can be substituted in eq.1.2 to give a general expression for the rate of propagation,

$$R_p = \frac{k_p k_{dec}^{1/2}}{k_t^{1/2}} f^{1/2}[M][I]^{1/2} \qquad \textbf{eq.1.6}$$

From eq.1.6, it can be seen that the radical polymerisation is first order with respect to the monomer but depends only of the square root of the concentration in initiator.

In the case of living radical polymerisation, the rate of initiation will be faster than the rate of propagation for all the polymer chains to grow in parallel. Also, in the absence of termination and chain transfer reactions, the rate of propagation can be expressed by:

$$R_p = -\frac{d[M]}{dt} = k_p[P_n^*][M] \qquad \textbf{eq.1.7}$$

with $[P_n^*]$, the concentration in active growing chains, equal in the ideal case to the initial concentration in initiator.

This expression is more simple than in classic free radical polymerisation, and gives indication for following a LRP.

By integrating eq.1.7, we obtain :

$$R_p = \ln\left(\frac{[M]_0}{[M]}\right) = k_p[P_n^*]t \qquad \textbf{eq.1.8}$$

And, as the ratio $[M]_0 / [M]$ is directly linked to the monomer conversion, C, by

$$\frac{[M]_0}{[M]} = \frac{[M]_0}{[M]_0 - [P]} = \frac{1}{\frac{[M]_0 - [P]}{[M]_0}} = \frac{1}{1 - \frac{[P]}{[M]_0}} = \frac{1}{1-C} \qquad \textbf{eq.1.9}$$

with $[M]_0$, [M], [P] respectively the initial concentration in monomer (t=0), the concentration in monomer and in polymer at a time t.

Therefore, by plotting ln (1/(1-C)) *vs.* time, one should obtain a straight line, evidence of a constant concentration in active species $[P_n^*]$ and can measure the apparent rate of polymerisation, $k_p [P_n^*]$.

At any time, the number of monomers in the growing chains (DP, degree of polymerisation) should be the same for each chain, and can be calculated by eq.1.10:

$$DP = \frac{[M]_0 - [M]}{[I]} \qquad \textbf{eq.1.10}$$

This can also be written for the number average molecular weight:

$$M_n = \frac{[M]_0}{[I]_0} \times C \times FW(M) \qquad \textbf{eq.1.11}$$

where $[M]_0$ and $[I]_0$ are the initial concentration of monomer and initiator, C the monomer conversion and FW(M) the molecular weight of the initiator.

Therefore, when plotting the molecular weight of the growing chain *vs.* the conversion of the reaction, one should obtain a straight line, showing the parallel growth of each active chain in time. This leads also to the definition of the theoretical molecular weight, $M_{n,th}$ (eq.1.12):

$$M_{n,th} = \frac{[M]_0}{[I]_0} \times FW(M) \qquad \textbf{eq.1.12}$$

As a conclusion, linear kinetic plots and molecular weight evolution, together with a good correlation of $M_{n,th}$ and $M_{n,exp}$ and a narrow polydispersity of the polymer through the reaction are the parameters that will be considered throughout this work in order to define the living character of a polymerisation.

1.4. Transition metal mediated living radical polymerisation.

It has bee shown so far the general interest of living radical polymerisation in the synthesis of well-controlled macromolecular architectures. As this work is almost exclusively related to transition metal mediated LRP, we propose inhere a closer look at this technique.

Transition metal mediated living radical polymerisation was first reported almost simultaneously in 1995, by the research groups of Sawomoto[38] and Matyjaszewski.[39] Based on the same principle as the Kharasch reaction[65], a transition metal complexed by ligands is oxidised by the transfer of an atom (generally halogen) from a dormant molecule, transforming the latter in an active chain which can undergo polymerisation, hence the appellation *atom transfer polymerisation* (ATP).

In an example of the Kharasch reaction, a homolytic break occurs on a relatively weak carbon halogen bond in the presence of a transition metal catalyst, with transfer of the halogen to the metal complex. The radical formed undergoes then an addition to the least hindered end of a double bond, followed by transfer of the halogen atom to the other end. This process is known as *atom transfer radical addition* (ATRA) (figure 1.11). The same process is observed for intramolecular addition to form ring structures, known *atom transfer radical cyclisation* (ATRC).[71]

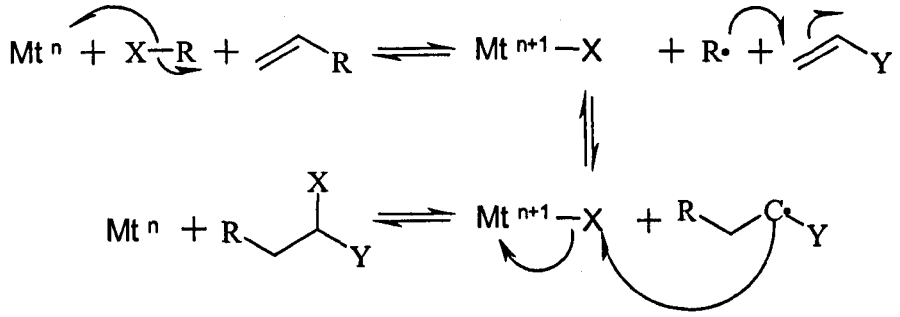

Figure 1.11: Mechanism of the Kharasch reaction.

If Y is an α-electron withdrawing group, the C-X bond is even more weakened and further Kharasch type reactions can occur, hence the principle of transition metal mediated living radical polymerisation of (meth)acrylates and styrenes.

As seen previously, the driving principle of LRP is to keep the concentration of propagating species low and constant to minimise bi-radical terminations. This is achieved here by the reversible capping of the propagating species by a halogen atom. A rapid equilibrium is established between dormant and active species and, for a rate of initiation faster than propagation, all chains begin to grow at the same time. This can lead to narrow polydispersity polymers (typically PDI <1.3) with M_n determined by the ratio [M]:[I].

The initiator used has generally a structure similar of the monomer polymerised, and introduce a halogen atom in the reaction.

The exact nature of the active catalyst is not well understood and might well vary from metal to metal and indeed even between similar and related ligands with the same metal.[40] For example, co-ordination of olefinic monomer would be expected for catalysts based on Ru(II), Rh(III) and Pd(II) but maybe less likely in the case of Cu(I).

However, there is no evidence that the propagation proceeds via attack of a propagating chain on to co-ordinated monomer in any system to date.

1.4.1. Rhodium mediated living radical polymerisation.

Wilkinson's catalyst ($RhCl(PPh_3)_3$) is well known for the reduction of olefins by a mechanism involving complexation of the substrate to the metal centre and has also been successfully applied to ATRA reactions[72]. The bulk polymerisation of styrene at 130 °C initiated by *p*-methoxybenzenesulphonyl chloride (MSC) and mediated by Wilkinson's catalyst was reported by Percec to give less control than systems based on ruthenium and copper[73]. An increase of the catalyst concentration resulted in lower polydispersity polymers, but the values still ranged from 3.0 to 1.8, considerably higher than those achieved in most of other controlled living radical polymerisations. Tessié also used Wilkinson's catalyst for the polymerisation of methyl methacrylate (MMA) initiated by 2,2'-dichloroacetophenone.[74] The polymer was obtained with relative narrow molecular weight distribution (PDI ~ 1.5) and polymerisation followed a first order kinetic in tetrahydrofurane THF solution. When changing the solvent to THF / 40% water, the same degree of control was obtained but a faster rate of polymerisation was observed.

1.4.2. Rhenium mediated living radical polymerisation

Sawamoto's group produced the use of $[ReO_2I(PPh_3)_2]$ / $Al(O_iPr)$ with alkyl iodide initiators to polymerise styrene:[75] With an initiator efficiency close to 100%, and polydispersities under 1.5, the polymerisation offered a good living character, and was

faster than a comparable reaction mediated by $RuCl_2(PPh_3)_3$ (~100 % conversion after 6 hours) at 100 °C in bulk. When extended to the polymerisation of substituted styrenes (*p*-chlorostyrene and *p*-methylstyrene) in toluene at 60°C, similar kinetics as for styrene were observed and all molecular weight distributions were relatively narrow (PDI ~ 1.3).[76]

1.4.3. Palladium mediated living radical polymerisation.

Otsu first reported in 1968 the use of palladium(0) for polymerisation: He used carbon black adsorbed Pd for the free radical polymerisation of MMA initiated by chlorophorm (CCl_4).[77] Fifteen years later, Tsuji reported that $Pd(OAc)_2$ in conjunction with PPh_3 was an efficient catalyst of the Kharasch addition of CCl_4 with olefins leading to high yields at room temperature[78]. The potential use of this system in the industrial application of living radical polymerisation was investigated for the stability of the catalyst substituents in water.[79] MMA was polymerised in toluene at 70 °C, but molecular weight distributions were broad (PDI = 1.6 – 2.3) and initiator efficiency was poor (f as low as 30 %). Increasing the level of PPh_3 lowered even further the initiator efficiency (f = 20 %) but reduced the polydispersity of the final product.

1.4.4. Nickel mediated living radical polymerisation.

The first living polymerisation catalysed by $[Ni\{o,o'(CH_2NMe_2)_2C_6H_3\}Br]$ (Figure 1.12) was reported by Teyssié on MMA and n-butyl methacrylate (^{n}BMA).[43]

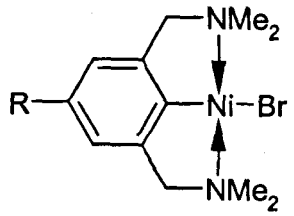

Figure 1.12: Structure of [Ni{o,o'(CH_2NMe_2)$_2$$C_6H_3$}Br].

In the polymerisation of MMA initiated by CCl_4 in toluene solution, narrow polydispersity polymers (typically PDI < 1.2) were produced in 22 hours at 80 °C. When stabilised organic bromides such as Ethyl-2-bromoisobutryrate (2EIBr) were used as initiators, M_n values were significantly higher than theoretical values and the initiator efficiencies ($f = M_{n,\,th} / M_{n,\,exp}$) were quoted as 60 % and 40 % for 2EIBr and 2-bromoisobutyrophenone respectively in toluene at 80 °C. Experiments using size exclusion chromatography (SEC) with differential refractive index (DRI) and ultra violet (UV) detectors showed that the UV active 2-bromoisobutyrophenone chromophore was fully incorporated in the polymer chain.

As the Ni complex is stable in water, the suspension polymerisation of MMA initiated by 2EIBr was investigated: High conversions were obtained with final products showing broad molecular weight distribution (M_n = 60,000 g mol^{-1}, PDI = 1.7), but the control was still better than the polymerisation in the absence of the nickel catalyst (PDI = 6.5).

Sawamoto *et al.*[80] undertook the polymerisation of MMA initiated with CCl_3Br in conjunction with $NiBr_2(PPh_3)_3$/ Al (O*i*Pr) activator, and obtained good control over the final product (PDI = 1.4 at 90 % conversion). When replacing the previous initiator by CCl_4, or mixed halides systems, significantly slower rates of

polymerisation and bimodal molecular weight distribution polymers were achieved. This was attributed to the greater strength of the Ni-Cl bond, differeing therefore from the Ru(II) systems which promote living radical polymerisation independently of the halogen atoms employed.

The same group showed that $NiBr_2(PBu_3)_3$/ Al(O*i*Pr) induced living polymerisation of MMA, methyl acrylate (MA) and n-butyl acrylate (^{n}BA) at higher temperatures (up to 120°C) and faster rates (90 % conversion in 2.5 hours) than those achieved by the less thermally stable $NiBr_2(PPh_3)_3$.[81] Addition of a second batch of monomer as conversion approached 100 % resulted in continued polymerisation at similar rates, unlike $NiBr_2(PPh_3)_3$ which experienced considerable slowing. The lowest polydispersity polymers (PDI ~ 1.1) were obtained when the higher molecular weight bromoester functionalised MMA dimer was used as the initiator.

1.4.5. Iron mediated living radical polymerisation.

As iron complexes have been reported to be good promoters in atom transfer radical addition reactions[72,82], their use in LRP appears logical. Matyjaszewski[83] and Sawamoto[84] reported for the first time in 1997 their uses in living radical polymerisation.

Matyjaszewski demonstrated the polymerisation of styrene and MMA with low polydispersity (typically PDI ~ 1.2) and M_n close to the theoretical values, by using FeX_2 (where X = Cl, Br) complexed by various ligands (e.g. substituted bipyridines, trialkylamines, trialkyl phosphines and trialkyl phosphates). Faster rates of polymerisation and lower polydispersity polymers were obtained for styrene using respectively a catalyst system of $FeBr_2/P(nBu)_3$ and fast initiating molecules such as

p-toluenesulphonyl chloride and 2EIBr. Sawamoto, at almost the same time, obtained living radical polymerisation of MMA initiated by CCl_4 in presence of $FeCl_2(PPh_3)_2$ (PDI ~ 1.4) with Al(O*i*Pr) as rate accelerator. Tessié investigated also this new polymerisation and, using $FeCl_3$/ PPh_3 in conjunction with the free radical initiator 2,2'-azobis-iso-butylnitrile (AIBN), was able to control the polymerisation of MMA[85]. M_n increased with monomer conversion, the concentration of active species remaining constant following an induction period attributed to the decomposition of AIBN and the establishment of the correct equilibrium between Fe(III) and Fe(II). Low polydispersities (< 1.4) were observed when the polymerisation was performed in solution and the incorporation of the CN fragment from AIBN initiation was confirmed by ^{13}C nuclear magnetic resonance (NMR). Under the same conditions, 4,4'-azobis-4-cyanopentanoic acid initiated a LRP and gave a carboxylic acid α-functionalised product[86]. 1,1,2,2,-tetraphenyl-1,2-ethanediol (a known free radical initiator[87]) in conjunction with $FeCl_3$ / PPh_3 has also been used to synthesise relatively high molecular weight poly(methyl methacrylate) PMMA with low polydispersity (e.g. M_n = 171 800, PDI = 1.13)[88]. The polymerisation took 8 hours to reach 100% conversion at 95°C but the poor initiator efficiency (f ~ 50 %) resulted in a much higher molecular weight than the theoretical one.

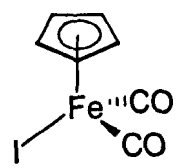

Figure 1.13 : $FeCp(CO)_2I$ used to mediate living radical polymerisation of styrene.

A novel half-metallocene Fe(II) complex (Figure 1.13) was introduced by Sawamoto *et al.* for the living polymerisation of styrene initiated by iodo analogue of 2EIBr[89]. A very slow rate of polymerisation was observed, in toluene solution at 60 °C with $Al(OiPr)_3$ or $Ti(OiPr)_4$ as activators. The product exhibited however a very low polydispersity (< 1.1) and its M_n agreed with the theoretical one. Higher temperature (80°C) resulted in a rate increase, without affecting the degree of control. An even faster rate was observed when polymerising without activator (unlike that observed for other metal complexes) but only oligomers were synthesised. Various other Fe (II) complexes were tried (FeLX(CO)2; X = I, Br; L = η^5-C_5H_5, η^5-C_5Me_5) without any improvements compared to the original complex[90]. When using bi-metallic clusters of type $Fe_2Cp_2(CO)_4$, good living radical polymerisation of styrene was observed, with reaction rates faster than single centred complexes (100 % conversion after 33 hours in dioxane at 80 °C) with an activating co-catalyst.

Very recently, the controlled polymerisation of MMA without organic halide or radical initiator was reported[91]. The active $FeCl_2$ catalysts and the halogenated initiator species Et_2NCS_2Cl were formed *in situ* by redox reaction of $FeCl_3$ with tetraethyl thiuram disulphide. The polymerisation of MMA was noticeably fast (40 % conversion after 8 minutes in anisole at 100 °C) and M_n increased linearly with conversion, following the theoretical values and polydispersities stayed below 1.5 during the polymerisation. The same observations were made when using Fe(III) tri(diethyldithiocarbamate) for the polymerisation of MMA.[92]

1.4.6. Ruthenium mediated living radical polymerisation.

Ruthenium based living radical polymerisation is based on the organic reaction of carbon tetrachloride addition on the double bond of an alkene catalysed by $[RuCl_2(PPh_3)_3]$.[93] The reaction is highly regioselective as the bulky CCl_3 group is binded to the least hindered end of the double bond, probably due to the formation of a radical intermediate which does not escape the co-ordination sphere of the Ru.[94,95] Living polymerisation of MMA was obtained with an activating species of methylaluminium bis-(2,6-di-*tert*-butylphenoxide) which achieved 90 % conversion in 4 hours at 60°C. First order kinetics were observed and polymers had M_n similar to those predicted with low polydispersity (typically PDI =1.3 – 1.4). Other monomers successfully polymerised by this technique include styrene[96] and *N,N*-dimethylacrylamide which polymerised faster but with a poorer molecular weight control (PDI ~1.6).[97] The same group studied the effect of additives and concluded that hindered Lewis acid such as $Al(OiPr)_3$, $Ti(OiPr)_4$ and $Sn(OiPr)_4$ accelerated controlled polymerisation whereas metal chlorides such as $TiCl_4$ and $SnCl_4$ were ineffective. NMR and cyclic voltametry experiments suggested that the former group interacted with the Ru species and not, as first thought, with the monomer or propagating polymer.[98]

The $RuCl_2(PPh_3)_3$/ $PhCOCHCl_2$ initiating system has been shown to be effective for the living radical polymerisation of MMA in toluene and water under an inert atmosphere. Although addition of $Al(OiPr)_3$ did increase the rate of reaction, it was found that polymerisation was significantly quicker in the water / toluene mixture than in water alone suggesting that complexation of water to the Ru catalyst was occurring[99].

Concerning the initiators, polydispersity was lowered when brominated rather than chlorinated α-haloesters were used and the dimeric initiator $(CO_2Me)CH_2C(CH_3)(CO_2Me)Br$ produced narrower distribution polymers than its unimer analogue 2EIBr certainly due to a more reactive C-Br bond and a higher molecular weight reducing the number of primary radical combination events[100].

Later, polymerisation mediated by $RuH_2(PPh_3)_4$ was found to occur at a faster rate than that mediated by $RuCl_2(PPh_3)_4$ and narrower polydispersities (PDI < 1.2) were observed without co-catalyst[101].

Ruthenium "half-sandwich" type cyclopentadienyl complexes are the most recent reported catalyst complexes for the living radical polymerisation of MMA and styrene using $CHCl_2COPh$ as the initiator with $Al(O\textit{i}\text{-}Pr)_3$ activator. Ruthenium indenyl complexes were even more active and did not require a co-catalyst to mediate smooth polymerisation. Polymers produced by this initiating system had very low polydispersity (typically PDI < 1.15) (figure 1.14).[100,102]

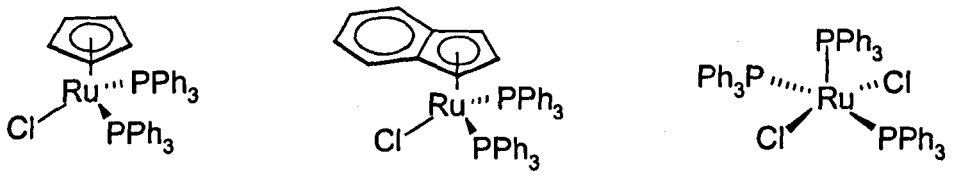

Figure 1.14: Ruthenium complexes catalysts for the living radical polymerisation of MMA.

Ruthenium mediated polymerisation has also been performed using a solid support system, using 2-Aminopropyl silica with $RuCl_2(PPh_3)_3$ for the polymerisation of MMA. The polymerisation occurred relatively fast (91% conversion after 4 hours) but the polydispersities of the final products (~ 1.5) were larger than the corresponding

homogenous reaction employing $Al(OiPr)_3$ as co-catalyst. The polymer obtained was successfully used to reinitiate polymerisation proving that living polymerisation had occurred. Alternative solid supports of silica gel and basic aluminium oxide were tested but it was concluded that the amino functionality was necessary to form the active catalyst.[103]

1.4.7. Copper mediated living radical polymerisation.

Copper mediated living radical polymerisation was one of the first transition metal mediated living radical systems to be reported, in 1995. Inspired from the atom transfer radical addition, Wang and Matyjaszewski polymerised styrene in bulk using 1-phenethyl chloride (1-PECl) as the initiator and Cu(I)Br / 2,2'-bipyridine (bipy) as the mediating species[39]. Relatively narrow polydispersity polystyrene (PDI ~ 1.5) was obtained and M_n increased linearly with conversion, with values in accordance with the ratio [Monomer]:[Initiator]. As the system seemed close to the organic reaction, the process was named *atom transfer radical polymerisation* (ATRP) by its authors. This communication was the first of many to follow, trying to understand the polymerisation process, increase the number of polymerisable monomers and adapt it to the industrial requirements. Today, copper mediated LRP is one of the most successful methods to polymerise a large number of monomers in a living and control manner.

In their following communication, Matyjaszewski and Wang investigated the use of several organic halides (X = Br, Cl) and CuCl / CuBr for the bulk and solution polymerisations of styrene, methyl acrylate, butyl acrylate and methyl methacrylate[104]. Stereochemical information from the ^{13}C NMR spectra of PMMA

prompted the authors to propose that the propagating species was a free radical, since the polymer had very similar stereochemistry to that synthesised with a free radical. The presence of a transition metal complex in the medium increases however the academic interest on the understanding of the process, as a potential copper coordination of the active species could occur, and be the source of the propagation.

1.4.7.1.Copper / ligand complex.

The role of the ligand in copper mediated LRP is to solubilise the copper, in its reduced and oxidised forms, and to help in the stabilisation of the redox equilibrium, key of the polymerisation (see above). Nitrogen donor species are known to be very good ligand for Cu(I) and Cu(II), and among them, 2,2'-bipyridine (bipy) is the most used in Cu(I)/Cu(II) chemistry, as a commercially available product.[105]

However, despite the encouraging results obtained when using bipy for LRP, the catalyst complex was not fully soluble and consequently heterogeneous catalysis occurred. Many research groups work on the elaboration of new ligands to increase the solubility of the catalyst complex keeping the right redox potential. The first efficient ligand to have been reported was a substituted bipy: 4,4'-Alkyl substituted bipyridines (Figure 1.15). Associated to Cu(I)X, it was employed for the homogenous polymerisation of styrene[73,106] and MMA[107,108] and lead to narrower polydispersity polymers than unsubstituted bipy.

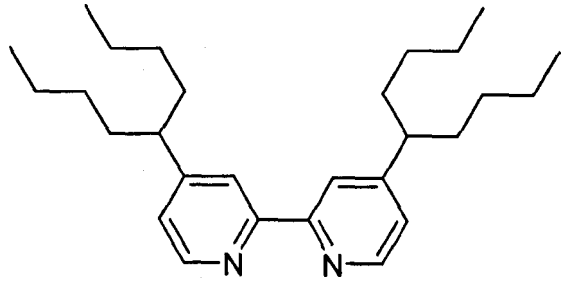

Figure 1.15: 4,4'-di(5-nonyl)-2,2'-bipyridine.

As the general synthesis of substituted bipyridines was not trivial, other ligands structure were proposed. Haddleton *et al.* demonstrated the use of *N*-alkyl-2-pyridylmethanimine complexes for the homogenous polymerisation of methacrylates[40,109]. The synthesis of such ligand is a simple condensation reaction of 2-pyridine carboxaldehyde with an appropriate amine. The main interest of these ligands is the possibility of changing the alkyl chain, either by varying its length to influence the solubility of the catalyst without influencing the polymerisation kinetics or by incorporating functionalities[110]. In the polymerisation of MMA, several alkyl-substituted pyridinalmethanimines were successful in promoting living character. Reaction rates were faster for straight chain alkyls and PDI was observed to increase for the branched alkyl ligands. The crystal structure of the isolated $Cu(L_2)BF_4$ shows a tetrahedral Cu centre (Figure 1.16) and for the first time, a structurally characterised Cu(I) complex was used for the polymerisation of MMA, rather than the formation of a complex *in situ.* However, there was no evidence to prove that the isolated structure resembled the structure of the active polymerisation catalyst[111].

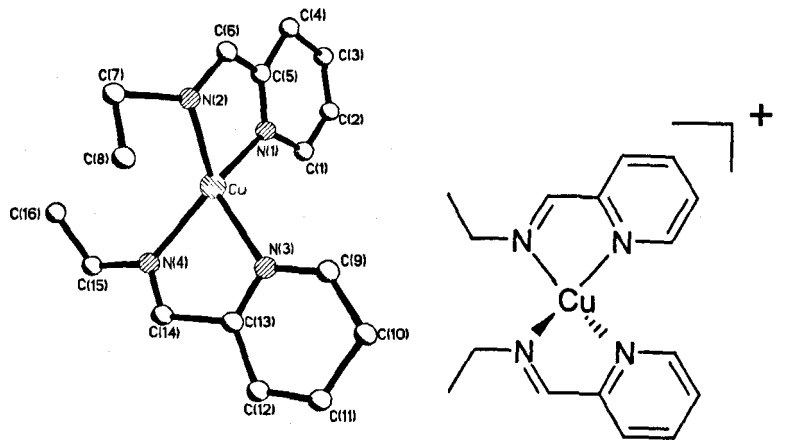

Figure 1.16: (*N*-ethyl-2-pyridinalmethanimine) Cu(I) BF_4.

In a constant concern of meeting industrial needs, commercially available multidentate amines, cheaper than bipy, have also been tried to efficiently complex the copper catalyst (Figure 1.17).

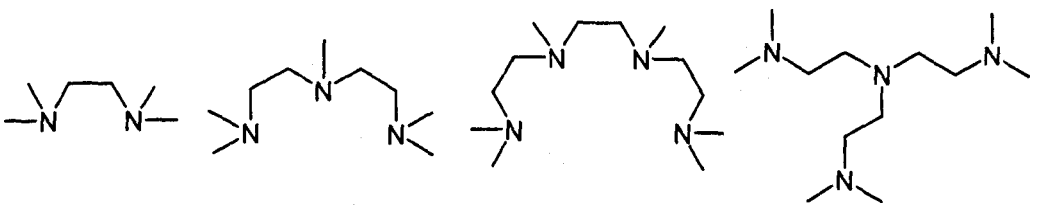

Figure 1.17: Multidentate amines for the Cu(I) based living polymerisation of Styrene, MMA and MA.

The amino ligands were used in the polymerisation of Styrene and methacrylate in bulk and methyl methacrylate in anisole. The homogeneous CuBr complex solutions led to living polymerisations characterised by narrow PDIs (PDI ~ 1.3 for styrene, 1.2 for MMA and 1.1 for MA) and linear increase of M_n with the conversion.[112] HMTREN however led to a heterogeneous system for the polymerisation of butyl

acrylate and styrene (PDI < 1.2) and was not efficient for MMA, with poor control and low conversion achieved.[113]

More recently, Johnson *et al.* reported the successful use of nine quadridentate nitrogen donor ligands for the polymerisation of MMA. The living system exhibited the best molecular weight control when catalysed by $[Cu\{en(Bn)py\}Cl]BPh_4$ (Figure 1.18), with PDI <1.1, 90 % conversion being achieved after 90 minutes in anisole 80°C[114]. This high rate of polymerisation (when compared to bipy system) was lowered by the addition of bulk to the pyridine ring, which decreased also the molecular weight control. Anisole, used as solvent, was found to increase both polymerisation rates and molecular weight control when compared to toluene. When fluorinated benzene rings were introduced in the ligands, slower polymerisation rates were observed, but the control remained the same.

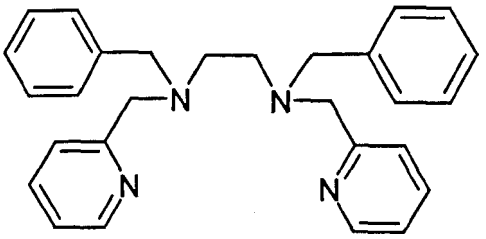

Figure1.18: Quadridentate ligand en(Bn)py.[114]

The use of flurinated ligands was also reported by Haddleton *et al.* in a concern of recycling the catalyst complex. The solvent used for the polymerisation system was an equivolume mixture of perfluoromethyl cyclohexane and toluene, only miscible at reaction temperature (90°C). As the catalyst complex was only soluble in the fluorous phase, homogeneous catalyse was achieved during the reaction, with easy separation of the catalyst from the product at room temperature. Three runs of polymerisation

could be achieved with the same catlalyst complex, leading to good control over the polymerisation (PDI increasing from 1.2 to 1.3 for each run) and final products showing a very low amount of residual catalyst.[115]

Efficient living radical polymerisation was also reported when using the oxidised form of copper(I) (Cu(II)). Firstly reported by Matyjaszewski and referred as "reverse Atom Transfer Polymerisation"[116], a system initiated by AIBN and catalysed by Cu(II)/dNbipy achieved high initiator efficiencies for styrene and methyl acrylate but not for MMA, which exhibited broader molecular weight distributions (PDI ~ 1.4). Maybe more surprising results were presented by Lin and co-workers who reported the polymerisation of solketal methacrylate using exclusively $Cu(II)Br_2$ in conjunction with an aliphatic tetra-amine ligand [117]. In this case acceptable rates were achieved and polydispersities < 1.20 were obtained.

1.4.7.2.Initiator.

The role of the initiator in copper mediated living radical polymerisation is of primary importance, as fast initiation and low side reaction induction is required to obtain a good control over the product molecular weight. As living radical polymerisation is tolerant to a wide range of functional groups the initiator is also an interesting way to introduce α–functionality in the polymer, or to build specific architecture. Generally, alkyl halides (R-X) with either inductive or resonance stabilising substituents are efficient initiators for copper mediated LRP. Often, the structure of the initiator is similar to the structure of the polymer end group (Figure 1.19). Fine tune can be

achieved by adjustment of the R group and the leaving group X in order to make the R-X bond more labile than the polymer-X bond.

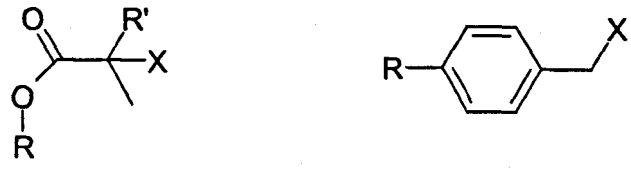

X = Cl, Br
R' = H, CH_3

Figure 1.19: Generic structures of typical initiators.

The facile reaction of hydroxyl group with 2-bromoisobutyryl bromide or 2-chloroisobutyroyl chloride allows any molecules showing a OH group to be potentially transformed in copper mediated LRP initiator. This leads to functionalised molecule capable of initiating polymerisation[118,119] (e.g. cholesterol or sugar[120]) or specific architectures as block copolymers (when the alcohol is part of a polymer; see chapter 2 for details and references), star polymers[120,121] and hyper-branched macromolecules.[122-124]

On a different approach, sulphonyl halides have been reported to be very efficient initiators because of their low tendency to dimerise and fast activation of olefins, and called "universal initiators" by their reporters.[41,125] The S-Cl bond found in sulphonyl halides is weaker than C-Cl, leading to a faster initiation than propagation, necessary for well controlled polymerisation. They have been successfully used with various styrenes, methacrylates and acrylates monomers.[126]

1.4.7.3.Monomer.

Styrene derivates[127], methacrylates[40] and acrylates[128] monomers can easily be polymerised in a control manner using copper mediated LRP, by simply using the right copper complex and/or initiator.

Functional monomers such as 2-hydroxyethyl acrylate,[129] glycidyl acrylates[130], acrylonitriles,[131] (meth)acrylamides[132] have also be polymerised in a controlled manner. Other monomers like vinyl acetate, isobutene and *N*-(cyclohexyl)maleimide were difficult to homopolymerised but copolymerised with monomers such as methyl acrylate, acrylonitrile and styrene.[133] Well-controlled structure bio-polymers (PDI < 1.1) can also be obtained from the polymerisation of specific monomers containing secondary hydroxyl, primary, secondary and tertiary amino, secondary amido, silyl ether and ester linkages.[134] This opens new possibilities for copper mediated LRP in the direction of the biology-polymer science interface, as the synthesis of possible Deoxyribose nucleic acid (DNA) interacting therapeutics could lead to the possible templated synthesis for the creation of artificial DNA analogues.[135,136]

1.4.7.4.Additives.

As it has been seen previously, copper mediated LRP is very robust regarding the presence of functional groups in the system. Their presence may even have a beneficial effect on the polymerisation. The various effects of additives or solvents will be reviewed and discussed in chapter 4, but one can quote, as an example, the effect of the addition of low levels of phenols (traditionally added as an inhibitor) to a living polymerisation system: It was shown to actually increase the rate of polymerisation without decreasing the degree of control of polymerisation of

MMA.[137] It was proposed that complexation of the phenol to the Cu centre modifies the structure of the catalyst and makes it more active.

1.5. Poly(ethylene oxide).

Poly(ethylene oxide) (PEO) is a crystalline, thermoplastic, water-soluble polymer with the general formula X-(O-CH_2- CH_2)$_n$-Y. The end groups are known to be hydroxyl groups only in the case of the lower molecular weight molecules. PEO is commercially available in a vast range of molecular weight, from ethylene glycol to polymer with repeating units greater than a million. The lower molecular weight molecules, with n up to around 150 (~ 6,600 g/mol) are generally referred as *poly(ethylene glycol)* (PEG) while the higher mass are known as *poly(ethylene oxide)*, polyoxyethylene or polyoxirane.

1.5.1. History.

PEO was first synthesised by Lourenco in 1859. Products with a degree of polymerisation as high as six were found when ethylene bromide was heated with ethylene glycol at 120°C.[138,139] At the same time, Wurtz reported the first synthesis of low molecular weight polymers from ethylene oxide, by heating it in presence of ethylene glycol for several weeks.[140] He noticed also that heating ethylene oxide with water[140] or with acetic acid[141] yielded low molecular weight polymers, while higher molecular weight products were obtained when eating the oxide in presence of zinc chloride or sodium hydroxide.

In the late 1920's, when developing the concept of polymers, Staudinger showed that poly(ethylene oxide) of higher molecular weight could be obtained, and studied its synthesis and properties extensively along with polyisoprene and polystyrene.[142] He proved that molecular weight higher than 100,000 g/mol could be achieved by mixing ethylene oxide and alkaline earth oxides. Yields of 50% were obtained after leaving the solution for two years.[143] It is in 1957 that the first commercial synthesise of high molecular weight PEO were reported using catalysts based on specially prepared alkaline earth carbonates.[144-146] In 1958, Union Carbide Corporation started the first industrial production of high molecular weight products under the trademark name POLYOX®. It still produces a large amount of this product with molecular weight up to several millions, while smaller chains are sold by numerous other companies, under various names, for example Polyglycol E (Dow), Polyethylene glycol, Carbowax® (Carbide), Pluracol®E (BASF).

1.5.2. Synthesis.

The synthesis of poly(ethylene oxide) is a classic example of ring-opening polymerisation of ethylene oxide (or epoxyde) encountered in many polymer textbook. The particularity of the synthesis is that either anionic or cationic polymerisation can be used because of the high degree of strain in the 3-menbered ring.

1.5.2.1.Cationic ring-opening polymerisation.[147]

The initiators are usually strong protonic acids or Lewis acids in conjunction with co-catalysts, all of the generic form: R^+A^-. Initiation take splace by addition of R^+ to the

epoxyde oxygen atom to yield a cyclic oxonium ion which is in equilibrium with the corresponding open-chain carbocation (Figure 1.20).

Initiation

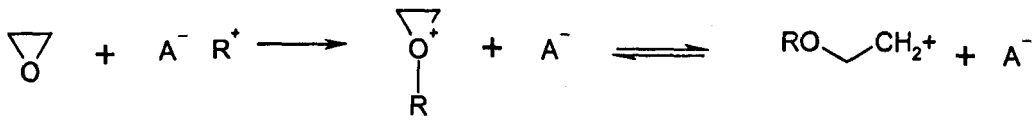

Figure 1.20: Initiation step of the cationic ring-opening polymerisation of ethylene oxide.

Both species can propagate either via ring-opening of the cyclic oxonium ion upon nucleophilic attack at a ring carbon atom by the epoxide oxygen atom in another monomer or via its addition to a monomer in a reaction similar as the initiation step (Figure 1.21).

Propagation

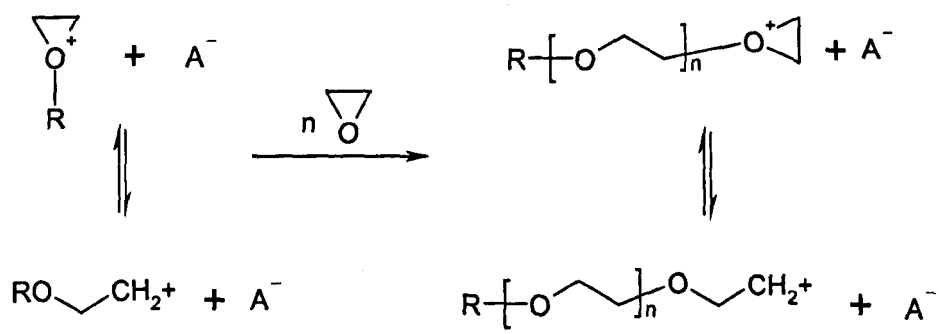

Figure 1.21: Propagation step of the cationic ring-opening polymerisation of ethylene oxide.

Termination can occur via ion-pair rearrangement of the two species in equilibrium to give a polymer with an unsaturated chain end, or by reaction with less stable counter-ion ($AlCl_3$ for instance).

Intramolecular and intermolecular chain transfer to polymer can occur: The former leads to the formation of rings, whereas the latter is an interchange reactions taking place with both linear-chain and ring molecules. This polymerisation is complicated by other mode of propagation (for instance via rearrangement of the growing chain intermediates, or via terminal –OH groups if an alcohol is present or if H^+ is the initiating species), which makes it difficult to control.

1.5.2.2.Anionic ring-opening polymerisation.[148]

This is the method the most used in industry to polymerise both poly(ethylene glycol) and poly(ethylene oxide). The polymerisation can be initiated by hydroxides, alkoxides, oxides and metal alkyls and aryls (figure 1.22).

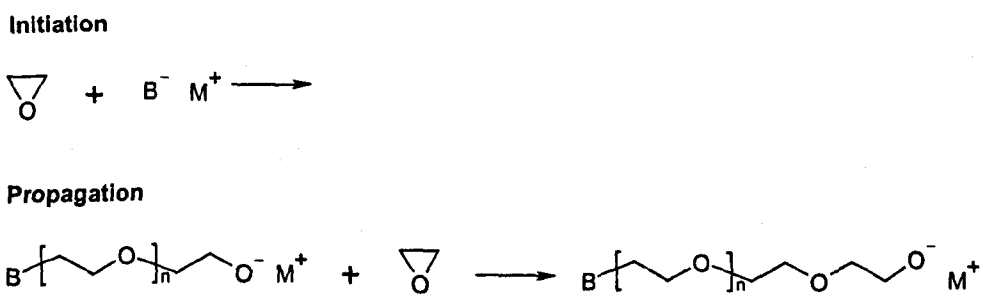

Figure 1.22: Initiation and propagation steps of the anionic ring-opening polymerisation of ethylene oxide.

Some initiators including adduct as ferric chloride-propylne oxide, Zn(OCH3), ([Zn(OCH3)2]2, bimetallic μ-oxoalkoxides, metallopophyrin derivatives of zinc, aluminium and manganese, etc. can undergo an anionic coordination mechanism. Propagation in this system involves a concerted process in which the monomer is inserte into a metal-oxygen bon (figure 1.23).

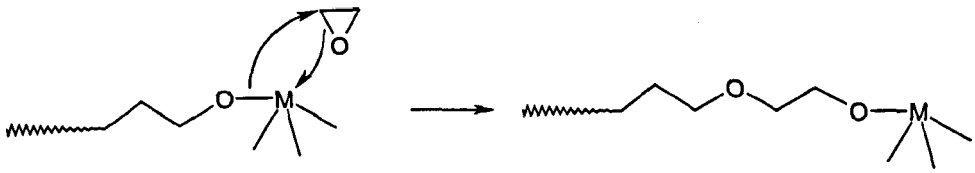

Figure 1.23: Propagation steps of the anionic ring-opening polymerisation of ethylene oxide by concerted process.

Polymerisations taking place in the presence of protonic substances such as water or alcohol (for example to solubilise the initiator when using metal alkoxide and hydroxides initiators) involve the presence of exchange reactions (figure 1.24).

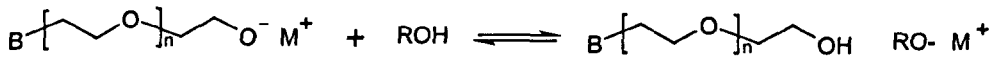

Figure 1.24: Exchange reaction during the anionic ring-opening polymerisation of ethylene oxide in presence of protonic substances.

Similar exchanges can occur between the newly formed polymeric alcohol and the propagating chains, resulting in equilibrium between dormant and active chains. This leads to the synthesis of poly(ethylene glycol) with a well-defined molecular weight distribution, limited to low molecular weights (usually under 10,000 g/mol).

However, this limitation does not apply when using aprotic polar solvents for an initiation by alkoxides and hydroxides or when using other initiators, including metal alkyls and aryls and the various coordination initiators, as they are fully soluble in

solvent such as THF. Poly(ethylene oxide) with molecular weight as high as a million can then be synthesised.

1.5.3. Properties.

PEO is a thermoplastic polymer, with a crystalline structure. In the crystalline state, the conformation reported is an internal rotation of O-CH_2, CH_2-CH_2 and CH_2-O bonds of trans, gauche, trans respectively.[149,150] In the molten state, the helix typical of the crystalline state is disordered, with the appearance of a considerable fraction of trans, trans, trans conformations.[150] These bonds give also a great flexibility to the polymer chain.

Low molecular weight poly(ethylene glycol) are characterised molecular weight wise by their number average molecular weight (M_n) and high molecular weight poly(ethylene oxide) are characterised by their weight average molecular weight (M_w).

PEO is soluble in water and in most of all common organic solvents such as acetonitrile, anisole, chlorophorme, dimethylformamide, etc. It is not soluble in aliphatic hydrocarbons, and although it has low room temperature solubility in aromatic hydrocarbons, PEO is fully soluble in benzene and toluene at elevated temperature.[151]

In water, PEO exhibits an inverse solubility-temperature relationship.[145,152] From being fully soluble at room temperature, the polymer precipitates when the temperature is raised close to the boiling point of the solvent. For very dilute solutions (0.2% or less), this precipitation is observed as a cloud point, whilst for more concentrate solution (0.5% or more), the polymer precipitates as a gel. This

temperature dependence solubility can be explained by the dual character of POE, as it presents both hydrophobic, due to the ethylene units and hydrophilic properties, due to the oxygen atoms.[153]

The same conformations are observed in solution as in the solid state. While the polymer adopts the crystalline state helix in water, its conformation is closer to the molten state when dissolved in organic solvent (Chloroform, benzene, etc.).[154]

In water, NMR spectrometry[155] and viscosity[156] analyses indicate that each ethylene oxide unit of the polymer chain is hydrated by three water molecules, while in chloroform or benzene evidences were found for intermolecular association of the polymer chains. This brings evidences of the difference in behaviour of PEO in water and in organic solvent, mainly attributed to the difference in the conformation of the polymer in these solvents. This leads to an application as surfactant at the interfaces of non-miscible liquids like water and organic solvents, and was extended to the interface water-air. Aqueous PEO solutions surface activity was shown to stay constant over molecular weight around 10,000 g/mol, but increases when the molecular weight was decreased under this value.[157-159]

Rheology properties appear to be the main interest of PEO solutions. When PEO with a molecular weight greater than about a million is dissolved in water with a concentration higher than 5%, the solution behaves as a gel. When the concentration is decreased up to 0.5%, the polymer solution exhibits a pseudoelastic behaviour.[145] Finally, and mainly, for highly diluted aqueous solution, PEO has been shown to be very efficient as a friction reduction agent, characteristic of the Toms effect.[160] In effect, PEO makes water more slippery. This friction reduction phenomenon is

obviously of considerable engineering interest: An example of application is the use of PEO polymers in the paint on the hull of a ship or a torpedo to decrease the drag of water and make them move faster.

1.5.4. Industrial applications.[161]

The main applications of high molecular weight PEO have been introduced in the 1960's. They are based on their thermoplastic character and their unique solubility and rheology properties, *e.g.* the ability to increase the flow of water slurries, as mentioned above. They are also used as stabilisers of aqueous colloids an dispersions, generally by physical adsorption followed by steric repulsion of the modified particles.

Low molecular weight PEG, (usually below 6,000-8,000) have been commercially available since the 1930's. They can be used as prepolymers in the synthesis of polyurethane, epoxies, silicones or other polymers, or, thanks to their exceptional compatibility and water solubility, they find their application as adjuvant in cosmetics (creams, lotions, powder, etc.), in industry as pigment dispersants, in agriculture as spreading agents, in starch adhesives industry as plasticiser, etc.

Chapter 2

Amphiphilic block copolymers synthesised by LRP with poly(ethylene glycol)-based macroinitiators.

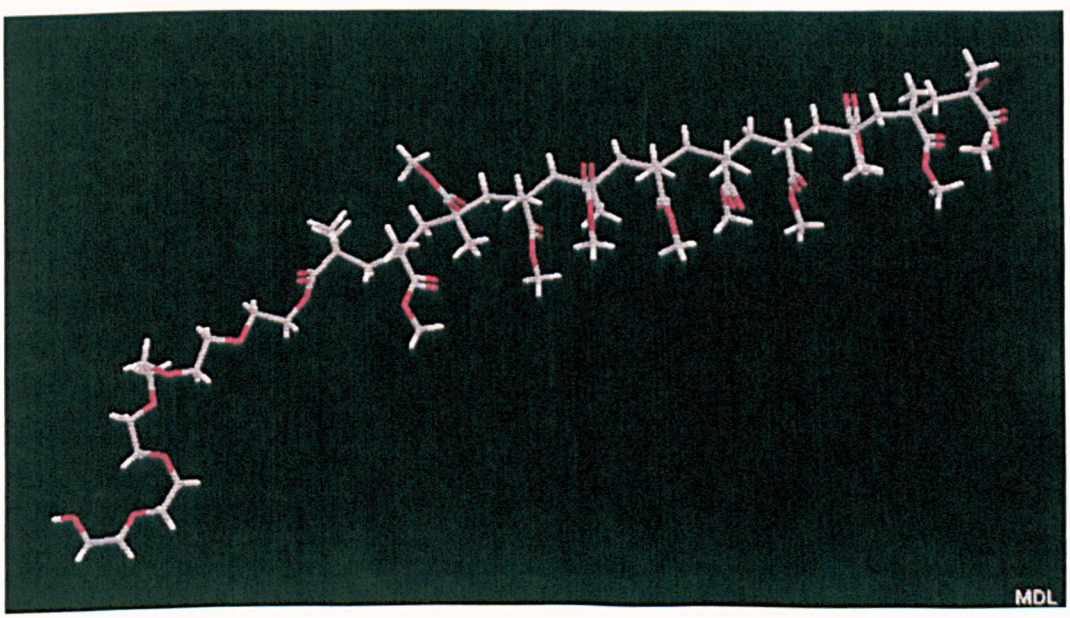

3D Schematic of a MeOPEG-*b*-PMMA copolymer.

2.1. Introduction.

Copper mediated living radical polymerisation offers a versatile method for the synthesis of di-block (A-B) and tri-block (B-A-B) copolymers. Polymers synthesised by any polymerisation technique, e.g. condensation, (A) can be transformed into macroinitiators by the introduction of an initiating end group via a simple esterification. The subsequent block(s) (B) can then be formed by living radical polymerisation. This results in block copolymers of well-defined structure. This method is especially interesting when the two monomers polymerise according to two different reactions and allows the preparation of a wide range of block copolymers.

LRP has been used to synthesise a variety of inorganic/organic polymer hybrids by the polymerisation of a range of monomers from poly(dimethyl siloxane) (PDMS) macroinitiators. Hydrosilylation of commercially available difunctional hydrosilyl terminal PDMS with allyl- or 3-butenyl 2-bromoisobutyrate has been used to form macroinitiators for the preparation of tri-block copolymers with acrylates, methacrylates[163] and styrene.[164] The same method has also been applied to hydrosilyl pendant PDMS to polymerise styrene from the backbone and form PDMS-g-PS.[164] Similar macroinitiators have been synthesised by anionic ring- opening polymerisation of hexamethylcyclotrisiloxane and hydrosilylation of an initiator onto telechelic vinyl- or hydrosilyl-terminal or -pendant PDMS, to form tri-block copolymers with polystyrene or isobornyl acrylate[165] and (meth)acrylates[163].

Polyalkylene chains have also been widely used to synthesise block or graft copolymers with styrene. Linear chains such as chlorophenylethyl telechelic poly(*iso*-butene) have been synthesised by cationic polymerisation to form block copolymers.[166] Commercially available *iso*-butene-*p*-bromomethylstyrene copolymer

have been utilised as macroinitiators for the preparation of poly(*iso*-butene)-*g*-polystyrene[167]. Di-block copolymers of polyethylene-co-polybutylene and PMMA[168], polystyrene[169] and poly(4-acetoxystyrene)[169] have also been synthesised by LRP using a 2-bromopropionic ester macroinitiator prepared from commercial monohydroxyl functional hydrogenated polybutadiene (Kraton).

More complex architectures have been formed by the preparation of polynorbornene-*b*-polystyrene and poly(dicyclopentadiene)-*b*-polystyrene using ring opening metathesis polymerisation of norbornene or dicyclopentadiene, and the addition of a bromo-aldehyde to give macroinitiators for the LRP of styrene.[170]

Dihydroxy telechelic poly(sulphone), synthesised by the polycondensation of bisphenol-A and 4,4'-difluorosulphone and subsequent condensation with acid bromide has been reported to provide a difunctional macroinitiator for copper mediated living radical polymerisation, from which styrene and BA were polymerised to give a ABA tri-block copolymers.[171]

Alternatively, conventional radical polymerisation and LRP have been combined to form A and B blocks respectively: Vinyl acetate (Vac) was polymerised via radical polymerisation to yield poly(vinyl acetate) PVAc with trichloromethyl end groups. This has been used as an initiator for the LRP of Styrene to form PVAc-b-PS.[172] *Radical polymerisation has also been used to prepare a bromine terminated* poly(vinylidene fluoride) macroinitiator by telomerisation of vinylidene fluoride with 1,2-dibromotetrafluoroethane. This macroinitiator was then used to synthesise polystyrene-*b*-poly(vinylidene fluoride)-*b*-polystyrene (PS-PVDF-PS) tri-block copolymers in the presence of copper(I) bromide and α-α-bispyridine complexes.[117]

Polar polymers have also been used to prepare macroinitiators, such as poly(tetrahydrofuran) from cationic ring opening polymerisation of tetrahydrofuran with 2-bromopropionyl bromide to prepare poly(tetrahydrofuran)-*b*-polystyrene by LRP.[173] This same approach has also been used for the synthesis of poly(propylene glycol)-g-polystyrene by CuCl-catalysed LRP of styrene with chloromethylated phenoxy poly(propylene glycol): the macroinitiator was prepared by ring-opening polymerisation of propylene oxide and glycidyl phenyl ether followed by chloromethylation.

Poly(ethylene glycol) has also been widely used to synthesis various block copolymers. Chen *et al.* coupled the hydroxyl group of HO-TEMPO with tosylated PEG to yield the macroinitiator terminated with a TEMPO unit, which was further used to prepare the di-block copolymer PS-b-PEG by LRP of styrene.[174] Wang *et al.* used a novel macroinitiator of poly(ethylene oxide) with a 4- hydroxy-2,2,6,6-tetramethylpiperidinyloxy end group, prepared by photochemical reaction, for the polymerisation of styrene by a living radical mechanism.[175]

In a different approach, commercially available poly(ethylene oxide) was reacted to form a macroinitiator terminated by ethyl 2-bromopropionate groups on either end of the chain and used to form A-B-A type tri-block copolymers by copper mediated living radical polymerisation with acrylamide,[176] methyl methacrylate and ter-butyl acrylate.[177] While the control over acrylamide polymerisation was incomplete and the initiation efficiency over MMA in bulk was low, good control was obtained with bulk ter-butyl acrylate.

Similar approaches were taken by Jankova *et al.*, who synthesised poly(ethylene glycol)-b-polystyrene di-and tri-block copolymers with polystyrene which showed a

PDI = 1.3, via LRP, initiated by a poly(ethylene glycol) macroinitiator prepared by quantitative esterification of PEG with 2-chloropropionyl chloride.[178]

In this chapter, the synthesis of poly(ethylene glycol) methyl ether macroinitiators, and its use for copper mediated living radical polymerisation of MMA, in order to form di-block copolymers showing amphiphilic properties is investigated.

2.2. Synthesis of poly(ethylene glycol) methyl ether based macroinitiator for copper-mediated LRP.

Commercially available (Aldrich) poly(ethylene glycol) methyl ether (MeOPEG) of three different molecular weights were used in this study. The actual DP of each macromolecule was determined to be 12 ($MeOPEG_{12}$), 45 ($MeOPEG_{45}$) and 113 ($MeOPEG_{113}$), using ^1H NMR spectroscopy.

2.2.1. Esterification.

Three different initiators with a terminal 2-bromoisobutyrate group were obtained from esterification of MeOPEG with 2-bromoisobutyryl bromide in THF, as described in the experimental section (Figure 2.1).

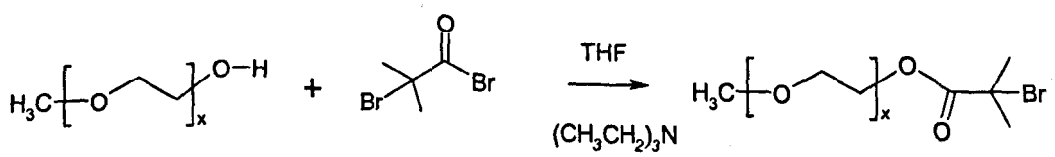

Figure 2.1: Esterification of $MeOPEG_X$ by 2-bromoisobutyryl bromide in THF (X=12, 45, 113).

As poly(ethylene glycol) is hydrophilic, it is necessary to dry the starting materials prior to esterification in order to avoid side reactions between water and acid bromide. MeOPEG was subsequently dissolved in toluene and the toluene-water azeotrope was removed under reduced pressure.

Moreover, due to their flexibility, poly(ethylene glycol) chains are intertwined together at high concentration in solution. This intermolecular hydrogen bonding made the reaction between the final hydroxyl group and the acid more difficult. It was consequently necessary to work at high dilution conditions in order to separate the polymer molecules. This effect was particularly strong for longer chains where the end group was in lower concentration.

2.2.2. Analysis of the macroinitiators.

The products of esterification were analysed by a range of technique in order to verify that 100% of the end groups were active, a condition required to obtain block copolymers of accurate molecular weights by macroinitiator-based LRP.

2.2.2.1.Infra red spectroscopy.

Infrared spectroscopy (IR) was used to confirm the esterification of the product. Figure 2.2 shows typical IR spectra of starting material and final product. The characteristic OH stretch of the starting material (black) is replaced by the C=O stretch of the ester (red).

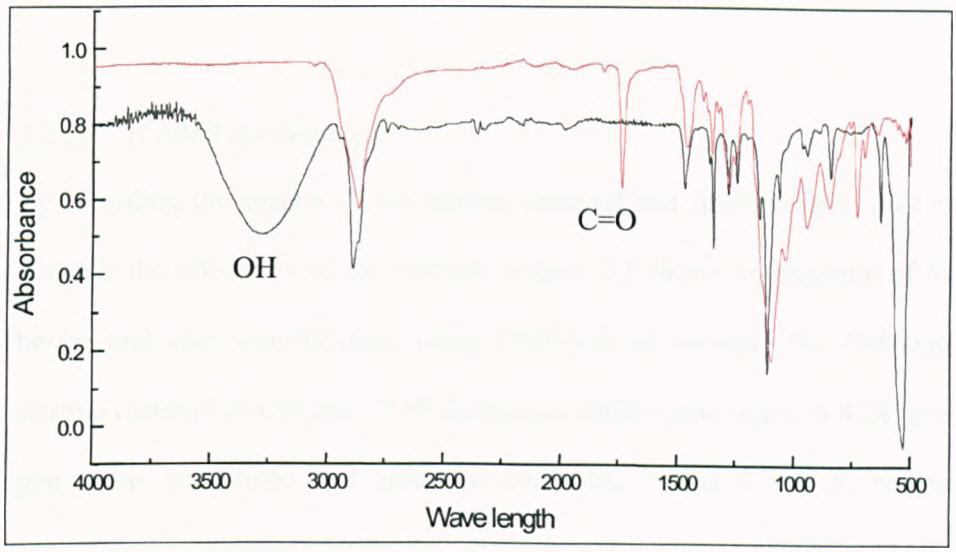

Figure 2.2: Typical Infra Red spectrum of starting material (MeOPEG, —) and initiator (MeOPEG-I, —).

2.2.2.2.Size exclusion chromatography (SEC).

The use of PMMA-calibrated SEC cannot give the absolute molecular weight of the PEG-based macroinitiator (See Appendix 2). However, the narrow polydispersity obtained did provide a good indication that the excess of acid used during the esterification did not react on the ether bonds of the poly(ethylene glycol) chains. Moreover, the product MWD was shifted to a slightly higher value than the starting material, due to the incorporation of a relatively large end group (149.9 mol/g) (Table 2.1).

X	Mwt of MeOPEG$_X$	PDI	Mwt of MeOPEG-I$_X$ (initiated)	PDI
12	560	1.08	710	1.06
45	2,000	1.02	2,200	1.05
113	5,000	1.02	5,200	1.11

Table 2.1: SEC analysis of the starting materials and final products.

2.2.2.3. ^{1}H NMR spectroscopy.

By recording the spectra of the starting material and final product, it is possible to quantify the efficiency of the reaction. Figure 2.3 shows an example of $MeOPEG_{45}$ before and after esterification, using DMSO-d_6 as solvent. The OH signal of the starting material at 4.60 ppm[179,180] disappears while a new signal at 4.24 ppm and 1.87 ppm (new substituted end group on MeOPEG, peaks 4 and 5, respectively) is observed. The quantitativity of the reaction is determined by integration of the peaks of interest (see experimental information).

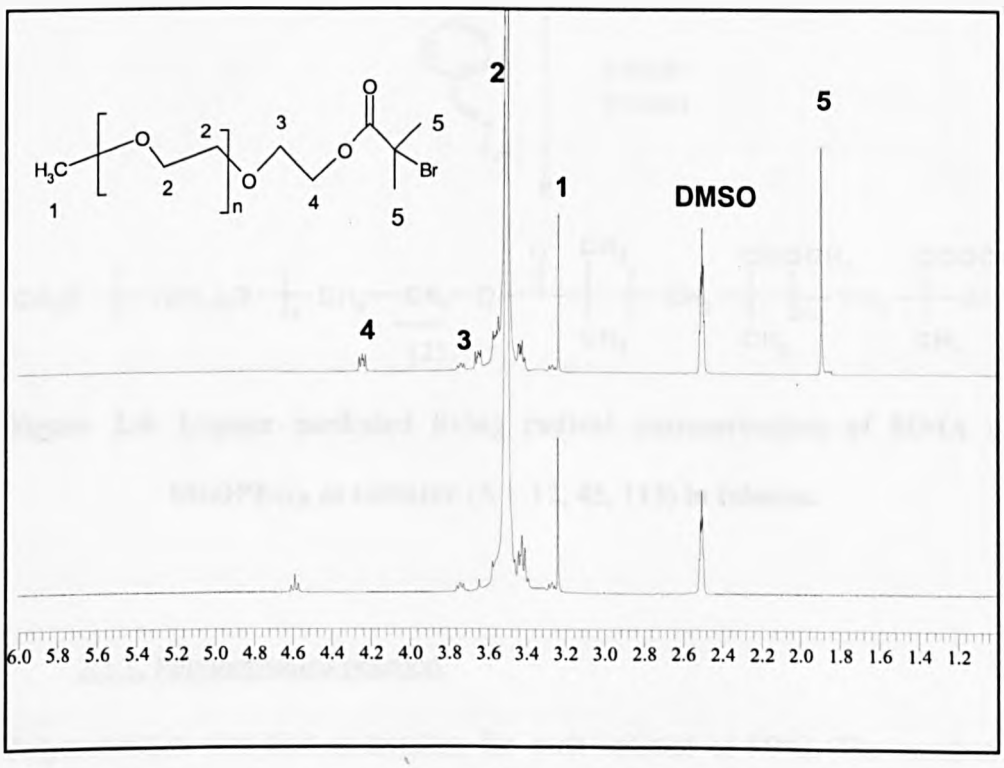

Figure 2.3: Example of typical ^{1}H NMR spectra of the $MeOPEG_{45}$ before (lower spectrum) and after (upper spectrum) esterification.

2.3. Copper-mediated radical polymerisation of PMMA using PEG-based macroinitiators.

Living radical polymerisation of MMA was initiated by MeOPEG initiators (Figure 2.4). Copper (I) was used as catalyst, complexed by the *N*-(*n*-propyl)-2-pyridylmethanimine ligand in a ratio 1 to 2 or 1 to 3, in order to ensure the solubility of the catalyst, and the stabilisation of the copper(I) / copper(II) equilibrium in toluene.

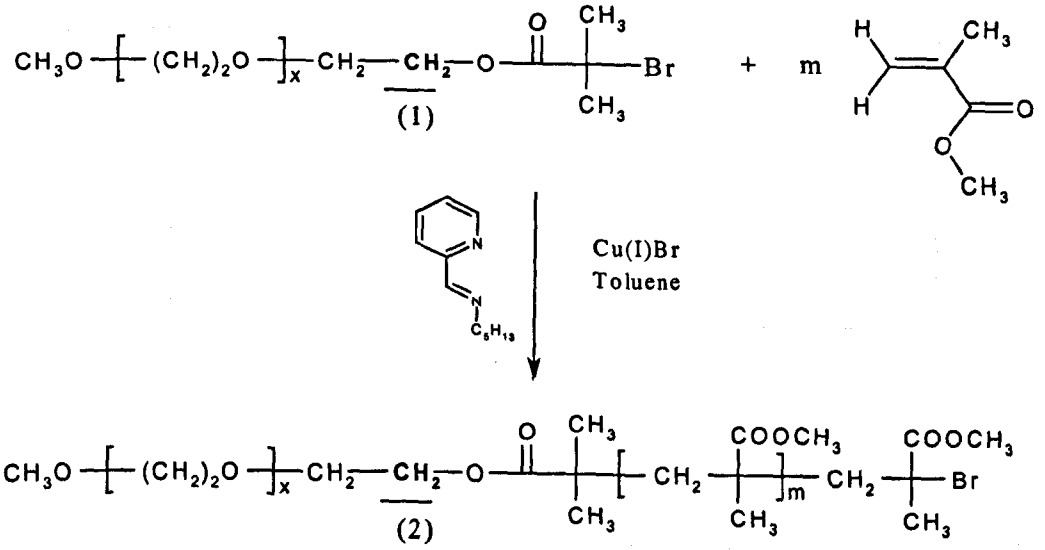

Figure 2.4: Copper mediated living radical polymerisation of MMA using $MeOPEG_X$ as initiator (X = 12, 45, 113) in toluene.

2.3.1. Polymerisation reaction.

Polymerisation was first undertaken for each initiator at 90°C. The reaction was followed for monomer conversion by ^1H NMR and the evolution of the MWD was measured by SEC samples. The monomer conversion was measured by integration of the vinyl resonance (5-6 ppm) relative to the CH_3 of the polymer backbone (1 - 1.5

ppm). Samples for SEC were filtered through basic alumina and subsequently dissolved in THF.

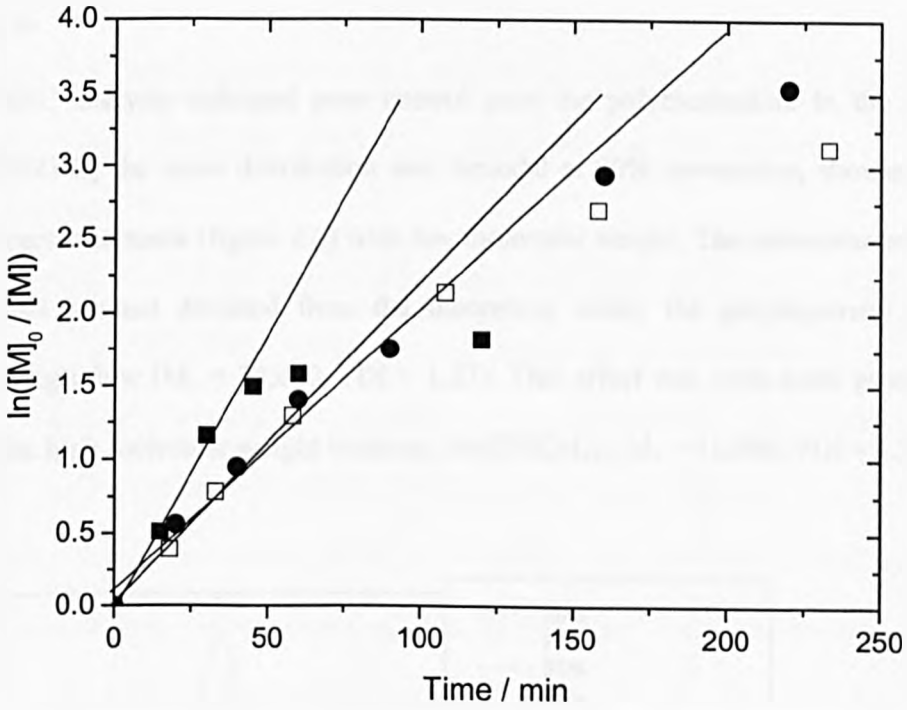

Figure 2.5: First order plot for the polymerisation of MMA with MeOPEG-I_{12} (■), MeOPEG-I_{45} (●) and MeOPEG-I_{113} (□) at 90°C.

A first attempt was made using a ratio of monomer / solvent = 1 / 1. Figure 2.5 shows the first order kinetic plot for this reaction. A clear deviation away from linearity was observed, with the reaction slowing down with time. This is indicative of termination which result in a reduction of the concentration of active species, i.e. a reduction of $k_p[P_n^*]$. After 90% conversion, the rate of polymerisation had decreased to a very low

value, the system became glassy and monomer could no longer be supplied to the propagating chain ends.

The rate of polymerisation for each macroinitiator is faster than LRP of MMA initiated by 2EIBr which gives approximately 90% conversion after 5 hours at 90°C.[181]

The SEC analysis indicated poor control over the polymerisation. In the case of MeOPEG-I_{12} the mass distribution was bimodal at 90% conversion, showing some non-reacted initiator (figure 2.6) with low molecular weight. The molecular weight of the final product deviated from the theoretical value, the polydispersity staying surprisingly low (M_n = 33,600, PDI = 1.23). This effect was even more pronounced with the high molecular weight initiator, MeOPEG-I_{113}, M_n = 18,400, PDI = 1.25.

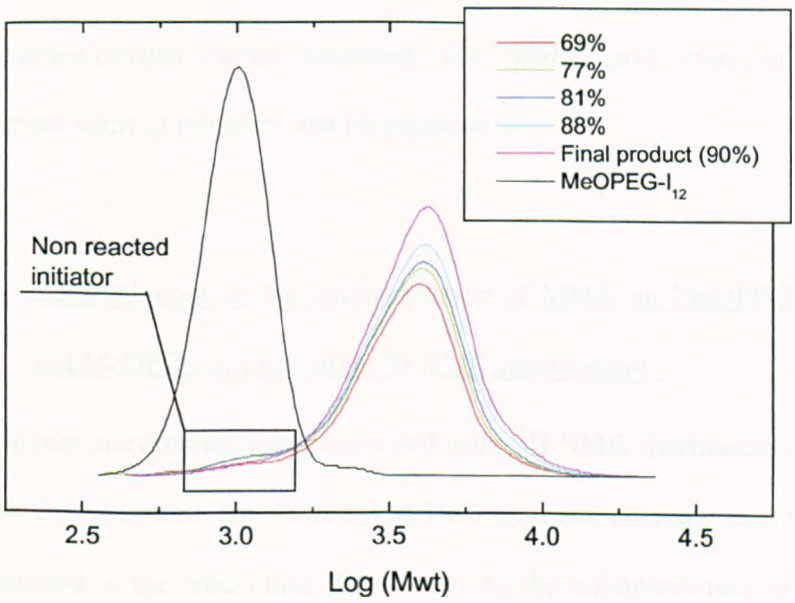

Figure 2.6: Evolution of the MWD from the polymerisation of MMA with MeOPEG-I_{12} as a function of conversion.

The absence of trace for the macroinitiator on the SEC analysis after 95% conversion indicates that initiation takes place over the course of the reaction, slower than the rate of propagation.

In order to improve to overall control of the polymerisation, the rate of reaction was decreased by diluting the solution, i.e. decreasing the ratio monomer to solvent (respectively 1 to 2).

Furthermore, in order to optimise the reaction conditions, the kinetics were followed *in-situ* by ^{1}H NMR. Polymerisations were carried out in toluene-d_8, in NMR tubes fitted with Young's tap, so as to maintain an inert atmosphere. This resulted in a plot of $\ln([M]_0/[M])$ as function of time with many more data points than from a *sampled* reaction described above. It also avoided the potential introduction of impurities/oxygen during sampling, and finally gave more information on the different steps of initiation and propagation.

2.3.2. Kinetics of the polymerisation of MMA on MeOPEG-I_{12}, MeOPEG-I_{45} and MeOPEG-I_{113} by online ^{1}H NMR spectroscopy.

Monomer conversions were monitored using ^{1}H NMR spectroscopy; the vinyl signals from the monomers appear at 5.3 and 6.0 ppm and decrease in intensity as they are consumed in the production of polymer. As the polymerisation proceeds, signals of the methacrylate backbone increase between 0.9-1.4 ppm (see Figure 2.7).

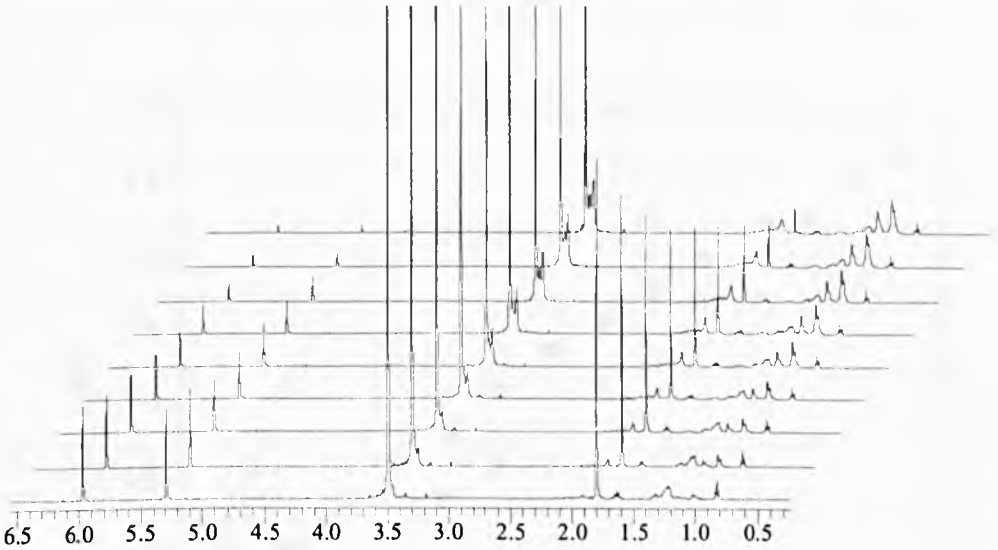

Figure 2.7: Selection of ^{1}H NMR spectra recorded during the polymerisation of MMA on MeOPEG-I$_X$ (X=12, 45, 113).

A comparison of the respective monomer and polymer signals allows the monomer conversion to be accurately determined. A first order plot was constructed for the polymerisation of MMA at 90°C with each macroinitiator (see Figure 2.8).

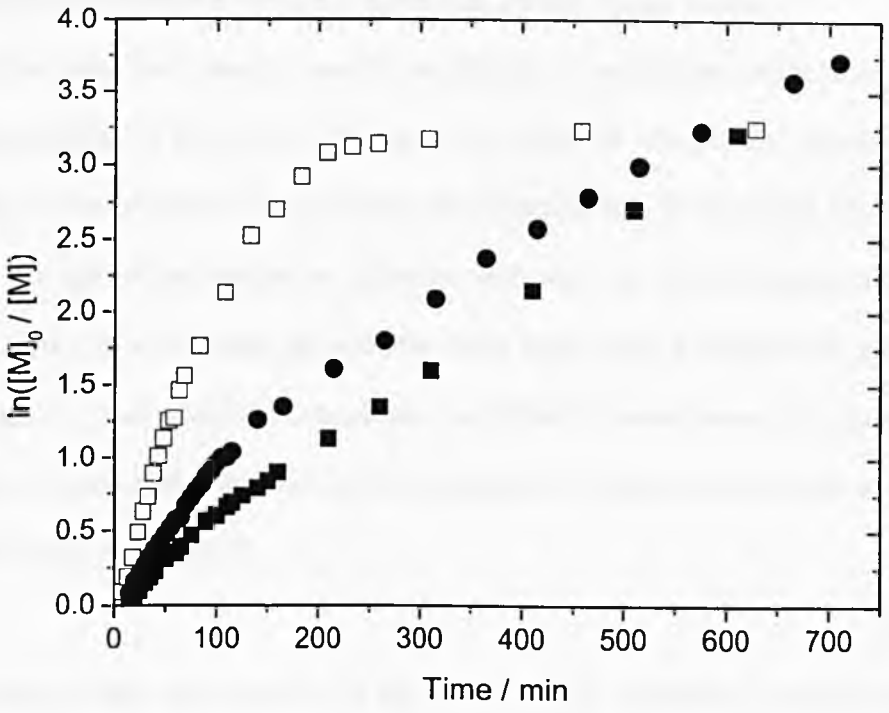

Figure 2.8: Kinetic plot of the polymerisation of MMA on MeOPEG-I_{12} (■), MeOPEG-I_{45} (●) and MeOPEG-I_{113} (□) at 90°C, followed by ^{1}H NMR spectroscopy.

A non-linear plot was observed for the highest molecular weight initiator, with a polymerisation stopping after 96% conversion. This indicates a higher contribution of termination reactions. The two smallest macroinitiators behaved similar to each other, as in both cases the initial rate decreased to a steadier rate. This can be explained by the high concentration of active species at the start of the reaction due to the presence of Cu(I) only, while the equilibrium Cu(I) / Cu(II) is established as Cu(II) is

produced. It is noteworthy that this equilibrium takes longer to be reached in the case of the highest molecular weight initiator than for the smaller chains.

The first order rate obtained once the equilibrium is established indicates that (i) the polymerisation is first order with respect to monomer and (ii) the concentration of active centres remains constant during the polymerisation. From Figure 2.8, it is clear that the rate of polymerisation increases with the size of the macroinitiator. This observation is in contradiction with that made when using a volume ratio monomer / solvent = 1 (see above). Furthermore, the different overall rates of polymerisation observed were higher than the one of a typical LRP of alkyl methacrylate with 2EIBr and similar conditions.[181]

In order to study the evolution of the Cu(I) / Cu(II) equilibrium, polymerisation of MMA using MeOPEG-I_{45} was carried out at lower temperature (see Figure 2.9). As can be seen, the first order plot is linear up to high conversions at 70°C (95% in 8 hours), with a rate close to that at higher temperature. At even lower temperatures (50°C), 80% conversion was achieved in 15 hours. In conclusion, 70°C is the best temperature in order to polymerise MMA using MeOPEG-I_{45} to obtain the best overall control of the molecular mass.

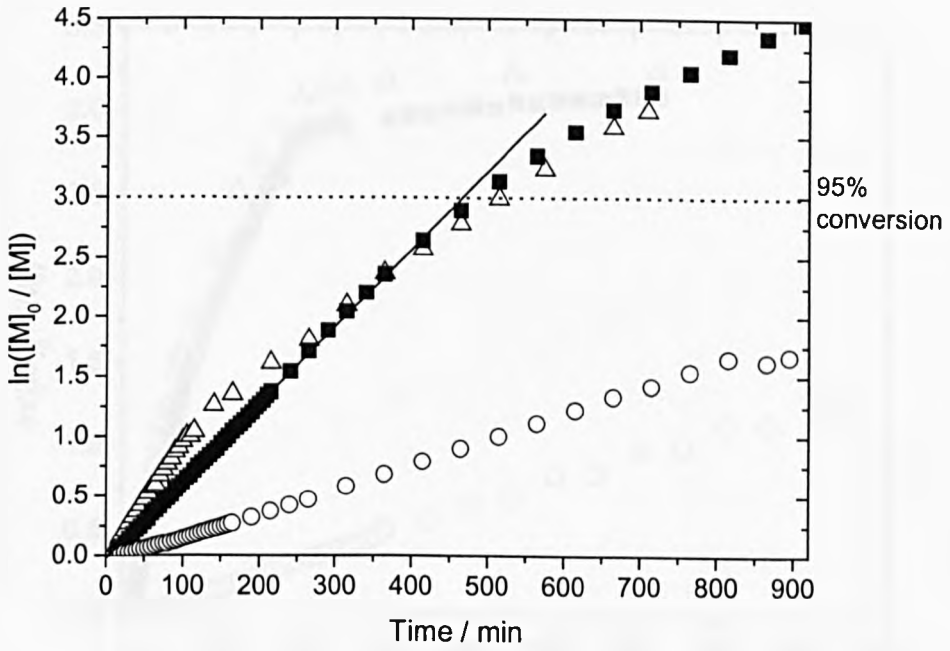

Figure 2.9: Kinetic plot of the polymerisation of MMA on MeOPEG-I_{45} at 90°C(Δ), 70°C (■) and 50°C(O), followed by ^{1}H NMR spectroscopy.

As the polymerisation using MeOPEG-I_{113} gave poor mass control at elevated temperatures, the polymerisation was carried out at 70°C and 50°C (Figure 2.10). The reaction at 70°C followed closely the behaviour of the higher temperature. At 50°C, the reaction occurred over a longer time period (80% conversion in 13 hours), but led to a kinetic plot more expected for living polymerisation.

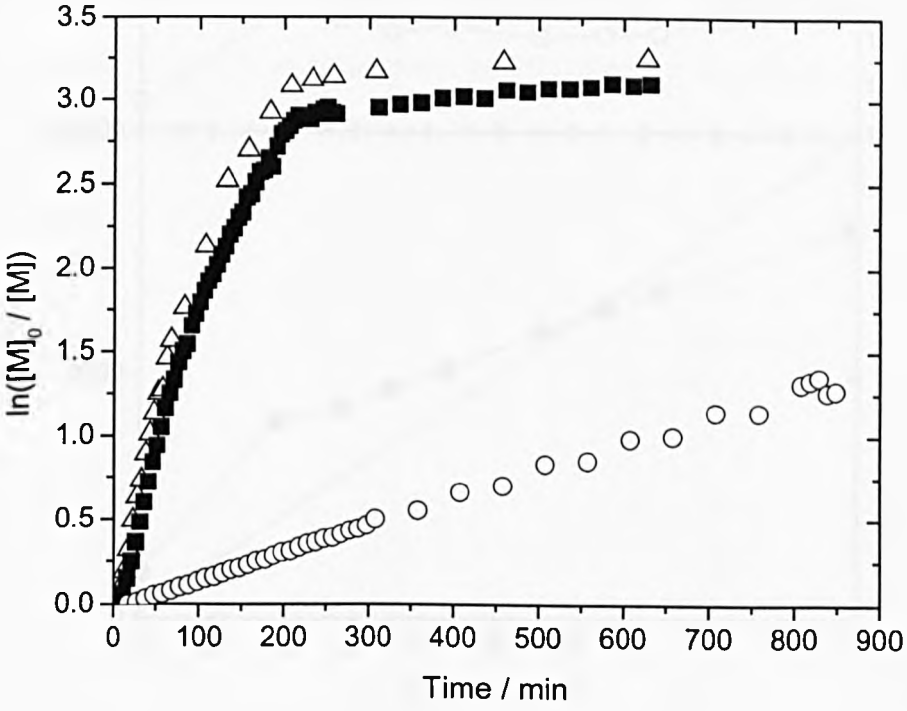

Figure 2.10: Kinetic plot of the polymerisation of MMA on MeOPEG-I_{113} at 90°C(Δ), 70°C (■) and 50°C(O), followed by ^{1}H NMR spectroscopy.

2.3.3. Molecular weight evolution.

Figure 2.11 shows typical plots of the evolution of both molecular weight and polydispersity, estimated by PMMA calibrated SEC, as a function of conversion for the polymerisation at 90°C using MeOPEG-I_{12}.

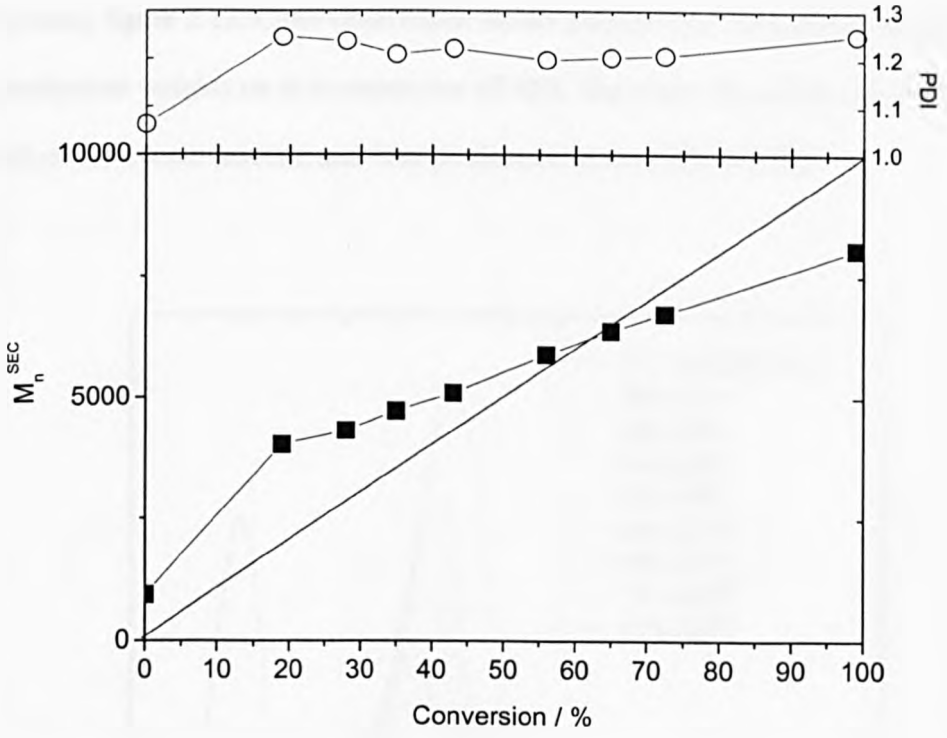

Figure 2.11: Evolution of M_n^{GPC} (■) and PDI (O) of the polymerisation of PMMA on MeOPEG-I_{12} as a function of conversion. The straight line represents the theoretical M_n.

In an ideal living system, M_n evolues linearly following the theoretical molecular weight. The measured M_n (PMMA-calibrated SEC), gives a different result from the actual M_n of the copolymer. As the poly(ethylene glycol) chains are more flexible than the PMMA ones, the hydrodynamic volume of the co-polymer will be different than a PMMA homopolymer (See Appendix 2). The graph shows therefore an increase of the molecular weight during reaction, the polydispersity remaining under 1.3, to give a final product with narrow PDI (1.25).

The MWD evolution is followed by plotting the SEC traces of each sample to 96% conversion, figure 2.12. Close observation shows the traces of non-reacted initiator at low molecular weights up to a conversion of 50%. However, as seen above, this does not affect the overall reaction and final product in terms of M_n and PDI.

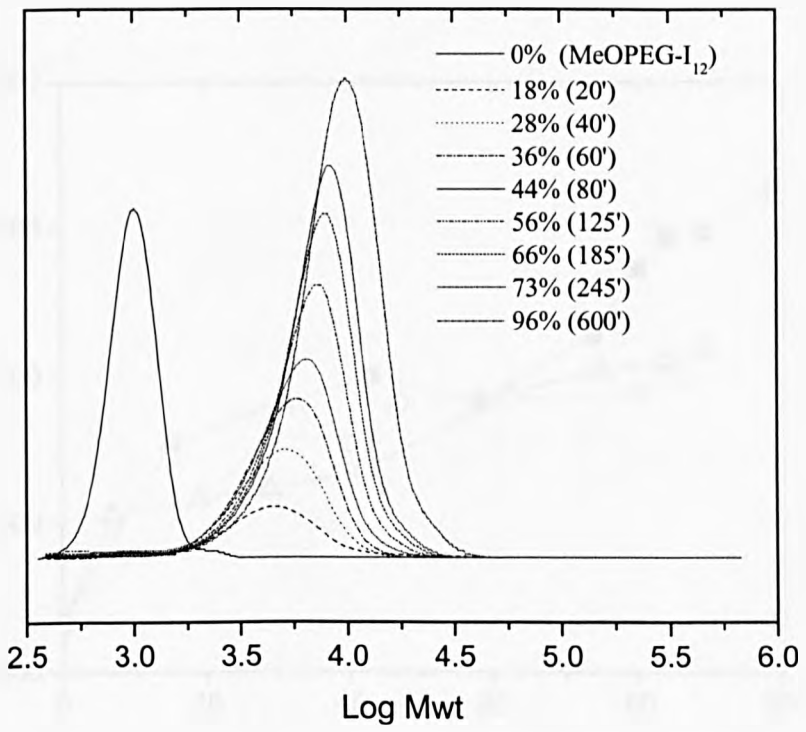

Figure 2.12: Evolution of the SEC trace of the polymerisation of MMA on MeOPEG-I_{12} with the conversion.

In conclusion, MeOPEG-I_{12} appears to be a good initiator for copper-mediated LRP of MMA at 90°C. The final PMMA block molecular weight, obtained by integration of the ^1H NMR was calculated to be 10,200 g/mol (targetted M_n = 10,000) for 710 g/mol in MeOPEG. The polydispersity was found to be 1.19 ($M_n^{SEC}{}_{copolymer}$ = 9,900).

When using MeOPEG-I_{45} as a macroinitiator at low temperature, the SEC analysis shows a steady evolution of the molecular weight with conversion at low temperature (See Figure 2.13). At 90°C, a remarkable increase in the trend was observed after 60% conversion.

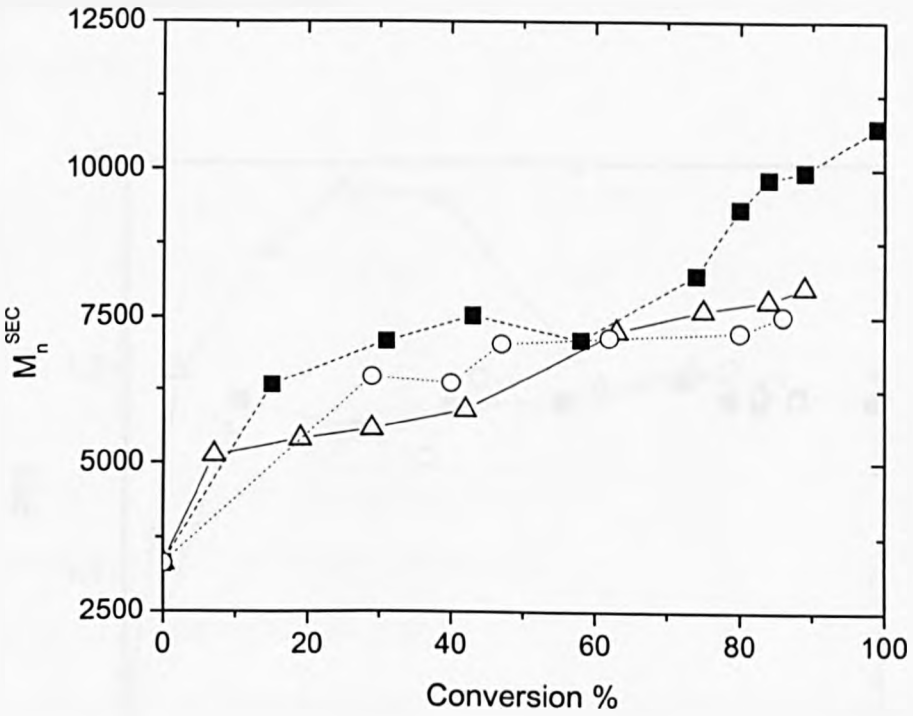

Figure 2.13: Evolution of the molecular weight as function of conversion for the polymerisation of MMA on MeOPEG-I_{113} 90°C(Δ), 70°C (■) and 50°C(O).

The reason for this can be seen in the MWD traces appearing bimodal up to a conversion at approximately 60%, then became monomodal. At low conversions, the

M_n is lowered by the presence of low molecular weight species, while at high conversions, the broadening of the MWD is decreased, giving M_n closer to that predicted. Indeed the PDI was high up to 60% conversion, before decreasing at higher conversions (see Figure 2.14).

In the case of the two lower temperature reactions, the macroinitiator trace could still be observed up to 60% conversion, but the reactions being slower, this did not seem to influence the kinetics, or MWD.

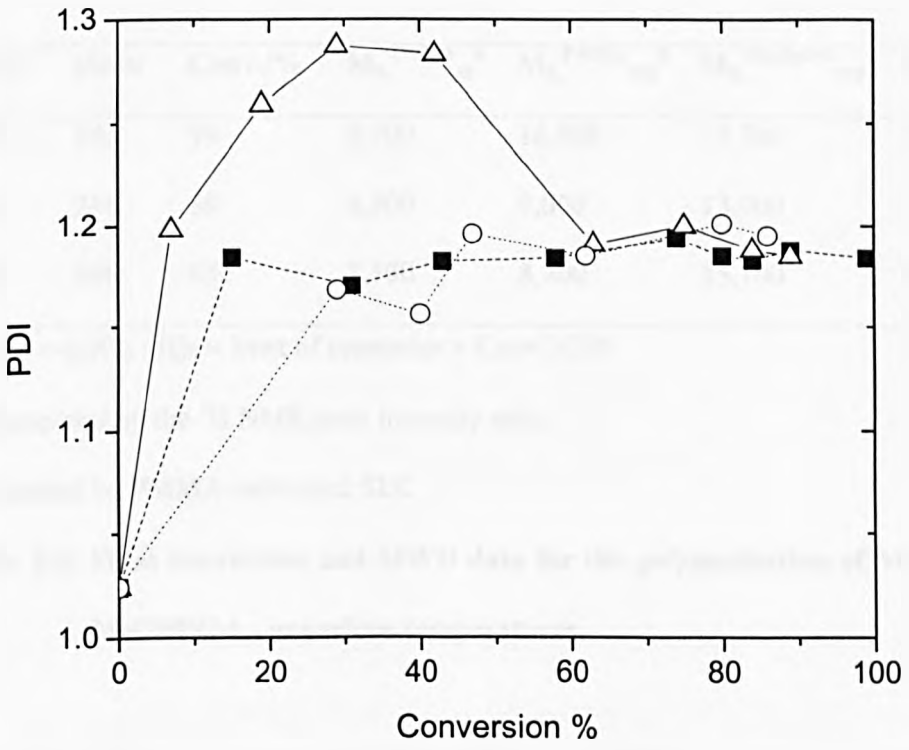

Figure 2.14: Evolution of the PDI as function of conversion for the polymerisation of MMA on MeOPEG-I_{113} 90°C (Δ), 70°C (■) and 50°C(O).

Table 2.2 gives a summary of the final products properties from these reactions. It is noted that the theoretical M_n and the M_n calculated by ^1H NMR spectroscopy are the molecular weight of the PMMA block only. However, the SEC analysis gives the M_n and PDI of the whole block copolymer. One will notice the difference between the SEC molecular weights and PDI of the final product and of the last reaction sample. This can be explained by the loss of small molecular weight species during the purification process, leading to a higher average molecular weight and lower polydispersity.

T/°C	t/min	Conv./%	$M_{n,\ th}^{PMMA\ a}$	$M_{n,\ exp}^{PMMA\ b}$	$M_{n,\ exp}^{copolymer\ c}$	PDI[c]
90	183	99	9,900	16,900	13,700	1.14
70	216	89	8,900	9,000	13,900	1.11
50	808	83	8,300	8,700	15,100	1.12

[a] $M_{n,\ th} = ([M]_0 / [I]_0 \times$ Mwt of monomer $\times$ Conv.$)/100$

[b] Determined by the ^1H NMR peak intensity ratio.

[c] Estimated by PMMA-calibrated SEC

Table 2.2: Final conversion and MWD data for the polymerisation of MMA on MeOPEG-I_{45} at various temperatures.

The polymerisation of MMA using MeOPEG-I_{45} as initiator at 70°C and 50°C gave an apparent well-defined copolymer, of low PDI.

In the case of MeOPEG-I_{113}, the molecular weight showed a dramatic increase toward high conversion for the two highest temperatures (see Figure 2.15). As seen

previously, this could be justified by the presence of non-reacted macroinitiator up to 90% and fast growing chains, giving a broad MWD, with lowering of the M_n. However, at lower temperature (50°C) and slow reaction, the non-reacted initiators do not influence to the same extent M_n.

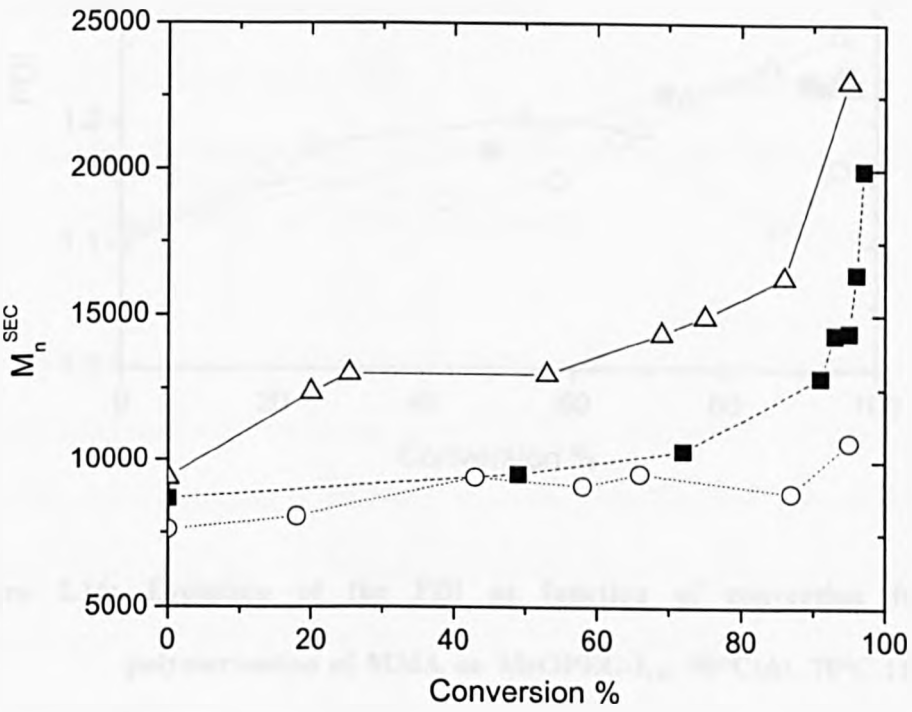

Figure 2.15: Evolution of the molecular weight as function of conversion for the polymerisation of MMA on MeOPEG-I_{113} 90°C(Δ), 70°C (■) and 50°C(O).

The PDI of the reactions at 70°C and 90°C increased slowly throughout the course of polymerisation, while it stayed almost constant at 50°C. The polydispersity of almost all the various polymers stayed under 1.3 during reaction (Figure 2.16).

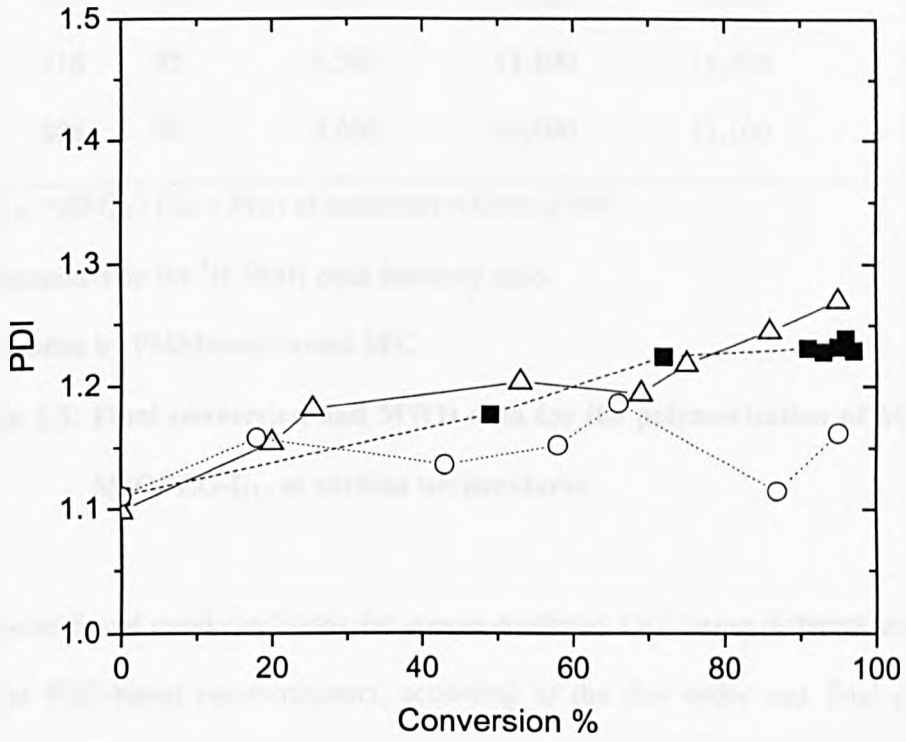

Figure 2.16: Evolution of the PDI as function of conversion for the polymerisation of MMA on MeOPEG-I_{113} 90°C(Δ), 70°C (■) and 50°C(O).

Table 2.3 summarises the properties of the final products. The two experiments at 90°C and 70°C gave products with molecular weights different than expected while the experiment at 50°C led to a block copolymer close to the expected value. The polydispersity and molecular weight of the purified product analysed by SEC was lower than the final reaction sample.

T/°C	t/min	Conv./%	$M_{n,th}^{PMMA}$ [a]	$M_{n,exp}^{PMMA}$ [b]	$M_{n,exp}^{copolymer}$ [c]	PDI[c]
90	183	95	9,500	12,300	15,200	1.22
70	216	95	9,500	13,300	15,300	1.13
50	808	96	9,600	10,200	17,100	1.18

[a] $M_{n,th} = ([M]_0 / [I]_0 \times \text{Mwt of monomer} \times \text{Conv.})/100$

[b] Determined by the ^1H NMR peak intensity ratio.

[c] Estimated by PMMA-calibrated SEC

Table 2.3: Final conversion and MWD data for the polymerisation of MMA on MeOPEG-I_{113} at various temperatures

We have found good conditions for copper-mediated LRP using different molecular weight PEG-based macroinitiators, according to the first order and final products properties (M_n being close to the theory with low PDI). The SEC traces recorded at different conversion, and for various temperature polymerisations showed however bimodal peaks up to high conversion (see for example Figure 2.17). The high molecular weight peak is assigned to the growing polymer while the smaller molecular weight one was the non-reacted macro-initiator trace. This was evidence that part of MeOPEG-I in solution did not react with the monomers, or reacted later in the reaction. As the SEC analysis can not quantify the amount of non-reacted macroinitiator, in order to understand how apparent control over the polymerisations could be obtained despite the slow initiation, online ^1H NMR experiment data were considered.

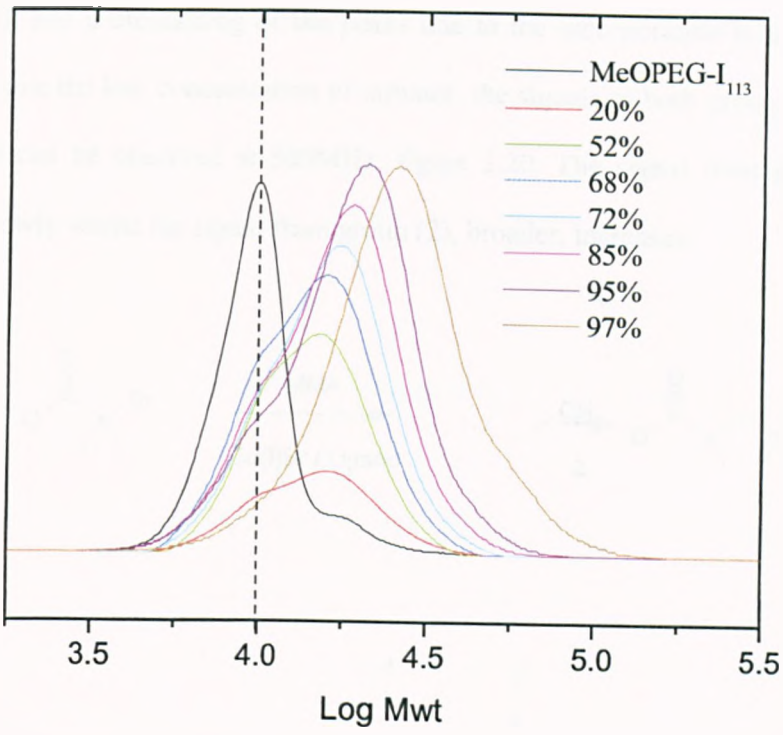

Figure 2.17: Evolution of the MWD for the polymerisation of MMA on MeOPEG-I_{113} during the reaction.

2.3.4. Initiatior efficiency.

PEG based macroinitiators have been previously reported to exhibit low initiation efficiency for the bulk polymerisation of MMA, but are reported to be efficient for the bulk polymerisation of ter-butyl acrylate.[177]

The actual initiation efficiency can be followed by ^{1}H NMR. On addition of monomers, group (1) from the initiator was transformed in (2) at the junction points of the two blocks in the block copolymer (Figure 2.18). In ^{1}H NMR, this is observed by

the shift of the triplet signal toward high shield (as the bromine atom is replaced by a carbon atom), and a broadening of the peaks due to the incorporation to a polymer chain[177]. Despite the low concentration of initiator, the signals of both groups are well resolved and can be observed at 500MHz, figure 2.20. The signal from group (1) disappears slowly whilst the signal from group (2), broader, increases.

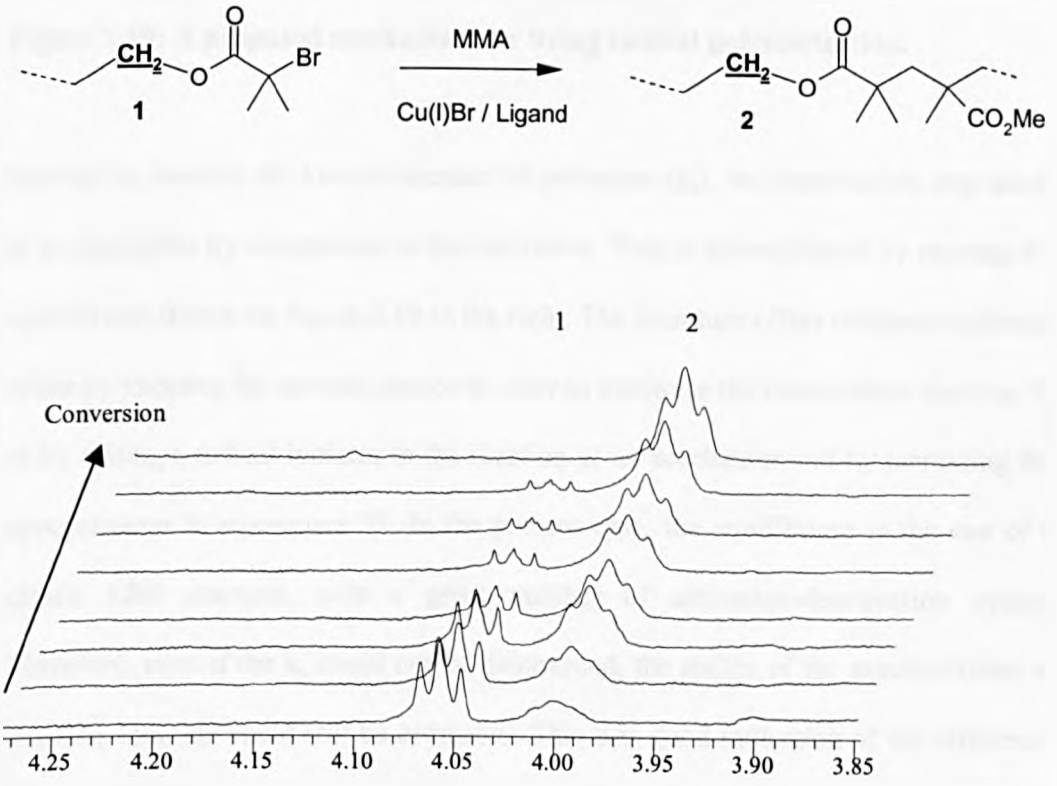

Figure 2.18: ^{1}H NMR spectra of the region of group 1 and 2 during the polymerisation of MMA with PEG-based macroinitiator followed by ^{1}H NMR spectroscopy.

This allows the measurement of the loss the initiator. As Figure 2.19 shows, the activation step can be summarised in the equilibrium between Cu(I) and Cu(II).

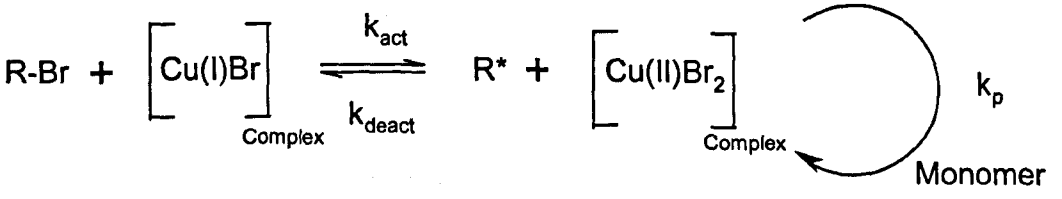

Figure 2.19: A proposed mechanism for living radical polymerisation.

In order to measure the kinetic constant of activation (k_a), the deactivation step needs to be negligible by comparison to the activation. This is accomplished by moving the equilibrium shown on Figure 2.19 to the right. The literature offers different methods, either by trapping the reacted species in order to minimise the deactivation reaction [182] or by adding a radical initiator to the reaction as an accelerator and by increasing the concentration in monomers [183]. In the present case, the equilibrium is the one of a classic LRP reaction, with a great number of activation-deactivation cycles. Therefore, even if the k_a could not be determined, the ability of the macroinitiator to loose its bromide could still be estimated. This was good indication of the efficiency of a macroinitiator. In the case of activation faster than propagation, all the chains would grow in parallel. If competition between activation and the propagation, some initiators would stay 'non-initiated' while other chains would be growing, leading to a bimodal molecular weight distribution.

In order to study the influence of the macroinitiators molecular weight, a graph of the conversion of non-reacted initiator into reacted initiator versus conversion of

monomer was plotted. This will be referred as 'initiator efficiency' in the remains of the study. In an ideal living polymerisation, the initiator efficiency should be 100% as soon as the polymerisation starts. In the case of PEG-based macroinitiator, the initiator efficiency appeared to be very low.

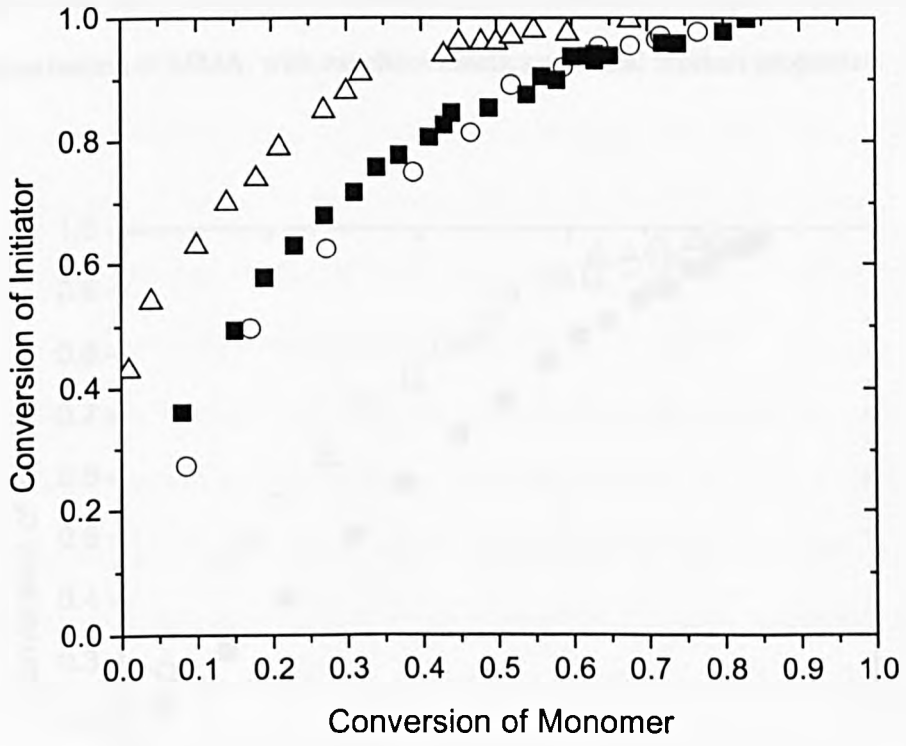

Figure 2.20: Evolution of the conversion of initiator in reacted initiator as a function of the conversion of monomer for the polymerisation of MMA with MeOPEG-I_{113} (O), MeOPEG-I_{45} (■) and on MeOPEG-I_{12} (Δ) at 90°C in toluene-d_8.

Figure 2.20 shows the evolution of the initiation for each initiator at 90°C. The efficiencies of the two highest molecular weight initiators were similar, whilst

MeOPEG-I_{12} was slightly better throughout the reaction. All of the initiators had reacted after a conversion of 60% for MeOPEG-I_{12}, while MeOPEG-I_{113} and MeOPEG-I_{45} needed 80% conversion. In the case of MeOPEG-I_{12}, an almost instantaneous initiation was obtained up to 40% of the initiator, and then the process was slowed down.

Despite this slow initiation, MeOPEG-I_{12} was efficient enough to perform living polymerisation of MMA, with excellent kinetics and final product properties.

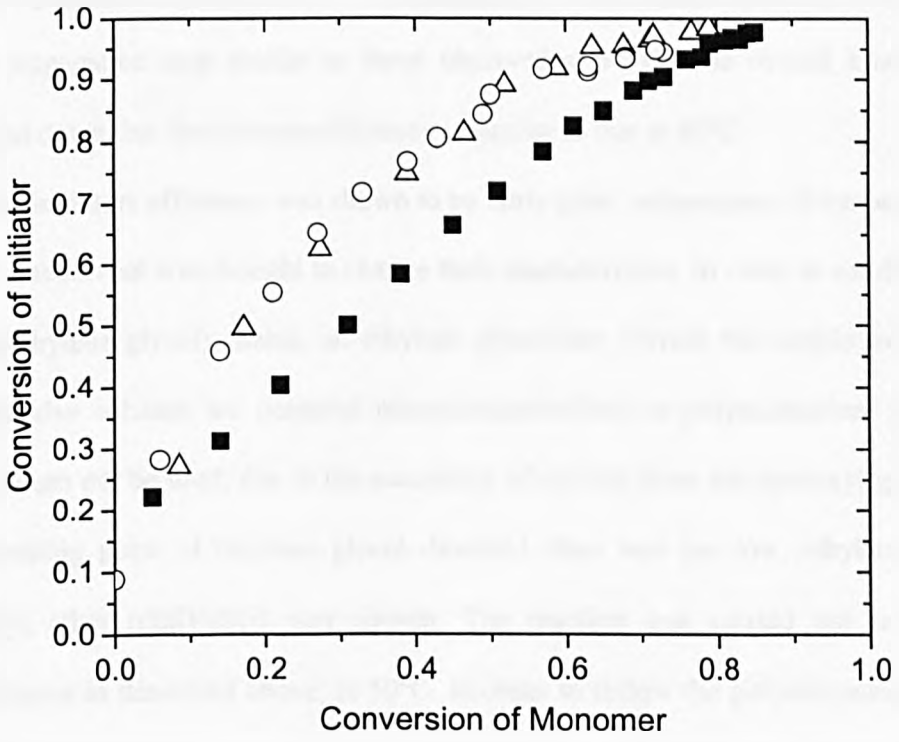

Figure 2.21: Evolution of the conversion of initiator as a function of the conversion of monomer for the polymerisation of MMA on MeOPEG-I_{113} at 90°C(Δ), 70°C (■) and 50°C(O).

MeOPEG-I_{113}, was the least efficient initiator, with 100% of initiator activated at 80% conversion at best (see Figure 2.21). Furthermore, experiments at 90°C and 50°C showed similar initiator efficiency, while it decreased at 70°C. At 90°C, the activation and propagation steps were very fast (as indicated by the kinetic plot, figure 2.10), but propagation was faster than initiation. Some initiators start chains, whilst the remains are not reacted. At 70°C, activation is more slown down than propagation. This results in chains propagating too fast, leading to a high conversion in monomer whilst some initiators have still not reacted. Full initiation is observed after 80% conversion. When the temperature is lowered to 50°C, propagation is more affected, leading to activation and propagation step similar to those observed at 90°C. The overall kinetics are slowed down, but the initiator efficiency is similar to that at 90°C.

As the initiators efficiency was shown to be fairly poor, independent of temperature, a different solvent was thought to change their characteristics. In order to solubilise the poly(ethylene glycol) chains, an ethylene glycol-like solvent was employed, which might also enhance the potential macroinitiator-effect on polymerisation. Ethylene glycol can not be used, due to the possibility of transfer from the hydroxyl group. As the boiling point of ethylene glycol dimethyl ether was too low, ethylene glycol diethyl ether ($(EtO)_2EG$) was chosen. The reaction was carried out in similar conditions as described above, at 50°C. In order to follow the polymerisation by ^1H NMR spectroscopy, a small amount of toluene-d_8 was added in the solution (10% of the solvent), figure 2.22.

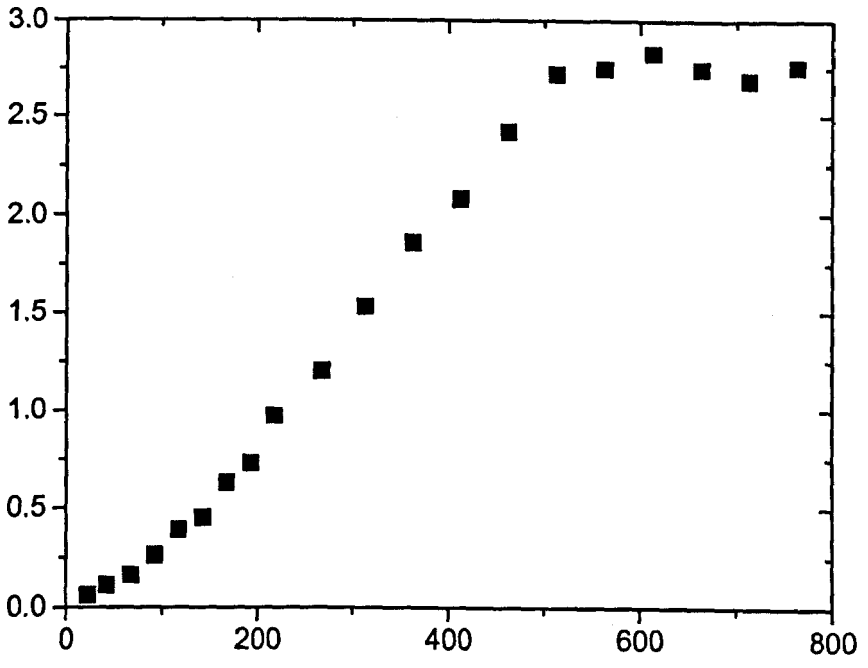

Figure 2.22: Kinetic plot for the polymerisation of MMA using $MeOPEG_{113}$ as initiator at 50°C in 90% $(EtO)_2EG$ / 10% toluene-d_8, followed by ^1H NMR spectroscopy.

The first order plot deviates significantly from linearity. An increase in $k_p[P_n^*]$ is observed over the first three hours of reaction. This can be explained either by an increase in the concentration of the active species or by an increase in k_p, or both. At high conversion (94%), the reaction slows down, accounted to the glassy effect of the solution. Furthermore, the reaction is faster than when using toluene as solvent; 70% conversion was reached in 5 hours instead of 12 hours in toluene.

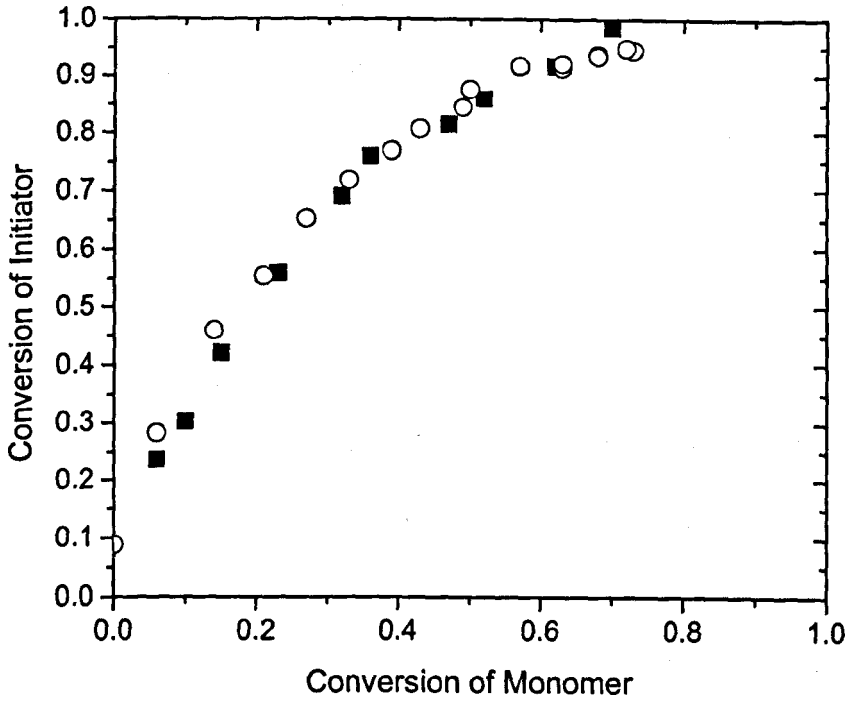

Figure 2.23: Evolution of the conversion of initiator in reacted initiator as function of the conversion of monomer for the polymerisation of MMA on MeOPEG-I_{113} at 50°C in toluene-d_8 (O) and in 90% $(EtO)_2EG$ / 10% toluene-d_8 (■)

The initiator efficiency (Figure 2.23) is similar to that at 50°C in toluene. This leads us to conclude that (i) the solvent has little effect on the initiator efficiency and (ii) the concentration of the active species increases during the reaction. When comparing to the same polymerisation in toluene, this could imply that k_p undertakes also some changes.

In conclusion, it has been demonstrated that PEG-based macroinitiators are relatively slow initiators for copper mediated living radical polymerisation. Temperature or solvent have little effects, but the chain length of the macroinitiator influences the initiator efficiency, shorter chain molecules being faster initiators than longer chain macromolecules.

2.3.5. SEC analysis of the final products.

As poly(ethylene glycol) based initiators are relatively slow initiators for living polymerisation, it was surprising to observe linear plots with narrow polydispersity final products.

As the SEC gave the molecular weight of the overall product, copolymer of PMMA and MeOPEG-I, one could wonder the influence of the low PDI of the macroinitiator (see table 2.1) on the polydispersity of the block copolymer.

As described in appendix 3, considering a classic free radical polymerisation of MMA, the MWD expected would follow a Schulz-Flory distribution, and give a polydispersity of 1.99. Considering the use of a macroinitiator of narrow polydispersity and high molecular weight, and assuming that the block copolymer will be analysed as the summation of the molecular weights of macroinitiator and PMMA block, we can estimate the effect of the two extreme molecular weight macroinitiators. Both number and weight average molecular weights will be increased by the SEC molecular weight of the macro-initiator (respectively 1,000 g/mol and 9,000 g/mol for MeOPEG-I_{12} and MeOPEG-I_{113}). This difference will dramatically affect the PDI analysis of the SEC, giving a value as low as 1.52 (table 2.4) for the higher molecular weight initiator. This is evidence that SEC analyses need to be

handed with care. However, in the case of a shorter initiator chain, the influence is less important.

	M_n	M_w	PDI
Classic Initiator (2EIBr)	10,012	19,922	1.99
MeOPEG-I_{12}	11,012	20,922	1.90
MeOPEG-I_{113}	19,012	28,922	1.52

Table 2.4: Summary of the different average molecular weights and polydispersity.

2.3.6. Gradient polymer elution chromatography (GPEC) analysis of the final products.

In order to demonstrate the broad polydispersity of the product, structural analysis in regard to the final polymer molecule were undertaken. This was also an opportunity to prove that the product was a copolymer, and not a blend of PMMA and MeOPEG. A methodology that has proved effective in analysing the chemical composition of polymers, is Gradient Polymer Elution Chromatography (GPEC).[184,185] While analysing polymers by separating them by size with SEC methods is common in polymer synthesis, the separation of polymers on the basis of chemical composition is a technique that is more rarely employed. The GPEC system works on the basis of the differing solubilities of the different monomers comprising the co-polymers or mixture of polymers. The polymer is dissolved in a good solvent and injected into the GPEC system where the eluent is initially a non-solvent for the polymer. This causes the polymer to precipitate at the column head. The ratio of solvent to non-solvent is

gradually increased at a constant rate until the eluent is purely comprised of the good solvent. At some stage during the elution the polymer is re-dissolved at a solvent mixture determined by the chemical composition and also the molecular weight of the polymer. The solvents for GPEC must be chosen carefully to allow good separation of the polymers while ensuring that the solvents remain miscible to allow good mixing. The solvent system employed in this work was a water / THF gradient. It was reasoned that any free unreacted macroinitiator would elute in pure water, any PMMA homopolymer in pure THF and a block copolymer at some intermediate time.

Figure 2.24 shows the summary of the data when using MeOPEG-I_{113} initiator for MMA polymerisation. PMMA prepared by copper mediated LRP (M_n = 10,900 ; PDI = 1.15) was used as reference and eluted in pure THF. The macroinitiator eluted in a mixture of water/THF in four different signals. By comparing these signals to the trace of $MeOPEG_{113}$ (before esterification), figure 2.24, it did not seem that any starting material was still present in the macroinitiator sample. These signals were then attributed to four major MeOPEG chains, probably differing on their size.

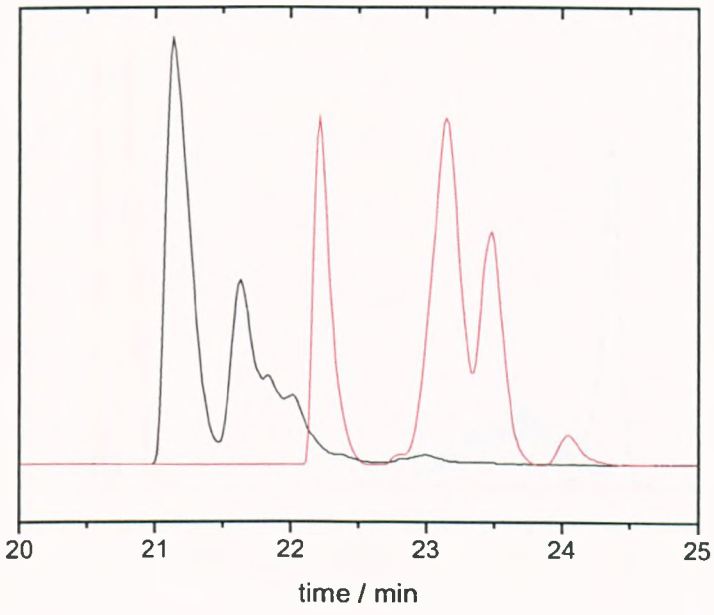

Figure 2.24: GPEC signal from $MeOPEG_{113}$ (black) and $MeOPEG\text{-}I_{113}$ (red).

The polymerisation product was then injected, which eluted between PMMA and $MeOPEG\text{-}I_{113}$. Two peaks were still observed at the MeOPEG elution time, certainly due to 'dead' chains that could not undertake polymerisation. The product signal is a multiplet, eluting at a time close to the PMMA. This was evidence that (i) the product was indeed a block copolymer, as it eluted between the two reference peaks, and that (ii) it was actually a mix of different sizes block copolymers.

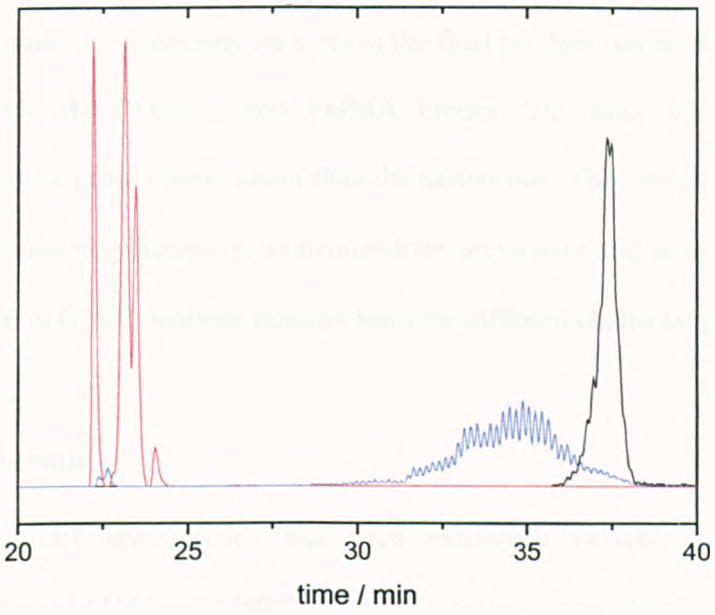

Figure 2.25: GPEC traces for MeOPEG-I_{113} (red), PMMA standard (black) and the copolymer (blue).

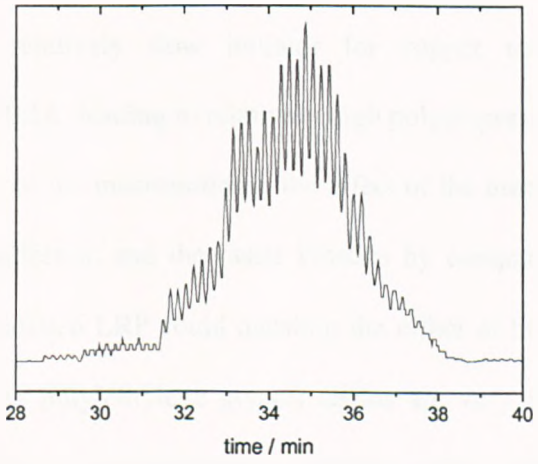

Figure 2.26: Expansion of the GPEC trace of the block copolymer $MeOPEG_{113}$–*b*-PMMA.

This distribution of macromolecule sizes in the final product comes from the different sizes of both MeOPEG-I_{113} and PMMA blocks. The later initiated MeOPEG molecules would grow shorter chain than the earlier one. This would result in a final product of broad polydispersity, as demonstrate previously and would give different elution signal in GPEC analysis, coming from the different chains length.

2.4. Conclusion.

Online ^{1}H NMR spectroscopy has been extremely valuable in studying the polymerisation of MMA on MeOPEG-based macroinitiators. While the kinetic plot observed seem to be the one of a typical living polymerisation, SEC analysis showed the presence of non-reacted initiator during the reaction. Analysis of the ^{1}H NMR spectra recorded during the reaction, has been quantified to determine optimum conditions for living polymerisation. Furthermore studies by GPEC confirmed that MeOPEG was a relatively slow initiator for copper mediated living radical polymerisation of MMA, leading to relatively high polydispersity block copolymers.

The poor efficiency of the macroinitiator, the effect of the macroinitiator chain length on the catalyst equilibrium and the faster kinetics by comparison to a more classic initiators copper-mediated LRP could question the effect of the macroinitiator on the catalyst complex. As poly(ethylene glycol) chains are very flexible, the active site could be trapped by the macroinitiator structure, away from the catalyst or the monomer. This effect would be even more important for longer chain initiators. When the catalyst reaches the active site, it finds itself trapped in the polymer chain. One can even imagine the co-ordination of the copper to the macroinitiator chain. This would

explain the difficulty of the monomer to react with the initiator, due to the steric hindrance. We observed indeed the impact of initiator chain length, but noticed the absence of effect of temperature and solvent.

If such co-ordination occurred, the equilibrium between Cu(I) and Cu(II) would be disturbed, leading to original kinetics, as previously observed (change of rate during the polymerisation and higher rate than usually observed, both depending on the chain length of the macroinitiator).

The aim of this chapter was to describe the synthesis of PEG-b-PMMA copolymers. Thus, this potential co-ordination effect, as well as the original kinetics of the reactions will be discussed in chapter 4.

The final block copolymer showed however a hydrophilic group of well known size, and a more or less well-defined hydrophobic block. A range of different products with different chain lengths of PMMA was then synthesised and purified in order to test their amphiphilic properties (see chapter 5).

2.5. Supplementary information.

Experiment	$MeOPEG_X$	$M_n^{PMMA\ a}$	M_n^{GPC} (PDI) [b]
sp34	12	1,870	3,700 (1.17)
sp31	12	3,400	8,160 (1.07)
sp40	12	3,600	6,470 (1.10)
sp199	12	9,500	10,500 (1.98)
sp28	12	11,100	11,400 (1.08)

sp44	45	4,850	9,150 (1.10)
sp38	45	4,970	12,160 (1.11)
sp43	45	5,970	9,050 (1.10)
Sp204	45	11,000	14,050 (1.08)
sp29	113	6,400	24,380 (1.27)
sp45	113	9,400	20,800 (1.21)
Sp200	113	11,050	19,080 (1.20)
sp39	113	15,200	29,600 (1.19)

[a] Determined by the ^{1}H NMR peak intensity ratio.

[b] Estimated by PMMA-calibrated SEC

Chapter 3

Amphiphilic block copolymers synthesised by LRP with poly(ethylene glycol)-based macromonomers.

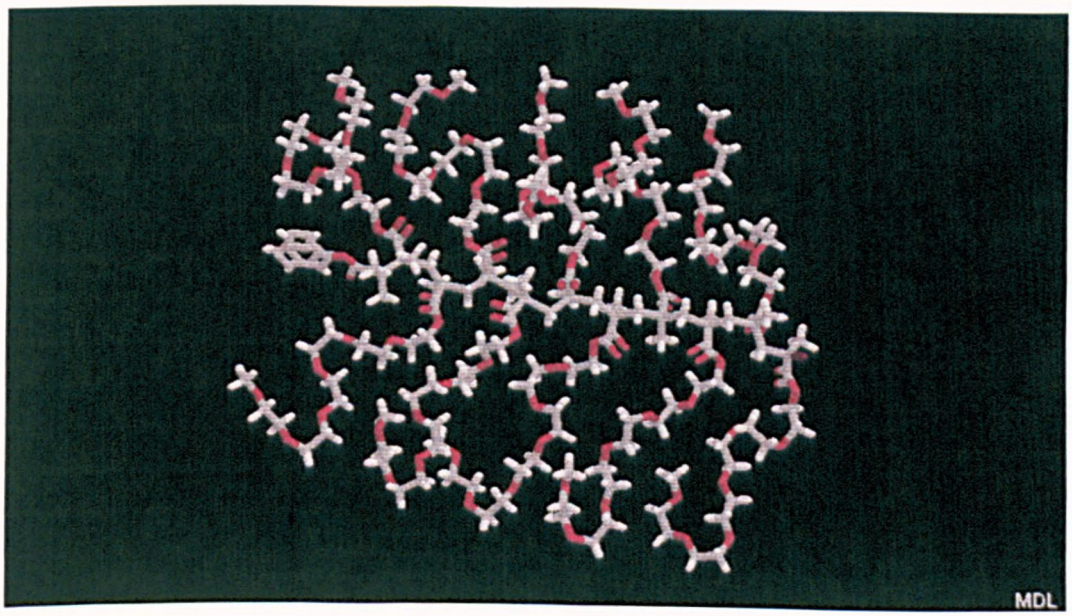

3D Schematic of poly(MeOPEG-MA) initiated by phenyl-2-bromoisobutyrate.

As MeOPEG based macroinitiators show poor efficiency for the synthesis of block copolymers of well-determined structure via copper mediated living radical polymerisation, a different approach was considered. Still aiming to introduce PEG based polymers in amphiphilic block copolymers, MeOPEG was considered as a potential methacrylate monomer (poly(ethylene glycol) methyl ether methacrylate, MeOPEG-MA) in living radical polymerisation. If successful, such polymerisation using hydrophobic initiators should lead to a final product showing amphiphilic properties.

3.1. Study of a new hydrophilic PEG-based macromonomer.

3.1.1. Introduction.

Water-soluble polymers are so widely used that novel methods for their synthesis are of considerable interest. In order to be water-soluble, a polymer needs to contain functionalities which hydrogen-bond in water. In the case of poly(ethylene glycol) or poly(ethylene oxide), this is accomplished by the presence of polar ethylene oxide repeat units. Poly(ethylene oxide) (PEO) containing polymers[186,187] are used in many diverse applications, including surfactants, e.g. polystyrene-*b*-poly(ethylene oxide)[188], poly(methyl methacrylate)-*b*-poly(ethylene oxide),[189] and poly(soaps).[190]

An interesting utilisation of poly(ethylene oxide)s is in *so-called* polymer brushes[186], which are characterised by a high branch-density along a 'backbone', *e.g.* solid surfaces *via* covalent bonding or physisorption, or a polymer chain. The conventional route towards homogeneous polymer brushes is homopolymerisation of macromonomers, to give poly(macromonomers). Such poly(macromonomers) are of

increasing interest and are commonly synthesised via free-radical polymerization.[191] This type of polymer brush is distinct from the more widely demonstrated graft-copolymers, which have a lower branch-density, obtained via copolymerisation of macromonomers commonly based on acrylic esters or styrene, with more conventional vinylic monomers.[192] Formation of poly(macromonomers) is complicated by the intrinsic low concentration of polymerisable groups in the system and a possible reduction in the rate of monomer addition as a result of steric hindrance. Thus, low degrees of polymerisation (DP) are generally obtained. However, Tsukahara *et al.* [193] have reported high DP polymer brushes synthesised by radical polymerisation. Polymers incorporating oxyethylene units have been previously prepared using nitroxide-mediated living radical polymerisation[194] and transition-metal mediated polymerisation to produce dendrimer-like polymers star block and amphiphilic copolymers.[195] Homopolymerisation of vinylether-based PEO derived macro-initiators have also been used to prepare block copolymers.[196,197]

This chapter describes the use of copper mediated living radical polymerisation to achieve low molecular weight homopolymers, using a (i) low molecular weight initiator to investigate the actual polymerisation, then (ii) various macro-initiators to synthesise different amphiphilic block copolymers.

3.1.2. Polymerisation of (PEG)-MA in toluene.

Living radical polymerisation of poly(ethylene glycol) methacrylate (PEG-MA) was carried out using copper(I)bromide / *N*-(*n*-propyl)-2-pyridylmethanimine and phenyl-2-bromoisobutyrate as initiator, in toluene solution over a range of temperatures. The final product appeared to be a cross-linked polymer gel, insoluble in all solvents

making analysis impossible. A potential explanation for this result is the presence of low amount of di-functional macromonomer present as an impurity or possibly formed by trans-esterification, or chain transfer reactions to polymer or monomer during the polymerisation, leading to cross-linking.[198] An alternative explanation is the possible complexation of the hydroxyl group from the polymer pendant chains with the copper (II) species[199]. This would create a network between the graft polymer and copper(II) present in solution (see Figure 3.1).

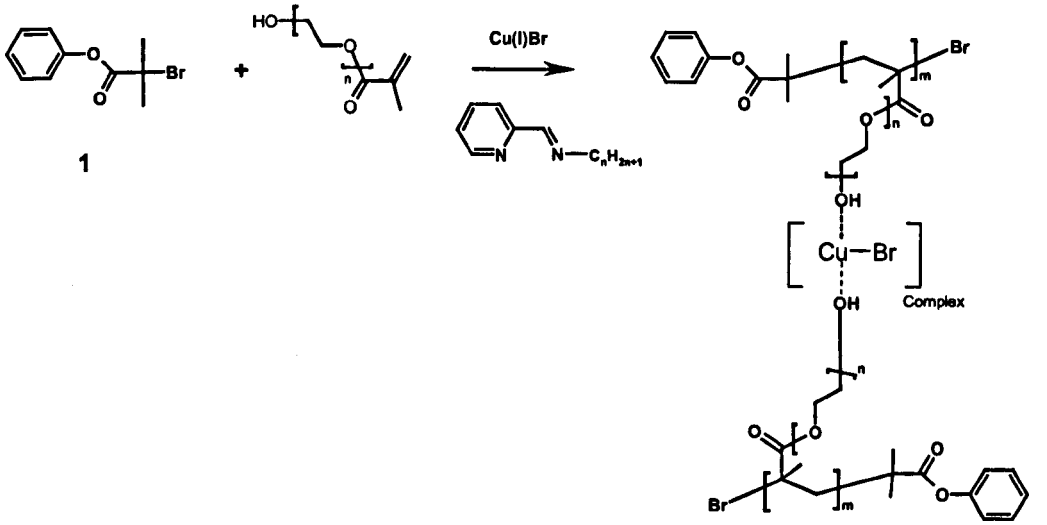

Figure 3.1: Proposed mechanism of the copper-mediated polymerisation of PEG-MA.

3.1.3. Polymerisation of poly(ethylene glycol) methyl ether methacrylate MeOPEG-MA in toluene.

As PEG-based macromonomers proved difficult to polymerise without protection of the terminal hydroxyl group, polymerisation of poly(ethylene glycol) methyl ether methacrylate (MeOPEG-MA) was carried out.

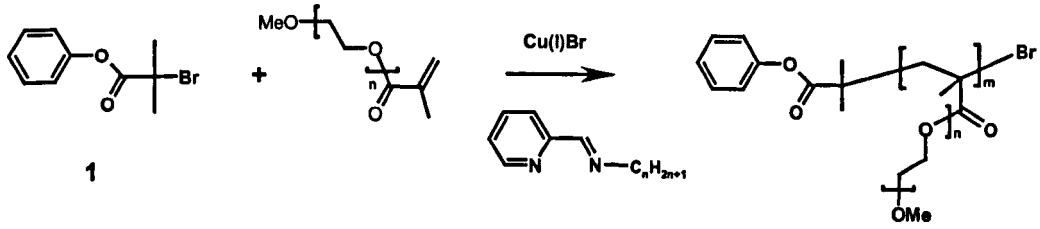

Figure 3.2: Copper mediated polymerisation of MeOPEG-MA.

Polymerisation of MeO(PEG)-MA was carried out with copper(I)bromide/*N*-(*n*-propyl)-2-pyridylmethanimine (*n*-Pr-L) using phenyl-2-bromoisobutyrate, **(1)**, as initiator (Figure 3.2) in toluene solution over a range of temperatures. Compound **(1)** was chosen as initiator so as to enable the number average molar mass, M_n, of the final polymer product to be determined from ^{1}H-NMR. Integration of the oxyethylene proton resonances, 3.5 - 4.5 ppm, and the aromatic resonances, 6.9 - 7.5 ppm, were used for the calculation of M_n. Polymerisations were carried out at various temperatures using typical living radical polymerisation conditions, as used for alkyl methacrylates with these catalysts (Chapter 2), with initial molar ratios = $[M]_0/[I]_0/[Cu(I)Br]_0/[n\text{-Pr-L}]_0 = 10/1/1/2$ (Figure 3.3).

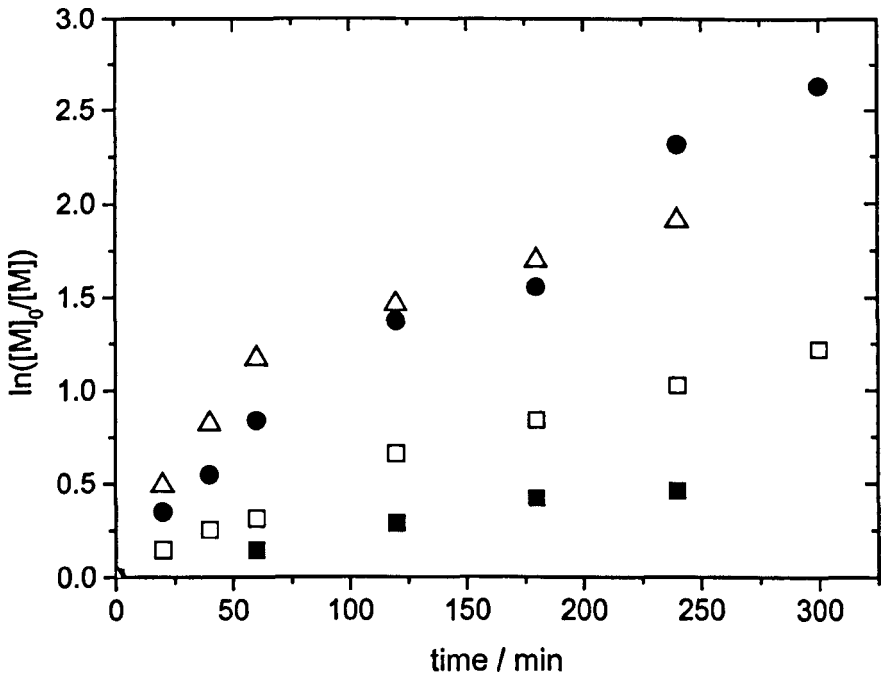

Figure 3.3: Kinetic data for the polymerization of MeO(PEG)-MA, $[M]_0/[I]_0/[Cu(I)Br]_0/[n\text{-Pr-L}]_0$ = 10/1/1/2 in toluene at 25°C (■), 40°C (□), 60°C (●) and 90°C (Δ), reaction sampled with time.

Observed rates of polymerisation were unusually high, with polymerisation at 90 °C resulting in a conversion greater than 70% within 1 h (as measured by ^{1}H NMR). Moreover, polymerisation proceeded to 81% conversion after 15 hours even at 25°C. It is apparent from figure 3.3 that at higher temperatures, 90 °C, the first order plots show significant curvature, prompting us to investigate these reactions in more detail.

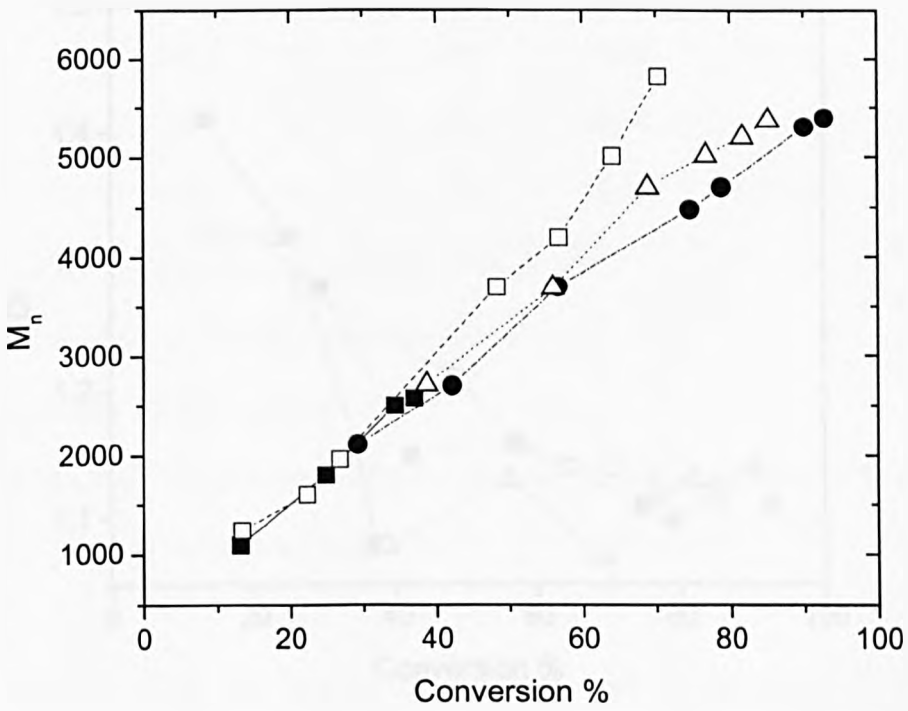

Figure 3.4: Evolution of molecular weight distribution for the LRP of MeO(PEG)-MA in toluene (50% v/v) at 25°C (■), 40°C (□), 60°C (●) and 90°C (Δ) initiated by α-bromo-isobutyric acid phenyl ester and mediated by Cu(I)Br / *N*-(*n*-octyl)-2-pyridylmethanimine.

Evolution of M_n was followed by SEC analysis, figure 3.4.

While the polydispersity stayed low during the whole reaction at 90°C, a decrease of value with the conversion was observed for the other temperatures (Figure 3.5). The final product showed, however, a low PDI in all cases (< 1.20).

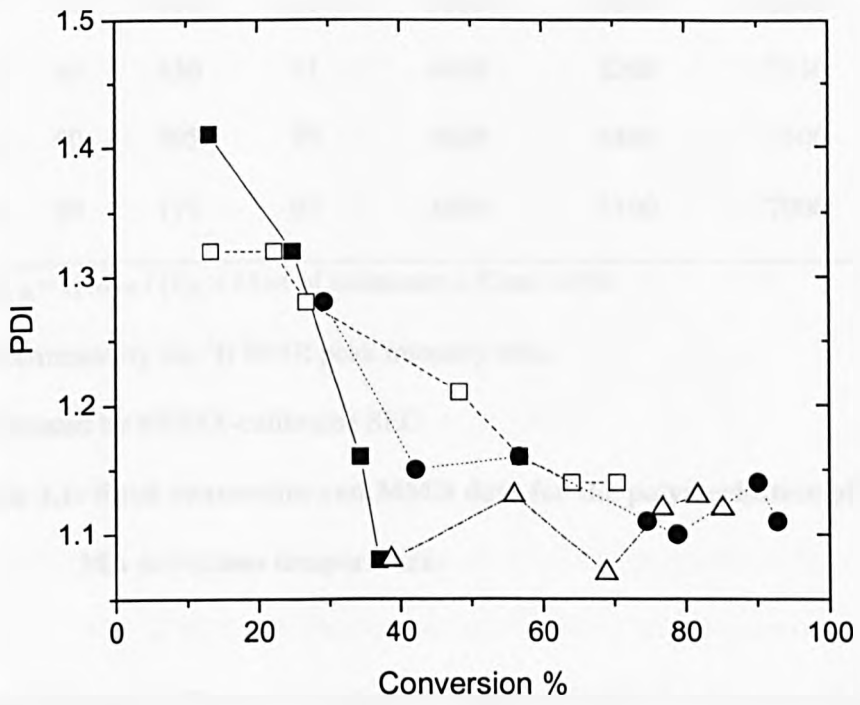

Figure 3.5: Evolution of polydispersity for the LRP of MeOPEG-MA in toluene (50% v/v) at 25°C(■), 40°C (□), 60°C (●) and 90°C (Δ) initiated by α-bromo-isobutyric acid phenyl ester and mediated by Cu(I)Br / *N*-(*n*-octyl)-2-pyridylmethanimine.

The final properties of the products from these reactions are summarised in Table 3.1; for full data sets, see supplementary information.

	T/ °C	t/ min	Conv./%	$M_{n,th}$ [a]	$M_{n,exp}$ [b]	$M_{n,exp}$ [c]	PDI[c]
A	25	910	81	3900	4600	6000	1.16
B	40	430	91	4400	5200	7530	1.12
C	60	595	99	4800	5400	7500	1.12
D	90	175	95	4600	5100	7000	1.14

[a] $M_{n,th} = ([M]_0 / [I]_0 \times \text{Mwt of monomer} \times \text{Conv.})/100$

[b] Determined by the ^{1}H NMR peak intensity ratio

[c] Estimated by PMMA-calibrated SEC

Table 3.1: Final conversion and MMD data for the polymerisation of MeOPEG-MA at various temperatures

The M_n from NMR was in excellent agreement with the theoretical M_n and the polydispersity remained below 1.20 in all cases. Moreover, experiments were carried out where the [monomer]/[initiator] ratio was varied at 60°C (Table 3.2, E-G). Overall these results show that the experimental values of the number average molar mass, $M_{n,exp}$, are in reasonable agreement with theoretical values, $M_{n,th}$, as would be expected for living polymerisation, and low polydispersity, < 1.2, was achieved in each case. Lowering the amount of catalyst with respect to the initiator (E, H and I, Table 3.2) reduced the rate of polymerisation. However, even at reduced levels of catalyst, efficient polymerisations ensued and narrow polydispersity polymers with M_n close to the theory were obtained.

	$[M]_0 / [I]_0 / [Cu(I)]_0$	t/min	Conv./%	$M_{n,th}$ [a]	$M_{n,exp}$ [b]	PDI [c]
E	10/1/1	360	93	4500	4200	1.11
F	10/0.5/1	360	89	8600	9600	1.10
G	10/0.25/1	360	80	15 600	16 000	1.09
H	10/1/0.5	360	68	3400	4000	1.11
I	10/1/0.25	360	44	2200	2400	1.13

[a] $M_{n,th} = ([M]_0 / [I]_0 \times$ Mwt of monomer $\times$ Conv.$)/100$

[b] Determined by the ^{1}H NMR peak intensity ratio

[c] Estimated by PMMA-calibrated SEC.

Table 3.2: Final conversion and MMD data for the polymerisation of MeOPEG-MA at 60 °C for different targeted degrees of polymerisation

3.1.4. Monitoring polymerisation using on-line ^{1}H NMR spectroscopy.

In order to investigate the polymerisation of MeOPEG-MA in more detail, reactions were followed *in-situ* by ^{1}H NMR, as described in chapter 2. Polymerisations were carried out at over a range of temperatures, 25, 40, 60 and 90°C in NMR tubes fitted with Young's taps, so as to maintain an inert atmosphere. In order to ensure a homogeneous polymerisation with both soluble copper(I) and copper(II) species *N*-(*n*-octyl)-2-pyridylmethanimine (*n*-Oct-L) was used as a ligand with a ratio of $[n\text{-Oct-L}]_0/[CuBr]_0 = 3$. Monomer conversion was measured by ^{1}H NMR, by integration of the vinyl resonances (6-5 ppm) relative to the combined values of the CH_2 α to *OC=O* from the monomer and polymer (4.1 ppm).

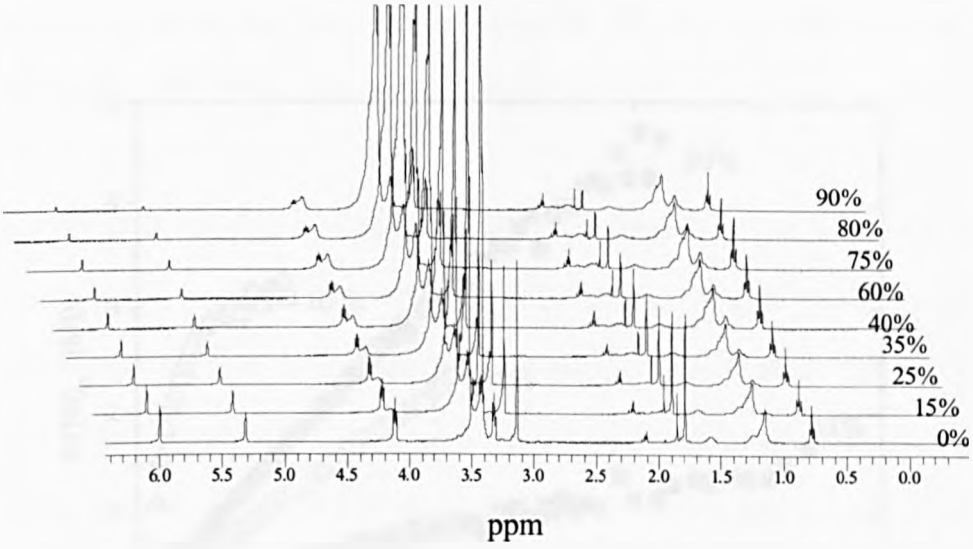

Figure 3.6: Partial ^{1}H NMR spectra at different stages of monomer conversion for the polymerization of MeOPEG-MA at 40°C.

Figure 3.6 shows a selection of the spectra obtained from the reaction carried out at 40°C. Analysis of the data results in $\ln([M]_0/[M])$ *vs.* time plots (Figure 3.7), which show that the concentration of active species remains relatively constant throughout polymerisation.

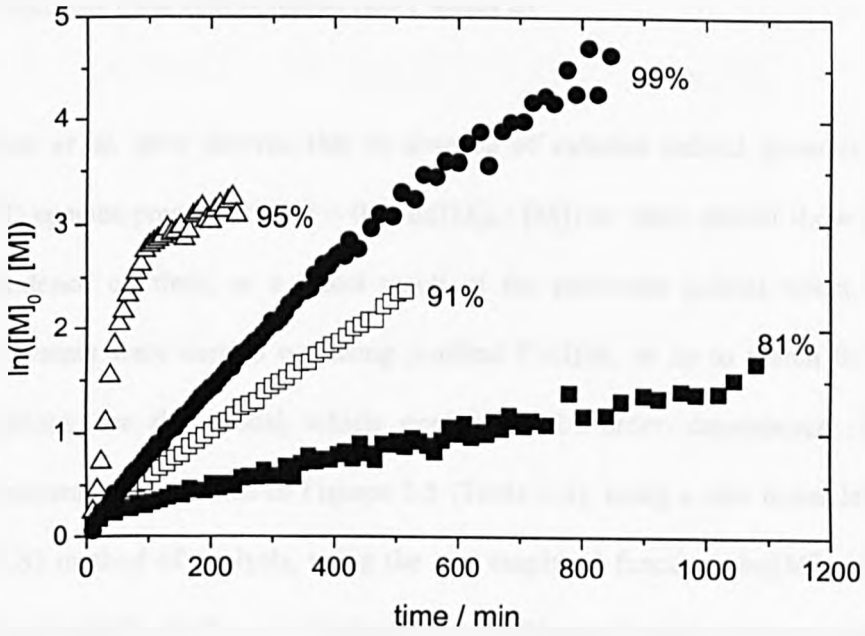

Figure 3.7: First order kinetic plots for the polymerization of MeO(PEG)MA in toluene at at 25°C (■), 40°C (□), 60°C (●) and 90°C (Δ) as monitored by ^{1}H NMR.

A striking observation from the polymerisation reactions discussed above is that the overall rate of polymerisation is very fast, when compared with polymerisation of *n*-alkyl methacrylate monomers under similar experimental conditions. For example, 90% conversion is reached after *ca.* 1 h at 90 °C for MeOPEG-MA whereas only about 35% conversion is achieved for methyl methacrylate under similar conditions.[181] Kinetic data available for the rate coefficients of propagation for *n*-alkyl methacrylates under conventional free-radical polymerisation do not show such large effects due to a change in monomer structure or due to solvent effects.[200] This unusual fast rate of

polymerisation, already observed when using MeOPEG as macroinitiator, stimulated us to investigate these effects further (see Chapter 4).

Fischer *et al.* have derived that in absence of external radical generation with no Cu(II) species present at time = 0 s, $\ln([M]_0 / [M])$ *vs.* time should show a 2/3-order dependence on time, as a direct result of the persistent radical effect.[201] All our experiments were carried out using purified Cu(I)Br, so as to match the boundary conditions for the model which predicts a 2/3-order dependence. Fitting the experimental data shown in Figures 3.5 (Table 3.4), using a non linear least squares (NLLS) method of analysis, using the two empirical functions $\ln([M]_0 / [M]) = a + bt^{2/3}$ and $\ln([M]_0 / [M]) = a + bt$ show an overall better fit with a linear dependence on time, the second expression. The empirical constant is used as it accounts for deviation from ideal conditions at the start of the reaction arising from normal experimental errors. The fit parameters, *a* and *b*, together with r^2 and the standard fit error are listed in table 3.3.

$\ln([M]_0/[M]) = a + bt$

T/ °C	a	b	r^2	Standard fit error
25	0.22445716	0.001255233	0.9736	0.0591
40	0.13511358	0.004311053	0.9989	0.0215
60	0.10216744	0.006543862	0.9978	0.0282
90[a]	-0.28717	0.0456458	0.9898	0.0770

$\ln([M]_0/[M]) = a + bt^{2/3}$

T/ °C	a	b	r^2	Standard fit error
25	0.019295006	0.013824547	0.9746	0.0580
40	-0.23409561	0.03834569	0.9884	0.0710
60	-0.26047872	0.049957482	0.9944	0.0449
90[a]	-0.8617699	0.20689868	0.9797	0.0770

[a] Data used up to $\ln([M]_0/[M]) = 2.10$.

Table 3.3: Fitting Results for the Data set for the polymerisation of MeOPEG-MA in toluene-d_8.

One of the restrictions of the current models is that they do not take into account chain-length dependence for the rate coefficients. Other points of criticism are that the nature of catalyst is only divided into two structures, a Cu(I) and Cu(II) compound, and that chain-growth is assumed to occur via conventional free-radical propagation. The current models are too oversimplified to describe transition-metal mediated living radical polymerisation and the kinetics are more complex and not well understood. It is also noted that even small deviations in starting materials e.g. a small amount of Cu(II) present at the start of the reaction will cause deviation from ideal kinetics. Thus it is difficult to make precise statements concerning the mechanism of the reaction from kinetic data alone.

A clear deviation from the expected monomer conversion profile is seen in Figure 3.5 at high conversion (> 90%) and high temperature. There are a number of possible explanations for this behaviour. Firstly, the enhanced viscosity of the reaction medium

results in the rate of macromonomer diffusion becoming important in the overall rate coefficient of polymerisation, k_p. This results in a suppression of values of $k_p[P_n^*]$. It has previously been reported that propagation in the metal-mediated living radical polymerisation of *iso*butyl vinyl ether methacrylate (PIBVE- MA) becomes diffusion controlled[196], Fukuda *et al.*, and also in conventional radical polymerisation systems with macromonomers of a variety of chemical structures.[200,202] This effect would be more likely to happen at elevated temperatures as a direct result of a higher activation energy for propagation for methacrylates (typically 20-28 kJ mol^{-1}) than for monomer diffusion (7-15 kJ mol^{-1}). An alternative explanation is the occurrence of termination reactions or certain chain transfer events, *e.g.* from monomer to polymer, which would generate secondary and primary carbon centred radicals and thus logically the corresponding brominated dormant analogues. This would result in a reduction of the concentration of activated species due to a lower rate coefficient of activation, and thus to a reduction in $k_p[P_n^*]$. An accurate estimation of the extent and relative contribution of these two explanations for the observed deviation in monomer conversion is, however, not known from the present data.

3.1.5. Conclusion

Copper-mediated LRP of MeOPEG-MA macromonomer was shown to be efficient in toluene, and led to well defined polymers, showing a hydrophobic methacrylate backbone and hydrophilic poly(ethylene glycol) pendent chains.

3.2. Copper-mediated living radical polymerisation of MeOPEG-MA macromonomers in aqueous solution.

3.2.1. Introduction.

Water has recently been successfully investigated for the copper mediated LRP of poly(ethylene glycol) based macromonomers.[203] It appears to be a solvent of choice for the synthesis of water-soluble polymers with well-defined structure. However, if 2,2'-bipyridine (bipy) was proved to be an efficient ligand in such conditions, the *N*-(*n*-alkyl)-2-pyridylmethanimine ligands used through this study did not appear to be an attractive option for water LRP. The synthesis of these ligands involves a condensation reaction with the evolution of water which could lead to a hydrolytically unstable ligand when water is present in the medium. As we show in part 4.2.3.1. that copper complexes based on this type of ligands are however surprisingly stable in water at ambient temperature, copper mediated LRP using the previous defined system was investigated at 25°C. Optimisation of the polymerisation conditions were carried out to give good control of the polymerisation by careful balancing of temperature, [Cu(I)] and [Cu(II)] yielding polymers of predictable molecular mass and narrow polydispersity.

3.2.2. Polymerisation of MeOPEG-MA in aqueous solution.

Poly(ethylene glycol) methyl ether methacrylate (MeOPEG-MA, **2**) was polymerised using 1,2-dihydroxypropane-3-oxy-2-bromoisobutyrate (**1**) as a water-soluble initiator in presence of copper(I) bromide and *N*-(*n*-propyl)-2-pyridylmethanimine (**3**) in water (homogeneous system).

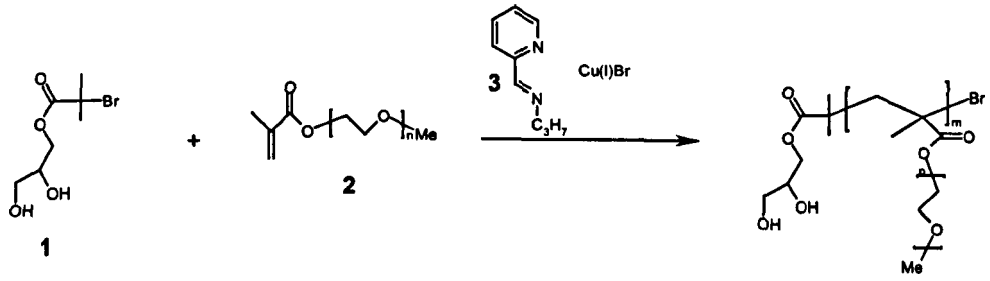

Figure 3.8: Polymerisation of poly(ethylene glycol) methyl ether methacrylate (MeOPEG-MA) using 1,2-dihydroxypropane-3-oxy-(2-bromo-2-methylpropionyl) as a water-soluble initiator mediated by Cu(Br)/*N*-(*n*-propyl)-2-pyridylmethanimine.

Polymerisations were followed by on-line ^{1}H NMR, as described previously (Chapter 2), using D_2O as solvent. Although the inhibitors were not removed from the monomer for practical reasons, both monomethyl ether hydroquinone and butylated hydroxytoluene are phenols and are not very effective inhibitors under the reaction conditions, *i.e.* in the absence of oxygen. Our group has previously reported that such additives do not inhibit this type of polymerisation; indeed slight acceleration effects have been observed, ascribed to co-ordination of the phenol group at the copper.[204] In the present case the acceleration observed by the much higher concentration of water is of a much higher magnitude than would be expected for co-ordination of phenols in their present concentration (approximately 3-4 times). When using reagent concentrations in similar ratios to that when polymerisations are carried out in organic solvents ([Monomer] / [1] / [Cu(I)Br] / [3] = 10 / 1/ 1/ 3, 50% w/w -% monomer with respect to D_2O) polymerisation occurred too fast for efficient monitoring to be carried out. Quantitative conversion to polymer was reached in less than 5 minutes. Size

exclusion chromatography (SEC) indicated a relatively broad mass distribution with a tail to high mass, polydispersity (PDI = 1.40), figure 3.9.

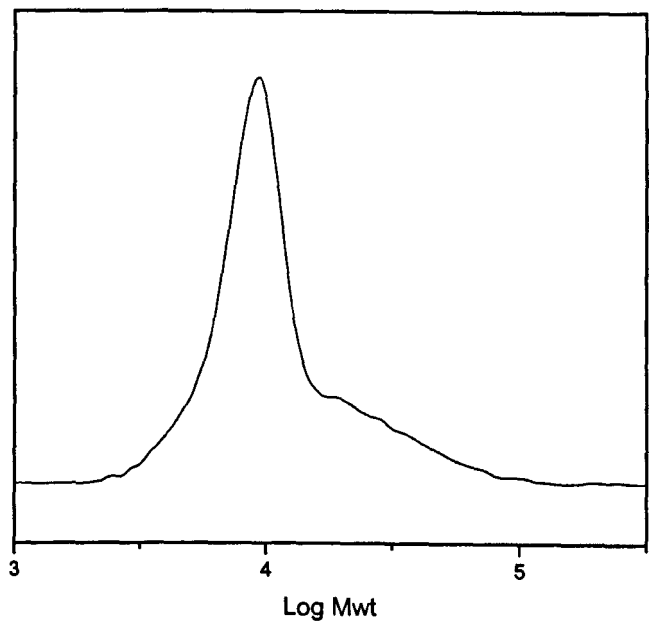

Figure 3.9: Mass distribution of the product of the of MeOPEG-MA in D_2O, at [M]/[1]/[CuBr]/[3] = 10/1/1/3, 50 w/w % monomer with respect toD_2O (100% conversion in less than 5 minutes).

When the catalyst concentration was reduced by two orders of magnitude the rate of polymerisation was lowered with 100% conversion being achieved after 60 minutes. Under these conditions the measured M_n of the final product was far higher than that predicted for efficient initiation and effective living polymerisation, indicating low initiator efficiency, giving a polymer with a polydispersity of 1.43. The conversion versus time plot, as obtained from NMR, Figure 3.10, showed an increase in the rate of polymerisation at the start of the reaction.

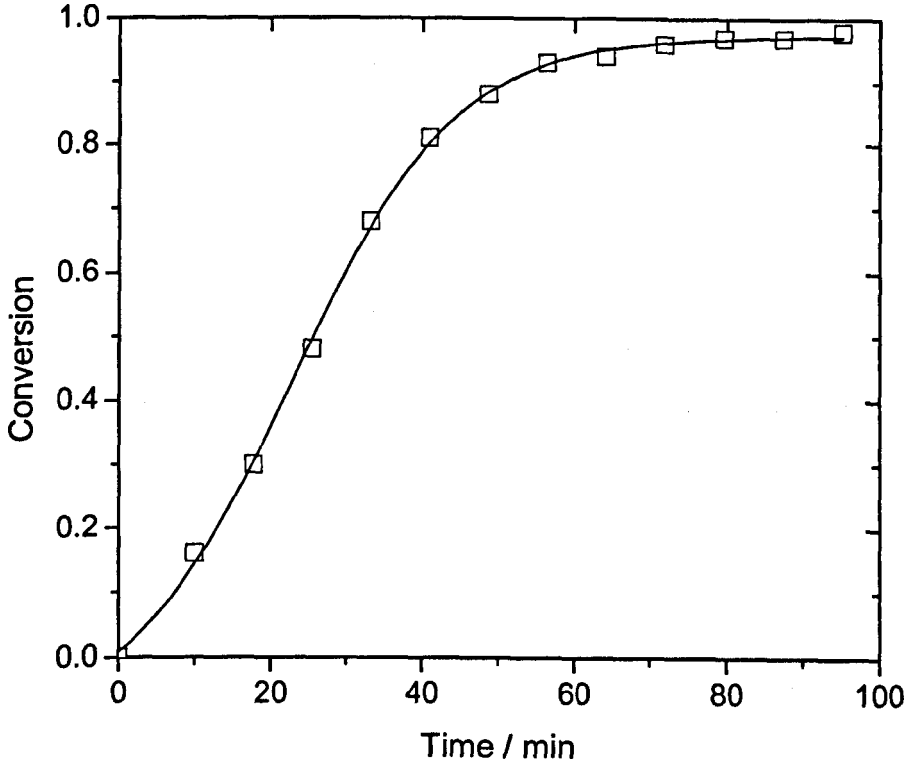

Figure 3.10: Conversion-time plot for the polymerisation of MeOPEG-MA in D_2O solvent at 25°C, [M]/[1]/[CuBr]/[3] = 10/1/0.01/0.03. Conversion was measured by ^1H NMR every 5 min.

This polymerisation had been slowed down but the polymer formed did not show the characteristics required for successful controlled polymerisation as expected for these catalysts, M_n = 28,800, PDI = 1.43. The SEC trace, from this reaction, showed a bimodal mass distribution. The high mass part of the bimodal distribution is formed at early stages of the reaction (60 minutes), whereas the low mass product increases with increasing conversion.

Copper-mediated radical polymerisation can be represented by three steps including activation, propagation and deactivation, Figure 3.11.

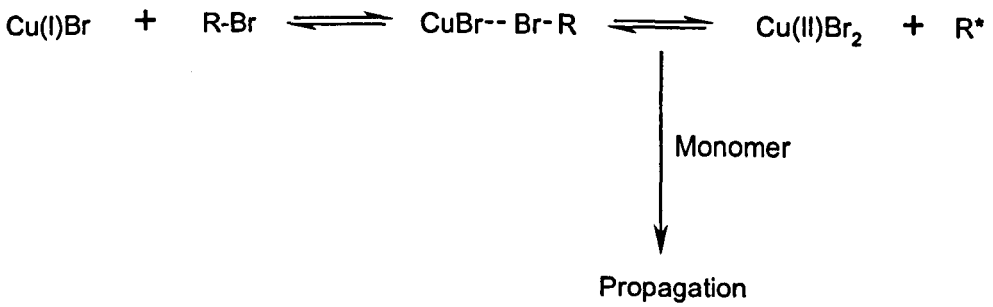

Figure 3.11: Representation of the mechanism of copper-mediated living radical polymerisation.

The two main steps, activation and deactivation, are governed by the redox equilibrium of [Cu(I)]/[Cu(II)] under the reaction conditions. Where the equilibrium lies too far to the right propagation is fast. This results in the formation of both living chain growth and free radical chain growth, giving rise to the bimodal mass distribution. In an attempt to circumvent termination, copper(II) was added as an inhibitor to move the equilibrium to the left, decreasing the concentration of active chains. Our first experiment involved replacing 10% of the Cu(I) by Cu(II) maintaining a ratio ([Cu(I)] + [Cu(II)])/[1] = 1/100) while maintaining all other reaction conditions as before. The mass distribution shows a bimodal distribution indicating at least two different polymerisation mechanisms with high mass polymer formed early in the reaction and growth of lower mass polymer over 22 hours (Figure 3.12). Furthermore, the rate of polymerisation was significantly decreased.

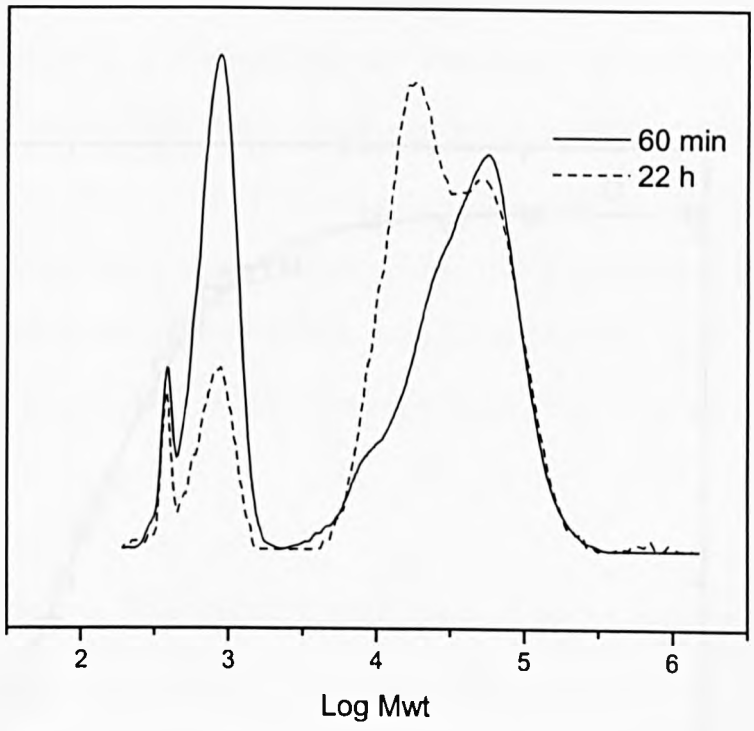

Figure 3.12: SEC traces of polymerisation of MeOPEG-MA in D_2O at 25°C, [1]/[Cu(I)Br]/ [Cu(II)Br_2]/[3] = 1/0.009/0.001/0.03.

The catalyst composition was subsequently changed to [Cu(I)]/[Cu(II)] = 0.5/0.5 again maintaining the overall ([Cu(I)] + [Cu(II)])/[I] = 1/100). Polymerisation proceeded slowly with 80% conversion reached after 22 h, M_n deviated significantly from the predicted value. The concentration of Cu(I) was thus further reduced to [Cu(I)]/[Cu(II)] = 10/90, ([Cu(I)] + [Cu(II)])/[**1**] = 1/100). The system now contained [**1**]/[Cu(I)] = 1000/1 and [**1**]/[Cu(II)] = 1000/9. The reaction reached 50% after 5h with the polymer having M_n close to the theoretical value and with a narrow

polydispersity, PDI = 1.15. However, the reaction terminated after approximately 4 hours, Figure 3.13.

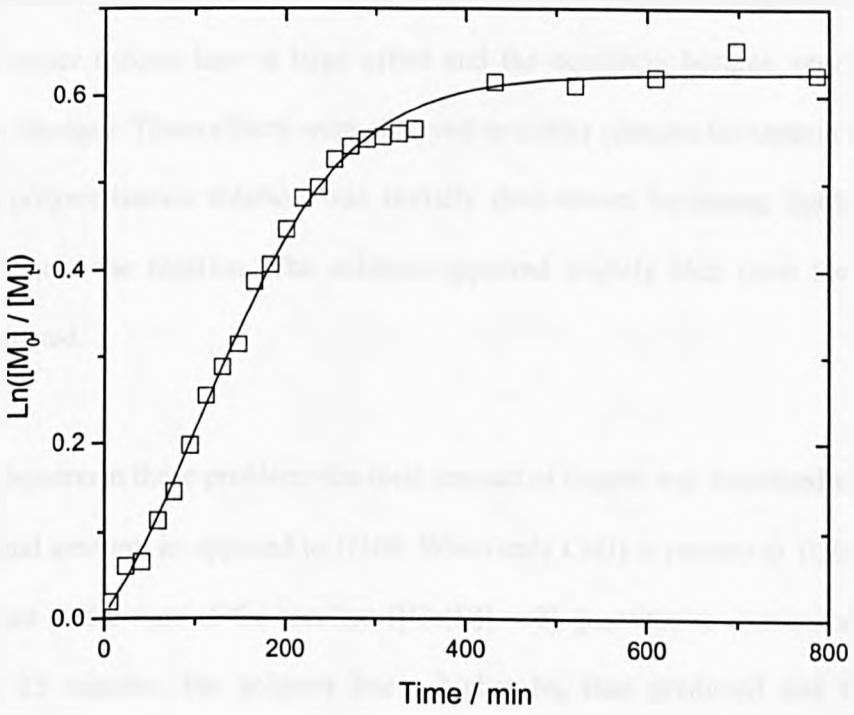

Figure 3.13: First order kinetic plot for the polymerisation of MeOPEG-MA in D_2O, [M]/[1]/[Cu(I)Br]/[Cu(II)Br2]/[3] = 10/1/0.001/0.009/0.03.

This is surprising, as the catalyst is stable in water at 25 °C (see chapter 4). It is noted that both oxygen and nitrogen donors are excellent ligands for copper(II) relative to halide ions [199]. In aqueous solution, nitrogen bidentate ligands can replace 4 water ligands on $Cu(H_2O)_6^{2+}$, but replacement of the third and fourth are kinetically less favourable.[205] Water is usually a better ligand for copper(II) relative to copper(I), resulting in a competition between the N bidentate ligand and water on copper(II)

displacing the equilibrium towards Cu(II), which in turn acts as a polymerisation inhibitor. As relatively stable Cu(II) is formed during the reaction the equilibrium is such that polymerisation is effectively retarded. Furthermore, as relatively low levels of catalyst were used ($1/100^{th}$ of the normal concentration), changes in the nature of the copper species have a large effect and the equilibria become very sensitive to these changes. These effects were observed as colour changes throughout the reaction. The polymerisation solution was initially dark-brown becoming lighter in colour throughout the reaction. The solution appeared slightly blue once the reaction is terminated.

To circumvent these problems the total amount of copper was increased to 1/20 of the original amount, as opposed to 1/100. When only Cu(I) is present at 1/20 the original amount at the start of the reaction ([Cu(II)] = 0) quantitative conversion is reached after 25 minutes, but polymer has a higher M_n than predicted and PDI = 1.61. However, when a mixture of copper(I) and (II) was used with Cu(I) / Cu(II) = 0.1 / 0.9 a conversion of 97.2% was seen after 17 h, with the product showing a molecular weight close to the theoretical value, and a PDI of 1.13.

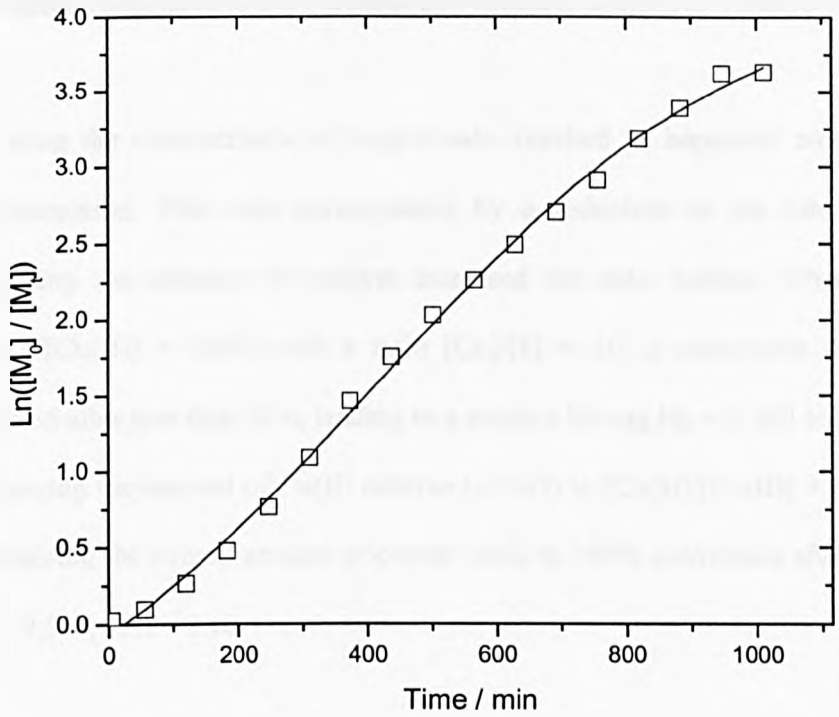

Figure 3.14: First order kinetic plot for the polymerisation of MeOPEG-MA in D_2O, [M]/[1]/[Cu(I)Br]/ [Cu(II)Br_2]/[3] = 10/1/0.005/0.045/0.1.

Figure 3.14 illustrates the first order kinetic plot for this reaction. In this case, the amount of catalyst used was high enough to avoid the reduction in catalyst efficiency during the polymerisation after 4 hours as previously seen. It is noted that measured polydispersities appear to be narrower than theoretical Poisson distribution at these low conversions. These effects were ascribed to the difference in hydrodynamic volume between the linear PMMA used as narrow standards for the SEC and the current polyether comb polymers which seems to result in a lower value for M_w and hence a narrower observed polydispersity. The true polydispersity would prove

difficult to measure accurately for these low molecular weight polymers and it is thus considered reasonable to use the measured values as indicative, relative values.

Lowering the concentration of copper salts resulted in improved control over the polymerisation. This was accompanied by a reduction in the rate of reaction. Increasing the amount of catalyst increased the rate. Indeed, when a ratio of [Cu(I)]/[Cu(II)] = 10/90 with a ratio [Cu]/[1] = 1/1 a conversion of 100% was achieved after less than 20 h, leading to a product having M_n = 8,500 and PDI = 1.15. Decreasing the amount of Cu(II) relative to Cu(I) to [Cu(I)]/[Cu(II)] = 0.5/0.5, while maintaining the overall amount of copper leads to 100% conversion after 75 minutes, M_n = 9,500, PDI = 1.10.

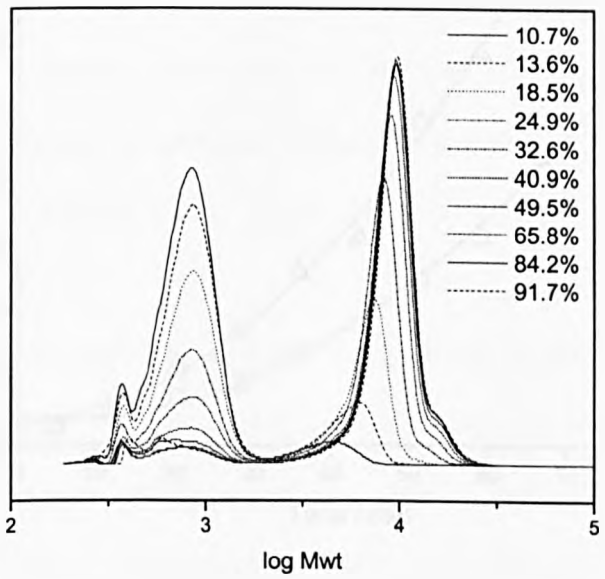

Figure 3.15: SEC traces for the polymerisation of MeOPEG-MA in D_2O, [M]/[1]/[Cu(I)Br]/ [Cu(II)Br_2]/[3] = 10/1/0.5/0.5/2 as a function of time, samples taken every 5 min.

Figure 3.15 demonstrates SEC traces for samples taken at regular time intervals in this reaction. These SEC traces can be used to follow the kinetics of polymerisation. After 30% conversion, we observe the appearance of a small amount of higher molecular weight material, due to termination by recombination as nearly always observed in all types of living radical polymerisation. The proportion of termination was calculated to be 5% at the end of the polymerisation. The first order kinetic plot, Figure 3.16, shows that the polymerisation occurs over a short time period (approximately 70 minutes for 90% conversion).

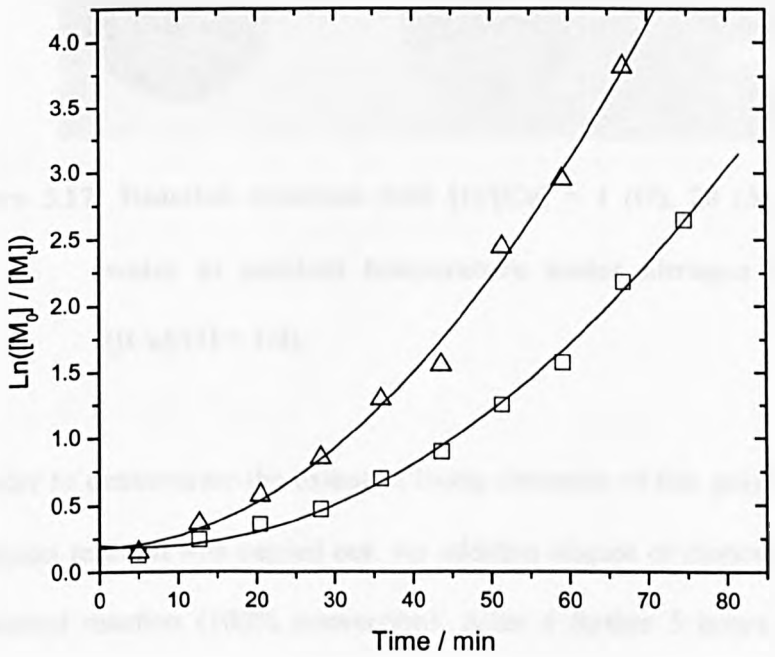

Figure 3.16: Kinetic plot for the polymerisation of MeOPEG-MA in D_2O, [M]/[1]/[Cu(I)Br]/ [Cu(II)Br_2]/[3] = 10/1/0.5/0.5/3 at 25°C (□) and 35°C(Δ).

In this case the rate of polymerisation increased throughout the course of the reaction showing an apparent increase in $k_p[P_n^*]$. As the control of both M_n and PDI are good we are confident that $[P_n^*]$ remains at least approximately constant.

The changes in the coloration of the reaction mixture on changing the levels of total copper and the ratio of copper(I) to copper(II) is quite remarkable, Figure 12. With the lowest levels of catalyst, the solution is water-white however, it is noted that this resulted in loss of rate after 4 hours. The median amount of copper ([2]/[Cu] = 20) is a semi-transparent green solution indicative of copper(II).

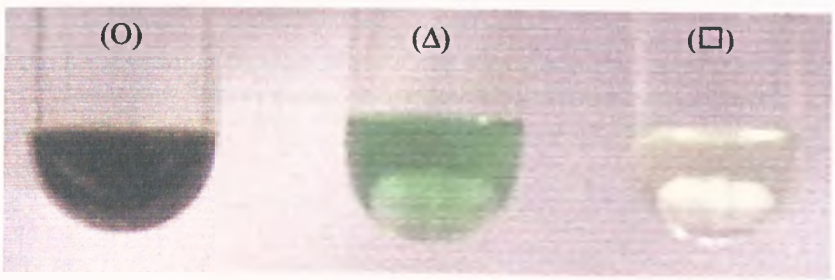

Figure 3.17: Reaction solutions with [1]/[Cu] = 1 (O), 20 (Δ), and 100 (□) in water at ambient temperature under nitrogen in Schlenk tubes ([Cu]/[3] = 1/3).

In order to demonstrate the extent of living character of this polymerisation, a chain extension reaction was carried out. An addition aliquot of monomer was added to a completed reaction (100% conversion). After a further 5 hours, the reaction was stopped and the product isolated. The molecular weight of the resulting polymer was then compared to the molecular weight of the *macro-initiator*. Figure 3.18 shows that the M_n of the final product was approximately twice the M_n of the polymer used as macro-initiator. This is good evidence for living polymerisation.

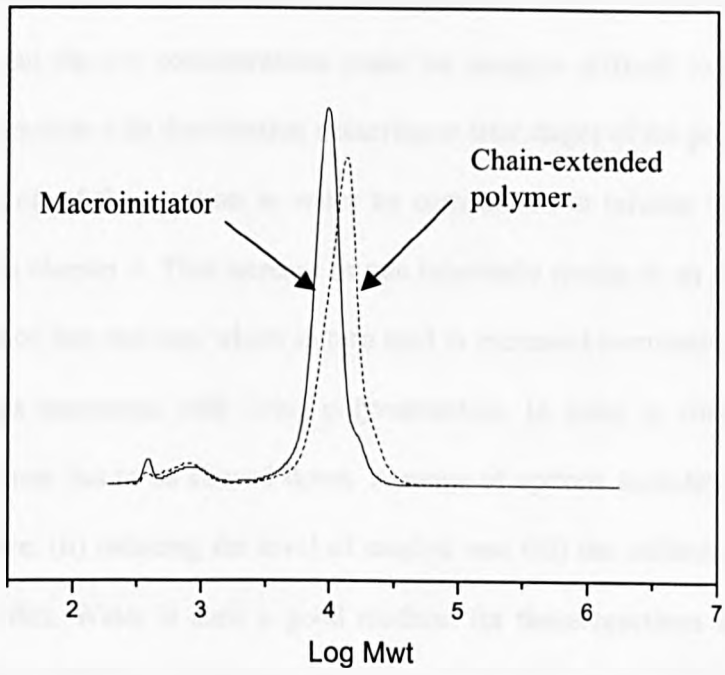

Figure 3.18: SEC traces for the reinitiation polymerisation of MeOPEG-MA initiated by a macroinitiator.

3.2.3. Conclusion.

Controlled polymerisation was obtained by polymerisation at ambient temperature with reduced level of copper than would normally be used in organic solvents. An appreciable amount of copper(II) has to be added to the reaction as an inhibitor in order to slow the reaction down to acceptable levels. Although it may be surprising that polymerisation occurs in the presence of such large quantities of copper(II) these observations are certainly not without precedence. A recent article from Zhang *et al.*[117] reported that the polymerisation of solketal methacrylate using exclusively

$Cu(II)Br_2$ in conjunction with an aliphatic tetra-amine ligand. In this case acceptable rates are achieved and polydispersities < 1.20 obtained. Copper levels can be reduced even further but the low concentrations make the reagents difficult to work with on this scale of reaction with deactivation occurring at later stages of the polymerisation. The acceleration of the reaction in water by comparison to toluene will be further investigated in chapter 4. This increase in rate inherently results in an increase in the concentration of free radicals, which in turn lead to increased termination, and loss of the advantages associated with living polymerisation. In order to circumvent these problems the rate has to be slowed down. A range of options including (i) lowering the temperature, (ii) reducing the level of catalyst and (iii) the addition of inhibitors may achieve this. Water is such a good medium for these reactions that empirical change of all of these parameters proved necessary in order to obtain controlled polymerisation. However, we have demonstrated that it is possible to obtain narrow polydispersity polymer of controlled molecular mass with good first order kinetics by appropriate choice of reaction conditions. Indeed it is possible to prepare block copolymers by sequential monomer addition. Thus water can be used as an effective polymerisation medium but the large increase in the rate introduce unexpected problems thus the nature of the solvent used for polymerisation has to be carefully considered in each case. Thus the controlled radical polymerisation of water soluble monomers to water soluble polymers can be carried out using bis(*N*-(*n*-propyl)-2-pyridylmethanimine)copper(I) complexes as catalyst with the polymerisation showing many attributes associated with living polymerisation.

3.3. Synthesis of new surfactant molecules.

The graft polymer obtained previously presents a *hydrophobic* methacrylate backbone, with *hydrophilic* poly(ethylene glycol) pendant chains. As seen in chapter 2, functional copper-mediated LRP initiators can be synthesised by the reaction of an appropriate alcohol with an α-bromo acid bromide. It is therefore possible to choose different initiators that would enhance the backbone hydrophobicity in order to investigate the amphiphilic properties of different MeOPEG-MA polymers. Such LRP was performed in toluene to give products showing various hydrophobic blocks.

3.3.1. Use of phenyl-2-isobutyrate as initiator.

As outlined in section 3-1, polymerisation of MeOPEG-MA using α-bromo-isobutyric acid phenyl ester initiator was efficient leading to a polymers of well described structure. The polymer obtained was the simplest structure possible, and the properties of this amphiphilic polymer are investigated in chapter 5.

The non-volatile nature of the MeOPEG-MA macromonomer coupled with the low T_g of poly(MeOPEG-MA) makes the usual procedures for purification (monomer evaporation or precipitation) unusable. Furthermore, the copolymer showed a strong green colour coming from Cu(II) present in the polymer, even after filtration throw a basic alumina column. The block copolymer was dissolved in distilled water and the solution was subjected to ultrafiltration by dialysis with a molecular barrier of ~ 1000 g/mol: The macromonomer of smaller molecular weight and Cu(II) dissolved in water, by formation of the water-soluble complex $Cu(H_2O)_6^{2+}$.[105] were therefore

eliminated. The purified aqueous solution was concentrated by high vacuum rotary evaporation and freeze dried overnight.

3.3.2. Use of octadecyl-2-bromoisobutyrate as initiator.

In order to add a longer alkyl chain to the graft polymer, a 18 carbon chain showing a final hydroxyl group was transformed into an initiator and used to polymerise MeOPEG-MA.

3.3.2.1.Synthesis.

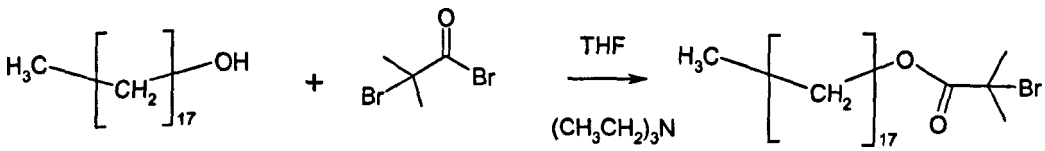

Figure 3.8: Esterification reaction of octadecanol.

As described in part 2.2, the initiator was synthesised by esterification with 2-bromoisobutyryl bromide (Figure 3.8). The product of the reaction was analysed by ^{1}H NMR and infrared spectroscopy to confirm the presence of active chain-end.

3.3.2.2.Polymerisation of MeOPEG-MA with octadecyl-2-bromoisobutyrate.

Copper(I)bromide / *N*-(*n*-propyl)-2-pyridylmethanimine living radical polymerisation of MeOPEG-MA was performed using octadecane-2-bromoisobutyrate as initiator, in toluene at 60°C.

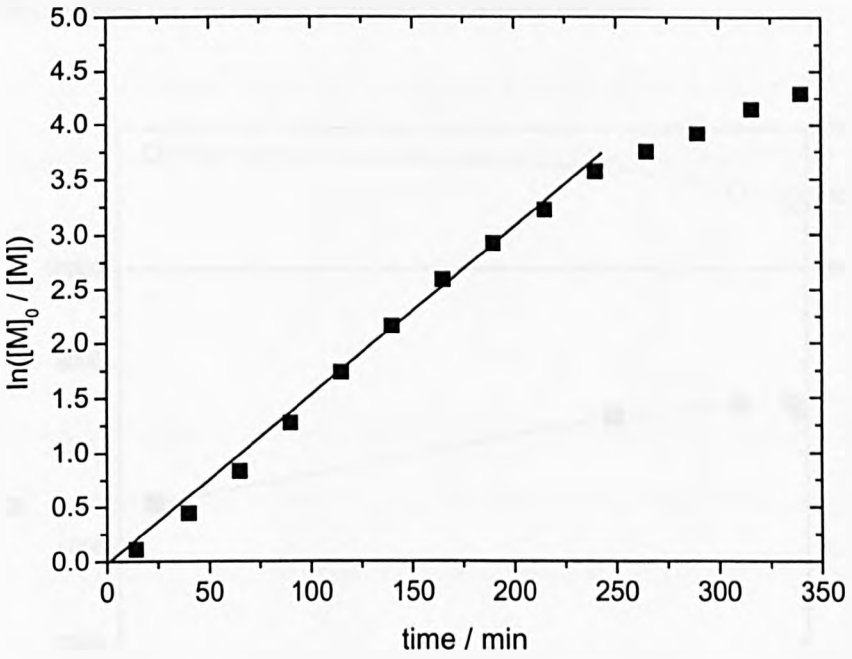

Figure 3.9: First order rate plot for the LRP of MeOPEG-MA in toluene at 60°C initiated by octadecyl-2-bromoisobutyrate and mediated by Cu(I)Br / *N*-(*n*-propyl)-2-pyridylmethanimine ([M] / [I] / [Cu] / [L] = 10 / 1/ 1 / 2)

Figure 3.9 shows the kinetic plot of the reaction. A linear behaviour was observed up to high conversion (98%), as expected by the previous study (section 3-1), demonstrating the constant concentration of reactive species. The molecular weight increased regularly with the conversion and the PDI stayed low during the reaction (see figure 3.10). A final product of molecular weight close to the theoretical one, with narrow molecular weight distribution was obtained. In order to avoid any

reaction of termination, the reaction was stopped after 90% conversion and the product isolated for surfactant properties characterisations.

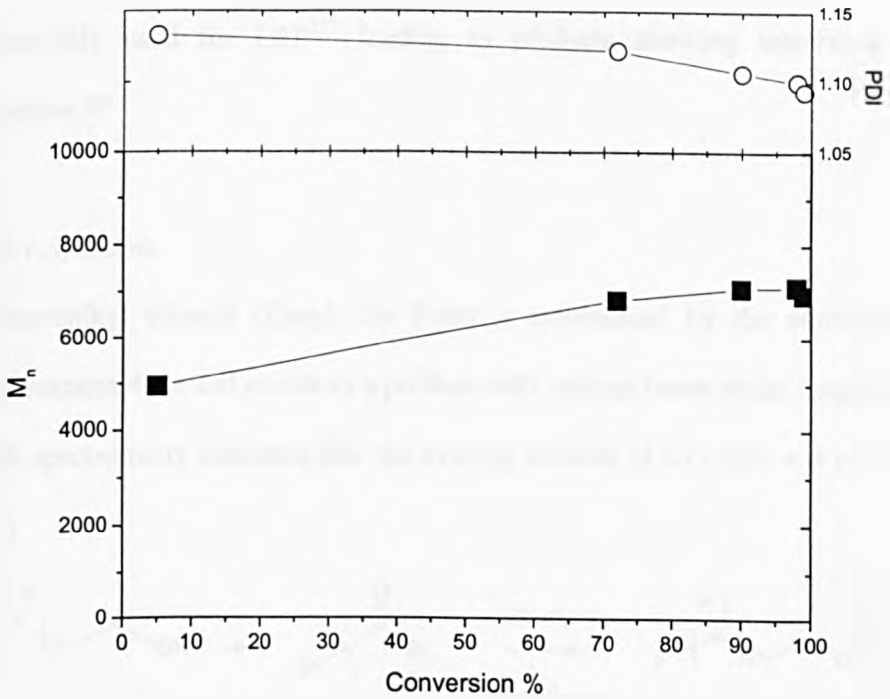

Figure 3.10: Evolution of molecular weight distribution and PDI for the LRP of MeOPEG-MA in toluene (50% v/v) at 60°C initiated by octadecyl-2-bromoisobutyrate and mediated by Cu(I)Br / *N*-(*n*-propyl)-2-pyridylmethanimine.

The resulting water-soluble block copolymer, with enhanced hydrophobic backbone, had a DP in MeOPEG-MA ~ 10 (calculated by NMR, M_n^{SEC} = 6,200) and a narrow polydispersity (1.12). The polymer was purified by dialysis as above, and isolated for further surfactant property studies (Chapter 5).

3.3.3. Use of α-perfluoroalkyl-2-bromoisobutyrate.

In order to enhance even more the hydrophobicity of the backbone, a fluorinated chain was introduced into the molecule. Fluorinated macroinitiators have been successfully used for LRP[117] leading to products showing interesting solution properties.[206]

3.3.3.1.Synthesis.

Perfluoroalkyl ethanol (Zonyl, Du Pont) is synthesised by the telomerisation of tetrafluoroethylene and results in a product with various linear chain lengths[207,208]. ^{19}F NMR spectrometry indicated that the average number of CF_2 unit was n = 8 (Figure 3.11).

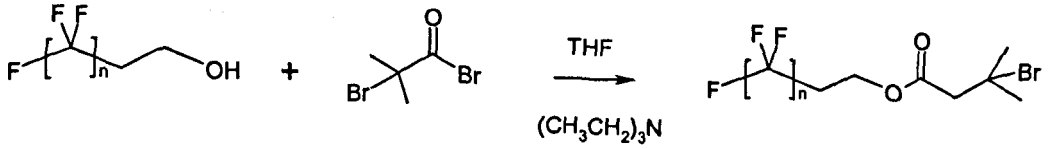

Figure 3.11: Esterification reaction of perfluoroalkyl ethanol.

The macroinitiator was formed by esterification with 2-bromoisobutyryl bromide (see Experimental for details).

3.3.3.2.Polymerisation of MeOPEG-MA α-perfluoroalkyl-2-bromoisobutyrate.

LRP of MeOPEG-MA initiated by α-perfluoroalkyl-2-bromo-isobutyrate at 60°C occurs at a faster rate than when initiated by phenyl-2-bromoisobutyrate, with 95% conversion achieved in 2 hours (see Figure 3.12). The rate of polymerisation increases after 20 minutes (20%) and stays constant up to a conversion of 90%. At high

conversion, terminations, chain transfer reactions and high viscosity of the solution slow down the reaction, as discussed above.

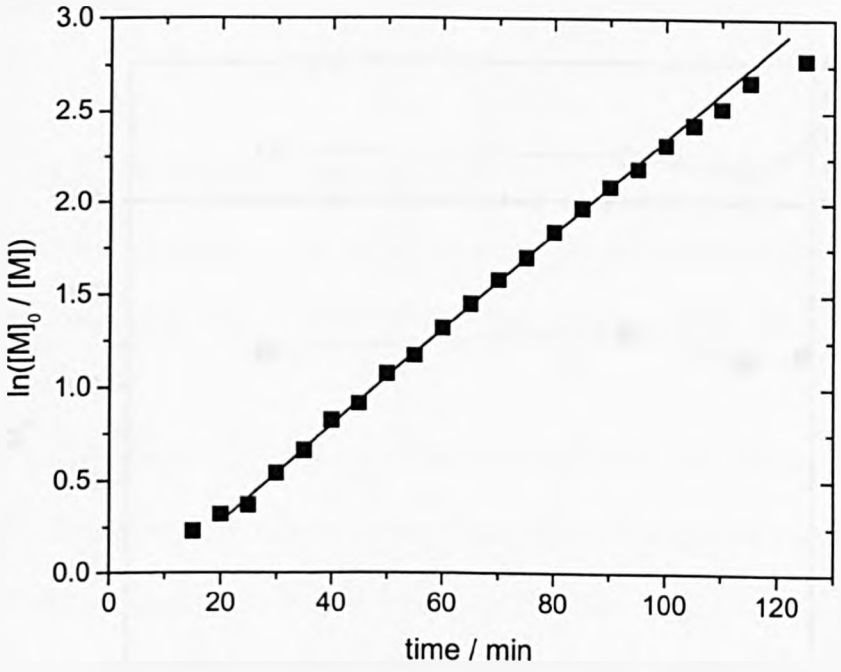

Figure 3.12: First order rate plot for the LRP of MeOPEG-MA in toluene at 60°C initiated by α-perfluoroalkyl-2-bromoisobutyrate and mediated by Cu(I)Br / *N*-(*n*-propyl)-2-pyridylmethanimine ([M] / [I] / [Cu] / [L] = 10 / 1/ 1 / 2)

Figure 3.13 shows the evolution of the molecular weight in function of the polymer conversion, which seems to stay constant. This can be explained by the presence of the fluorinated initiator. In THF, the polymer could act as a shell, trapping the fluorinated initiator away from the solvent. This would explain why the

hydrodynamic volume of the product appears constant, independent of the poly(MeOPEG-MA) DP.

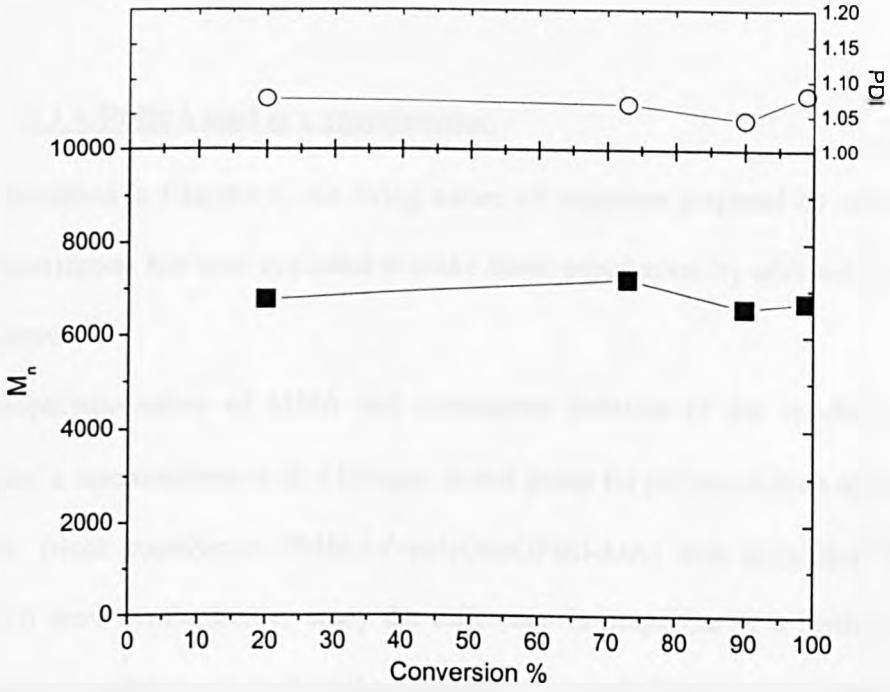

Figure 3.13: Evolution of molecular weight distribution and PDI for the LRP of MeO(PEG)-MA in toluene (50% v/v) at 60°C initiated by α-perfluoroalkyl-2-bromoisobutyrate and mediated by Cu(I)Br / *N*-(*n*-propyl)-2-pyridylmethanimine.

The water-soluble copolymer was purified by dialysis, to give a polymer of M_n^{SEC} = 6,700 g/mol and PDI = 1.07. The M_n^{NMR} was difficult to calculate, as no initiator peaks were clear enough for integration. However, as the SEC results gave a logical molecular weight regarding to the polymerisation of MeOPEG-MA with a more

classic initiator (with M_n slightly higher) or the LRP using octadecyl-2-bromoisobutyrate we were confident in the achievement of a final DP close to the theoretical one, and narrow MWD. The polymer was submitted to surfactant property studies (Chapter 5).

3.3.4. PMMA used as a macroinitiator.

As described in Chapter 1, the living nature of polymers prepared by atom transfer polymerisation has been exploited to make block copolymers by addition of a second monomer.

Homopolymerisation of MMA and subsequent isolation of the resultant polymer yielded a macroinitiator with a halogen ω-end group for polymerisation of the second block. Block copolymers PMMA-*b*-poly(MeOPEG-MA) with respective DP of 50 and 10 were synthesised to study the difference in properties of a better-controlled structure copolymer, as well as the influence of a graft block versus linear block by comparison to the copolymer $MeOPEG_{112}$-*b*-$PMMA_{50}$ formed in chapter 2.

3.3.4.1.Synthesis of PMMA.

In order to obtain a product of molecular weight close to 5,000 g/mol, and showing active chain end groups, a copper(I)bromide / *N*-(*n*-propyl)-2-pyridylmethanimine LRP of MMA was performed in toluene at 90°C using 2EIBr as initiator, with a small amount of copper(II) introduced in the medium (Cu(I) / Cu(II) = 0.95 / 0.05). The resulting polymerisation was subsequently slowed down and a better control over the reaction was obtained at the very beginning. The polymerisation was stopped around a

conversion of 70%, in order to insure that the end groups stay active. The product was then precipitated in petroleum spirit and purified, yielding to an oligomer of M_n=5,200 g/mol and PDI = 1.14, showing an active ω-end group, and therefore used as macroinitiators.

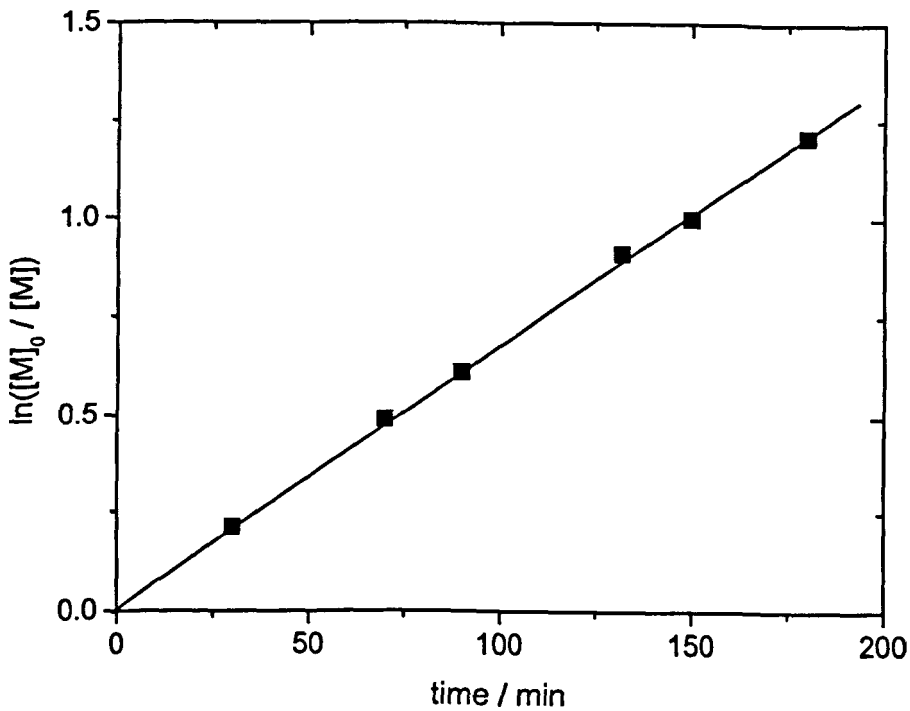

Figure 3.14: First order rate plot for the LRP of MMA in toluene at 90°C initiated by Ethyl-2-bromoisobutyrate and mediated by Cu(I)Br / Cu(II)Br_2 / *N*-(*n*-propyl)-2-pyridylmethanimine ([M] / [I] / [Cu(I)] / [Cu(II)] / [L] = 60 / 1/ 0.95 / 0.05 / 2)

The molecular weight evolution measured by SEC showed a linear increase as expected for a living polymerisation. The polydispersity stayed remarkably low, even at low conversion (See figure 3.15).

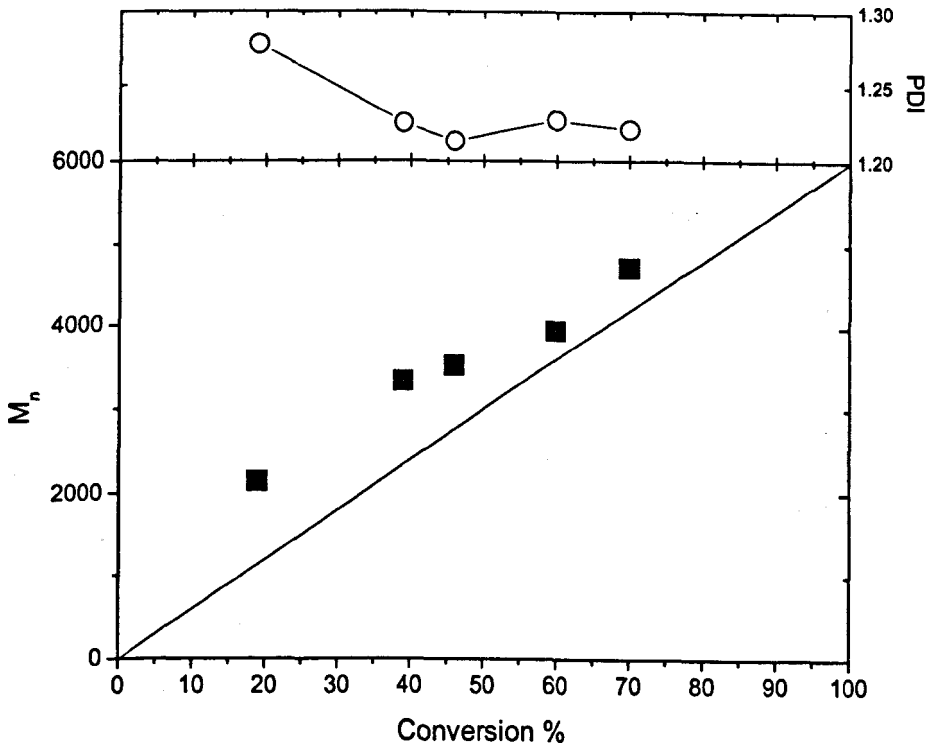

Figure 3.15: Evolution of molecular weight distribution and PDI for the LRP of MMA in toluene (50% v/v) at 90°C initiated by Ethyl-2-bromoisobutyrate and mediated by Cu(I)Br / Cu(II)Br_2 / *N*-(*n*-propyl)-2-pyridylmethanimine ([M] / [I] / [Cu(I)] / [Cu(II)] / [L] = 60 / 1/ 0.95 / 0.05 / 2)

3.3.4.2.Polymerisation of MeOPEG-MA on PMMA macroinitiator.

PMMA initiated LRP of MeOPEG-MA was undertaken at 60°C. The polymerisation showed a higher rate for the first few minutes, and then followed good first order kinetics up to a conversion of 95% (Figure 3.15). It is noteworthy that, as observed with the previous initiators, the rates is slowed down after 95% conversion. This can be explained by the concentration of active species decreasing due to termination and transfer reactions, or the propagation becoming more diffusion controlled, as the viscosity of the solution is increased by the presence of the macroinitiators.

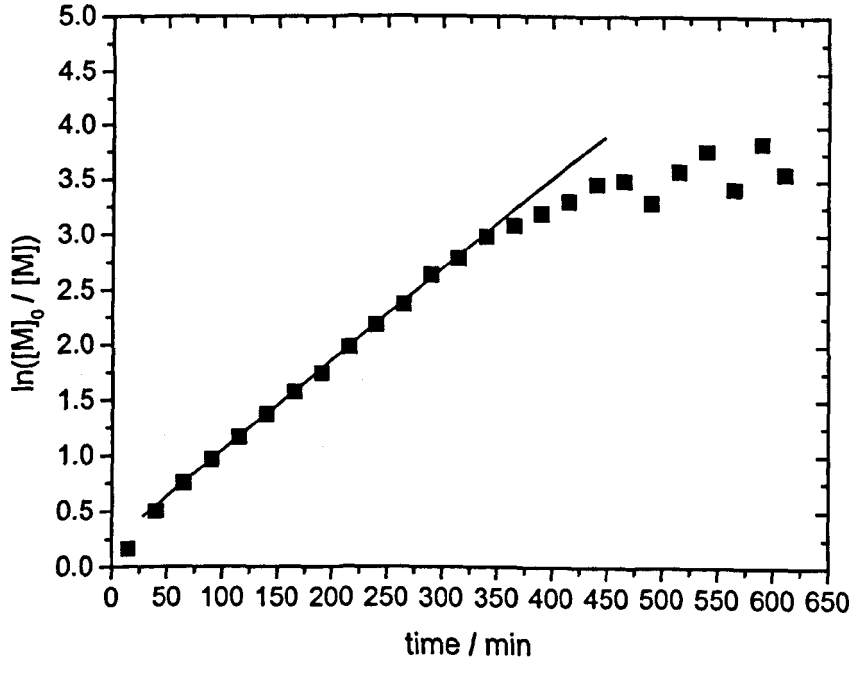

Figure 3.16: First order rate plot for the LRP of MeO(PEG)-MA in toluene (50% v/v) at 60°C initiated by $PMMA_{50}$ and mediated by Cu(I)Br / *N*-(*n*-propyl)-2-pyridylmethanimine ([M] / [I] / [Cu] / [L] = 10 / 1/ 1 / 2)

The molecular weight increased regularly with the conversion and the PDI stayed low during the reaction (see Figure 3.17).

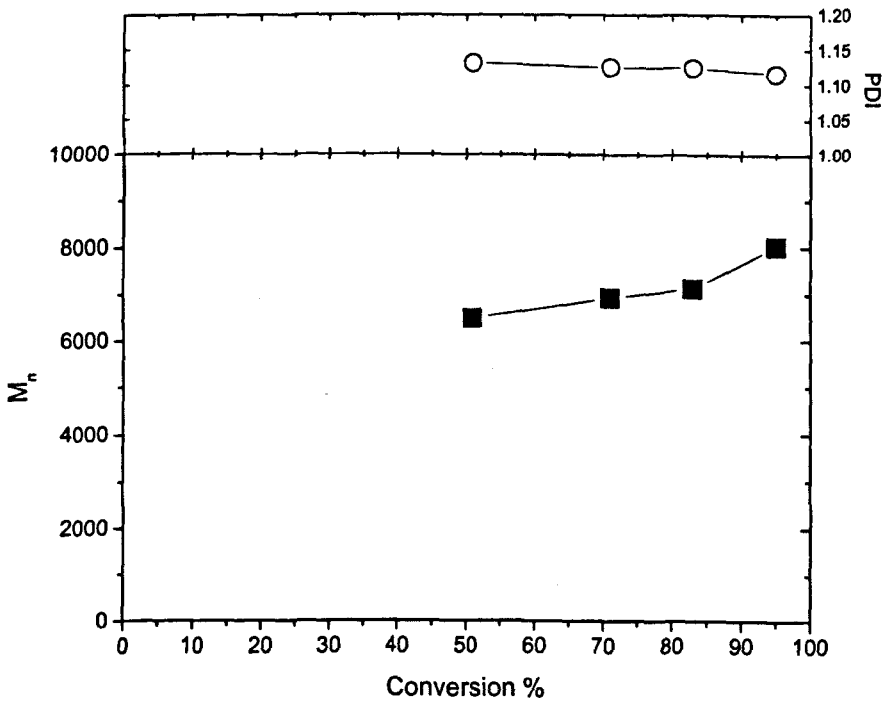

Figure 3.17: Evolution of molecular weight distribution and PDI for the LRP of MeOPEG-MA in toluene (50% v/v) at 60°C initiated by $PMMA_{50}$ macroinitiator and mediated by Cu(I)Br / *N*-(*n*-propyl)-2-pyridylmethanimine.

3.4. Conclusion

In this chapter, LRP of MeOPEG-MA was shown to be efficient, leading to well defined graft water-soluble oligomers, of low molecular weight. Furthermore, water was shown to be an interesting solvent for such polymerisation, leading to an

improvement of the speed of the reaction, and an evolution in the experimental procedure.

MeOPEG-MA was then used as monomer in the living radical polymerisation with various initiators, in order to synthesis different copolymers showing surfactant properties. Surfactant properties of the resulting products will be tested in chapter 5.

3.5. Supplementary information.

T/K	t/min	Conv.[a]	$<Mn>_{th}$	$<M_n>^{a}_{exp}$	$<M_n>^{b}_{exp}$	PDI[b]
298	60	13.2	638		1090	1.41
	120	24.9	1204		1800	1.32
	180	34.4	1664		2500	1.16
	240	37.0	1760	2010	2570	1.08
313	20	13.4	648		1240	1.32
	40	22.3	1078		1600	1.32
	60	26.8	1296		1960	1.28
	120	48.3	2336		3700	1.21
	180	56.8	2747		4200	1.16
	240	64.1	3100		5010	1.14
	300	70.4	3405	3700	5820	1.14
333	20	29.3	1417		2110	1.28
	40	42.2	2041		2700	1.15
	60	56.7	2742		3700	1.16

	120	74.6	3608		4480	1.11
	180	78.9	3816		4700	1.10
	240	90.1	4357		5300	1.14
	300	92.8	4488	4620	5390	1.11
363	20	38.7	1872		2710	1.08
	40	56.0	2708		3690	1.13
	60	68.9	3330		4700	1.07
	120	76.8	3716		5020	1.12
	180	81.7	3950		5200	1.13
	240	85.2	4120	5460	5370	1.12

[a] Determined by the ^{1}H NMR peak intensity ratio

[b] Estimated by PMMA-calibrated SEC.

Chapter 4

Mechanistic approach of the polymerisation: Solvent Effects.

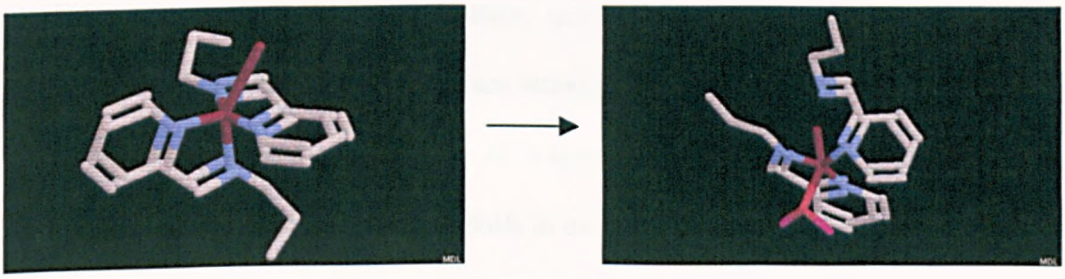

3D Schematic of the potential copper coordination competition between oxygen containing molecules and ligands.

4.1. Introduction.

The nature of the solvent in copper mediated living radical polymerisation plays an important role in the mechanism and rate of polymerisation. For example, THF can even copolymerise, while 2-propanol[209], DMF[210], ethylene or propylene carbonate[211], diethyl ether[211] and ethylene glycol diethyl ether (see chapter 2 and chapter 3) enhance the rate of polymerisation. Indeed careful reading of the literature shows that non-polar solvents such as toluene are preferred to $(bpy)_2Cu(I)$ mediated polymerisations whilst more polar ethers, anisole or diphenyl ether, are preferred for methacrylates. There seems no apparent rational for these different reaction conditions other than differences in solubility of reagents. Therefore it seems that a careful consideration of the solvent with regards to co-ordination of various species that may be present in the reaction and its ability to solubilise monomer, polymer and catalyst is always required.

We have seen in the previous chapters an original behaviour of the polymerisation (kinetics and catalyst complex evolution) during copper-mediated living radical polymerisation in presence of poly(ethylene glycol) species.

In chapter 2, unusual fast kinetics were observed when using poly(ethylene glycol) methyl ether based macroinitiators for the LRP of alkyl methacrylates. The rate of the polymerisation was shown to increase with the size of the macroinitiator chain. For molecular weight of ~2,000 and ~500 g/mol, a variation of rate was observed at the beginning of the reaction, with a decrease after few minutes of polymerisation. When using ethylene glycol diethyl ether as solvent for the LRP initiated by MeOPEG-I_{113}, a constant increase of $k_p[P_n^*]$ was noticed, with an overall kinetic faster than the polymerisation carried out in toluene.

In chapter 3, the LRP of MeOPEG-MA in toluene appeared again faster than classic LRP of alkyl methacrylate in the same conditions. When carried in water, the reaction is speeded up, with $k_p[P_n^*]$ increasing regularly in time. Finally, water was found to affect the catalyst complex, destroying it after a long period, at low concentration in copper.

These observations motivated us to investigate further the solvent effect on the copper-mediated living radical polymerisation presented in this work.

4.2. Potential Co-ordination effect on the catalyst complex.

4.2.1. Effect of ethylene oxide groups on copper-mediated LRP.

As the presence of ethylene glycol groups proved to influence the copper-mediated LRP of MMA, further studies were undertaken. In order to determine if alkyl ether groups affect the rate of polymerisation, living radical polymerisations in presence of ethylene glycol diethyl ether were carried out.

Benzyl methacrylate (BzMA) monomer was chosen as monomer-model for the polymerisation followed *in-situ* by ^1H NMR, as described in chapter 2. Monomer conversion could be easily measured by integration of the vinyl resonances (6-5 ppm) relative to the combined values of the CH_2 α to *OC=O*, shifted by the presence of the aromatic ring, from the monomer and polymer (5.10 ppm) (see Figure 4.1).

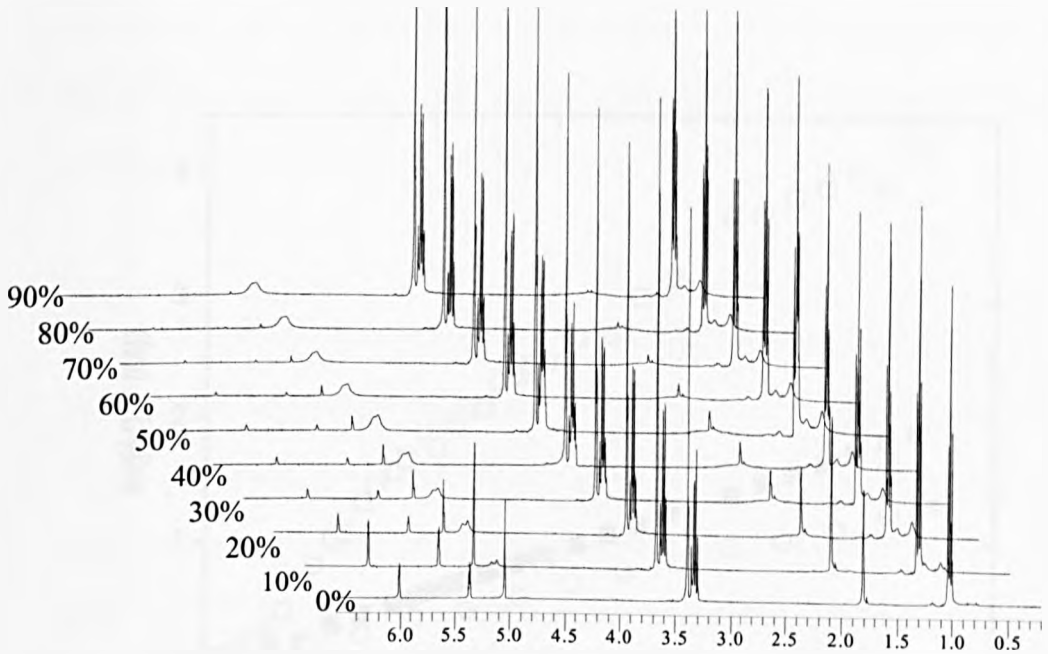

Figure 4.1: Figure 3.6: Partial ^{1}H NMR spectra at different stages of monomer conversion for the polymerization of BzMA in $(EtO)_2EG$ at 50 °C.

Living radical polymerisations of benzyl methacrylate (BzMA) were carried out in a toluene-d_8 solution with (i) a PEG-based macroinitiator, MeOPEG-I_{113} (**2**), and (ii) ethylene glycol diethyl ether as co-solvent. According to the previous study (see chapter 2), the reaction temperature was kept at 50°C in order to keep control over the polymerisation.

The use of oxyethylene containing macro-initiators increased the overall rate of polymerisation markedly in comparison to a similar living radical polymerisation with ethyl 2-bromoisobutyrate as initiator (Figure 4.2). The addition of ethylene glycol diethyl ether as co-solvent in the polymerisation of BzMA also showed a large rate enhancement, in comparison to reactions carried out in neat toluene-d_8 (Figure 4.2).

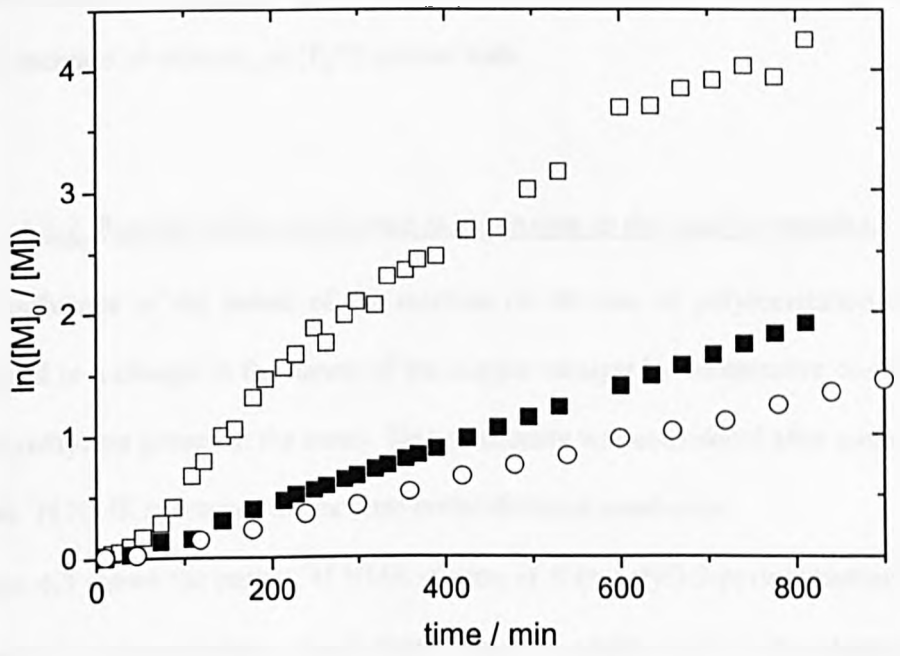

Figure 4.2: First order kinetic plots for the polymerization of benzyl methacrylate (BzMA) in toluene-d_8 at 50 °C (O), in toluene using an oxyethylene macroinitiator, MeO(PEG)-I_{113} (M_n = 5000 g/mol ; ■), and in toluene-d_8 / diethyl ether ethylene glycol (4/1 g/g; □). Conversion monitored by ^{1}H NMR.

While the reaction initiated by MeOPEG-I_{113} appeared controlled up to approximately 85% conversion, the reaction in $(EtO)_2EG$ showed a clear deviation from a first order behaviour. $k_p[P_n^*]$ increases regularly up to a conversion of 85%, then decreases up to 98% conversion. This behaviour is similar as the one observed in chapter 2, figure 2.22, when polymerising MMA in $(EtO)_2EG$ initiated by MeO(PEG)-I_{113}. While the decrease of rate toward the end of the polymerisation can be understood as

termination reactions decreasing the concentration in active species, then $k_p[P_n^*]$, the kinetic behaviour during the first 3 hours is more difficult to understand. This is due to an increase of either k_p or $[P_n^*]$ or even both.

4.2.2. Possible effect of ethylene oxide groups on the catalyst complex.

The influence of the nature of the reaction on the rate of polymerisation could be ascribed to a change in the nature of the copper-catalyst by competitive co-ordination of oxyethylene groups at the metal. This possibility was considered after measurement of the ^{1}H NMR spectra of the catalyst under different conditions.

Figure 4.3 shows the partial ^{1}H NMR spectra of *N*-(*n*-octyl)-2-pyridylmethanimine in toluene-d_8, using ethylene glycol diethyl ether as additive, (a) in the absence of the additive and (b) in presence of the additive, (c) bis(*n*-Oct-L)copper in the absence of the additive (d) bis(*n*-Oct-L)copper with ethylene glycol diethyl ether (1:1) and (e) bis(*n*-Oct-L)copper with ethylene glycol diethyl ether (1:5). In the case of a complexed ligand, a broad signal is observed.

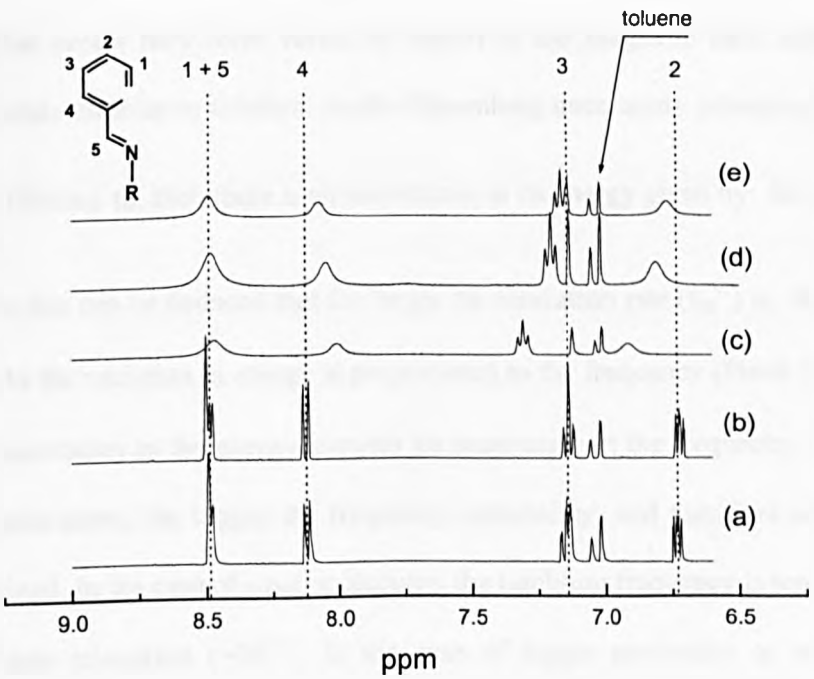

Figure 4.3: Partial ^{1}H NMR spectra, aromatic region, of (a) *N*-(*n*-octyl)-2-pyridylmethanimine in toluene-d_8 (b) *N*-(*n*-octyl)-2-pyridylmethanimine with the addition of 2 equivalents of diethyl ether ethylene glycol (c) bis(*N*-(*n*-octyl)-2-pyridylmethanimine)copper(I) (2:1, ligand to CuBr) (d) bis(*N*-(*n*-octyl)-2-pyridylmethanimine)copper(I) (2:1, ligand to CuBr) with 2 equivalents of ethylene glycol diethyl ether and (e) bis(*N*-(*n*-octyl)-2-pyridylmethanimine)copper(I) (2:1, ligand to CuBr) with 5 equivalents of ethylene glycol diethyl ether.

Classically, this type of broadening observed by ^{1}H NMR spectroscopy can be explained in two ways.[212] A first explanation is the *efficient relaxation* of the

molecule: The relaxation of a ^{13}C or ^{1}H is promoted by a neighbour atoms, as the dipolar vector they form varies by regard to the magnetic field applied when the molecule tumbles in solution. As the Heisenberg uncertainty principle states, if a state as a lifetime τ_m, then there is an uncertainty in its energy given by: $\delta E = \frac{h}{2\pi\tau_m}$.

From this can be deduced that the larger the relaxation rate (τ_m^{-1}) is, the larger δE will be. As the variation in energy is proportional to the frequency (Plank's law: $\Delta E = h\nu$), an uncertainty in the energy requires an uncertainty in the frequency. Thus, the faster the relaxation, the bigger the frequency uncertainty, and therefore a broad signal is obtained. In the case of small molecules, the tumbling frequency is too fast to promote efficient relaxation ($\sim 10^{-11}$). In the case of bigger molecules or viscous solution, however, the tumbling frequency will be around $10^9 s^{-1}$ or less, resulting in a broaden line. A typical example of this effect is the broadening of the ^{1}H NMR spectrum signal observed for the protons of a polymer backbone during its formation.

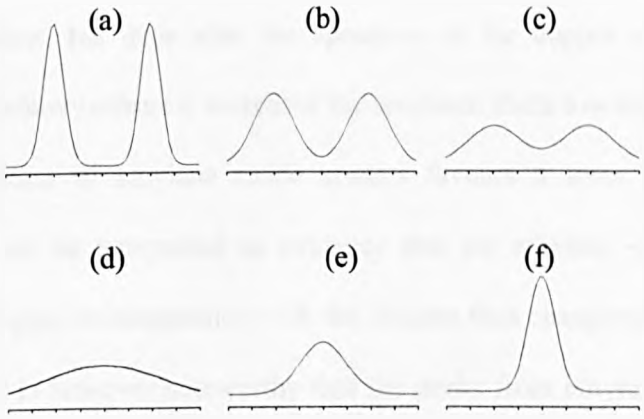

Figure 4.4: Variation of the ^{1}H NMR spectroscopy proton signal when the rate of exchange from different environments varies from very slow (a) to very fast (f) with the evoluting intermediates ((b) to (e)). [212]

A second explanation is an *environmental exchange.* When the rate constant for the exchange between one environment and another is greater than the frequency difference of the proton resonances in the separate environments, a broadening in the signal will be observed. When the rate of exchange is very low, the protons will appear as separate signals, but when the rate of exchange is very fast, they will appear as a line, seen as the average of the two signals (see figure 4.4).

In the present case, this last possibility appears to be the most probable. Our group has already observed fast exchanges between complexed and free ligand, as the ^{1}H NMR spectroscopy signal of the aromatic protons shifts and broadens with the increase of the temperature.[213] The ligand is in fast dynamic coordination equilibrium on the copper centre on the NMR time-scale and as the observed NMR spectrum is an average of complexed and uncomplexed ligand, the peaks appear broader.

Ethylene glycol diethyl ether does not influence the spectrum of *N*-(*n*-octyl)-2-pyridylmethanimine, but does alter the spectrum of the copper complex. As the amount of 1,2-diethoxy ethane is increased the spectrum shifts towards that of the free ligand. An addition of ethylene oxide species favours a more "loose" catalyst structure. This can be interpreted as evidence that the ethylene oxide groups co-ordinate to the copper in competition with the diimine thus changing the nature of the active species. It is however noteworthy that the peaks from ethylene glycol diethyl ether does not seem to be influenced by the complexation, as no obvious shifts are observed when in presence of copper.

In order to investigate this effect further, the experiments designed to follow the kinetics of the polymerisation *in-situ* by NMR were used to monitor the complex throughout the reaction.

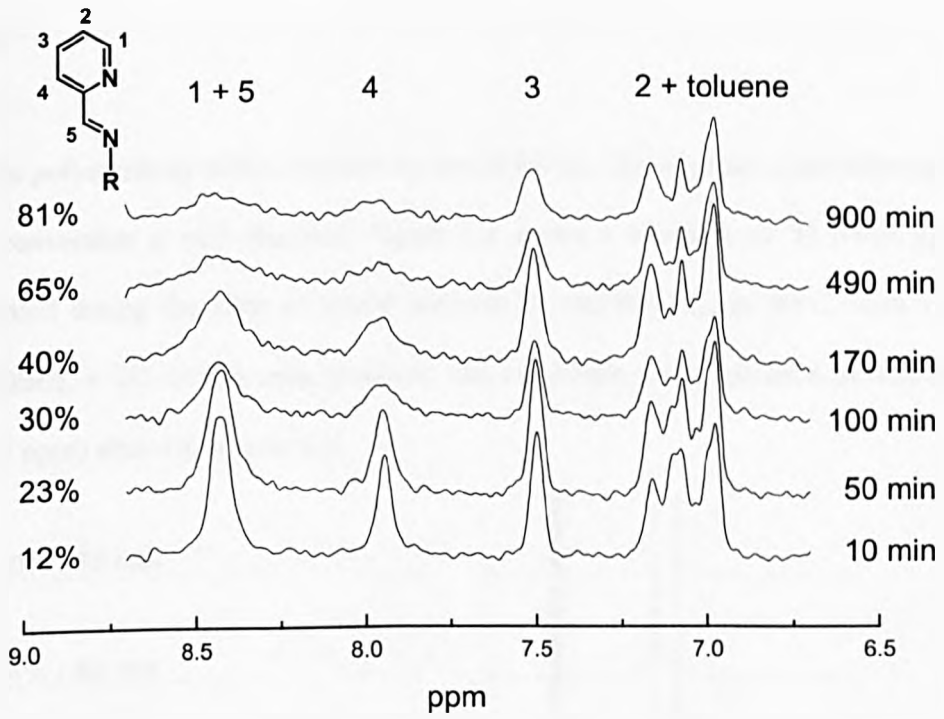

Figure 4.5: Partial ^{1}H NMR spectra of *N*-(*n*-octyl)-2-pyridylmethanimine ligand during the polymerisation of MeOPEG-MA in toluene-d_8 at 25 °C using 3 equivalents of ligand to CuBr.

Figure 4.5 shows the evolution of the copper complex during polymerisation of MeOPEG-MA at 25°C in toluene-d_8. Firstly it is noted that only one set of resonances is observed for the ligand even though it is present in excess, supporting our belief of rapid exchange between complexed and non-complexed ligand. A continuous broadening of the aromatic peaks is observed upon increasing polymerisation

conversion. This can be ascribed to a decrease in mobility of the complex, as the viscosity increases, resulting in the efficient relaxation effect described above. Broadening due to the accumulation of paramagnetic Cu(II) species in the medium can be ruled out as explanation as the other peaks (*e.g.* toluene) do not alter in this way.

When polymerising MMA initiated by MeOPEG-I_{45}, the increase of broadening with the conversion is still observed. Figure 4.6 shows a selection of ^{1}H NMR spectra recorded during the LRP of MMA initiated by MeOPEG-I_{45} at 50°C, with a ratio Cu(I)Br/L = 1/2. In this case, however, one can notice the appearance of free ligand (8.52 ppm) after 4% conversion.

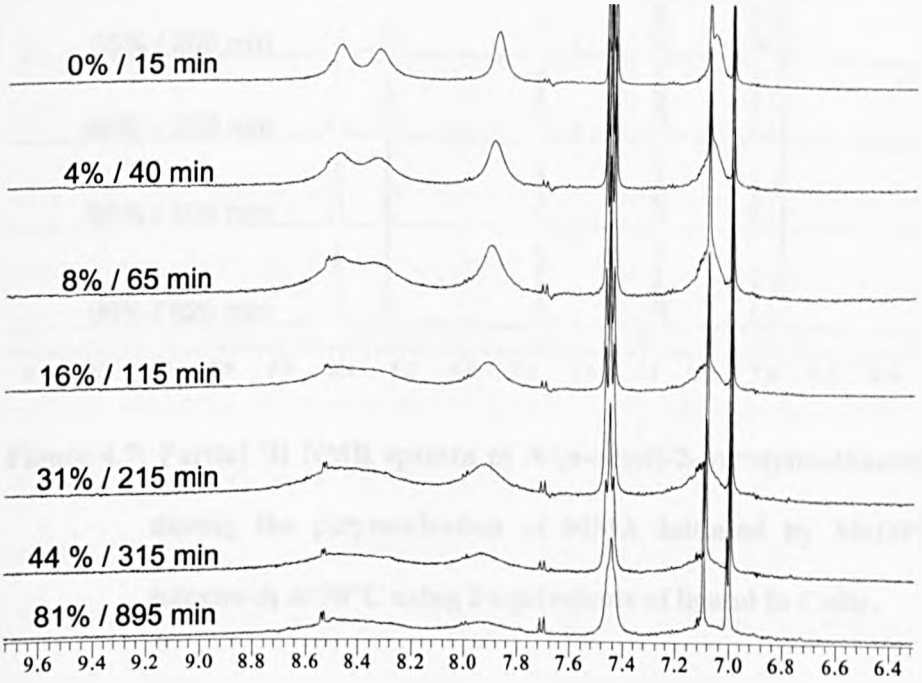

Figure 4.6: Partial ^{1}H NMR spectra of *N*-(*n*-octyl)-2-pyridylmethanimine ligand during the polymerisation of MMA initiated by MeOPEG-I_{45} in toluene-d_8 at 50°C using 2 equivalents of ligand to CuBr.

In the case of the polymerisation of MMA initiated by MeOPEG-I_{113} at 90°C, the combination of higher viscosity due to a bigger macroinitiator and higher temperature resulted in highly broad signals, up to a conversion of 90% (see figure 4.7). We observed then the loss of complex with time, and after 7 hours, only free ligand was present.

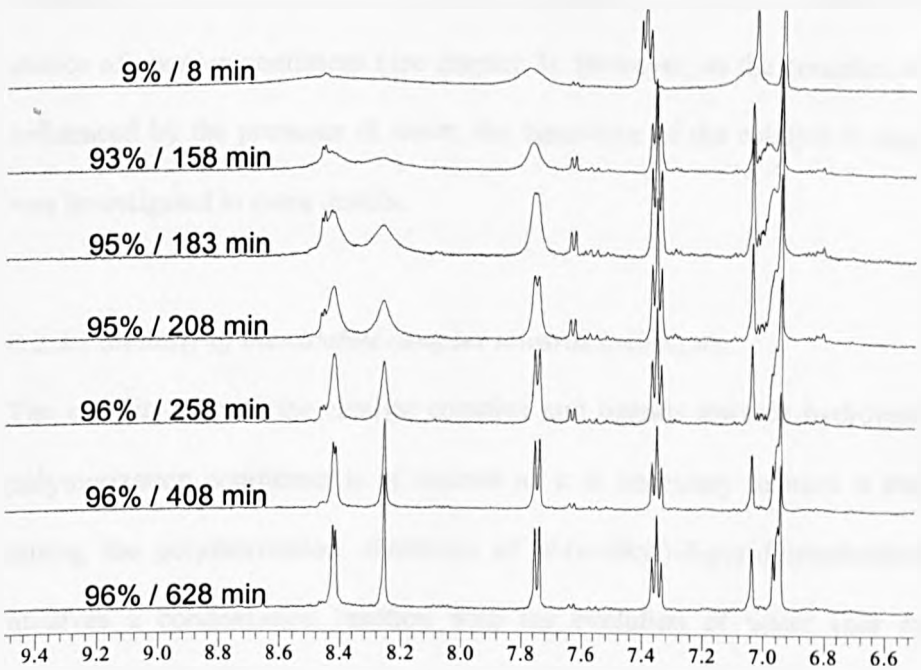

Figure 4.7: Partial ^{1}H NMR spectra of *N*-(*n*-octyl)-2-pyridylmethanimine ligand during the polymerisation of MMA initiated by MeOPEG-I_{113} in toluene-d_8 at 90°C using 2 equivalents of ligand to CuBr.

From these observations, it appears that when using an alkyl ether-based species in solution, the complexation of the ligand with copper is in competition with the possible complexation of the alkyl ether group. We observe that (i) the increase of the

solution viscosity slow down the whole complex giving a weak and broad signal and (ii) some free ligand appears. This is coherent with the previous observation made on the complex by itself: the alkyl ether species might replace the ligand on complexation on copper.

4.2.3. Effect of water on copper-mediated LRP.

Water has been shown to be an efficient solvent for LRP, but needs an appropriate choice of reaction conditions (see chapter 3). However, as the complex seemed to be influenced by the presence of water, the behaviour of the catalyst in aqueous media was investigated in more details.

4.2.3.1.Stability of the catalyst complex towards hydrolysis.

The stability of both the catalyst complex and ligands towards hydrolysis under the polymerization conditions is of interest as it is necessary to have a stable catalyst during the polymerization. Synthesis of *N*-(*n*-alkyl)-2-pyridylmethanimine ligands involves a condensation reaction with the evolution of water (see experimental section) such aliphatic imines can be hydrolytically unstable with addition of water reversing the equilibrium back to aldehyde and primary amine. However, in the present case both the catalyst complex and ligands are stable in water, under ambient conditions. Catalysts based on a range of *N*-(*n*-alkyl)-2-pyridylmethanimine ligands, **L**, and copper(I) bromide were used throughout this study (Figure 1), in ratios of [**L**]/[CuBr] of 3 to 1. [40] Catalyst stability under polymerisation conditions was followed by ^{1}H NMR spectroscopy in D_2O recording spectra every 15 mins, under an inert atmosphere. When *N*-(*n*-Octyl)-2-pyridylmethanimine is used, the complex acts

as a surfactant with a hydrophilic metalated head group and hydrophobic C-8 chain. This results in an inhomogeneous reaction mixture unsuitable for efficient polymerization. When the alkyl chain is shortened to C-5, *N*-(*n*-pentyl)-2-pyridylmethanimine, a water insoluble copper complex is formed, as observed by oily droplets dispersed in the aqueous medium. With C-3 and C-2 alkyl groups, *N*-(*n*-propyl)-2-pyridylmethanimine and *N*-(*n*-ethyl)-2-pyridylmethanimine, CuBr complexes lead to homogeneous dark-brown aqueous solutions.

Following these observations *N*-(*n*-propyl)-2-pyridylmethanimine was used for all further work. At 25 °C no decomposition of bis(*N*-(*n*-propyl)-2-pyridylmethanimine)copper(I) is observed after 10 hours in water under ambient conditions with no changes in the ^{1}H NMR spectrum, Figure 4.8.

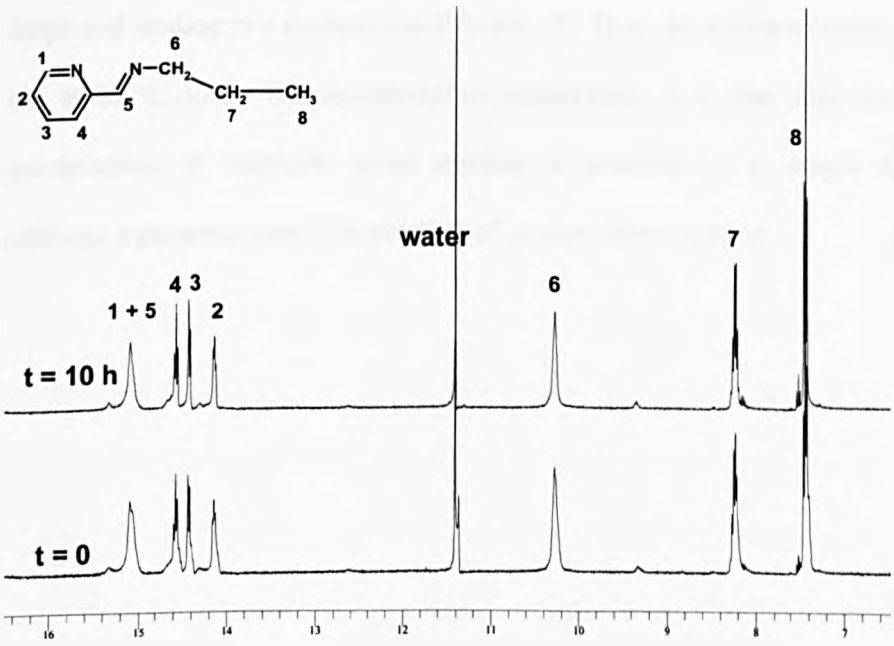

Figure 4.8: Selection of ^{1}H NMR (400 MHz) spectra of the bis(*N*-(*n*-Propyl)-2-pyridylmethanimine) copper(I) complex in D_2O recorded every 15 mins under Nitrogen at 25 °C.

At 50°C the complex begins to decompose after approximately 1 hour, releasing free ligand after 100 mins, Figure 4.9. The free ligand is stable towards hydrolysis, even at 50 °C, as seen by the lack of a peak at low attributable to an aldehyde proton. The formation of a red/orange precipitate accompanies the release of ligand, suspended in a slightly blue solution. Copper(I) is not generally stable in aqueous solution usually disproportionates to Cu(0) and Cu(II).[105] This disproportionation is thought to occur following the displacement of the bidentate N donor ligands on co-ordination of water to give the thermodynamic product. At 50°C exchange of both ligands occurs forming $Cu(I)_{aq}$ which disproportionates precipitating Cu(0) leaving $Cu(H_2O)_6^{2+}$ in solution. At 25°C there is insufficient kinetic driving force for both diimine ligands to be displaced leading to a dynamic equilibrium. [214] Thus, the polymerisations were carried out at 25 °C, under the decomposition temperature. It is also important to note that precipitation of insoluble metal residues is possible by a simple heat treatment offering a potential route for isolation of product from catalyst.

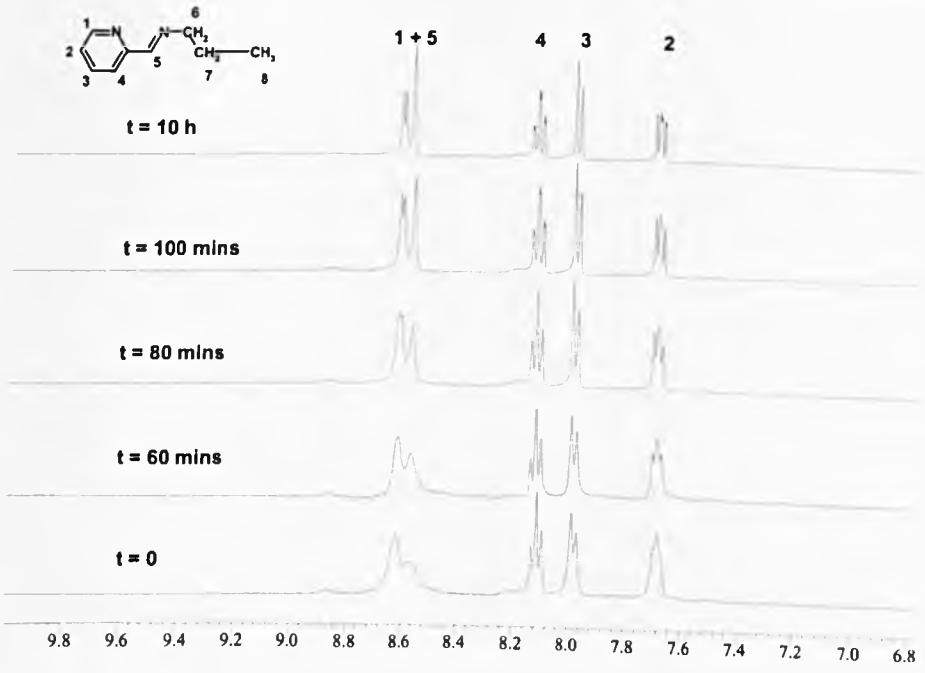

Figure 4.9: Selection of the aromatic area of ^{1}H NMR (400 MHz) spectra of the bis(N-(n-Propyl)-2-pyridylmethanimine)copper(I) complex in D_2O recorded every 15 mins under Nitrogen at 50 °C.

Bis(*N*-(*n*-propyl)-2-pyridylmethanimine)copper(I) is surprisingly stable in aqueous solution at ambient temperature. Hydrolysis of the complex, but not the ligand, occurs at 50°C over a short time period precipitating insoluble copper salts from solution. During the polymerisation, however, we observed an increase in rate (see part 3.2.) as noticed in presence of alkyl ether groups. Furthermore, the semilogarithmic plot showed an original behaviour, with $k_p[P_n^*]$ increasing during the reaction (part 3.2.2., figure 3.16). A parallel can be established between this observations and the catalyst behaviour in presence of alkyl ether groups (part 4.2.1.): a change could occur in the nature of the catalyst complex. Competition between co-ordination of both ligand, water and/or monomer changes the position of the Cu(I) / Cu(II) equilibrium resulting

in an increase in the overall rate of polymerisation. These effects are observed in each polymerisation reaction irrespective of the concentration of Cu(I) and Cu(II). In the extreme case we see the reaction stopping due to the loss of the catalyst from the system.

4.3. Potential polarity effect of the reaction medium.

An alternative explanation to the enhancement of the reaction is the increase of the polarity of the medium. The presence of alkyl ether in the polymerisation medium might increase the polarity of the solution, which might have a marked influence on the stability of the reactants/intermediates involved in the events typical of the transition-metal mediated living radical polymerisation process, *e.g.* the activation/deactivation process. Charge separation in the transition-state would be stabilised by an increase in polarity of the medium. In the present case higher rate coefficients for activation and lower rate coefficients for deactivation would explain the observed increase in the overall rate of polymerisation. Enhanced rate coefficients of activation upon increase of solvent polarity have been found by Chambard *et al.*[215] for poly(butylacrylate) macroinitiators using 4,4'-di-*n*-heptyl-2,2'-bipyridine, which can be explained by a change in catalyst structure and/or the above elucidated change in energy levels. Contradictory results, however, were found for poly(styrene) macroinitiators[215].

Solvent polarity is often characterised by dielectric constants, refractive indexes, or dipole moments. As the interactions between solvent and solute are not taken into account in these cases, empirical methods to determine solvent polarity have been

developed. One of these approaches is the use of solvatochromic dyes for which the absorption or emission band maxima shift according to the polarity of the medium in which they are dissolved.[216-221]

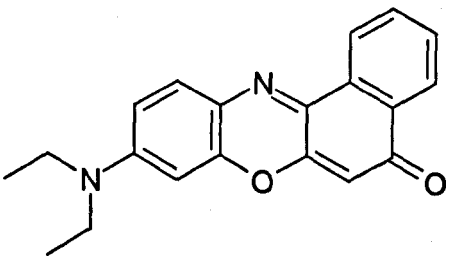

Figure 4.10: Structure of the solvatochromic dye Nile Red.

In the present case, Nile Red (Figure 4.10) was considered in order to investigate the change in polarity for different polymerisation solutions. Amongst positively solvatochromic dyes, Nile Red presents one of the largest bathochromic shifts known: when dissolved in increasingly polar media, the wavelength of its visible absorption maximum (λ_{max}) moves to longer wavelengths (lower energies). Thus, on changing solvent from water to pentane, a change in λ_{max} of 110 nm is observed.[222]

Nile Red has been used to determine the polarity of conventional solvents and binary mixtures[222-225] of supercritical fluids,[222,226] ionic liquids,[227] and used to probe the microenvironment of polymers,[223] xerogels, [228] liquid crystals,[229] and zeolites.[230] It has also been incorporated, as the sensing element, into fibre-optic devices capable of identifying and quantifying a range of organic vapours.[231,232]

Polarity measurements were undertaken in a range of different media including the polymerisation medium of BzMA, as studied in part 4.2.1. Nile Red concentration was

chosen so that absorbance would stay in the 0.5 to 1.0 range. This was achieved by preparing a stock solutions of Nile Red in the different solvents of interest (*n*-hexane, toluene, ethylene glycol diethyl ether, water) or monomer (BzMA) and diluted accordingly. Table 4.1 presents the different results obtained by UV spectroscopy for the wavelength of its visible absorption maximum (λ_{max}) and the corresponding energy E_{NR}.

	λ_{max} / nm	E_{NR} [a]
Water	593.2	201.7
Benzyl methacrylate (BzMA)	535.1	223.6
MeO(PEG)MA/toluene (50/50)	533.6	224.2
1,2-Diethoxy ethane/BzMA (50/50)	532.0	224.9
BzMA/toluene (50/50) + 0.9 M MeO(PEG)I	531.0	225.3
BzMA/toluene (50/50)	530.4	225.5
P(BzMA)/toluene (50/50)	530.2	225.6
Diethyl ether ethylene glycol	522.3	229.0
Toluene	521.5	229.4
n-Hexane	484.4	247.0

[a] $E_{NR} = (h*c*Na / \lambda_{max})*10^6$ kJ mol^{-1}

Table 4.1. λ_{max} and E_{NR} for Nile red in different media.

These results give information about the relative polarity of the media considered in this study and seems relevant when compared to the values of E_{NR} observed in the polarity table generated by Deye *et al.*[222] Furthermore, it confirms the relationship between the overall rate of polymerisation and the polarity of the medium: As expected,

the media of highest polarity present the highest polymerisation rate, water appearing to be the 'fastest' solvent.

4.4. Conclusion.

The solvent effect of alkyl ether and water on copper mediated living radical polymerisation has been investigated. The enhancement of the reaction rate seems to be due to the possible competition between the components and the ligand on the copper catalyst, modifying the activation/deactivation equilibrium of the copper complex. An alternative explanation was considered, as the influence of the polarity of the medium on the reactive bond Copper-Bromide. An increase of polarity would weaken this bond, increasing the concentration in active species and therefore the rate of the polymerisation.

Chapter 5

Physical properties of the surface active agents synthesised.

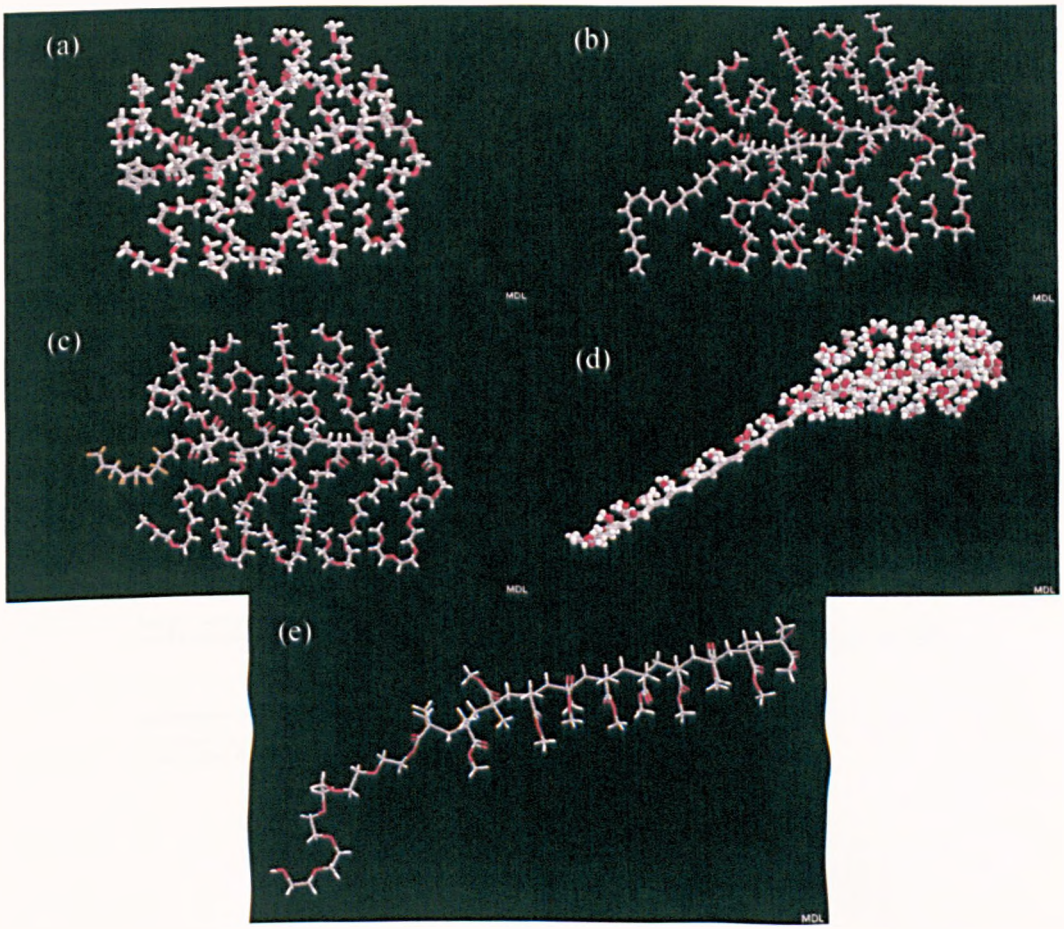

3D schematic of poly(MeOPEG-MA) initiated by (a) phenyl-2-bromoisobutyrate, (b) octadecyl-2-bromoisobutyrate, (c) α-perfluoroalkyl-2-bromoisobutyrate, (d) PMMA and (e) PMMA-*b*-MeOPEG.

5.1. Introduction.

As seen in chapter 1, living radical polymerisation is a technique of choice for the synthesis of well-defined architecture polymers. It has been demonstrated in the previous chapters that copper mediated LRP can be undertaken using poly(ethylene glycol)-based monomers or macroinitiators. Moreover, our group as developed an efficient procedure to synthesise methacrylate polymers in a living manner, using the copper-based system previously defined.[40] As PEG is a well-known crystalline polymer, widely used as surfactant due to its hydrophilic properties, it was interesting to associate it with a different polymer type. PMMA, an amorphous and hydrophobic polymer, was chosen, as both polymers are reported to be compatible (miscible in the solid state).[233,234] The use of MeOPEG as macroinitiator or macromonomer influenced the structure of the resulting copolymer. In the first case, an AB linear block copolymer was obtained, while the second case led to an AB graft block copolymer (the polymerisation of MeOPEG-MA results in a graft polymer, with a methacrylate backbone), as schematise in figure 5.1.

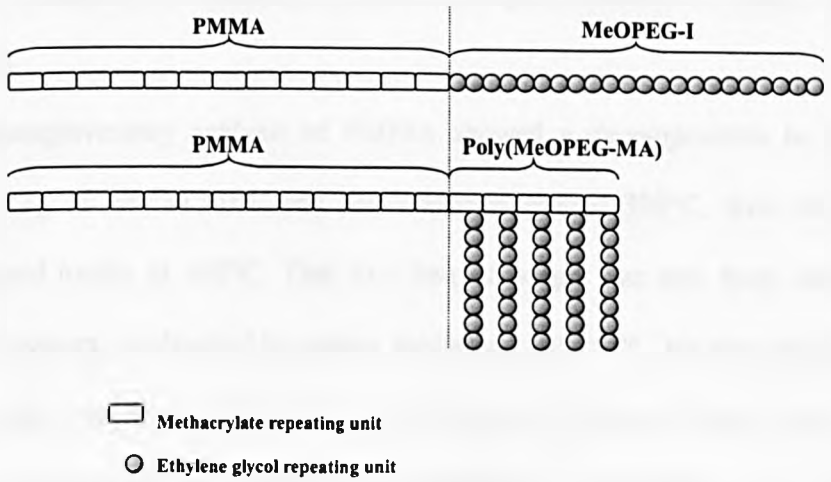

Figure 5.1: Schematic of the various block PMMA-*b*-MeOPEG copolymers studied in this chapter.

This final chapter reports the study of various physical properties of the products previously synthesised. Firstly, the thermal properties of the block and graft polymer were compared, then the modification of the surface properties of PMMA was investigated by incorporation of PEG blocks, and finally aggregates properties of PEG based polymers in aqueous media were considered.

5.2. Thermal properties.

In order to test the thermal properties, thermogravimetry analysis (TGA) and differential scanning calorimetry (DSC).

5.2.1. Thermogravimetry.

5.2.1.1.PMMA containing block copolymers.

TGA was used to test the influence of a MeOPEG block on the thermal stability of the PMMA. Compounds including a linear and graft MEOPEG block were also compared.

The thermogravimetry analysis of PMMA showed a decomposition in two steps (Figure 5.1). A loss of 10% was first observed around 300°C, then the polymer decomposed totally at 400°C. This first loss of weight has also been observed on similar polymers, synthesised by copper mediated LRP.[235,236] This was ascribed to the loss of methyl bromide followed by the cyclisation of the two final units to give a lactone end group. On the other hand, MeOPEG-I_{113} was slightly more stable, and decomposed totally in one step, at 450°C (Figure 5.2).

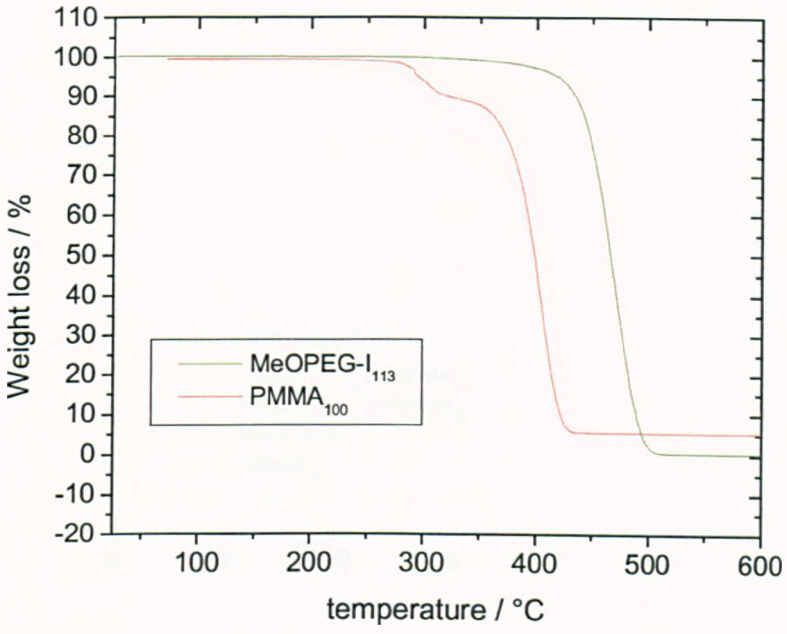

Figure 5.2: Thermal decomposition of PMMA and MeOPEG-I_{113}.

Following these observations, one would expect a three-steps decomposition for a PMMA-*b*-MeOPEG copolymer, corresponding respectively to the chain-end group, PMMA and MeOPEG blocks. However, TGA measurements exhibited only two steps, in a similar way as those observed for the PMMA homopolymer. Figure 5.3 shows the TGA of various PMMA-*b*-$MeOPEG_{113}$ polymers, with different PMMA chain lengths. In each case, the first loss appeared more important (15-20 %wt/wt) than the one observed on PMMA homopolymer and happened at a lower temperature (280°C). The second step corresponds to the total decomposition of the polymer; the decomposition of the methacrylate chain initiates the MeOPEG block one, leading to a one step decomposition. Upon variation of the length of the PMMA block, no change were observed.

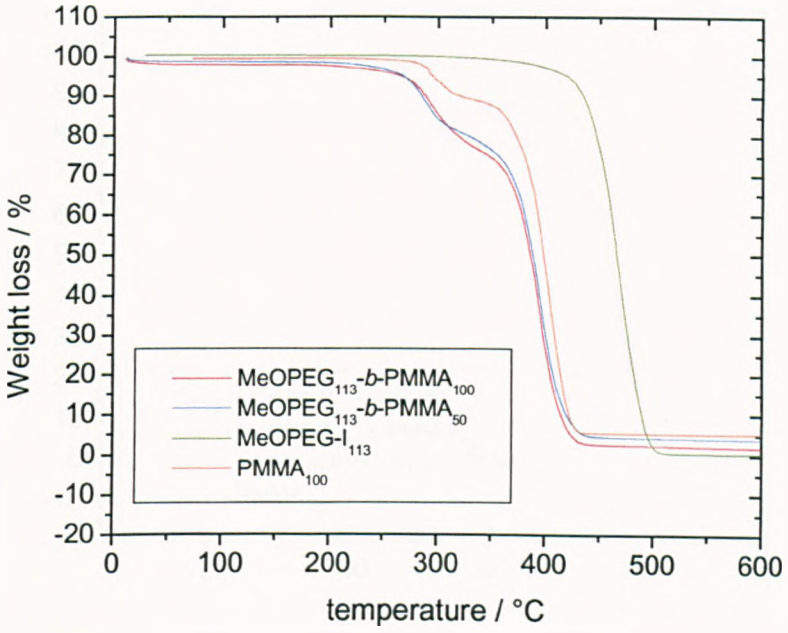

Figure 5.3: Thermal decomposition of PMMA, MeOPEG-I_{113} and PMMA-*b*-MeOPEG$_{113}$ block copolymers with various PMMA molecular weight.

In order to verify the influence of the MeOPEG block, the same analysis were carried out with MeOPEG$_{12}$ and poly(MeOPEG-MA) in the copolymer (Figure 5.4). The copolymer containing the MeOPEG$_{12}$ block behaved similarly as the PMMA homopolymer, probably due to the small size of the macroinitiator. However, when comparing two PEG chains of similar size but different structure, the two-step decomposition occured at the same temperature, but the first weight loss was more important for the MeOPEG-I_{113} containing copolymer (20%) than for the polymer containing poly(MeOPEG-MA) (15%) or the PMMA homopolymer (10%).

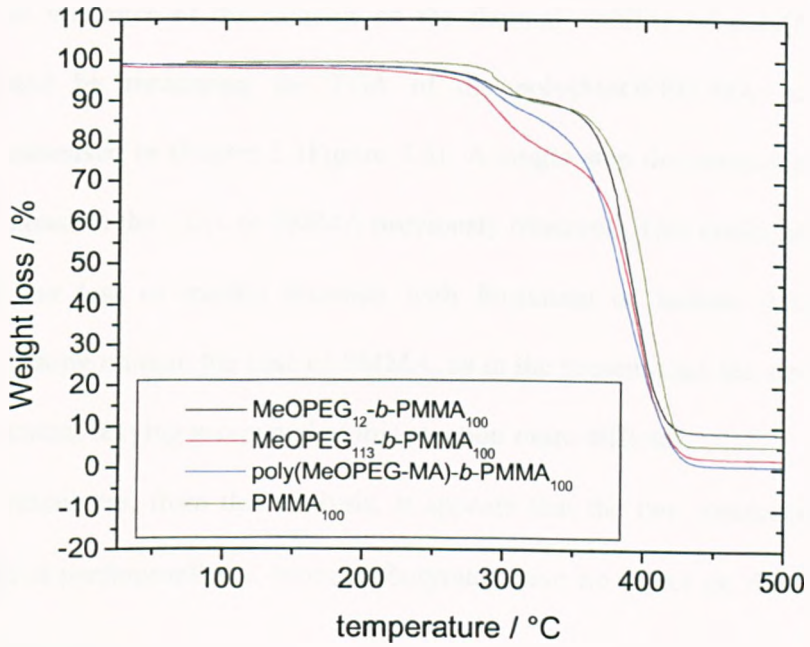

Figure 5.4: Thermal decomposition of $PMMA_{100}$, $PMMA_{100}$-b-$MeOPEG_{12}$, $PMMA_{100}$-b-$MeOPEG_{113}$ and $PMMA_{100}$-*b*-poly(MeOPEG-MA) block copolymers.

The close behaviour of PMMA-*b*-poly(MeOPEG-MA) with PMMA can be explained by the similarity in their structure, as poly(MeOPEG-MA) backbone is a methacrylate chain. The decomposition initialised by the PMMA chains propagates through the methacrylate backbone of poly(MeOPEG-MA), which initiates the decomposition of the ethylene glycol pendant chains, as described above. The first weight loss was however not fully understood.

5.2.1.2.Poly(MeOPEG-MA) containing polymers.

The influence of the initiator on the thermal stability of poly(MeOPEG-MA) was tested by measuring the TGA of the poly(MeOPEG-MA) containing products synthesised in chapter 3 (Figure 5.5). A single step decomposition was obtained, in contrast to the TGA of PMMA previously observed. This could justify the hypothesis of the loss of methyl bromide with formation of lactone between the two last repeating units in the case of PMMA, as in the present case the steric hindrance of the potential leaving group makes this reaction more difficult.

Furthermore, from this analysis, it appears that the two macroinitiators (Octadecyl- and α-perfluoroalkyl-2-bromoisobutyrate) have no effect on the thermal stability of the polymer.

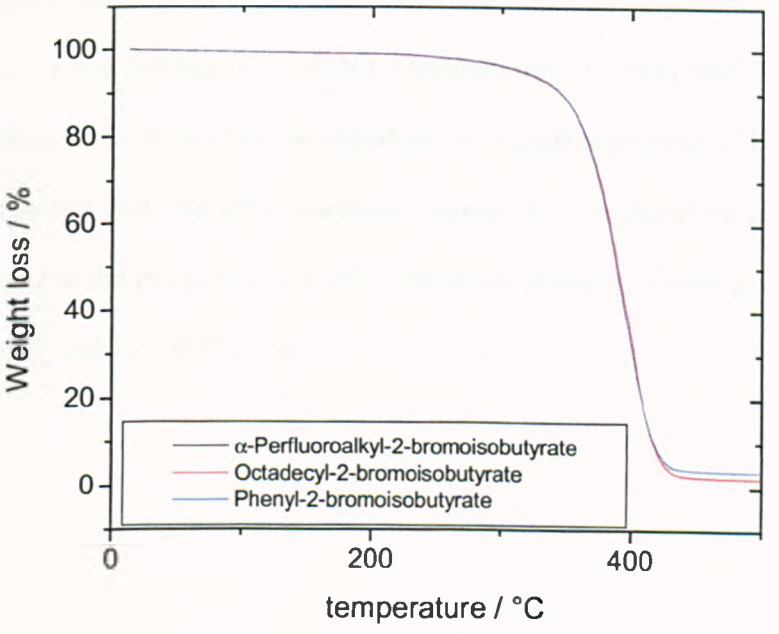

Figure 5.5: Thermal decomposition of poly(MeOPEG-MA) with various initiators.

5.2.2. Differential scanning calorimetry.

As MeOPEG is a crystalline polymer and PMMA is amorphous, the thermal behaviour of the block copolymer was investigated by DSC. MeOPEG-I_{12} and MeOPEG-I_{113} were considered to study the influence of the poly(ethylene glycol) block molecular weight over the copolymer, while varying the molecular weight of PMMA. The influence of the nature of the MeOPEG block (linear or graft) was also studied.

Table 5.1 gives a summary of the different thermal transition temperatures. PMMA is a well-known amorphous polymer, exhibiting a glass transition temperature (T_g) around 110°C (a). In the case of high molecular weights (M_n ~ 5,000 g/mol) Poly(ethylene glycol) is a crystalline polymer, showing both crystallisation (T_c = 37.8°C) and melting (T_m = 62.9°C) temperatures (b). Poly(MeOPEG-MA) with M_n ~ 5,000 g/mol can however be considered as a graft copolymer of PMMA (methacrylate backbone) and MeOPEG (pendent chains). It was therefore not surprising that it exhibited the properties of a semi-cristalline polymer, showing a T_g < -20°C, T_c = -13.6°C and T_m = 0.2°C (c).

		T_g	T_c	T_m
a	$PMMA_{105}$	107.0°C	-	-
b	MeOPEG-I_{113}	-	37.8°C	62.9°C
c	Poly(MeOPEG-MA)	<-20°C	-13.6°C	0.2°C
d	$MeOPEG_{12}$-*b*-$PMMA_{100}$	104.2°C	-	-
e	$MeOPEG_{12}$-*b*-$PMMA_{63}$	90.1°C	-	-
f	$MeOPEG_{113}$-*b*-$PMMA_{100}$	35.5°C	-	-
g	$MeOPEG_{113}$-*b*-$PMMA_{200}$	66.0°C	-	-
h	Poly(MeOPEG-MA)-*b*-$PMMA_{100}$	41.0°C	-	-
i	Poly(MeOPEG-MA)-*b*-$PMMA_{200}$	92.9°C	-	-
j	PMMA / MeOPEG blend	105°C	14.2°C	58.4°C

Table 5.1: Summary of the transition temperatures for the various PMMA-*b*-MeOPEG copolymers.

The block copolymers showed the loss of the semi-crystalline properties of MeOPEG (no T_c or T_m observed) by opposition to the blend (d-j). This can be understood by a better mix of the two polymers when copolymerised, the PMMA chains influencing the structure adopted by the molecules of MeOPEG. This led to a homogeneous product, showing only one glass transition. This T_g could be adjusted by varying the length of the PEG or PMMA blocks (d, e, f. g): In each case, an increase of the proportion of the PEG block resulted in the decrease of the T_g of the copolymer.

The influence of the nature of the MeOPEG chain was also reported: For same blocks length, at lower proportion of PMMA (f, h), the influence of the graft or block PEG chains does not influence the T_g of the copolymer (35.5°C in the case of $PMMA_{100}$–*b*-

$MeOPEG_{113}$ and 41.0°C for $PMMA_{100}$–*b*-poly(MeOPEG-MA). However, when the proportion of PMMA is increased to a DP of 200, the temperature dropped from 92.9°C in the case of poly(MeOPEG-MA) (i) to 66.0°C for MeOPEG-I_{113} (g). In the case of the $PMMA_{200}$–*b*-poly(MeOPEG-MA), the percentage of methacrylate backbone was more important than for $PMMA_{200}$–*b*-$MeOPEG_{113}$, increasing the stiffness of the copolymer. The former copolymer needed therefore more energy for flexibility than the latter, resulting in a higher glass transition temperature.

5.3. Surface Properties.

5.3.1. Surface and Interfacial Tension.[237-239]

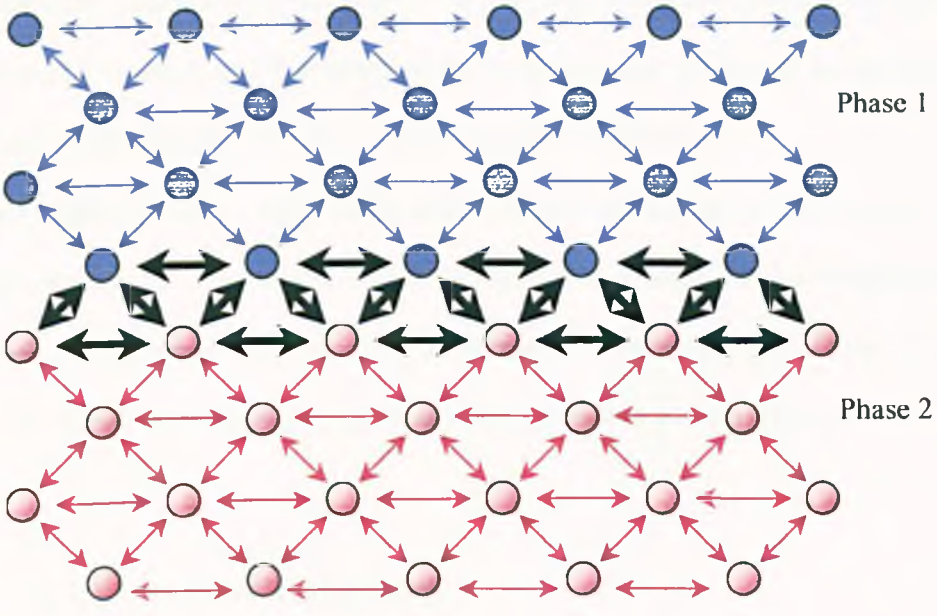

Figure 5.6: Scheme of the forces applied to molecules in a liquid and at the interface air-liquid.

Surface tension is a measurement of the cohesive energy present at an interface. As an equal attractive force in all directions balances the interactions of a molecule in a defined phase, molecules situated on the interface experience an imbalance of forces (see figure 5.6).

The net effect of this situation is the presence of free energy at the interface. This excess energy is called surface free energy and can be quantified as a measurement of energy/area. It is also possible to describe this situation as having a line tension or surface tension which is quantified as a force/length measurement. The common units for surface tension are dynes/cm or mN/m. When one of the phases is the vapour phase of a liquid being tested the measurement is referred to as *surface tension.* If the surface investigated is the interface of two liquids the measurement is referred to as *interfacial tension.* In either case the more dense fluid is referred to as the 'heavy phase' and the less dense fluid is referred to as the 'light phase'.

Polar liquids, such as water, have strong intermolecular interactions and thus high surface tensions. Any factor, which decreases the strength of this interaction, will lower surface tension. Therefore as an increase in the temperature of the system or any contamination, especially by surfactants, will lower surface tension.

5.3.2. Contact angle measurement.

Contact angles are used as a measure of the wetting interaction between a liquid and a solid. Two different approaches are commonly used to measure contact angles of non-porous solids: goniometry and tensiometry. Goniometry involves the observation of a sessile drop of test liquid on a solid substrate. Tensiometry involves measuring the

forces of interaction as a solid is contacted with a test liquid. Both techniques were used and compared with the products synthesised in the precedent parts.

5.3.2.1.Contact angle by the Sessile Drop method.

5.3.2.1.1.Introduction.[240-242]

Contact angle measurement is a straight forward method for surface analysis related to surface energy and surface tension. Contact angle describes the shape of a liquid drop resting on a solid surface. By drawing a tangent line from the drop shape to the touch of the solid surface, contact angle is defined as the angle between the tangent line and the solid surface. The measurement provides information to study the bonding energy of the solid surface and surface tension of the liquid droplet. Due to the simplicity of this technique and measurement, it has been broadly accepted in various research environments and industries for material surface analysis related to wetting, adhesion and absorption.

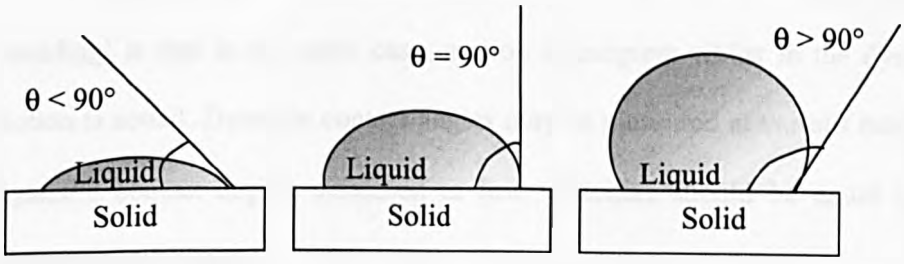

Figure 5.7: Different behaviour of liquid on a solid surface.

Contact angle, θ, is a quantitative measure of the wetting of a solid by a liquid. It is defined geometrically as the angle formed by a liquid at the three-phase boundary where a liquid, gas and solid intersect. It can be seen from figure 5.7 that low values

of θ indicate that the liquid spreads, or wets well, while high values indicate poor wetting. If the angle q is less than 90° the liquid is said to wet the solid. If it is greater than 90° it is said to be non-wetting. A zero contact angle represents complete wetting.

The measurement of a single static contact angle to characterise the interaction is no longer thought to be adequate. For any given solid/ liquid interaction there exists a range of contact angles which may be found. The value of static contact angles is found to depend on the recent history of the interaction. When the drop has recently expanded the angle is said to represent the 'advanced' contact angle. When the drop has recently contracted the angle is said to represent the 'receded' contact angle. These angles fall within a range with advanced angles approaching a maximum value and receded angles approaching a minimum value.

If the three-phase (liquid/solid/vapour) boundary is in actual motion, the angles produced are called Dynamic Contact Angles and are referred to as 'advancing' and 'receding' angles. The difference between 'advanced' and 'advancing', 'receded' and 'receding' is that in the static case, motion is incipient whilst in the dynamic case, motion is actual. Dynamic contact angles may be measured at various rates of speed. Dynamic contact angles measured at low velocities should be equal to properly measured static angles.

The difference between the maximum (advanced/advancing) and minimum (receded/receding) contact angle values is called the contact angle hysteresis. It has been used to help characterise surface heterogeneity, roughness and mobility. For surfaces that are not homogeneous there will exist domains on the surface that present barriers to the motion of the contact line. For the case of chemical heterogeneity these

domains represent areas with different contact angles than the surrounding surface. For example when wetting with water, hydrophobic domains will pin the motion of the contact line as the liquid advances thus increasing the contact angles. When the water recedes the hydrophilic domains will hold back the draining motion of the contact line thus decreasing the contact angle. From this analysis it can be seen that, when testing with water, advanced angles will be sensitive to the hydrophobic domains and receded angles will characterise the hydrophilic domains on the surface. For situations in which surface roughness generates hysteresis the actual microscopic variations of slope in the surface create the barriers which pin the motion of the contact line and alter the macroscopic contact angles.

Contact angle can also be considered in terms of the thermodynamics of the materials involved. This analysis involves the interfacial free energies between the three phases and is given by:

$$g_{lv} * \cos\theta = g_{sv} - g_{sl}$$

with g_{lv} ,g_{sv} and g_{sl} referring to the interfacial energies of the liquid/vapour, solid/vapour and solid/liquid interfaces.

The production of drops with advanced and receded edges involves one of two strategies. Drops can be made to have advanced edges by addition of liquid. Receded edges may be produced by allowing sufficient evaporation or by withdrawing liquid from the drop. Alternately, both advanced and receded edges are produced when the stage on which the solid is held is tilted to the point of incipient motion. By using an instrument with high-speed image capture capabilities, shapes of drops in motion may be analysed (Figure 5.8).

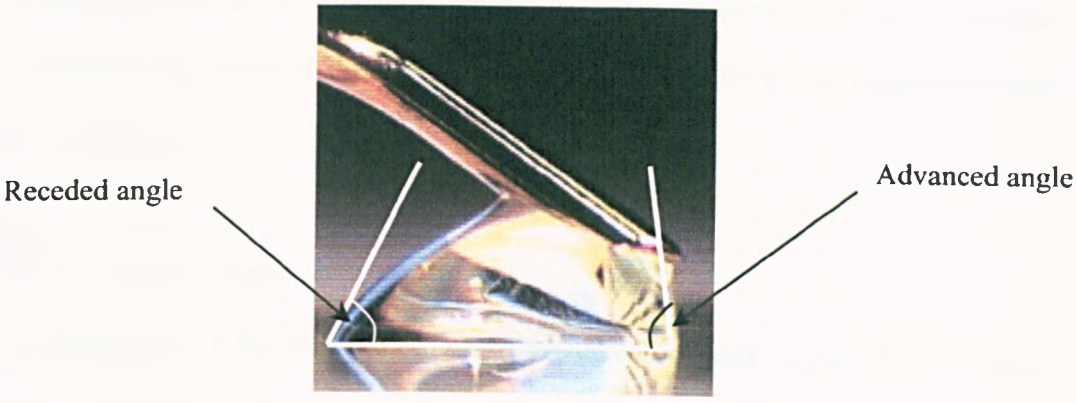

Figure 5.8: Example of a drop in motion, showing the advanced and receded angles.

Goniometry can be used in many situations where tensiometry cannot. A great variety of solid substrates can be used, provided they have a relatively flat portion for testing and can fit on the stage of the instrument. Substrates with regular curvature, such as contact lenses are also easily analysed.

Testing can be done using very small quantities of liquid. It is also easy to test high temperature liquids such as polymer melts.

The assignment of the tangent line that will define the contact angle is a factor that can limit the reproducibility of contact angle measurements. Conventional goniometry relies on the consistency of the operator in the assignment of the tangent line. This can lead to significant error, especially subjective error between multiple users.

The conditions that produce advanced and receded angles are sometimes difficult to reproduce. Although drops in motion can produce data on dynamic contact angles the velocity of motion cannot be controlled. It is also less suited, when compared to tensiometry, to analysis of the effects of wetting on changes in contact angle. In

addition the amount of surface sampled for each measurement is limited and multiple measurements should be used to characterise a surface. Fibbers are not easily studied by goniometry.

5.3.2.1.2.Measurements

Measurements of the sessile drop were undertaken on block co-polymers of PMMA and MeOPEG, the latter being either a linear chain MeOPEG-I or a graft chain Poly(MeOPEG-MA). The molecular weights of the PMMA homopolymer and the PMMA block in the co-polymer were kept above 10,000 g/mol, in order to avoid dissolution of the co-polymer when in contact with water. Measurements were undertaken on both freshly spin coated film and 24 hours annealed cast at 140°C (above the polymers T_g).

	Advanced angle (°)	**Receded angle (°)**
PMMA	75.1	59.3
$MeOPEG_{12}$-*b*-$PMMA_{50}$	57.1	39.5
$MeOPEG_{12}$-*b*-$PMMA_{100}$	66.7	47.3
$MeO(PEG)_{113}$-*b*-$PMMA_{100}$	51.0	32.1
$MeO(PEG)_{113}$-*b*-$PMMA_{200}$	60.1	41.8
Poly(MeOPEG-MA)-*b*-$PMMA_{100}$	54.5	27.7
Poly(MeOPEG-MA)-*b*-$PMMA_{200}$	62.4	35.1

Table 5.2: Summary of the advanced and receded contact angles measured by the sessile drop on freshly cast films.

From table 5.9, the influence of the molecular weight of the poly(ethylene glycol) chain can be discussed on the freshly cast films: For small initiator chains, only the receded angle was changed. This showed that the hydrophilic character of PMMA was increased, while the hydrophobicity stayed unchanged (decrease of the receded angle from 51.2° to 47.3° while the advanced angle stays around 67°). When increasing the chain length of the macro-initiator, the effects on both hydrophobicity and hydrophilicity of the resulting co-polymer surface were more obvious: The surface appeared less hydrophobic (advanced angle = 51.0°) but more hydrophilic (receded angle = 32.1°).

A different effect was observed when changing the structure of the macro-initiator: For a PMMA of DP= 100, when using the graft PEG, the hydrophobicity of the surface changed less (advanced angle = 54.5° when using poly(MeOPEG-MA) against 51.0° when using MeOPEG-I_{113}), while its hydrophilic character was enhanced (receded angle = 27.7° when using poly(MeOPEG-MA) against 32.1° when using MeOPEG-I_{113}). The same observations were made for $PMMA_{200}$ .It seems therefore that the graft PEG has a stronger influence on the surface than the linear PEG. This can be attributed to the similarity in structure of the two methacrylate blocks, resulting in a better incorporation of the hydrophilic block in the PMMA structure.

	Advanced angle (°)	Receded angle (°)
$PMMA_{100}$	75.5	60.2
$MeOPEG_{12}$-*b*-$PMMA_{50}$	75.7	51.3
$MeOPEG_{12}$-*b*-$PMMA_{100}$	75.2	57.7
$MeOPEG_{113}$-*b*-$PMMA_{100}$	73.6	53.6
$MeOPEG_{113}$-*b*-$PMMA_{200}$	74.6	54.8
Poly(MeOPEG-MA)-*b*-$PMMA_{100}$	74.2	55.6
Poly(MeOPEG-MA)-*b*-$PMMA_{200}$	75.7	55.7

Table 5.3: Summary of the advanced and receded contact angles measured by the sessile drop on annealed cast films.

After annealing the film, the products behave in a complete different way (see table 5.3). The advanced angle of all the products is very close to the PMMA one, while a decrease in the receded angle is noticed. No major differences were observed between the different structures of the PEG block. It appears therefore that when heated above its T_g the products saw its polymer chains mixing together. This is logical with the thermal properties already observed above, as PEG and PMMA were found to be compatible. The resulting products showed a hydrophobic character unchanged from the original PMMA, while their hydrophilicity was increased.

5.3.2.2.Contact angle by the Wilhelmy Technique.

5.3.2.2.1.Introduction.[240,243-246]

The tensiometric method for measuring contact angles measures the forces that are present when a sample of solid is brought into contact with a test liquid. If the forces

of interaction, geometry of the solid and surface tension of the liquid are known, the contact angle may be calculated. Measurement of the surface tension of the liquid was first made using a DuNouy ring. The sample of the solid to be tested was hung on the balance and tarred. The liquid is then raised to contact the solid. When the solid contacts the liquid the change in forces is detected and the tensiometer registers this elevation as zero depth of immersion. As the solid is pushed into the liquid the forces on the balance are recorded. The forces on the balance are:

F_{total} = wetting force + weight of probe - buoyancy

The tensiometer has tarred the weight of the probe and can remove the effects of the buoyancy force by extrapolating the graph back to zero depth of immersion. The remaining component force is the wetting force which is defined as:

Wetting force = $g_{LV} * P * \cos(\theta)$

with g_{lv} is the liquid surface tension, P is the perimeter of the probe and θ is the contact angle. This contact angle, which is obtained from data generated as the probe advances into the liquid, is called the *advancing contact angle*. The sample is immersed to a set depth and the process is reversed. As the probe retreats from the liquid data collected is used to calculate a *receding contact angle*. The process will appear as shown on figure 5.9.

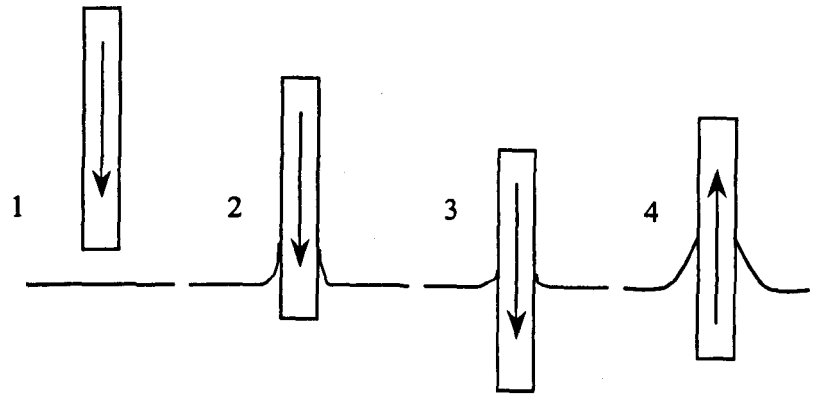

Figure 5.9: Process of the measurement of advancing (3) and receding (4) angle using the Wilhelmy technique.

The evolution can then be followed as a graph of force/wetted length *vs.* depth of immersion (see Figure 5.10).

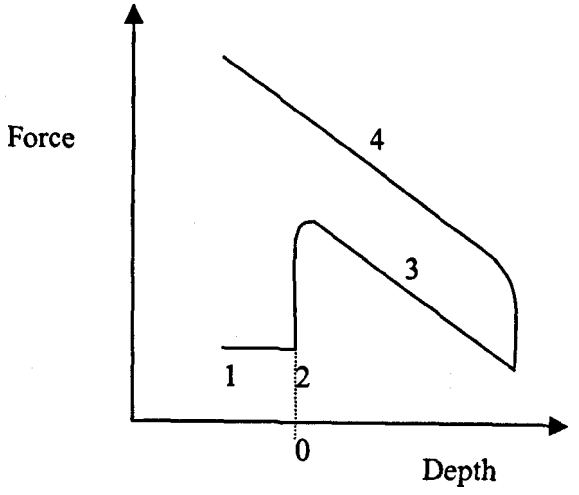

Figure 5.10: Graph of force/wetted length *vs.* depth of immersion.

Firstly, the sample is above the liquid and the force/ length is set to zero (1). When the sample hits the surface with a contact angle < 90° (2), the liquid rises up causing a positive force. The sample is then immersed, resulting in the buoyant force to increase, which causes a decrease in the force on the balance (3). The forces measured

are the one of the advancing angle. After having reached the desired depth the sample is pulled out of the liquid (4). The forces are then measured for the receding angle.

The use of tensiometry for measurement of contact angle has several advantages over conventional goniometry. At any point on the immersion graph, all points along the perimeter of the solid at that depth contribute to the force measurement recorded. Thus the force used to calculate θ at any given depth of immersion is already an averaged value. An averaged value can be calculated for the entire length of the sample or average any part of the immersion graph data to assay changes in contact angle along the length of the sample. Hysteresis, the difference between advancing and receding angles, is very easy to determine using this method. By using multiple cycles it is possible to identify variations in surface structure and notice adsorption phenomena.

There are two major limitations for the application of this technique. Firstly the user must have enough of the liquid being tested available so that he can immerse a portion of his solid in it. Secondly the solid sample must be formed in a regular geometry such that it has a constant perimeter over a portion of its length. This is easily achieved when coating the product on a well-known shape support, keeping the same surface on all sides which contact the liquid.

5.3.2.2.2.Measurements.

Film of non-annealed copolymers were observed to degrade through the dipping cycles and resulted in non-reproducible results. However, annealed sample gave better hysteresis (see figure 5.11) and were the only ones taken into account for the discussion.

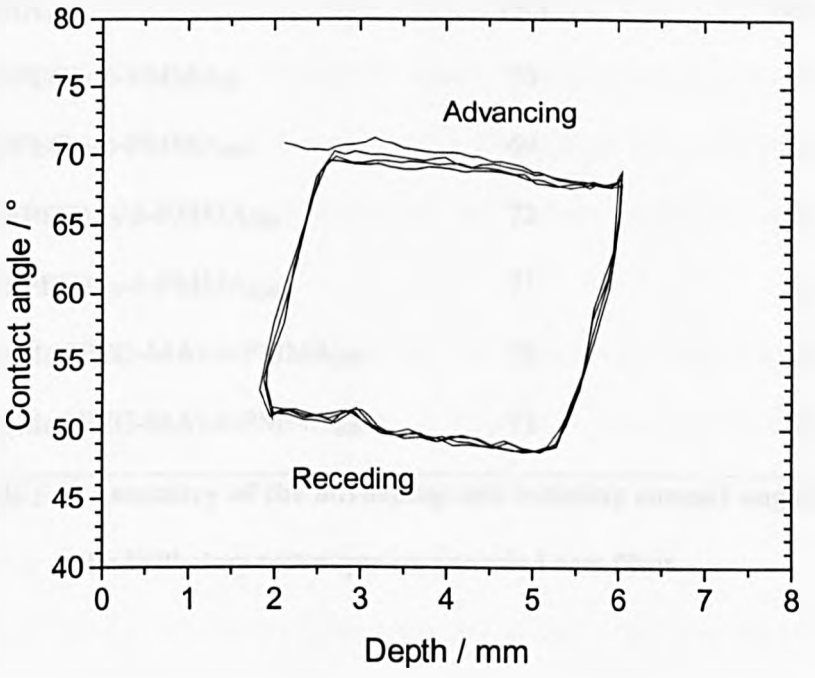

Figure 5.11: Example of contact angle hysteresis loops for water on $MeOPEG_{12}$-*b*-$PMMA_{50}$ cast on glass slide measured by the Wilhelmy technique.

Table 5.4 gives a summary of the contact angles measured for various products. Overall, the angles are found slightly smaller than in the case of the sessile drop method, but the same trend is kept: While the advancing angle is close to the PMMA one, the receding angle is slightly smaller, sign of an increase of the hydrophilicity of the surface.

	Advancing angle (°)	Receding angle (°)
$PMMA_{100}$	75.5	60.2
$MeOPEG_{12}$-*b*-$PMMA_{50}$	70	51
$MeOPEG_{12}$-*b*-$PMMA_{100}$	69	53
$MeO(PEG)_{113}$-*b*-$PMMA_{100}$	72	44
$MeO(PEG)_{113}$-*b*-$PMMA_{200}$	71	48
Poly(MeOPEG-MA)-*b*-$PMMA_{100}$	73	49
Poly(MeOPEG-MA)-*b*-$PMMA_{200}$	71	52

Table 5.4: Summary of the advancing and receding contact angles measured by the Wilhelmy technique on annealed cast films.

As a conclusion, both sessile drop and Wilhelmy technique were found to give accurate results concerning the surface properties of the copolymers films.

5.4. Aggregate properties.

Certain molecules may be said to contain two distinct components, differing in their affinity for solutes. The part of the molecule that has an affinity for polar solutes, such as water, is said to be hydrophilic. The part of the molecule that has an affinity for non-polar solutes, such as hydrocarbons, is said to be hydrophobic. Molecules containing both types of components are said to be amphiphilic.

Such molecules display distinct behaviour when interacting with water. The polar part of the molecule 'seeks' to interact with water while the non-polar part 'shuns' interaction with water. There are two ways in which such a molecule achieves both these states.

An amphiphilic molecule can arrange itself at the surface of the water such that the polar part interacts with the water and the non-polar part is held above the surface (either in the air or in a non-polar liquid) as shown below. The presence of these molecules on the surface disrupts the cohesive energy at the surface and thus lowers the surface tension. Such molecules are called 'surface active' molecules or surfactants.

Another arrangement of these molecules can allow each component to interact with its favoured environment. Molecules can form aggregates in which the hydrophobic portions are oriented within the cluster and the hydrophilic portions are exposed to the solvent. Such aggregates are called micelles.

The proportion of molecules present at the surface or as micelles in the bulk of the liquid depends on the concentration of the amphiphile. At low concentrations surfactants will favour arrangement on the surface. As the surface becomes crowded with surfactant more molecules will arrange into micelles. At some concentration the surface becomes completely loaded with surfactant and any further additions must arrange as micelles. This concentration is called the Critical Micelle Concentration (CMC). In the present study, until evidences of micelles presence is given, this concentration would be considered as the critical *aggregate* concentration (CAC).

It has been seen in introduction that poly(ethylene glycol) shows interesting surfactant properties. As poly(MeOPEG-MA) present an hydrophobic methacrylate backbone and hydrophilic pendant PEG chains, it should exhibit amphiphilic properties. In order to enhance and test these properties, the hydrophobic character of the graft polymer was increased by introduction of hydrophobic initiators. Therefore, block copolymers were formed showing an enhanced hydrophobic block with an alkyl chain of 18

carbon atoms, a fluorinated chain of 12 fluorinated carbon atoms and a $PMMA_{50}$ oligomer (M_n = 5,000 g/mol). In order to test the difference in behaviour of the graft and linear PEG chains, the latter product was also compared to a $PMMA_{50}$-*b*-$MeOPEG_{113}$ copolymer (See chapter 5-2). Figure 5.12 summarises the products of interest.

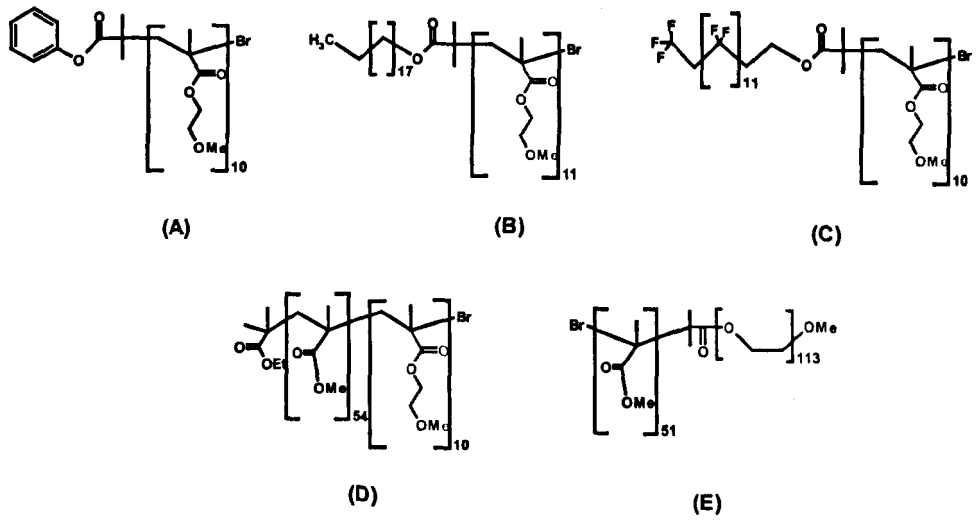

Figure 5.12: Surfactants molecules synthesised in the previous chapter and tested in the present study: Phenol ester poly(MeOPEG-MA) (A), Octadecyl-2-bromoisobutyrate poly(MeOPEG-MA) (B), α-perfluoroalkyl-2-bromoisobutyrate poly(MeOPEG-MA) (C), $PMMA_{50}$-*b*-poly(MeOPEG-MA) (D) and $PMMA_{50}$-*b*-$MeOPEG\text{-}I_{113}$ (E). The grey bonds represent the hydrophilic block.

As (D) and (E) were not directly water soluble, the solution were prepared by dissolving the block copolymers in THF (1 wt%) and dispersing the organic solution in water (changing the concentration from 1 g/l to 10^{-6} g/l). In the case of (D), as soon as water was added, the copolymer precipitated. The same process was unsuccessfully

repeated at various concentrations in THF and water. This non-water-solubility can be explained by the similarity in the backbone structure of PMMA and poly(MeOPEG-MA), as already observed for the DSC analysis: The product, showing a too strong hydrophobic character, does not dissolve in water.

See chapter 2 and 3 for the details of the synthesis.

5.4.1. CAC measurement by tensiometry.

5.4.1.1.Introduction.[240,247-249]

Measurement of surface tension may be used to find CAC. A graph of surface tension *vs.* log of concentration of surfactant added will appear as represented on figure 5.13.

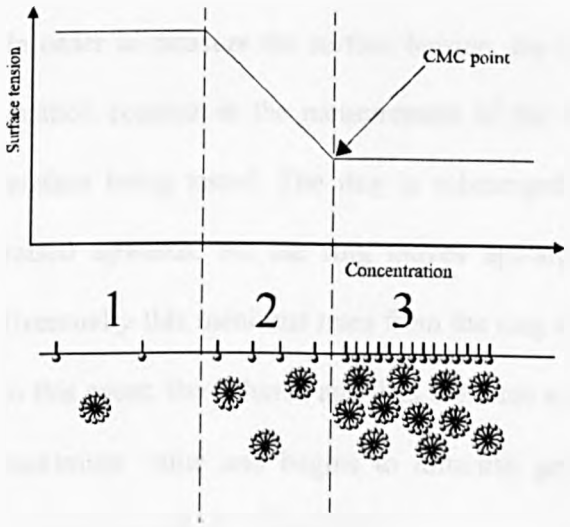

Figure 5.13: Evolution of the surface tension with the surfactant concentration.

In this graph, three phases are observed: At very low concentrations of surfactant only slight change in surface tension is detected (1). Upon addition of surfactants, the

surface tension decreases (2). Finally, the surface becomes fully loaded and no further change in surface tension is observed (3).

As shown above the technique for assaying CAC by measurement of surface tension is simple and straightforward. A graph of surface tension *vs.* log concentration is produced by measuring a series of manually mixed surfactant solution. The CAC is found as the point at which two lines intersect; the baseline of minimal surface tension and the slope where surface tension shows linear decline.

Many researchers are interested in finding the CAC for surfactants in order to optimise detergency and minimize waste. Beyond the calculation of CAC the researcher will also produce a graph which shows surface tension across a range of concentrations. Data is also produced which shows the change in surface tension after mixing and time required to reach equilibrium.

In order to measure the surface tension, the DuNouy ring method was utilised. This method consists in the measurement of the interaction of a platinum ring with the surface being tested. The ring is submerged below the interface and subsequently raised upwards. As the ring moves upwards it raises a meniscus of the liquid. Eventually this meniscus tears from the ring and returns to its original position. Prior to this event, the volume, and thus the force exerted, of the meniscus passes through a maximum value and begins to diminish prior to the actually tearing event. The process is shown in figure 5.14.

The ring is firstly kept above the surface as the force is set to zero (1). When the ring hits the surface, a slight positive force appears because of the adhesive force between the ring and the surface (2). Then, the ring must be pushed through the surface (due to the surface tension) which causes a small negative force (3). It

breaks through the surface and a small positive force is measured due to the supporting wires of the ring (4). When lifted through the surface the measured force starts to increase (5) and keep increasing (6) until the maximum force is reached (7). After the maximum to be reached, a small decrease of the force is observed until the lamella breaks (8).

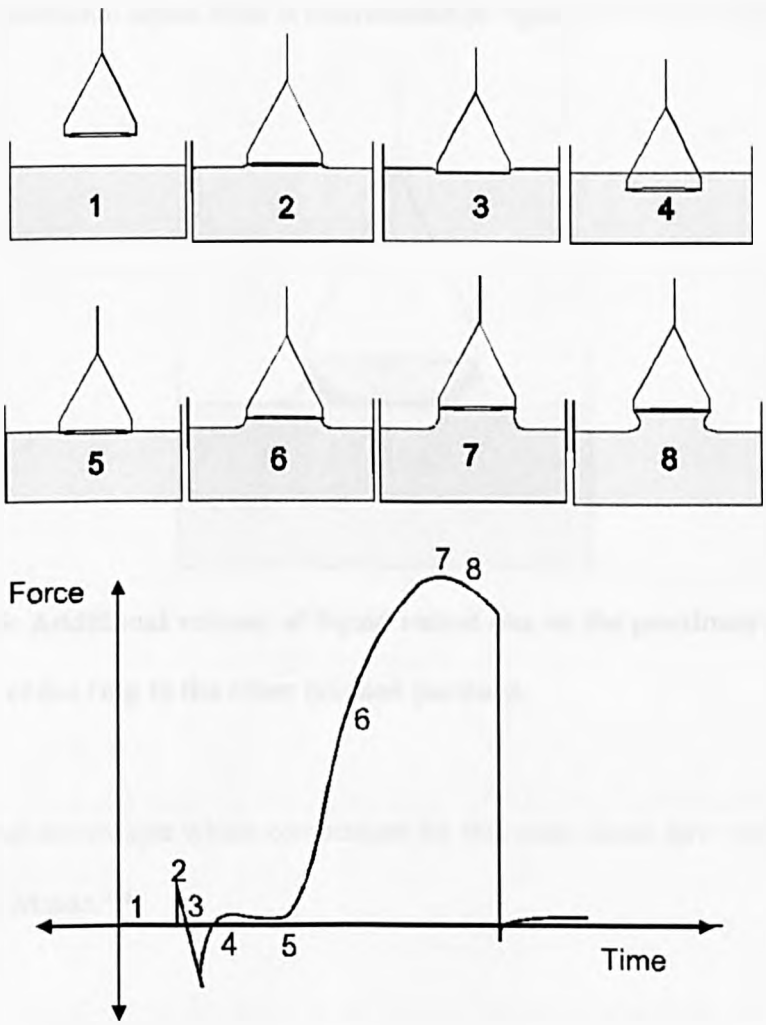

Figure 5.14: Process of surface tension measurement using a DuNouy ring.

The calculation of surface or interfacial tension by this technique is based on the measurement of this maximum force. The depth of immersion of the ring and the level to which it is raised when it experiences the maximum pull are irrelevant to this technique. The original calculations based on the ring technique were based on theories which apply to rings of infinite diameter and do not consider an additional volume of liquid which is raised due to the proximity of one side of the ring to the other. This additional liquid lifted is diagrammed on figure 5.15 as the shaded portion.

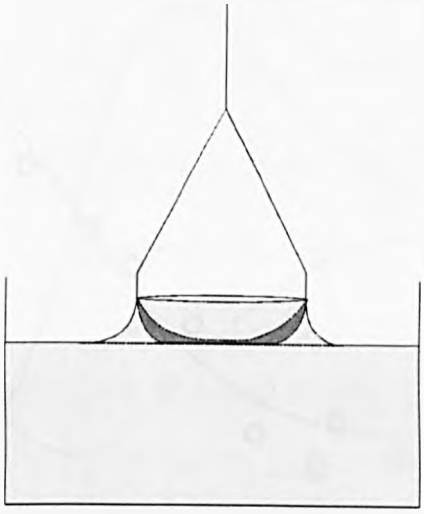

Figure 5.15: Additional volume of liquid raised due to the proximity of one side of the ring to the other (shaded portion).

Mathematical corrections which compensate for this extra liquid have been produced by Huh and Mason.[249]

5.4.1.2.Measurements.

The graph surface tension *vs.* concentration obtained did not show a clear enough inflexion point for the determination of the CAC_{tensio}. Therefore, a mathematical

sigmoid fitting was adopted, and the CAC_{tensio} was assimilated to the maximum of the second derivative (red curve).

Figures 5.16 to 5.19 show the surface tension *vs.* concentration plot for each product. Samples with the lowest concentration in copolymer give generally the surface tension of water at 25°C, 72.8 mN/m.

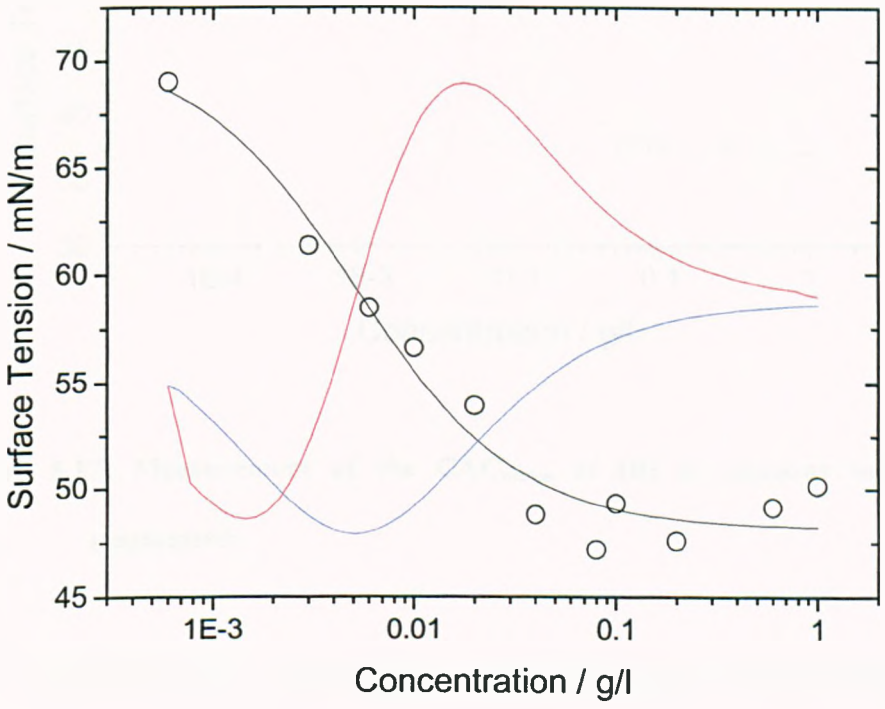

Figure 5.16: Measurement of the CAC_{tensio} of (A) in aqueous solution by tensiometry.

The CAC_{tensio} for (A) and (B) were found to be similar, respectively 0.018 g/l and 0.017 g/l (see figure 5.16 and 5.17), certainly due to a too short hydrophobic chain incorporated into the poly(MeOPEG-MA) copolymers.

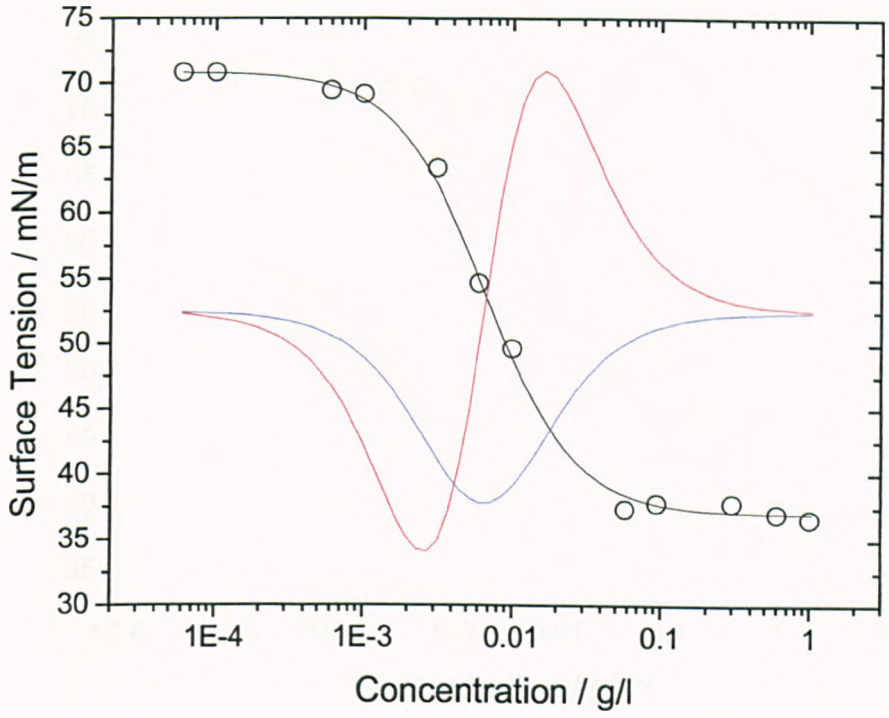

Figure 5.17: Measurement of the CAC_{tensio} of (B) in aqueous solution by tensiometry.

When a fluorinated chain was added, (compound (C), figure 5.18), the CAC_{tensio} was increased to 0.079 g/l. This was surprising according to our initial thoughts, as an increase of the hydrophobicity part of the copolymer should decrease the CAC_{tensio}. A potential explanation could rely on (a) a too short hydrophobic chain introduced by the zonyl initiator and/or (b) an important phase separation between the fluorinated oligomers and PEG chains, changing the equilibrium elaboration.

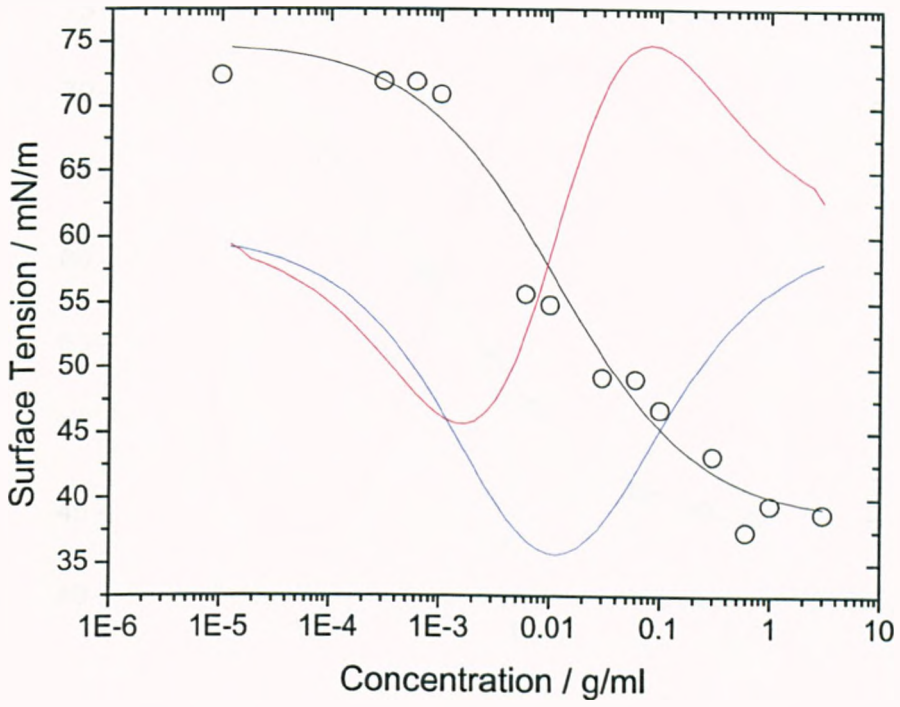

Figure 5.18: Measurement of the CAC_{tensio} of (C) in aqueous solution by tensiometry.

Following the previous observation and in order to improve (*i.e.* decrease) the CAC_{tensio}, a PMMA block was introduced in the copolymer, as a longer and more PEG-compatible hydrophobic chain (Figure 5.19). In this case, the CAC_{tensio} value decreased noticeably to 0.0014 g/l.

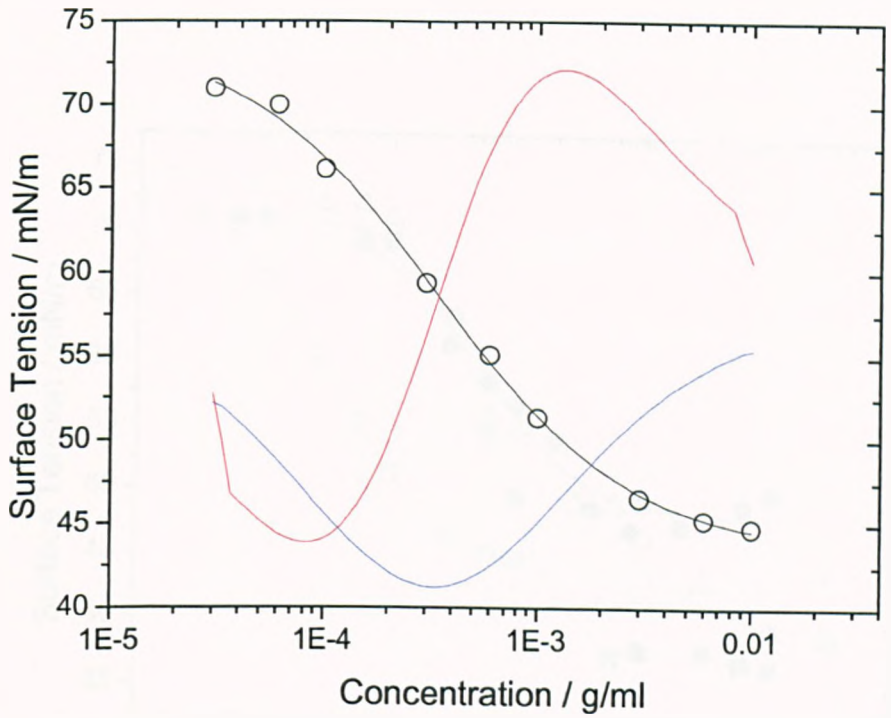

Figure 5.19: Measurement of the CAC_{tensio} of (E) in aqueous solution by tensiometry.

When comparing the decrease of surface tension of the four products (figure 2.20), (B) appears to induce the lowest surface tension, with the fastest decrease (37 mN/m). (C) leads to a close value (39 mN/m), with a slower drop. (A) shows the highest surface tension after CAC_{tensio} (48 mN/m), which seems logical, the product having the smallest hydrophobic group. (E) leads to a surface tension of 45 mN/m, which appears to be average by comparison to the other products. In this latter case, the presence of THF could interfere with the actual product aqueous solution surface tension.

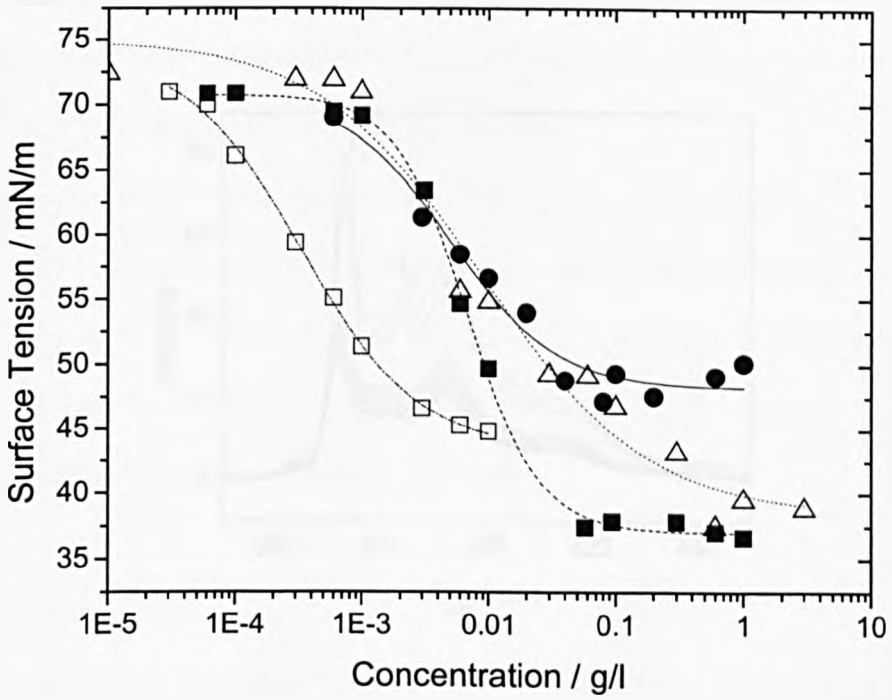

Figure 5.20: Surface tension evolution of (A) (●), (B) (■), (C) (Δ) and (E) (□) in function of the concentration in product in solution.

5.4.2. CMC measurement by Fluorescence.

5.4.2.1.Introduction.[250-253]

Fluorescence spectroscopy was used to determine the presence of micelles in the products solutions. Pyrene was utilised as a probe which preferentially partitions into the hydrophobic micelle cores. As shown in figure 5.21, the emission and excitation spectra of pyrene vary depending on the surrounding environment. In the emission spectra, the third intensity peak is higher when pyrene is in the hydrophobic micelle

core rather than in water. As shown in the excitation spectra, the intensity peak at 333 nm shifts to higher wavelengths when pyrene is surrounded by a hydrophobic environment.

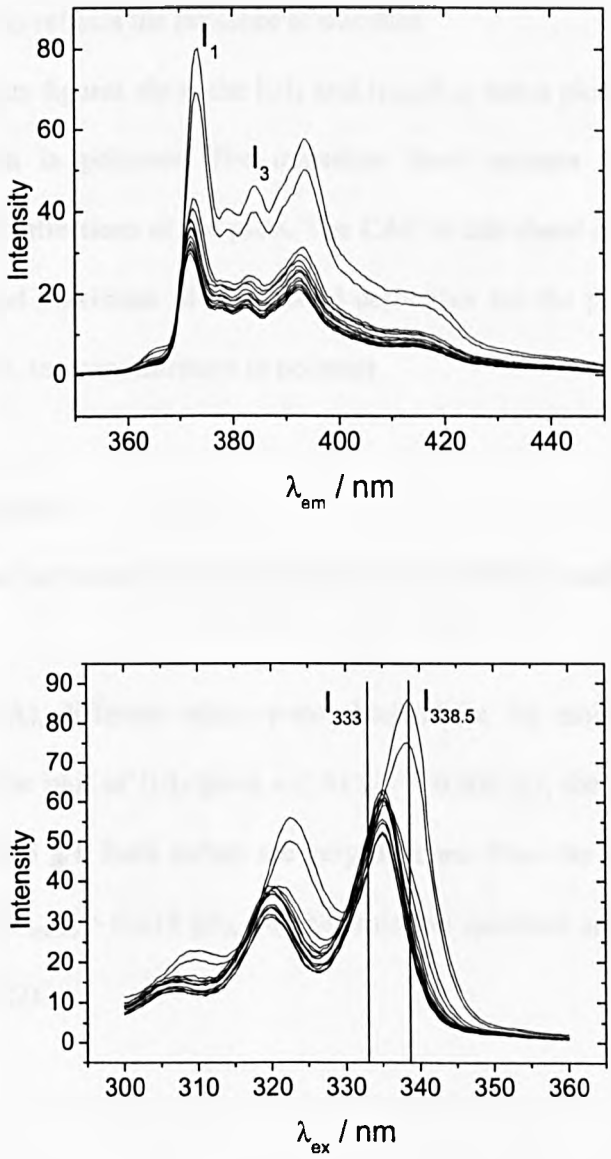

Figure 5.21: Emission (above) and excitation (below) spectra of pyrene changing according to its surrounding environment.

The differences in the emission spectra can be characterised by the intensity ratio of the first and third peaks, I_1/I_3, where a low I_1/I_3 indicates the presence of micelles. Similarly, the excitation spectra can be characterized by the $I_{338.5}$ / I_{333} ratio, where a high $I_{338.5}/I_{333}$ ratio reflects the presence of micelles.

The measurements figures show the I_1/I_3 and $I_{338.5}/I_{333}$ ratios plotted as a function of the concentration in polymer. The transition from unimers to micelles can be identified by the inflections of the plots. The CAC is calculated as being respectively the minimum and maximum of the second derivative for the plots of the I_1/I_3 and $I_{338.5}/I_{333}$ ratios *vs.* the concentration in polymer.

5.4.2.2.Measurements.

The same product as in part 5.4.1 were considered, in order to confirm the tensiometry results.

In the case of (A), different values were obtained for the emission and excitation spectra. While the plot of I_1/I_3 gives a CAC_{I_1/I_3} = 0.005 g/l, the plot $I_{338.5}/I_{333}$ gives $CAC_{I_{338.5}/I_{333}}$ = 0.085 g/l. Both values are very different from the CAC determined by tensiometry (CAC_{tensio} = 0.018 g/l), but the emission spectrum seems to give a closer result (Figure 5.22).

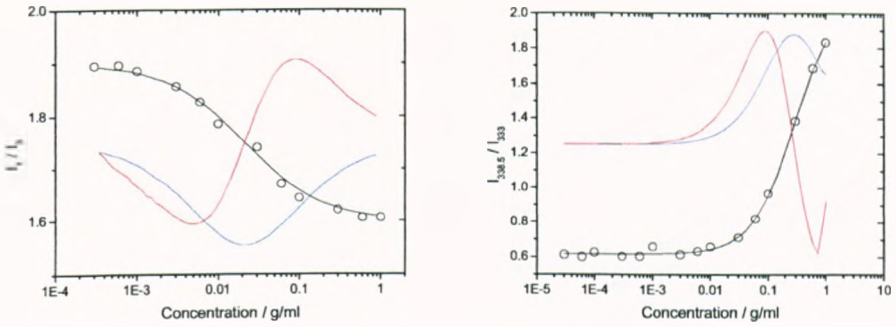

Figure 5.22: Plots of the I_1/I_3 (left) and $I_{338.5}/I_{333}$ (right) ratios *vs.* the concentration in polymer for (A).

The same observation was made for (B), with I_1/I_3 giving CAC_{I_1/I_3} = 0.0005 g/l and $I_{338.5}/I_{333}$ giving $CAC_{I_{338.5}/I_{333}}$ = 0.0085 g/l. In this case, the excitation spectra experiment seems the closest to the tensiometry data (CAC_{tensio} = 0.017 g/l) (Figure 5.23).

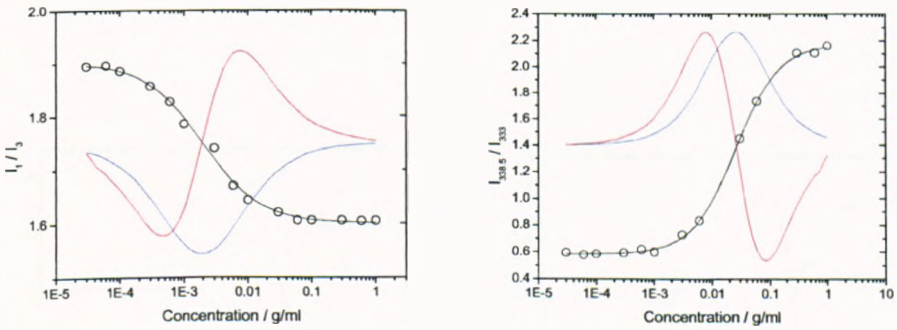

Figure 5.23: Plots of the I_1/I_3 (left) and $I_{338.5}/I_{333}$ (right) ratios *vs.* the concentration in polymer for (B).

When considering (C), the two CAC calculated seems closer from each other (CAC_{I_1/I_3} = 0.0047 g/l and $CAC_{I_{338.5}/I_{333}}$ = 0.0185 g/l, but still different from the CAC_{tensio} = 0.079 g/l) (Figure 5.24).

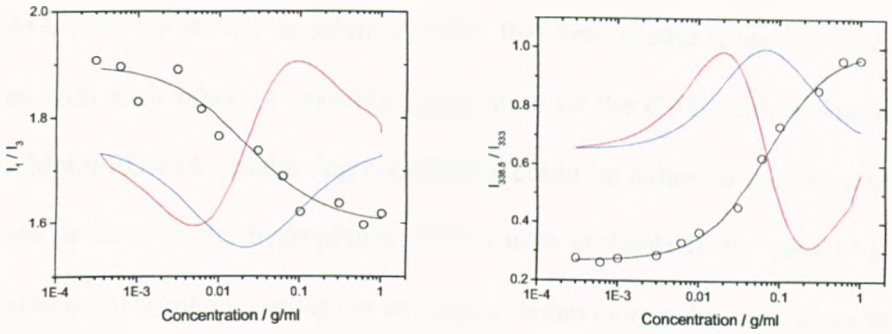

Figure 5.24: Plots of the I_1/I_3 (left) and $I_{338.5}/I_{333}$ (right) ratios *vs.* the concentration in polymer for (C).

Finally, in the case of (E), a better correlation in the values was found, with CAC_{I_1/I_3} = 0.0017 g/l and $CAC_{I_{338.5}/I_{333}}$ = 0.0020 g/l. These values were in good agreement with the CAC_{tensio} = 0.0014 g/l (Figure 5.25).

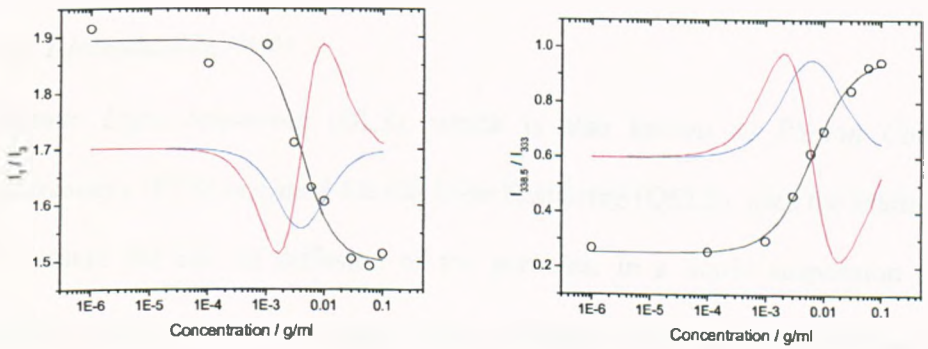

Figure 5.25: Plots of the I_1/I_3 (left) and $I_{338.5}/I_{333}$ (right) ratios *vs.* the concentration in polymer for (E).

From these measurements, it appears that the product containing poly(MeOPEG-MA) give poor correlation between the tensiometry and fluorescence method. However, the

PMMA-*b*-MeOPEG-I_{113} copolymer shows that both methods are consistent and can agree with each other. A possible justification of the CAC scatter obtained for the poly(MeOPEG-MA) containing copolymers could be either an incompatibility of the pyrene probe with the hydrophobic block (more probable in the case of (C), and its fluorinated hydrophobic group) or an original behaviour of the aggregates formed.
In both cases, further investigation was necessary. As the size of the aggregates formed could be an important parameter to conclude on the validity of the various CAC found, dynamic light scattering experiments were undertaken.

5.4.3. Aggregates size measurement by Dynamic Light Scattering (DLS).

In order to investigate further the aqueous behaviour of the different copolymers synthesised, the structure of the aggregates were studied by light scattering.

5.4.3.1.Introduction.[254-257]

Dynamic Light Scattering (DLS), which is also known as *Photon Correlation Spectroscopy* (PCS) or *Quasi-Elastic Light Scattering* (QELS), uses the scattered light to measure the rate of diffusion of the particles. In a liquid suspension of small particles, molecules of the liquid strike randomly the suspended particles making them move with what is called a *Brownian motion*. When the laser light is passed through the suspension, some of the light is scattered with a frequency related to the speed of the particles. As the smaller particles move faster than the larger one, they scatter light at a higher frequency. By measuring and analysing the scattered light over time (dynamic light scattering), the size distribution of the suspended particles can be determined.

In the Stokes model for motion of a hard sphere through a viscous liquid, the resistance to motion is related to the shearing force between adjacent solvent planes moving at different velocities (see figure 5.26). The shearing force per unit area (F_s/A) at each slippage plane is described with the following differential equation: $\frac{F_s}{A} = \frac{m}{A} \times \frac{dv}{dt} = \eta \times \frac{dv}{dy}$, where m is the mass, A is the surface area, dv/dt is the acceleration, h is the viscosity of the medium, and dv/dy is the velocity gradient across the shearing planes.

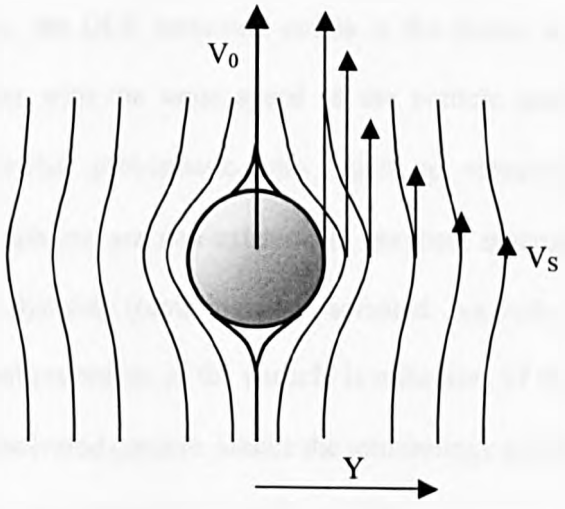

Figure 5.26: Schematic of the Stokes model for motion of a hard sphere through a viscous liquid.

For stick boundary conditions, assuming that the fluid layer adjacent to the particle has the same velocity as the particle, solution of the above equation gives the total force of viscous resistance: $F_{vis} = 6\pi\eta R_H(v_s)$, where R_H is the particle radius and v_s is the limiting steady state velocity of the fluid when y becomes very large.

The proportionality factor in the above expression is defined as the frictional coefficient ($f = 6\pi\eta R_H$), used to calculate the radius of a particle from the measured diffusion coefficient (D) in dynamic light scattering studies.

The radius (R_H) of the particle is calculated from the diffusion coefficient (D) via the Stokes-Einstein equation, where k is the Boltzmann constant, T is the temperature, h is the solvent viscosity, and $f = 6\pi\eta R_H$ is the frictional coefficient for a compact sphere in a viscous medium: $D = \frac{kT}{f} = \frac{kT}{6\pi\eta R_H}$ $\quad R_H = \frac{kT}{6\pi\eta D}$

By definition then, the DLS measured radius is the radius of a hypothetical hard sphere that diffuses with the same speed as the particle under examination. This definition is somewhat problematic with regard to visualisation however, since hypothetical hard spheres are non-existent. In practice, macromolecules in solution are non-spherical, dynamic (tumbling), and solvated. As such, the radius calculated from the diffusional properties of the particle is indicative of the apparent size of the dynamic hydrated/solvated particle. Hence the terminology *hydrodynamic radius*.

A typical DLS measurement proceeds as follow: A solid state laser sends a monochromatic light beam through a small quartz sample cell. Light is scattered in all directions by the molecules in solution. Photons scattered at 90 degrees to the beam path are collected by a small lens and transmitted to a photodiode through a monomode optical fiber. The photodiode receives the photons and converts them to electrical pulses so they can be processed and analysed. Molecules undergoing Brownian Motion cause intensity fluctuations in the scattered light intensity due to constructive and destructive interference. This fluctuation has a time scale related to the speed of the movement of the molecules, and hence, their size. The collection of

photons into time windows or channels and the subsequent analysis (autocorrelation) of this data yields the Translational Diffusion Coefficient (D_t). Once D_t has been determined, the Hydrodynamic Radius (R_H) can be calculated using the Stokes-Einstein equation (see Appendix 4 for details on the mathematical treatment of analysis data).

5.4.3.2.Measurements.

All the reported values below are calculated by correlation of the experimental data with the mathematical algorithm *CONTIN*. However, in all cases, it was verified that the algorithm NNLS gives similar results.

As the sample (E) needed to be first dissolved in THF, and in order to test the influence of this co-solvents on the aggregates sizes, the same treatment was applied to all the others sample. Table 5.3 gives a summary of the various results obtained with the samples A, B, C, D and E.

The hydrodynamic radii measured for the Poly(MeOPEG-MA)-based polymer appear to be too high for the aggregates to be micelles. In the extreme case of Poly(MeOPEG-MA), no data were acquired, because of a too high polydispersity of the sample. This could be justified by the double behaviour of poly(ethylene glycol) chains which can be hydrophilic or hydrophobic depending on the environment. As PEG and PMMA have been shown to be compatible, and the structure of poly(MeOPEG-MA) being close to the one of PMMA (same methacrylate backbone), it seems logical to expect some copolymers to migrate *inside* the core, increasing therefore the size of the overall particle. Considering the results obtained for the CAC, this could justify the difference observed between the tensiometric and fluorescence

methods: The presence of copolymer inside the core could influence the excitation and emission wavelength of the pyrene once migrated in the aggregate. It is however remarkable that the fluorine containing polymers shows a hydrodynamic radius lower than the ones containing an alkyl chain, probably due to the phase separation between fluorine and methacrylate backbone.

In the case of the PMMA-*b*-MeOPEG$_{113}$ block copolymer, however, the data obtained appeared more encouraging: A hydrodynamic radius of 51.8nm was calculated, value more logical for the diameter of micelles, and the PDI of 0.320 was far lower than the values previously obtained.

When comparing the hydrodynamic radii of the same products initially dissolved in THF, we observed a decrease of size in the case of (B), but an increase for (C). In the case of the alkyl hydrophobic chain, this was understood as the solvatation by THF of the whole aggregate, resulting in a shrinking, while, in the case of the fluorinated chain, THF would only solvate the crown of PEG, increasing the size of the overall aggregate.

		Water (0.1%wt/wt)		**THF (1%wt/wt) / Water (0.1%wt/wt)**	
		Z (nm)	**PDI**	**Z (nm)**	**PDI**
A	Poly(MeOPEG-MA)	-	-	-	-
B	Octadecyl-*b*-Poly(MeOPEG-MA)	161.1	0.385	139.6	0.56
C	α-perfluoroalkyl-*b*-Poly(MeOPEG-MA)	149.8	0.430	163.6	0.61
E	PMMA$_{50}$-*b*-MeOPEG$_{113}$	-	-	51.8	0.320

Table 5.5: Summary of the average hydrodynamic radius and PDI for the different surfactants considered.

5.5. Conclusion

PEG-*b*-PMMA block copolymers were tested on their physical properties, by varying the sizes of both chains, and the character of the PEG block (either graft or linear).

In the case of longer PMMA chains, thermal analysis showed that the decomposition temperature of the block copolymers were closer to the PMMA one. The products appeared homogeneous, as only one T_g was found, decreasing when increasing the PEG block size. In both case, the effect of the structure of PEG was neglectable. The incorporation of PEG chains in PMMA resulted in an increase in its hydrophilic character, more obvious when using a graft PEG block. However, after bringing the copolymer above its T_g, this effect was decreased, certainly due to the homogenisation of the product.

Blocks copolymers of equal length of chains were tested as surfactant. While the copolymer showing a graft block of PEG was proved to be inefficient (insoluble in water), the linear block PMMA-*b*-MeOPEG gave a low CMC with micelles of 51.8 nm.

Various poly(MeOPEG-MA) were also tested on their thermal properties and surfactant abilities. While the change of macroinitiator did not affect the decomposition temperature, found slightly above the one of PMMA, it varied the surfactant properties. In any cases, poly(MeOPEG-MA) products were found to be poor surfactants, forming only highly polydispersed aggregates in aqueous solution.

Chapter 6

General conclusion.

It has been shown through this study that poly(ethylene glycol) containing copolymers can be synthesised via copper mediated living radical polymerisation. The living character of the polymerisations was justified and more or less well-defined polymers were obtained.

The on-line *in situ* ^{1}H NMR experiment was shown to be an easy and accurate method to follow the kinetics of polymerisation, and brought multiple information regarding the polymerisation process.

In the chapter 2, the polymerisation of MMA on MeOPEG-based macroinitiators has been studied. While the kinetic plot observed seem to be the one of a typical living polymerisation, SEC analysis showed the presence of non-reacted initiator during the reaction. Analysis of the ^{1}H NMR spectra recorded during the reaction, has been quantified to determine optimum conditions for living polymerisation. Furthermore studies by GPEC confirmed that MeOPEG was a relatively slow initiator for copper mediated living radical polymerisation of MMA, leading to relatively high polydispersity block copolymers. The poor efficiency of the macroinitiator, the effect of the macroinitiator chain length on the catalyst equilibrium and the faster kinetics by comparison to a more classic initiators copper-mediated LRP could be explained by the macroinitiator structure. As poly(ethylene glycol) chains are very flexible, the active site could be trapped by the ethylene glycol chain, away from the catalyst or the monomer. This effect would be even more important for longer chain initiators. When the catalyst reaches the active site, it finds itself trapped in the polymer chain. One can even imagine the co-ordination of the copper to the macroinitiator chain. This would explain the difficulty of the monomer to react with the initiator, due to the steric hindrance. We observed indeed the impact of initiator chain length, but noticed the

absence of effect of temperature and solvent. The final block copolymer showed however a hydrophilic group of well known size, and a more or less well-defined hydrophobic block. A range of different products with different chain lengths of PMMA was then synthesised and purified in order to test their amphiphilic properties.

In chapter 3, LRP of MeOPEG-MA was shown to be efficient, leading to well defined graft water-soluble oligomers, of low molecular weight. Furthermore, water was shown to be an interesting solvent for such polymerisation, leading to an improvement of the speed of the reaction, and an evolution in the experimental procedure. MeOPEG-MA was then used as monomer in the living radical polymerisation with various initiators, in order to synthesis different copolymers showing surfactant properties.

Chapter 4 described the study of the solvent effect of alkyl ether and water on copper mediated living radical polymerisation, as a model for the effects observed when using PEG as initiator or monomer. The enhancement of the reaction rate appeared to be due to the possible competition between the components and the ligand on the copper catalyst, modifying the activation/deactivation equilibrium of the copper complex. An alternative explanation was considered, as the influence of the polarity of the medium on the reactive bond Copper-Bromide. An increase of polarity would weaken this bond, increasing the concentration in active species and therefore the rate of the polymerisation.

Finally, in chapter 5, PEG-*b*-PMMA block copolymers were tested on their physical properties, by varying the sizes of both chains, and the character of the PEG block (either graft or linear).

In the case of longer PMMA chains, thermal analysis showed that the decomposition temperature of the block copolymers were closer to the PMMA one. The products appeared homogeneous, as only one T_g was found, decreasing when increasing the PEG block size. In both case, the effect of the structure of PEG was neglectable. The incorporation of PEG chains in PMMA resulted in an increase in its hydrophilic character, more obvious when using a graft PEG block. However, after bringing the copolymer above its T_g, this effect was decreased, certainly due to the homogenisation of the product.

Blocks copolymers of equal length of chains were tested as surfactant. While the copolymer showing a graft block of PEG was proved to be inefficient (insoluble in water), the linear block PMMA-*b*-MeOPEG gave a low CMC with micelles of 51.8 nm.

Various poly(MeOPEG-MA) were also tested on their thermal properties and surfactant abilities. While the change of macroinitiator did not affect the decomposition temperature, found slightly above the one of PMMA, it varied the surfactant properties. In any cases, poly(MeOPEG-MA) products were found to be poor surfactants, forming only highly polydispersed aggregates in aqueous solution.

Chapter 7

Experimental

7.1. General Characterisation.

^{1}H, ^{13}C and ^{19}F NMR spectra were recorded on Brüker ACF 250, DPX 300, ACP 400 or DPX 400 spectrometers using deuterated solvents obtained from CEA or Aldrich. Polymerisation kinetics followed by ^{1}H NMR were ran using a Brucker built-in kinetics program. Mass spectra were recorded on a Kratos MS80 or Micromass Autospec spectrometer using chemical ionisation (CI) or electrospray ionisation (EI) techniques. Elemental analyses were performed on a Leeman Labs CE 440 elemental analyser. ICP analysis was performed on a Leeman Labs ICP PS instrument. DSC was performed on a Perkin-Elmer Pyris 1 system equipped with a cooling unit. Thermogravimetric analysis was performed on a Perkin-Elmer TGA 7 system under a nitrogen atmosphere. Infrared absorption spectra were recorded on a Brücker Vector 22 FTIR spectrometer equipped with a Golden Gate diamond attenuated total reflection (ATR) sample platform. Freeze-drying was performed on an Edwards Minifast 680. Fluorescence spectra were measured on a Perkin-Elmer LS 50 luminescence spectrometer thermostated at 25 °C. Surface tension was measured on a Nima Technology DST 9005 automated tensiometer. Polymer films were spin coated onto glass slides or silicone wafers using a Chemat Technology KW 4A spin coater. Dialysis was performed using a Millipore cellulose TFF cartridge with a 1000 g mol^{-1} limit.

Molecular weight distribution were measure as follows:

Polymers made by living radical polymerisation were dissolved in THF and the solution passed through a short column of activated basic alumina to remove metal containing species. Molecular mass analyses were carried out by gel permeation (size exclusion) chromatography on a Polymer Laboratories system using THF as the

eluent at 1.0 mL/min and equipped with a PL autoinjector, a PL-gel 5 μm (50 x 7.5 mm) guard column, two PL-gel 5 μm (300 x 7.5 mm) mixed-C columns and a refractive index detector. Samples were compared against narrow standards of either poly(styrene), M_p = 580 to 3.15 x10^6 gmol^{-1}, or poly(methyl methacrylate), M_p = 200 to 1.577 x10^6 gmol^{-1}, obtained from Polymer Laboratories, except for the methyl methacrylate dimer, trimer, and tetramer which were prepared by catalytic chain transfer at the University of Warwick.

7.2. Copper mediated living radical polymerisation – General procedure.

7.2.1. Reagents.

Methyl methacrylate (Aldrich, 99 %), benzyl methacrylate (Aldrich, 99 %) were passed through a short column of activated, basic alumina to remove inhibitors and acidic impurities, degassed by bubbling with dry nitrogen gas for 30 minutes and then stored at 0 °C before use. Polyethylene glycol methyl ether methacrylate (Aldrich, 98 %) was bubbled with dry nitrogen gas for 30 minutes before use. Toluene, ethylene glycol diethyl ether and water were degassed by bubbling with dry nitrogen gas for 30 minutes and kept in sealed flasks under nitrogen prior to use.

7.2.2. Polymerisation procedure.

All polymerisations were carried out using Schlenk apparatus under dry nitrogen. In a typical reaction the solid reagents were added to a pre-dried Schlenk tube which was sealed with a rubber septum. The tube was evacuated and flushed with nitrogen three

times so as to remove oxygen and the liquid reagents added via oven dried, degassed syringes. All liquid reagents were degassed prior to use by bubbling through with nitrogen for at least 15 minutes or were degassed in the Schlenk tube by three freeze-pump-thaw cycles. The tube was brought to reaction temperature in a stirred, thermostatted oil bath and held for 5 minutes to allow the copper complex to fully dissolve before initiator was added. Samples for kinetic data were taken using degassed syringes and polymer conversion data obtained by gravimetry. A sample was accurately weighed into a pre-weighed aluminium pan and then volatile solvents and monomers removed under vacuum in an oven at 60 °C until constant sample weight was achieved. For polymerisations involving non-volatile monomers or solvents polymer conversions were obtained by integration of the appropriate regions of the ^{1}H NMR spectrum. Conversion of methacrylic monomers was also measured by gel permeation chromatography using infra-red absorption detection by comparison of monomer and polymer peak integrals. The system used chloroform as the eluent at 1.0 mL/min and consisted of an LKB HPLC pump, a PL-gel 5 μm (50 x 7.5 mm) guard column, two PL-gel 5 μm (300 x 7.5 mm) mixed-C columns, a Wilks Miran 1A-CVF IR absorption detector and a PL EMD 950 evaporative mass detector.

7.2.3. Isolation and purification of polymers.

Polymerisation undertaken for kinetics data were prepared using *N*-*n*-octyl-2-pyridylmethanimine ligands, leading to a catalyst complex fully soluble at any temperature. Polymers in synthetic experiments were prepared by reactions mediated by copper bromide complexed with *N*-*n*-propyl-2-pyridylmethanimine ligands. This

complex was fully soluble in a monomer and toluene solution at reaction temperature, but relatively insoluble at room temperature. After the polymerisation was complete the solution was cooled to room temperature, the solution filtered over a bed of Celite and the polymer precipitated into petroleum ether (40 - 60 °C). After collection and drying in air the polymer was redissolved in dichloromethane, the solution passed down a column of activated, basic alumina to remove brown and green coloured copper containing impurities and the polymer re-precipitated into petroleum ether (40 - 60 °C). Polymers purified in this way where usually white or pale green in colour and contained less than 50 ppm copper by weight (as found by ICP). Polymerisations of poly(ethylene glycol)methyl ether methacrylate were filtered by the same method, dissolved in distilled water and submitted to dyalisis using an ultracentrifugation cartridge (Millipore, 1000 g/mol limit). Water was removed by freeze drying.

7.2.4. Purification of copper (I) halides.

Copper (I) bromide (Avocado, 98 %) and copper (I) chloride (Avocado, 99 %) were purified by a method based on that of Keller and Wycoff.[258] For example, copper (I) bromide (50 g, 0.35 mol) was ground to a fine powder in a mortar and then dilute sulphuric acid (2 M, 30 drops) added to make a thick, brown paste. This was dropped into a stirred solution of sodium sulphite (2 M, 2 L) to give a fine, white suspension in a blue solution of the copper (II) species. The suspension was collected by careful vacuum filtration below a nitrogen blanket and the solid was washed with glacial acetic acid (250 mL), absolute ethanol (250 mL) and finally anhydrous diethyl ether (250 mL) each time ensuring that the level of liquid in the funnel was never allowed to sink below the level of the solid to ensure the minimum of oxygen contact. 41.3 g

of a cream coloured powder thus obtained was dried at 150 °C under vacuum for 12 hours and stored in a light proof container. Yield = 82.2 %. Very little green coloured impurity could be seen in the product, even after several weeks exposure to air.

7.2.5. Synthesis of ligands.

Synthesis of the range of Schiff base ligands was carried out by a modification of the procedure used by Baehr and Doege.[259]

7.2.5.1.Reagents.

Ethylamine (Avocado, 70% in water), *n*-propylamine (Lancaster, 98 %), *n*-pentylamine (Aldrich, 99 %), *n*-hexylamine (Avocado, 98 %), *n*-heptylamine (Avocado, 98 %), *n*-octylamine (Lancaster, 98 %), *n*-nonylamine (Avocado, 98 %), *n*-octadecylamine (Aldrich, 99 %), ethylene diamine (Aldrich, 99 %), pyridine-2-carboxaldehyde (Avocado, 99 %), sodium tetrahydroborate (Aldrich, 99 %) were all used as received.

7.2.5.2.N-n-Propyl-2-pyridylmethanimine.

An excess of *n*-propylamine (19.0 mL, 0.25 mol) was added dropwise to a stirred solution of pyridine-2-carboxaldehyde (20.0 mL, 0.21 mol) in diethyl ether (20 mL) and cooled in an ice bath. On complete addition of the amine dried magnesium sulphate (5 g) was added and the slurry stirred for 2 hours at 25 °C. The solution was filtered and distilled under reduced pressure to give 30.5 g of product at 43 °C, 0.05 mmHg. Yield = 98.2 %.

^{1}H NMR ($CDCl_3$, 298 K, 250 MHz): δ (ppm from TMS) = 8.63 (d, 1H, Pyr-H), 8.39 (s, 1H, Pyr-C<u>H</u>=N-), 8.00 (d, 1H, Pyr-H), 7.69 (t, 1H, Pyr-H), 7.27 (t, 1H, Pyr-H), 3.64 (t, 2H, J = 4.4 Hz, -C=N-C<u>H</u>$_2$-), 1.76 (sextet, 2H, J = 4.4 Hz, -CH_2-C<u>H</u>$_2$-CH_3-), 0.70 (t, 3H, J = 4.4 Hz, -CH_2-C<u>H</u>$_3$).

^{13}C NMR ($CDCl_3$, 298 K, 250 MHz): δ (ppm from TMS) = 161.0 (Pyr-<u>C</u>H=N-), 154.1, 148.7, 135.8, 123.9, 120.5 (<u>Pyr</u>), 62.6 (-C=N-<u>C</u>H_2-), 22.3 (-CH_2-<u>C</u>H_2-CH_3-), 11.3 (-CH_2-<u>C</u>H_3).

IR absorption: ν (cm^{-1}) = 3054, 3009 (Ar C-H str.), 2961-2834 (Alkyl C-H str.), 1651 (C=N str.), 1587, 1568, 1468, 1436 (Ar ring str.).

Mass spectrum: m/z = 149 [M + H].

Elemental analysis: 73.1 %C, 8.2 %H, 18.7 %N; (theoretical; 72.9 %C, 8.2 %H, 18.9 %N).

7.2.5.3.N-n-Octyl-2-pyridylmethanimine.

Synthesised as above except *n*-octylamine (18.6 g, 0.14 mol) and pyridine-2-carboxaldehyde (10 g, 0.093 mol) were used. The solution was filtered and distilled under reduced pressure to give 19.9 g of product at 101 °C, 0.03 mmHg. Yield = 97.6 %.

^{1}H NMR ($CDCl_3$, 298 K, 250 MHz): δ (ppm from TMS) = 8.61 (d, 1H, Pyr-H), 8.33 (s, 1H, Pyr-C<u>H</u>=N-), 7.95 (d, 1H, Pyr-H), 7.70 (t, 1H, Pyr-H), 7.27 (t, 1H, Pyr-H), 3.64 (t, 2H, -C=N-C<u>H</u>$_2$-), 1.68 (quintet, 2H, (-C=N-CH_2-C<u>H</u>$_2$-), 1.27 (m, 10H, alkyl H), 0.83 (t, 3H, -CH_2-C<u>H</u>$_3$).

^{13}C NMR ($CDCl_3$, 298 K, 250 MHz): δ (ppm from TMS) = 161.5 (Pyr-CH=N-), 154.6, 149.3, 136.4, 124.4, 121.0 (Pyr), 61.5 (-C=N-CH_2-), 31.8 (-C=N-CH_2-CH_2-), 30.6, 29.3, 29.2, 27.2, 22.5 (alkyl C), 14.0 (-CH_2-CH_3).

IR absorption: ν (cm^{-1}) = 3053, 3008 (Ar C-H str.), 2955-2856 (Alkyl C-H str.), 1650 (C=N str.), 1587, 1568, 1468, 1436 (Ar ring str.).

Mass spectrum: m/z = 219 [M + H].

Elemental analysis: 76.8 %C, 10.1 %H, 13.0 %N (theoretical; 77.0 %C, 10.2 %H, 12.8 %N).

7.3. Chapter 2: Amphiphilic block copolymers synthesised by LRP with poly(ethylene glycol)-based hydrophilic initiators.

7.3.1. Synthesis of (poly(ethylene glycol) methyl ether)-2-bromoisobutyrate (MeOPEG-I_X, X = 12, 45, 113).

2-bromoisobutyryl bromide (Lancaster, 98 %) was stored under dry nitrogen. Triethylamine (BDH, 99 %) was stored over sodium hydroxide pellets and 4 Å molecular sieves for 48 hours and then filtered before use. Anhydrous THF (Romil "Hi-Dry", 99.99 %) were stored over activated 4 Å molecular sieves under dry nitrogen. All other reagents, unless otherwise stated, were used as received.

Poly(ethylene glycol) (Aldrich, 0.5 g (X = 12), 2 g (X = 45), 5 g (X = 113), 1 mmol) was dissolved in anhydrous THF (50 mL) with triethylamine (0.21 ml, 1.5 mmol). 2-bromoisobutyryl bromide 0.18 mL, 1.5 mmol) was added dropwise under an atmosphere of dry nitrogen. The reaction was left for 48 hours at 25 °C before the solution was taken up in dichloromethane (100 mL) and washed successively with

saturated, aqueous sodium hydrogen carbonate solution (3 x 100 mL). The resultant organic phase was dried over anhydrous magnesium sulphate and the solvent removed under vacuum to give a yellowig liquid for X = 12. In the case of X = 45 and 113, the product was precipitated in cold diethyl ether. Yield = 85 % (X = 12), 82 % (X = 45), 79 % (X = 113).

^{1}H NMR ($CDCl_3$, 298K, 300 MHz) δ (ppm from TMS) 4.27 (t, *J* = 4.9 Hz, 2 H, -$C\underline{H}_2$-O-CO-), 3.69 (t, *J* = 4.9 Hz, 2 H, -$C\underline{H}_2$- CH2-O-CO -), 3.59 (m, 48 H (X = 12), 180 H (X = 45), 452 H (X = 113), ($C\underline{H}_2$-$C\underline{H}_2$-O)x)), 3.41 (s, 3 H, -O-$C\underline{H}_3$), 1.89 (s, 6 H, -CH_3),

^{13} C {^{1}H} NMR ($CDCl_3$, 298K 100.6 MHz) δ 170.13, 77.09, 67.57, 64.00, 54.78, 29.68

IR absorption ν (cm^{-1}) 2865, 1733 (C=O), 1462, 1348, 1276, 1096, 947, 853, 748

Elemental analysis: (X = 12) 49.15% C, 8.21% H (theoretical: 49.08% C, 8.10% H)

(X = 45) 53.01% C, 8.92% H (theoretical: 52.74% C, 8.81% H)

(X = 113) 53.80% C, 9.07% H (theoretical: 53.78% C, 9.01% H)

7.3.2. Copper mediated LRP of MMA initiated by MeOPEG-based macroinitiators.

7.3.2.1.Schlenk polymerisation.

A degree of polymerisation, DP_{Theo} = 100 was targeted CuBr (9.99×10^{-4} mol, 0.1429 g) was placed in a Schlenk tube and placed under a nitrogen atmosphere. Deoxygenated MMA (9.99×10^{-2} mol, 10.0000 g), toluene (50vol.%) and

(poly(ethylene glycol) methyl ether)-2-bromoisobutyrate (9.99×10^{-4} mol, 0.5594 g (X = 12), 2.0100 g (X = 45), 4.9989 g (X = 113)) were added at room temperature. The mixture was deoxygenated by three freeze-pump-thaw cycles after which the *N*-(*n*-propyl)-2-pyridylmethanimine ligand was added (2 mol equiv. to CuBr, 19.98×10^{-4} mol, 0.31 mL). Next the Schlenk tube was immersed in a thermostated oil bath at the reaction temperature (time = 0 s). Samples for analysis of the molar mass distribution (MMD) and monomer conversion were taken at different intervals throughout the reaction. Catalyst residues were removed by passing the samples through a short column of basic alumina prior to SEC and NMR analysis.

When DPs under 100 were targeted, polymerisations were stopped at lower conversions equivalent to the molecular weight aimed for (e.g. PMMA = 5,000 g/mol was obtained by stopping the reaction at 50% conversion).

7.3.2.2. ^1H NMR polymerisation.

For the reactions followed *in-situ* by ^1H NMR, *N*-(*n*-octyl)-2-pyridylmethanimine was used as ligand, with a molar ratio of 3:1, with respect to CuBr so to ensure that the complex was fully soluble, for all temperatures. For a DP_{th} = 100, the procedure was as above. MMA (1.99×10^{-2} mol, 2.0000 g), Copper (1.99×10^{-4} mol, 0.0286 g), *N*-(*n*-octyl)-2-pyridylmethanimine (5.97×10^{-4} mol, 0.156 ml), (poly(ethylene glycol) methyl ether)-2-bromoisobutyate (4.99×10^{-4} mol, 0.1119 g (X = 12), 0.4020 g (X = 45), 0.9998 g (X = 113)) and toluene-d_8 (2.00 g). An aliquot of 2 mL of this solution was transferred to a Young's tap NMR tube and with time = 0 s taken once the tube was at reaction temperature within the NMR spectrometer.

When ethylene glycol diethyl ether was introduced as co-solvent, 1.80 g $(EtO)_2EG$ and 0.2 g toluene-d_8 was measured.

7.3.2.3.PMMA block Molecular weight calculation.

The calculation of the final molecular weight was obtained by integration of the ^1H NMR spectrum of the final product, comparing the signals between 0.0 and 2.5 ppm (CH_2 and CH_3 of PMMA) and between 3.0 and 4.5 ppm (O-CH_3 of PMMA and O-CH_2-CH_2 of MeOPEG-I_{12}).

7.3.2.4.GPEC analysis.

Gradient Polymer Elution Chromatography was performed using Kontron system with UV detection. The eluents were THF and water, with a flow rate of 1 mL min^{-1}. THF (Aldrich) and water purified by reverse osmosis were used. The detector was a Kontron 332 UV/Vis, tuned at 254 nm. The column was a Spherisorb (5 micron particle size) ODS1 (C-18 bonded to a silica support), 100 mm by 14.6 mm. The system was calibrated with Polymer Laboratory poly(methyl methacrylate) standards and poly(ethylene glycol) standards.

7.4. Chapter 3: Amphiphilic block copolymers made by LRP from hydrophobic initiators.

7.4.1. Synthesis of phenyl-2-bromoisobutyrate.

2-bromoisobutyryl bromide (Lancaster, 98 %) was stored under dry nitrogen. Triethylamine (BDH, 99 %) was stored over sodium hydroxide pellets and 4 Å

molecular sieves for 48 hours and then filtered before use. Anhydrous THF (Romil "Hi-Dry", 99.99 %) were stored over activated 4 Å molecular sieves under dry nitrogen. All other reagents, unless otherwise stated, were used as received.

Phenol 18.85 g (0.20 mol) was dissolved in anhydrous THF (400 mL) with triethylamine (30.6 ml, 0.22 mol). 2-bromoisobutyryl bromide (26.4 mL, 0.22 mol) was added dropwise under an atmosphere of dry nitrogen. The reaction was left for 6 hours at 25 °C before the solution was taken up in dichloromethane (100 mL) and washed successively with saturated, aqueous sodium hydrogen carbonate solution (3 x 100 mL). The resultant organic phase was dried over anhydrous magnesium sulphate and the solvent removed under vacuum to give a slightly yellow/brown liquid. This was vacuum distilled at 58 °C and 0.2 Torr to give a colourless liquid Yield = 28.9 g (72.7 %)

^{1}H NMR ($CDCl_3$, 298K, 300 MHz) δ 7.41 (t, J = 7.6 Hz, 2 H), 7.26 (t, J = 6.9 Hz, 1H), 7.13 (d, J = 8.7 Hz, 2 H), 1.93 (s, 6 H)

^{13} C {^{1}H} NMR ($CDCl_3$, 298K 100.6 MHz) δ 169.40, 150.38, 129.09, 125.74, 120.74, 64.14, 29.09

IR absorption ν (cm^{-1}) 3044, 2985, 2936, 1754, 1591, 1456, 1389, 1371, 1265, 1186, 1161, 1140, 1107, 1070, 1006, 938, 911, 859, 745, 688

Mass spectrum: m/z = 200, 198 (mass peaks) 131, 94, 77, 65, 41

Elemental analysis: 60.36 %C, 5.58 %H, (theoretical; 60.46 %C, 5.58 %H).

7.4.2. Polymerisation of PEG-MA in toluene.

Targeted degree of polymerisation, $DP_{Theo} = 10$.

CuBr (0.442 g, 3.1 mmol) were placed in a Schlenk tube and placed under a nitrogen atmosphere. Deoxygenated (PEG)MA (14.8 mL, 0.031 mol), toluene (50vol.%) and phenyl-2-bromoisobutyrate (0.751 g, 3.1 mmol) were added at room temperature. The mixture was deoxygenated by three freeze-pump-thaw cycles after which the *N*-(*n*-propyl)-2-pyridylmethanimine ligand was added (2 mol equiv. to CuBr, 6.2 mmol, 0.97 mL). Next the Schlenk tube was immersed in a thermostated oil bath at the reaction temperature (time = 0 s). Samples for analysis of the molar mass distribution (MMD) and monomer conversion were taken at different intervals throughout the reaction. Catalyst residues were removed by passing the samples through a short column of basic alumina prior to SEC and NMR analysis.

7.4.3. Polymerisation of MeOPEG-MA in toluene.

7.4.3.1.Schlenk polymerisation.

Targeted degree of polymerisation, $DP_{Theo} = 10$.

CuBr (0.442 g, 3.1 mmol) were placed in a Schlenk tube and placed under a nitrogen atmosphere. Deoxygenated MeO(PEG)MA (10 mL, 0.031 mol), toluene (50vol%) and phenyl-2-bromoisobutyrate (0.751 g, 3.1 mmol) were added at room temperature. The mixture was deoxygenated by three freeze-pump-thaw cycles after which the *N*-(*n*-propyl)-2-pyridylmethanimine ligand was added (2 mol equiv. to CuBr, 6.2 mmol, 0.97 mL). Next the Schlenk tube was immersed in a thermostated oil bath at the reaction temperature (time = 0 s). Samples for analysis of the molar mass distribution

(MMD) and monomer conversion were taken at different intervals throughout the reaction. Catalyst residues were removed by passing the samples through a short column of basic alumina prior to SEC and NMR analysis.

7.4.3.2. ^1H NMR polymerisation.

For the reactions followed *in-situ* by ^1H NMR, *N*-(*n*-octyl)-2-pyridylmethanimine was used as ligand, with a molar ratio of 3:1, with respect to CuBr so to ensure that the complex was fully soluble, for all temperatures. For a DP_{th} = 10, the procedure was as above. MeOPEG-MA (10.3 mmol, 5.00 g), Copper (1.03 mmol, 0.147 g), *N*-(*n*-octyl)-2-pyridylmethanimine (3.09 mmol, 0.675 g), ethyl-2-bromoisobutyrate (1.03 mmol, 0.250 g) and toluene-d_8 (5.00 g). An aliquot of 2 mL of this solution was transferred to a Young's tap NMR tube and with time = 0 s taken once the tube was at reaction temperature within the NMR spectrometer.

7.4.4. Polymerisation of MeOPEG-MA in water.

7.4.4.1.Synthesis of (1,2-dihydroxypropane-3-oxy)-2-bromoisobutyrate.

2,2-Dimethyl-1,3-dioxolane-4-methoxy-2-bromoisobutyrate, 1.

1 was prepared by esterification of 2,2-dimethyl-1,3-dioxolane-4-methanol with 2-bromo-2-methylpropionylbromide. Triethylamine was dried over KOH pellets and glassware dried at 150°C overnight prior to use. 2,2-Dimethyl-1,3-dioxolane-4-methanol (0.04 mol, 5.29 g), triethylamine (0.08 mol, 8.10 g) and anhydrous tetrahydrofuran (50 mL) were charged in a 100 mL round-bottomed flask equipped with a magnetic stirrer and cooled to 0 °C with an ice-bath. 2-Bromo-2-

methylpropionylbromide (0.044 mol, 5.44 mL) was added dropwise via syringe. The mixture was subsequently stirred for 45 min while being brought to ambient temperature. The reaction mixture was poured into an excess of cold water and extracted with 50 mL of diethyl ether. The organic layer was washed with a saturated aqueous solution of Na_2CO_3 acidified water (pH ≈ 4.5), and a second aliquot of saturated aqueous solution of Na_2CO_3. The organic layer was dried over anhydrous Na_2SO_4, filtered and the solvent under vacuum. 1 was isolated as slightly yellowish oil (89%). ^{1}H NMR (DMSO-d_6) δ 1.30 and 1.37 (each s, 3H, OC(C$\underline{H}_3$)$_2$O), 1.92 (s, 6H, C(C$\underline{H}_3$)$_2$Br), 3.75 (dd, 1H, C5$\underline{H}_a$H$_b$, J_{ab} = 8.55 Hz, J_Z = 6.10 Hz), 4.05 (dd, 1H, C5H$_a\underline{H}_b$, J_{ab} = 8.55 Hz, J_E = 6.41 Hz), 4.15 (dd, 1H, C$\underline{H}_a$H$_b$, J_{ab} = 11.60 Hz, J_E = 4.89 Hz), 4.22 (dd, 1H, CH$_a\underline{H}_b$, J_{ab} = 11.60 Hz, J_Z = 3.97 Hz), 4.31 (m, 1H C4$\underline{H}$). ^{13}C NMR (DMSO-d_6) δ 25.6 and 26.8 (1C, OC($\underline{C}$H$_3$)$_2$O), 30.6 (2C, C($\underline{C}$H$_3$)$_2$Br), 57.3 (1C, $\underline{C}$(CH$_3$)$_2$Br), 65.5 (1C, $\underline{C}$5H$_a$H$_b$), 65.7 (1C, $\underline{C}$H$_a$H$_b$), 73.3 (1C, $\underline{C}$4H), 109.2 (1C, O$\underline{C}$(CH$_3$)$_2$O), 171.0 (1C, C=O).

1,2-dihydroxypropane-3-oxy-2-bromoisobutyrate, 2.

A mixture of 5.0 g of 1, 15 mL of glacial acetic acid, 40 mL of water and a catalytic amount of methoxybenzene were stirred for 30 min at 80 °C. The solution was cooled to room temperature prior to the addition of 50 mL of diethylether. The aqueous layer was saturated with sodium hydrogen carbonate by portionwise addition (CAUTION: formation of CO_2). The aqueous layer was separated and washed with 50 mL of diethyl ether. The crude product was obtained from the combined organic layers following removal of the solvent as yellowish oil. The product crystallized overnight on standing at ambient temperature. The crude yellowish solid was recrystallised from

toluene (1 g in 25 mL) to yield pearl crystals (72%). ^{1}H NMR (DMSO-d_6) δ ^{1}H NMR (DMSO-d_6) δ 1.91 (s, 6H, C(C$\underline{H}_3$)$_2$Br), 3.40 (app. d, 2H, C$\underline{H}$2OH J = 5.27 Hz), 3.70 (m, 1H, C$\underline{H}$OH), 4.04 (dd, 1H, C$\underline{H}_a$H$_b$OC=O, J_{ab} = 11.11 Hz, J_E = 5.93 Hz), 4.15 (dd, 1H, CH$_a\underline{H}_b$OC=O, J_{ab} = 11.11 Hz, J_Z = 4.53 Hz), 4.69 (br. s, 1H CH$_2$O$\underline{H}$), 4.97 (br. S, 1H, CHO$\underline{H}$). ^{13}C NMR (DMSO-d_6) δ 30.7 (2C, C($\underline{C}$H$_3$)$_2$Br), 57.6 (1C, $\underline{C}$(CH$_3$)$_2$Br), 62.8 (1C, $\underline{C}$H$_2$OH), 67.3 (1C, $\underline{C}$H$_2$OC=O), 69.4 (1C, $\underline{C}$HOH), 171.1 (1C, C=O).

7.4.4.2.Polymerisation of MeOPEG-MA in water.

7.4.4.2.1.Schlenk polymerisation.

Typical polymerisation procedure for poly[poly(ethylene glycol) methyl ether methacrylate] with a targeted degree of polymerisation (DP_{Theo} = 10) and a ratio M / I / Cu / Ligand = 10 / 1 / 1 / 3

CuBr (0.0589 g, 0.412 mmol) was placed in a Schlenk tube under a nitrogen atmosphere. Deoxygenated *N*-(n-propyl)-2-pyridylmethanimine ligand (3 mol equiv. to CuBr, 1.24 mmol, 0.190 mL) was added, followed by deoxygenated water (2 g). The solution was heated for 5 min at 40°C, to ensure the dissolution of the complex in water. MeO(PEG)MA (2.00 g, 4.12 mmol), and 1,2-dihydroxypropane-3-oxy-2-bromoisobutyrate initiator (0.412 mmol, 0.0993 g) were mixed separately and deoxygenated by three freeze-pump-thaw cycles. Finally the solution of macromonomer initiator was injected into the catalyst solution and the Schlenk tube immersed in a thermostated water bath (time = 0). Samples for analysis of the MMD and monomer conversion were taken at different intervals throughout the reaction.

When using a mixture of (Cu(I) / Cu(II) = 90/10, 50/50, 10/90 mole%) the quantity of Cu(I) and Cu(II) were modified keeping the overall amount of copper bromide = 0.412 mmol.

When a lower concentration of copper was used, a stock solution in water was prepared (0.412 mmol of copper, 0.19 ml of ligand in 10 ml of water). The stock solution (2 ml) was used where the [CuBr] was reduced by a factor of 20, 2 ml of the stock solution further diluted by x5 were where [CuBr] was reduced by 100.

7.4.4.2.2. ^{1}H NMR polymerisation.

For the reactions followed by on-line ^{1}H NMR, the procedure was essentially the same as above, replacing water by D_2O. An aliquot of 1 ml of the solution was transferred to a Young's tap modified NMR tube, time t = 0 was taken once the tube was at temperature in the NMR spectrometer.

7.4.5. Polymerisation of MeOPEG-MA in toluene with various initiators.

7.4.5.1.Octadecyl-2-bromoisobutyrate.

7.4.5.1.1.Synthesis of the initiator.

1-Octadecanol {Aldrich, 99%} (2.3263 g, 0.0086 moles) was suspended in Anhydrous THF {Romil Hi Dry}(10 mL). The mixture was heated and stirred until the 1-octadecanol dissolved. Triethylamine (1.226 mL, 0.0088 moles) and 2-bromoisobutyryl bromide {Aldrich, 98 %}(1.44 mL, 0.0088 moles) were added slowly and the mixture was stirred at room temperature for 8 hours.

The solution was filtered and THF was removed by rotary evaporation. The organic liquid was dissolved in dichloromethane and washed extensively with saturated

$NaHCO_3$ solution and distilled water. The product was dried over $MgSO_4$ and dichloromethane was removed by rotary evaporation to leave a pale yellow liquid.

Yield = 73 %, FW = 420

Elemental analysis: 63.00 % C, 10.40 % H, (theoretical; 62.99 % C, 10.33 % H).

^{1}H NMR ($CDCl_3$, 298 K, 300 MHz) δ (ppm from TMS) = 3.63 (t, 2H, J = 6.03 Hz, -$C\underline{H}_2$-OH), 1.90 (s, 6 H, -CH_3), 1.56 (m, 2H, $C\underline{H}_2$-CH_2-OH), 1.26 (m, 30 H, -$(CH_2)_{15}$-), 0.86 (t, J = 6.03 Hz, 3 H, CH_3-)

^{13}C NMR ($CDCl_3$, 298 K, 75 MHz) δ (ppm from TMS) 170.1, 65.6, 32.9, 32.0, 29.8, 29.6, 29.4, 25.9, 22.8, 14.1

IR absorption ν (cm^{-1}) 3308, 2956, 2917, 2860 (Alk. C-H stretch), 1636 (C=O stretch), 1473, 1463, 1409, 1378, 1123, 1072, 1063, 1051, 1039, 1022

7.4.5.1.2.Schlenk polymerisation.

Targeted degree of polymerisation, DP_{Theo} = 10.

CuBr (0.442 g, 3.1 mmol) were placed in a Schlenk tube and placed under a nitrogen atmosphere. Deoxygenated MeO(PEG)MA (10 mL, 0.031 mol), toluene (50vol%) and Octadecyl-2-bromoisobutyrate (1.2986 g, 3.1 mmol) were added at room temperature. The mixture was deoxygenated by three freeze-pump-thaw cycles after which the *N*-(*n*-propyl)-2-pyridylmethanimine ligand was added (2 mol equiv. to CuBr, 6.2 mmol, 0.97 mL). Next the Schlenk tube was immersed in a thermostated oil bath at the reaction temperature (time = 0 s). Samples for analysis of the molar mass distribution (MMD) and monomer conversion were taken at different intervals throughout the

reaction. Catalyst residues were removed by passing the samples through a short column of basic alumina prior to SEC and NMR analysis.

7.4.5.2. α-perfluoroalkyl-2-bromoisobutyrate.

7.4.5.2.1.Synthesis of the initiator.

Rf = $(CF_2)_n$, n ~ 8 from ^{19}F analysis

Zonyl BA {Du Pont, purity unknown} (4 g, 0.0086 moles) was suspended in anhydrous THF {Romil Hi Dry}(10 mL). The mixture was heated and stirred until the Zonyl BA dissolved. Triethylamine (1.226 mL, 0.0088 moles) and 2-bromoisobutyryl bromide {Aldrich, 98 %}(1.44 mL, 0.0088 moles) were added slowly and the solution was stirred at room temperature for 8 hours.

The solution was filtered and THF was removed by rotary evaporation. The waxy solids were dissolved in dichloromethane and washed extensively with saturated $NaHCO_3$ solution, 1M HCl, and distilled water. The product was dried over $MgSO_4$ and dichloromethane was removed by rotary evaporation to leave a pale yellow gelatinous solid.

Yield = 73 %, FW = 613

CH Theoretical 27.10, 1.50 found 27.74, 1.66

^1H NMR ($CDCl_3$, 298 K, 300 MHz) δ (ppm from TMS) = 4.45 (t, 2H, J = 6.03 Hz), 2.49 (tt, 2H, J_1 = 6.03 Hz, J_2 = 18.1 Hz), 1.90 (s, 6H)

^{13}C NMR ($CDCl_3$, 298 K, 75 MHz) δ (ppm from TMS) 171.6, 121-107 (heavily split CF signals), 58, 55, 30.5 (t), 30.7

^{19}F NMR ($CDCl_3$, 298K, 282.2 MHz) δ (ppm from TMS) –81.4, -114.1, -122.3, -122.5, -123.3, -124.2, 126.7

IR absorption ν (cm^{-1}) 3308, 2969, 2871, (Alk. C-H stretch), 1738, 1636 (C=O stretch), 1549, 1524, 1466, 1435, 1370, 1296, 1265, 1228, 1216, 1204, 1068

7.4.5.2.2.Schlenk polymerisation.

Targeted degree of polymerisation, $DP_{Theo} = 10$.

CuBr (0.442 g, 3.1 mmol) were placed in a Schlenk tube and placed under a nitrogen atmosphere. Deoxygenated MeO(PEG)MA (10 mL, 0.031 mol), toluene (50vol%) and α-perfluoroalkyl-2-bromoisobutyrate (1.9003 g, 3.1 mmol) were added at room temperature. The mixture was deoxygenated by three freeze-pump-thaw cycles after which the *N*-(*n*-propyl)-2-pyridylmethanimine ligand was added (2 mol equiv. to CuBr, 6.2 mmol, 0.97 mL). Next the Schlenk tube was immersed in a thermostated oil bath at the reaction temperature (time = 0 s). Samples for analysis of the molar mass distribution (MMD) and monomer conversion were taken at different intervals throughout the reaction. Catalyst residues were removed by passing the samples through a short column of basic alumina prior to SEC and NMR analysis.

7.4.5.3.PMMA macroinitiator.

7.4.5.3.1.Synthesis of the initiator.

Copper (I) mediated polymerisation of MMA ([MMA]:[I]:[Cu]:[L] = 100:1:1:2)

Cu(I)Br (0.1273 g, 0.89 mmol) and Cu(II)Br (0.0099 g, 0.0445 mmol) and a dry magnetic follower were charged to a dry Schlenk tube. The tube was sealed with a rubber septum underwent three vacuum / N_2 cycles. Toluene (10 mL), MMA (10 mL, $9.32 * 10^{-2}$ moles) and ethyl-2-bromoisobutyrate (0.136 mL, 0.932 mmoles) were added under N_2. The Schlenk tube was subjected to three freeze pump thaw cycles

and subsequently was heated to 90 °C with constant stirring. Once the reaction temperature had been reached, *N*-(*n*-propyl)-2-pyridylmethanimine (0.28 mL, 1.864 mmoles) was added under N_2 (t = 0). Samples were removed periodically using a degassed syringe for molecular weight and conversion analysis. The reaction was stopped after 2 hours, at 48% conversion.

M_n = 5,100 (PDI = 1.11)

7.4.5.3.2.Schlenk polymerisation.

Targeted degree of polymerisation, DP_{Theo} = 10.

CuBr (0.442 g, 3.1 mmol) were placed in a Schlenk tube and placed under a nitrogen atmosphere. Deoxygenated MeOPEG-MA (10 mL, 0.031 mol), toluene (50vol%) and PMMA (15.81 g, 3.1 mmol) were added at room temperature. The mixture was deoxygenated by three freeze-pump-thaw cycles after which the *N*-(*n*-propyl)-2-pyridylmethanimine ligand was added (2 mol equiv. to CuBr, 6.2 mmol, 0.97 mL). Next the Schlenk tube was immersed in a thermostated oil bath at the reaction temperature (time = 0 s). Samples for analysis of the molar mass distribution (MMD) and monomer conversion were taken at different intervals throughout the reaction. Catalyst residues were removed by passing the samples through a short column of basic alumina prior to SEC and NMR analysis.

7.5. Chapter 4: Understanding of the kinetics of polymerisation: Solvent effects.

7.5.1. Polymerisation of BzMA on 2EIBr, MeOPEG-I_{113} in tol and $(EtO)_2EG$ folowed by ^1H NMR.

7.5.1.1.Polymerisation of BzMA using (poly(ethylene glycol) methyl ether) 2-bromoisobutyrate (MeOPEG-I) as macroinitiator

A degree of polymerisation of 100 was targeted. CuBr (1.13×10^{-4} mol, 0.0162 g), BzMA (11.3 mmol, 2.00 g), (poly(ethylene glycol) methyl ether)-2-bromoisobutyrate (1.135×10^{-4} mol, 0.5855 g), *N*-(*n*-octyl)-2-pyridylmethanimine ligand (3.40×10^{-4} mol, 0.0743 g). The polymerisation was carried out as described in part 6.2.2.2 at 50 °C.

7.5.1.2.Polymerisation of BzMA in various solvents

A degree of polymerisation of 100 was targeted. CuBr (1.13×10^{-4} mol, 0.0162 g), BzMA (11.3 mmol, 2.00 g), solvent (2.0 mL of toluene-d_8, or 1.6 g toluene-d_8 + 0.4 g 1,2-diethoxy ethane), ethyl 2-bromoisobutyrate (1.13×10^{-4} mol, 0.0221 g), *N*-(*n*-propyl)-2-pyridylmethanimine ligand (1.13×10^{-4} mol, 0.0743 g). The polymerisation was carried out as described above at 50 °C.

7.5.2. ^1H NMR study of copper complex in toluene-d_8 + $(EtO)_2EG$.

Cu(I)Br (0.41 mmol, 58.9 mg) was placed in a Schlenk tube under a nitrogen atmosphere. *N*-(n-Octyl)-2-pyridylmethanimine ligand, was added (2 mol equiv. to Cu(I)Br, 0.82 mmol, 0.22 mL). Deoxygenated $(EtO)_2EG$ (2 mol equiv. to Cu(I)Br, 0.82 mmol, 0.1151 mL or 5 mol equiv. to Cu(I)Br, 2.05 mmol, 0.2878 mL) was added

under nitrogen and the solution was stirred for 5 min. Once the medium was homogeneous, 2 ml of the solution was transferred to a Young's tap modified NMR tube at ambient temperature, time t = 0 was taken once the tube was at temperature in the NMR machine.

7.5.3. ^{1}H NMR study of the stability of the copper complex in D2O.

Cu(I)Br (0.41 mmol, 58.9 mg) was placed in a Schlenk tube under a nitrogen atmosphere. *N*-(n-Propyl)-2-pyridylmethanimine ligand, was added (2 mol equiv. to CuBr, 0.82 mmol, 0.13 mL). Deoxygenated D_2O was added under nitrogen and the solution was stirred for 5 min. To achieve complete dissolution of the complex the solution was heated at 40°C for a further 5 minutes. Once the medium was homogeneous, 2 ml of the solution was transferred to a Young's tap modified NMR tube at ambient temperature, time t = 0 was taken once the tube was at temperature in the NMR machine.

7.5.4. UV spectrometry with Nile Red

Absorption spectra were recorded on a Perkin-Elmer Lambda 9 electronic absorption spectrophotometer. Solutions were examined using stoppered quartz cells of 1 mm path length. Absorption spectra of Nile Red in several conventional solvents were obtained and found to be in good agreement with published data.[260] The ionic liquids examined have no absorption bands in the region of interest.

7.6. Chapter 5: Physical properties of the surface modifier agents synthesised.

7.6.1. Thermal properties.

7.6.1.1.Thermogravimetry.

Thermogravimetric analyses were performed on a Perkin Elmer TGA 51 under nitrogen at 5°C min^{-1}. Approximately 10 mg of each sample were heated at a rate of 10°C min^{-1} under a dry nitrogen atmosphere and the weight loss of the polymer was measured as a function of temperature.

7.6.1.2.Differential Scanning Calorimetry.

DSC measurements were carried out on a Perkin Elmer DSC Pyris 1 calibrated with indium and cyclohexane. Each sample was scanned with a heating rate of 10 °C min^{-1}. Four subsequent scans were performed. The measured DSC data are averaged on three last subsequent scans. The glass transition temperature Tg, the change in specific heat ΔCp, and the width of the glass transition temperature region ΔTg were determined by standard extrapolating the linear portion of DSC traces.[261]

7.6.2. Surface properties.

7.6.2.1.Contact angle measurement.

7.6.2.1.1.Contact angle by the sessile drop method.

Polymer films were prepared from 1.5 wt. % solutions in dichloromethane. Glass slides were washed with water and acetone followed by tissue drying. Films were formed by spin coating. Static advanced and receded contact angles were measured on

a horizontal stage and viewed by microscope linked PC. Water (Millipore deionised) (typically 30 μL) was placed on the film using a manual micrometer driven syringe with the needle remaining in the droplet. The angle was advanced by either addition of 10 μL of liquid or by dragging the drop across the surface by means of the syringe needle mounted on a manually driven micrometer translational stage (both methods gave identical results). The drop was receded either by withdrawing 10 μL of liquid or observed as the trailing side of the displaced drop as outlined above (both methods gave identical results). Contact angles were measured from the recorded images using Adobe Photoshop. At least six measurements of each angle were recorded and the results quoted were an average. Results were normally subject to an error of ± 2°. Annealed samples were baked in an oven at 140°C for 12 hours.

7.6.2.1.2.Contact angle by the Wilhelmy technique.

Dynamic contact angles were measured for polymer films dip coated in 1.5 wt % solution in dichloromethane and annealed at 140°C for 24 hours.

7.6.2.2.Aggregate properties.

7.6.2.2.1.CMC measurement by tensiometry.

Solutions of varying concentrations of the polymer were accurately made up in doubly distilled, filtered (0.45 micron) water under dust free conditions.

A Pt ring was flame cleaned and mounted on the tensiometer DST9005 (Nima Technology) balance. Distilled water was added to the test vessel and the surface tension was verified as 72.8 mN m^{-1}. The test vessel was washed with filtered (dust free) acetone and dried using filtered compressed air. The Pt ring was flame cleaned

and the surface tension of the least concentrated polymer solution was measured. This procedure was repeated for all samples.

7.6.2.2.2.CMC measurement by fluorimetry.

The following method was followed as a modification to that outlined by Winnik *et al.*[262]

A stock solution on pyrene {Aldrich, 99%} (0.20 g) in filtered acetone {BDH, HPLC grade}(200 mL) was accurately made up. Aliquots of pyrene solution were added to volumetric flasks so that each had a concentration of $1 * 10^{-7}$ mol dm^{-3}. The flasks were then dried by filtered compressed air. Solutions of varying concentration the polymer were accurately made up in doubly distilled, filtered (0.45 micron) water under dust free conditions in these volumetric flasks. In the emission measurements, the solutions were irradiated with UV at 333 nm and the emission spectra were measured for wavelength between 360 nm and 460 nm. In the excitation experiments, the solutions were irradiated with a range of wavelength from 300 nm to 360 nm and the emission spectra were recorded for 394 nm. Intensities for $\lambda = 333$ nm and 338.5 nm were compared.

7.6.2.2.3.Aggregate size measurement by Dynamic Light Scattering (DLS).

Dynamic light scattering measurements were done using the Malvern Zetasizer 3000HS spectrometer equipped with a 5mW-helium neon laser operating at 633 nm and a 7132 correlator operating in 8 x 8 groups. Determination of the hydrodynamic diameter was done using the CONTIN and NNLS algorithms. All measurements were

carried out at a scattering angle 90° and a temperature of 25°C. A standard latex of 200 nm diameter (Duke scientific) was used as calibration standard.

Chapter 8

Appendix

8.1. Appendix 1

Molecular weight - Definitions

The molecular weight of a polymer is one of its most important characteristics, as it plays an important role in its properties, and therefore its application.

In most of the polymerisation processes, the product formed will not contain polymer chains of the same length (monodisperse species), but will show a distribution of differing length polymer chains and hence a distribution of molecular weights. Therefore, to give an idea of the actual size of the polymer chains, an *average* molecular weights is used, this average being calculated in different ways, and each way having its own value. The most commonly used are:

The Number Average Molecular Weight, $\mathbf{M_n}$:

The number average molecular weight is the total weight of all the polymer molecules in a sample, divided by the total number of polymer molecules in a sample.

$$M_n = \frac{M\,P(M)\,dM}{P(M)\,dM} \qquad \textbf{eq. A.1}$$

The Weight Average Molecular Weight, $\mathbf{M_w}$:

The weight average is based on the fact that a bigger molecule contains more of the total mass of the polymer sample than the smaller molecules do. Therefore, each molecule is 'weighted' by its concentration in the sample: $\frac{MP(M)}{MP(M)dM}$

To get the Weight Average Molecular Weight, we sum the different 'weighted' molecular weights:

$$M_w = \frac{M^2 P(M)\, dM}{M P(M)\, dM} \qquad \textbf{eq. A.2}$$

The Plot Thickens: Viscosity Average Molecular Weight, $\mathbf{M_v}$

Molecular weight can also be calculated from the viscosity of a polymer solution, based on the principle that bigger polymers molecules make a solution more viscous than small ones do.

M_v is closer to the weight average than the number average.

$$M_v = \left[\frac{M^{1+\alpha} P(M)\, dM}{M P(M)\, dM} \right]^{\frac{1}{\alpha}} \qquad \textbf{eq. A.3}$$

P(M) represents the number of *molecules of molecular weight M.* The weight of the molecules is defined as W(M) = M P(M).

Because of the different way of calculating the average molecular weight, it is more usual to consider the actual *molecular weight distribution* (MWD) of a polymer. Figure A1.1 gives an example of a distribution of molecular weight. The knowledge of this distribution could be critical in predicting the physical caracteristic and the performance of the polymer.

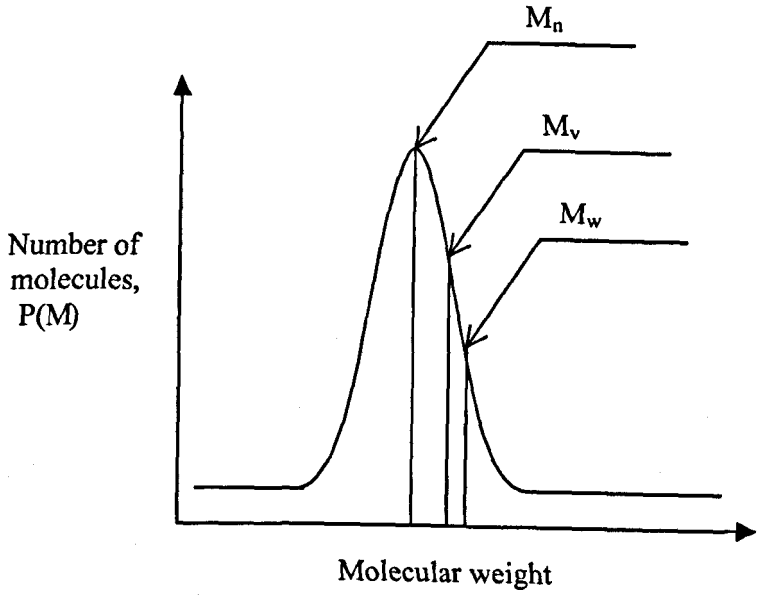

Figure A1.1: Example of a distribution of molecular weight.

The *polydispersity* of the sample is defined as:

$$PDI = \frac{M_w}{M_n} \qquad \textbf{eq. A.4}$$

The minimum value od the PDI is 1, for monodisperse samples. On figure A.1, it is represented by the width of the distribution.

8.2. Appendix 2

8.2.1. Molecular weight determination by gel permeation chromatography (GPC).

8.2.1.1.Theory – Principle

A wide range of methods can be used for the determination of the MWD. However, methods based on colligative properties, light scattering, or viscosity.[263,264] can only give an average of the MWD and not the whole distribution. Only gel permeation chromatography (GPC), based on the principle of size exclusion chromatography (SEC) can give the whole distribution of molecular weight.

A definition of chromatography similar to one originally stated by Harold H. Strain (Recipient of the first ACS award in chromatography, 1961) is as follows: *Chromatography* is a separation method in which a mixture is applied as a narrow initial zone to a stationary, porous sorbent and the components are caused to undergo differential migration by the flow of the mobile phase, a liquid or a gas.

The originator of chromatography as it is practiced today was a Russian botanist, Michael Tswett (1872-1919). In 1906 he published a paper describing the separation and isolation of green and yellow chloroplast pigments by column adsorption chromatography and stated that "Chromatography is a method in which the components of a mixture are separated on an adsorbent column in a flowing system". It is far later, in 1964, that J. C. Moore will develop the gel permeation chromatography as a practical method.

The principle of GPC is based on the separation of molecules by their size, or more accurately by their hydrodynamic volume (V_h). The hydrodynamic volume is the volume that a polymer chain will occupy in a certain solvent. For linear molecules, this volume is directly related to their molecular weight.

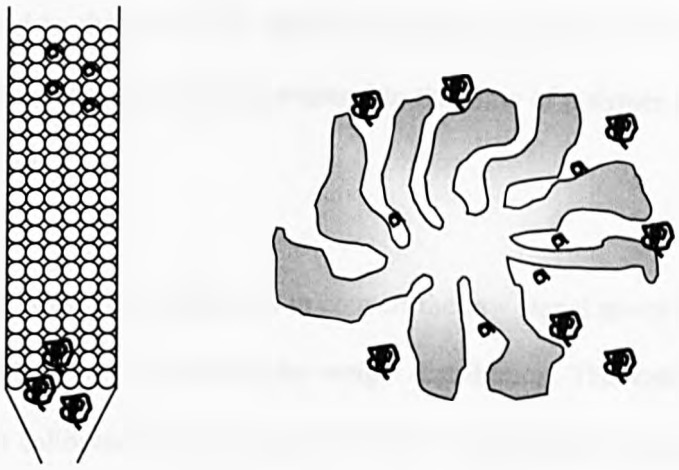

Figure A2.1: Schematic of the elution of polymer chains in a chromatographic column containing beads of cross-linked polymers.

A sample of polymer showing a range of different molecular weight is dissolved in a solvent, called eluent. The solution is injected in a column, containing beads of a cross-linked polymer, usually made of Poly(styren/divinylbenzene). While migrating, the different molecules can interact with the column. Molecules with a smaller V_h will have the opportunity to visit any cavities, staying longer in the column, while bigger V_h chains will be more excluded and therefore come out faster (Figure A2.1). Different columns are commercially available, showing a different range of cavity size, helping in a separation of a certain molecular weight range.

This results in the separation of the different molecules at the exit of the column, which are then analysed by a detector. The most common detector used is the

differential reffractive index (DRI) which measure the difference in refractive index between the sample and the pure eluent. One can find as well, for exemple, *UV absorbence detectors* more accurate because of a better signal to noise ratio, but dependent on the presence of UV chromophores in the polymer, or *IR absorbence detectors* limited to the use of IR sensitive polymers. In any cases, the raw signal given by the detector is directly proportionnal to the mass of polymer fraction passing throw the detector.

The task of GPC data interpretation is to convert the raw signal given by the detector, intensity vs. elution time, in a molecular weight distribution. This can be done by the knowledge of a calibration curve (LogM vs Elution time) and by the proportionality between detector signal and mass of polymer fraction. A calibration curve is usually created by the use of well characterised polymers of narrow polydispersity. The LogM vs Elution time plot resulting is generally fitted by a third order polynomial.

As the answer of the detector (h_v) is proportional to the mass of the polymer fraction of interest, the chromatogram has to be normalised to give the weight percentage of polymer by volume unit (V_{el}). This is done by dividing the value of the answer for a sample at an elution volume, V_{el}, by the sum of all the answers:

$$\frac{dw}{dV_{el}} = \frac{h(V_{el})}{h(V_{el})dV_{el}} \qquad \textbf{eq. A.5}$$

The normalised chromatogram is then combined with the calibration curve to give a distribution in term of logarithm of molecular weight rather than in term of volume:

$$W(\log M) = \frac{dw}{d(\log M)} = -\frac{dw}{dV_{el}} \times \frac{dV_{el}}{d(\log M)} \qquad \textbf{eq. A.6}$$

We obtain then the percentage differential logarithm molecular weight distribution of the sample, which is a molecular weight distribution on a log molecular weight axis. This can be converted into a linear weight distribution, W(M), as follows:

$$W(M) = \frac{dw}{dM} = \frac{dw}{d(\log M)} \times \frac{d(\log M)}{dM}$$

$$= \frac{dw}{d(\log M)} \times \frac{\log(e)}{M}$$

$$= W(\log M) \times \frac{\log(e)}{M} \qquad \textbf{eq. A.7}$$

Knowing the linear weight distribution W(M), the number distribution P(M) can be calculated:

$$P(M) = \frac{W(M)}{M} \qquad \textbf{eq. A.8}$$

If the standards and the sample are the same polymers, GPC will give the 'absolute' molecular weight. However, and this is the case most of the time, the standards for the polymer studied might not be available. Therefore, the simplest procedure is to use the *universal calibration.*

The universal calibration method is based on the fact that polymer of different type with the same molecular weight have different hydrodynamic volumes in solution. The hydrodynamic volume of a molecule in solution can be shown to be directly related to the *intrinsic viscosity* (η) and the molecular weight of the polymer:[265]

$$V_h = M_v \times \eta \qquad \textbf{eq. A.9}$$

The intrinsic viscosity is also related to the molecular weight by the Mark-Houwink-Sakurada equation:[264,266]

$$\eta = K \times M_v^{\alpha} \qquad \textbf{eq. A.10}$$

where K and α are parameters available in the literature, described for a specific polymer at a defined temperature in a certain solvent.

Combining these two equations leads to the universal calibration equation:

$$\log V_h = \log K + (\alpha + 1) \times \log M_v \qquad \textbf{eq. A.11}$$

This method, while readily applied, showed two major problems. Firstly, the molecular weight used is the M_v which is close to the M_w. Secondly, the literature shows a wide scatter of the Mark-Houwink parameters for a particular polymer. A way to overcome these problems is the use of on-line GPC coupling with viscosimeter[267,268] or differential light scattering.[269] Both of these methods being absolute functions of the molecular weight, the need for standards is avoided.[264]

8.2.1.2. Using Gel permeation chromatography.

As demonstrated earlier, the molecular weight is of first interest in living polymerisation. Plotting the evolution of the molecular weight with the conversion helps polymer chemist to show the 'living' character of the polymerisation. Theoretically, in a 'living' system, polymer chains grow in parallel, each of them keeping the same length as the others at any time. Therefore, by plotting the molecular weight and PDI versus conversion, a first order polynomial joining the origin to the 'aimed' molecular weight and low PDI values will demonstrate the living character of the polymerisation. As seen above, GPC is the most current method of finding the molecular weight of a product, and more specifically the M_n, M_w and PDI.

Therefore, it is generally accepted in most publications to plot molecular weight vs. conversion, trying to follow as much as possible the 'theoretical' first order plot, independently of the polymer analysed and the GPC standards.

We propose inhere a model of the analysis of the molecular weight evolution during the polymerisation in a 'perfect' living system, and its interpretation when analysed with a PMMA-calibrated GPC.

In a first time, we will assume the perfect living polymerisation of polystyrene (PS). If the final molecular weight aimed is 10,000, the plot of the evolution of molecular weight vs conversion can be modelised by the function F(x) = 100x, with a molecular weight of 10,000 at 100% conversion.

At any time, the PS molecular weight M_i^{PS} is dependant to the hydrodynamic volume, as follows, by transformation of equation A.11:

$$V_{h,i}^{PS} = K_i^{PS} \times (M_i^{PS})^{(\alpha_i^{PMMA}+1)} \qquad \textbf{eq. A.12}$$

When the molecules of molecular weight M_i^{PS} are injected through the column, their hydrodynamic volume makes them eluting at a volume V_{el}. However, using the PMMA calibration curve, this volume of elution V_{el} will be associated to a hydrodynamic volume $V_{h,i}^{PMMA}$. Therefore,

$$V_{h,i}^{PS} = V_{h,i}^{PMMA} \qquad \textbf{eq. A.13}$$

Then, transforming the equation A.12, we can calculate the equivalent molecular weight of PMMA given by the GPC:

$$M_1^{PMMA} = \left(\frac{1}{K_1^{PMMA} \times V_{h,1}^{PMMA}} \right)^{\frac{1}{\alpha_i^{PMMA}+1}} \qquad \textbf{eq. A.14}$$

It is then possible to link the actual PS molecular weight to the molecular weight answer of the GPC (i.e. the PMMA molecular weight) by combining the equations A.13 and A.14:

$$M_i^{PMMA} = \left(\frac{K_i^{PS}}{K_i^{PMMA}} \right)^{\frac{1}{\alpha+1}} \times (M_i^{PS})^{\frac{\alpha_i^{PS}+1}{\alpha_i^{PMMA}+1}} \qquad \textbf{eq. A.15}$$

This being true for any M_i, we can sum this equation for any molecular weight from 0 to 10,000:

$$M_i^{PMMA} = \left(\frac{K_i^{PS}}{K_i^{PMMA}} \right)^{\frac{1}{\alpha+1}} \times (M_i^{PS})^{\frac{\alpha_i^{PS}+1}{\alpha_i^{PMMA}+1}} \qquad \textbf{eq. A.16}$$

$$F^{PMMA}(x) = \left(\frac{K_i^{PS}}{K_i^{PMMA}} \right)^{\frac{1}{\alpha+1}} \times F^{PS}(x)^{\frac{\alpha_i^{PS}+1}{\alpha_i^{PMMA}+1}} \qquad \textbf{eq. A.17}$$

Knowing the K and α values for both polymer from the polymer handbook (table A.1), we can plot the two function, see figure A2.2.

Polymer	**α**	**K*10^3 (dl/g)**
PMMA(THF, 30°C)	0.69	0.000128
PS(THF, 30°C)	0.428	0.0017

Table A.1: Mark-Houwink parameters for PMMA and PS at 30°C in THF.

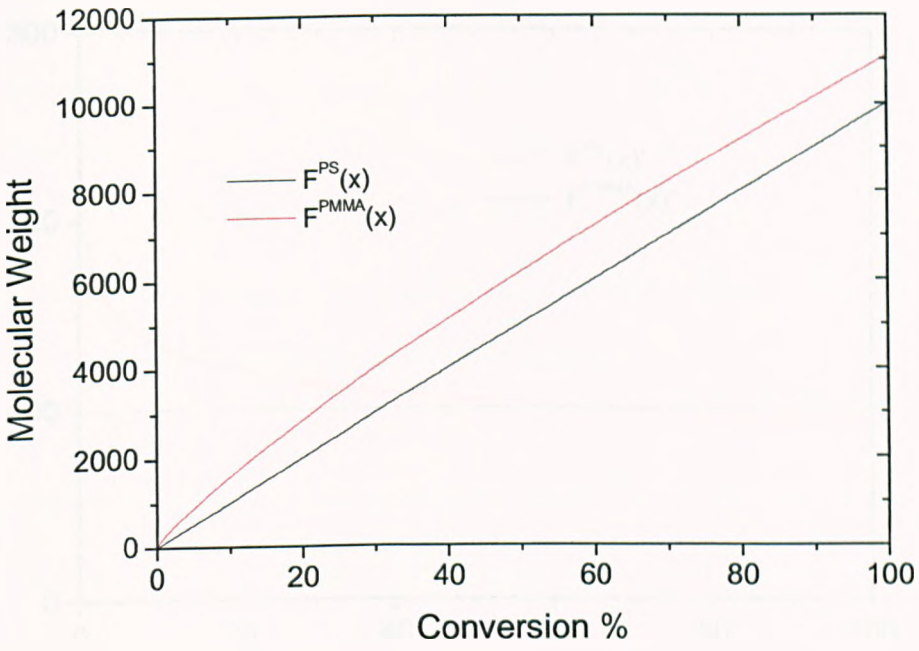

Figure A2.2: Theoretical evolution of the molecular weight during the living radical polymerisation of styrene (—) and as analysed by PMMA calibrated GPC(—).

While $F^{PS}(x)$, the actual molecular weight, is a first order polynomial, the plot resulting of the molecular weight given by PMMA-calibrated GPC is a curve. Therefore, a fitting of these results by a straight line would be wrong. Figure A2.3 shows the first derivative of each curves, with $F^{PS}(x)' = 100$ as expected, and $F^{PMMA}(x)'$ a function, confirming the non linearity of the 'GPC molecular weight'.

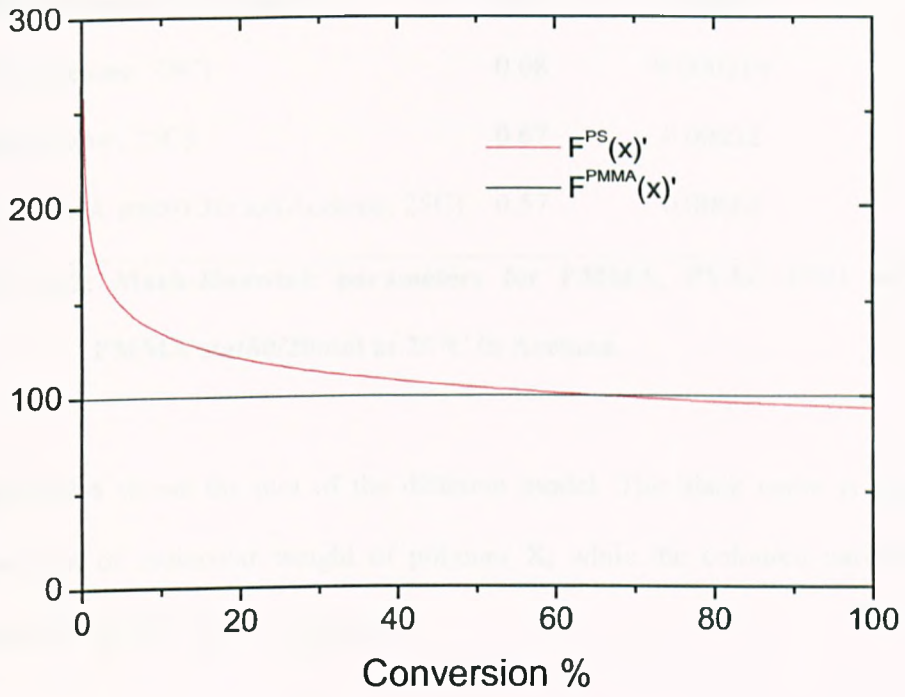

Figure A2.3: First order derivative of the theoretical evolution of the molecular weight during the living radical polymerisation of styrene (—) and as analysed by PMMA calibrated GPC(—).

In order to use a model for different cases, the same calculation was undertaken on different polymer, still using a PMMA-calibrated GPC. The case of a polymer close to the PMMA was studied (Poly Vinyl Acetate, PVAc), a polymer showing different chain properties, and of first interest in this work (Poly Ethylene Oxide, PEO), and a copolymer (statistic copolymer Poly Ethyl Acrylate- Poly Methyl Methacrylate, PEA-PMMA stat80/20mol). The different K and α values are summarised in table A.2.

Polymer	α	K*10^3 (dl/g)
PMMA(Acetone, 25C) atactic	0.71	0.000676
PVAc(Acetone, 25C)	0.68	0.000214
PEO(Acetone, 25C)	0.67	0.00032
PEA-PMMA stat80/20mol(Acetone, 25C)	0.57	0.00062

Table A.2: Mark-Houwink parameters for PMMA, PVAc, PEO and PEA-PMMA stat80/20mol at 25°C in Acetone.

Figure A2-4 shows the plot of the different model. The black curve is always the actual plot of molecular weight of polymer X, while the coloured curves are the answer of the GPC for the polymer X.

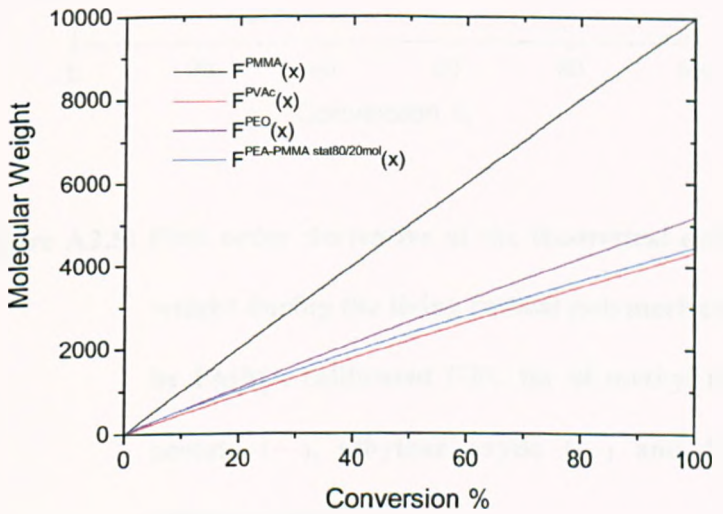

Figure A2.4: Theoretical evolution of the molecular weight during the living radical polymerisation (—)and as analysed by PMMA calibrated GPC for of methyl methacrylate (—), vinyl acetate (—), ethylene oxyde (—) and Ethyl Acrylate/ Methyl Methacrylate (—).

We observe a completely different behaviour of the different curves, giving a wrong final molecular weight. The plot of the derivatives of these functions shows again the non-linearity of the GPC molecular weight (Figure A2-5).

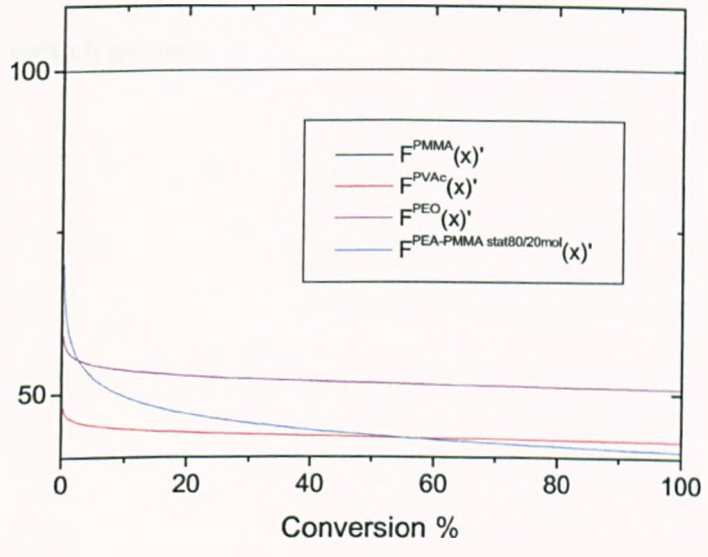

Figure A2.5: First order derivative of the theoretical evolution of the molecular weight during the living radical polymerisation (—)and as analysed by PMMA calibrated GPC for of methyl methacrylate (—), vynyl acetate (—), ethylene oxyde (—) and Ethyl Acrylate/ Methyl Methacrylate (—).

As a conclusion, it has been demonstrated by using this model that the use of GPC can be dangerous if not handled with care. While using a GPC calibrated with samples

different than the polymer analysed, one cannot expect the molecular weight obtained to be accurate, neither following the different theoretic molecular weight rules.

Conversely, the model studied above presents certain limits, as discussed previously. However, these problems are limited: Firstly, working with living polymerisation products implies a narrow MWD, which justifies the approximation of $M_v = M_w$. Secondly, the K and α values chosen have been reported and accepted by many research groups.

8.3. Appendix 3

8.3.1. Influence of a narrow PDI macro-initiator.

It has been shown in Appendix 2 that the use of GPC with polymers different than the calbration could give wrong molecular weights. We propose inhere to investigate the effect of AB block copolymer on the GPC analysis in the case of radical polymerisation initiated by a macroinitiator (A).

Modelling the polymerisation of MMA by free radical polymerisation can predict the molecular weight distribution, using a Schulz-Flory distribution.[266] The normalised number and weight molecular weight distributions of the product would be, respectively:

$$n(M) = M_{wt}(i) \times p^{i-1} \times (1-p) \qquad \textbf{eq. A.18}$$

$$w(M) = i \times M_{wt}(i) \times p^{i-1} \times (1-p)^2 \qquad \textbf{eq. A.19}$$

with, $M_{wt}(i) = i \times M_{wt}$ (i = number of units, M_{wt} = Molecular weight of the monomer), p = probability of reaction as $p = \frac{M_0 - M}{M_0}$ (M_0 = Monomer at t=0, M = Monomer at t).

Then, by definition,

$$M_n = \frac{i \times M_{wt} \times n(M) \times dM}{n(M) \times dM} \qquad \textbf{eq. A.20}$$

$$M_w = \frac{i \times M_{wt} \times w(M) \times dM}{w(M) \times dM} \qquad \textbf{eq. A.21}$$

$$PDI = \frac{M_w}{M_n} \qquad \textbf{eq. A.22}$$

with $n(M)\times dM = w(M)\times dM = 1$, as n(M) and w(M) are normalised.

In the case of the homopolymerisation of MMA, M_{wt} = 100.12 g/mol, and p = 0.99 will be used.

When using a macro-initiator of narrow PDI for the polymerisation of MMA, its polydispersity will be assumed to be 1, in order to simplify the calculations. Then, $M_{wt}(i) = i\times M_{wt} + M_I$ and p = 0.99. M_I is defined as being the GPC molecular weight of each initiator. Assuming that the GPC will analyse the copolymer as the summation of the molecular weights of the initiator and of the PMMA synthesised, figures A3.1 and A3.2 show respectively the plot of n(M) and w(M) versus Mwt(i) for the homopolymerisation of MMA initiated by Ethyl-2-bromoisobutyrate and two different macro-initiators (MeOPEG-I_{12} and MeOPEG-I_{113}).

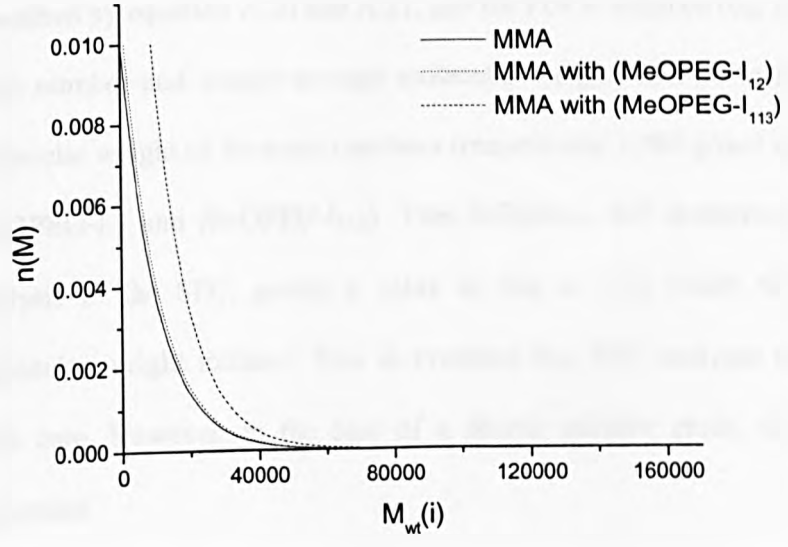

Figure A3.1: Number molecular weight distribution as function of the molecular weight of the units.

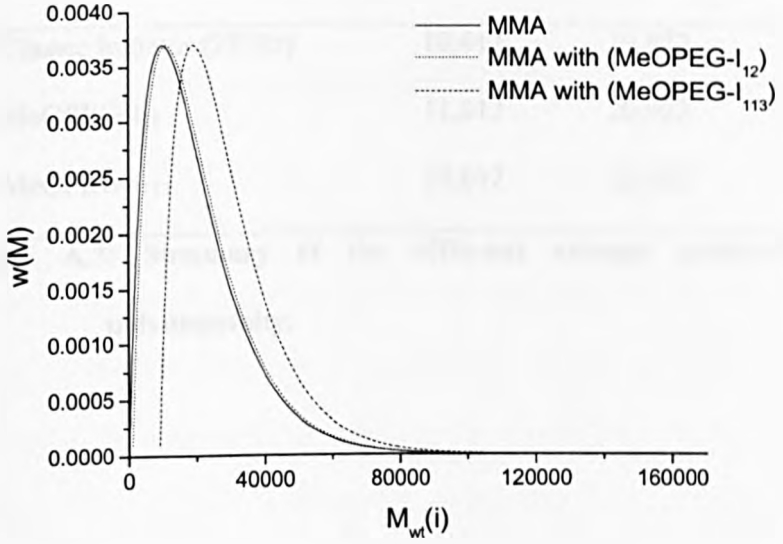

Figure A3.2: Weight molecular weight distribution as function of the molecular weight of the units.

The average number and weight molecular weights can then be calculated, as described by equation A.20 and A.21, and the PDI is deduced (eq. A.22).

Both number and weight average molecular weights will be increased by the SEC molecular weight of the macro-initiator (respectively 1,000 g/mol and 9,000 g/mol for MeOPEG-I_{12} and MeOPEG-I_{113}). This difference will dramatically affect the PDI analysis of the SEC, giving a value as low as 1.52 (table A.3) for the highest molecular weight initiator. This is evidence that SEC analyses need to be handled with care. However, in the case of a shorter initiator chain, the influence is less important.

	M_n	M_w	PDI
Classic Initiator (2EIBr)	10,012	19,922	1.99
MeOPEG-I_{12}	11,012	20,922	1.90
MeOPEG-I_{113}	19,012	28,922	1.52

Table A.3: Summary of the different average molecular weights and polydispersity.

8.4. Appendix 4

8.4.1. Dynamic Light Scattering (DLS): Mathematical approach.[255-257]

8.4.1.1.Correlation of the scattered signal.

Photon Correlation Spectroscopy (PCS), also known as Dynamic Light Scattering (DLS), is concerned with the investigation of correlation of photons. In a typical light scattering experiment single photons are detected with a single photon counting device. This detector transforms the signal from a single photon into an electronic signal, basically a '1' or a '0', depending on whether a photon was or was not detected in a certain time interval. The objective of PCS is to find any peculiar properties of the scattered signal which can be used to characterize and describe the seemingly random "noise" of the signal, and the correlation curve is used to achieve this objective.

A typical way to describe a signal is by way of its 'autocorrelation'. The autocorrelation function of the signal from the scattered intensity is the convolution of the intensity signal as a function of time with itself. In more abstract terms, if the detected intensity is described as a function I(t), then the autocorrelation function of this signal is given by eq.A.23, where t is the shift time.

$$G(\tau) = \int_0^{\infty} I(t) * I(t+\tau) d\tau \qquad \textbf{eq. A.23}$$

The above function is also called the intensity correlation function, and it is used to describe the correlation between the scattering intensities measured at t = 0 and some later time ($t_n = t_0 + t$). Considering for example the schematics shown figure A4.1, where the frame represents the scattering volume, the black circle represents the

particle, and the grey region represents the volume within which the particle must be contained. The scattering intensity at the detector is dependent upon the position of the particle relative to the detector. When considering very small time increments (micro-seconds), there is at t_0 ($t = 0$) a finite volume of space within which the particle can move during the first time increment. This finite volume of space is called the diffusional volume. At $t = t_1$, the particle has diffused a single step. Since the exact path is unknown, the diffusional volume or the volume of space within which the particle must reside considering all paths has expanded. The change in particle position is accompanied by a change in the measured scattering intensity at the detector. However, this new scattering intensity is still strongly correlated with that measured at t_0 due to the finite diffusional volume and the correlation between the current and initial positions. As the shift time increases, the diffusional volume also increases. The increased diffusional volume is accompanied by a decrease in the correlation between the current and initial particle positions. The correlation is still present however, as long as the diffusional volume is finite. At longer times (frame 6), the diffusional volume becomes infinite, and the correlation between the initial and current particle position and the respective scattering intensities is lost.

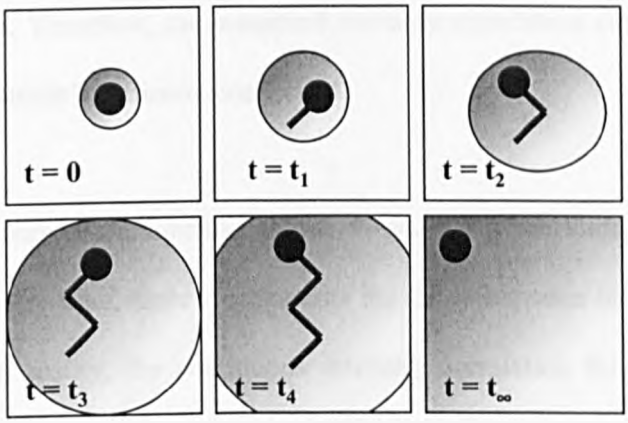

Figure A4.1: Schematic representing the scattering volume (frame) where a particle (black circle) moves in a defined volume (grey region) at different impulse time.

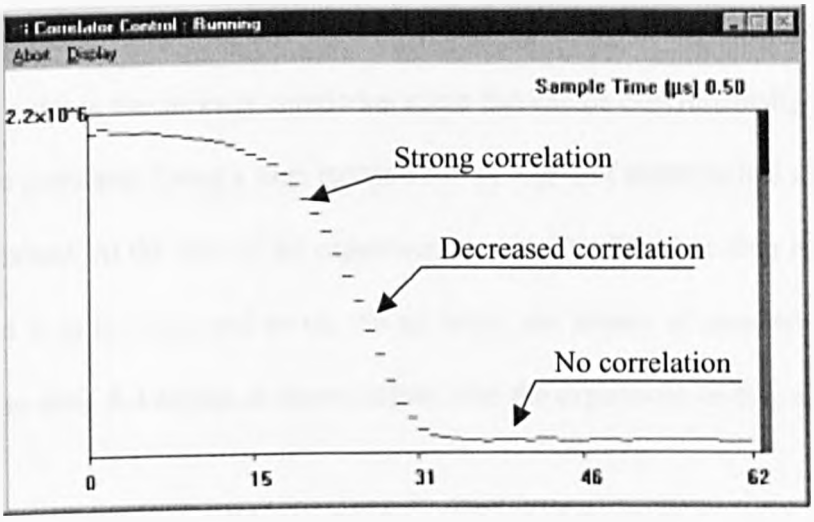

Figure A4.2: Intensity correlation function measured by DLS.

The correlation in particle position at small shift times is contained within the measured intensity correlation function, an example of which is shown figure A4.2. In the absence of any applied forces, the particle position is dictated by the degree of

Brownian motion. Therefore, the measured intensity correlation curve is an indirect measure of the particle's diffusion coefficient.

In the intensity correlation function shown in eq. A.23, the shift time (t) is often referred as the delay time, since it represents the delay between the original and the shifted signal. In reality, the continuous intensity correlation function can not be measured. It can however, be approximated with discrete points obtained by a summation over the duration of the experiment. This summation is performed by the correlator which continuously multiplies and adds measured intensity values.

A defining parameter for a correlator is its speed, i.e. its ability to add up numbers fast, or inversely expressed, the smallest delay time that can be handled. This delay time (α) determines the smallest accessible time of G(t). Hence, G(α) is the first numerical point in the intensity correlation curve that can be experimentally measured for a given correlator. Using a time increment of α, a grid of experimental data values can be obtained. At the start of the experiment, $t_0 = 0$. The first time then is at $t_1 = \alpha$, the second is at $t_2 = 2\alpha$, and so on. As an array, the stream of numbers could be displayed in table A.4 format as shown below, with the experiment ending at $t_n = n\alpha$.

Index	Time	Intensity
0	$t_0 = \alpha$	$I(t_0)$
1	$t_1 = \alpha$	$I(t_1)$
2	$t_2 = 2\alpha$	$I(t_2)$
...	...	...
n	$t_n = n\alpha$	$I(t_n)$

Table A.4: Number of intensity-signal received by the correlator during n acquisition.

The correlator now finds out how related these intensity numbers are to each other. It does this by comparing each number to its neighbour a defined time interval later. This comparison is carried through the duration of the experiment. As a summation, the comparison can be expressed as follows, where the upper summation limit is given by the appropriate index belonging to the largest available summation term for k.

$$G_k(\tau_k) = \sum_{i=0} I(t_i) * I(t_i + \tau_k) \qquad \textbf{eq. A.24}$$

The above expression is very general and holds true for both linear and arbitrary delay times. To understand the meaning of this summation, let's assume we would like to find $G(t_1) = G(a)$. According to the previous equation, $G(t_1)$ is defined as:

$$G(t_1) = I(t_0)I(t_0 + \alpha) + I(t_1)I(t_1 + \alpha) + I(t_2)I(t_2 + \alpha) + I(t_3)I(t_3 + \alpha) + \ldots$$

$$= I(t_0)I(t_1) + I(t_1)I(t_2) + I(t_2)I(t_3) + I(t_3)I(t_4) + \ldots \qquad \textbf{eq. A.25}$$

In the same fashion, $G(t_2)$ is defined as:

$$G(t_1) = I(t_0)I(t_0 + 2\alpha) + I(t_1)I(t_1 + 2\alpha) + I(t_2)I(t_2 + 2\alpha) + I(t_3)I(t_3 + 2\alpha) + \ldots$$

$$= I(t_0)I(t_2) + I(t_1)I(t_3) + I(t_2)I(t_4) + I(t_3)I(t_5) + \ldots \qquad \textbf{eq. A.26}$$

In table format, the correlation function values can then be written as given in table A.5.

Index	Time	Intensity	Correlation function value
0	$t_0 = \alpha$	$I(t_0)$	
1	$t_1 = \alpha$	$I(t_1)$	$G(t_1) = I(t_0)\times I(t_1) + I(t_1)\times I(t_2) + \ldots + I(t_{n-1})\times I(t_n)$
2	$t_2 = 2\alpha$	$I(t_2)$	$G(t_2) = I(t_0)\times I(t_2) + I(t_1)\times I(t_3) + \ldots + I(t_{n-2})\times I(t_n)$
...	...	...	...
n	$t_n = n\alpha$	$I(t_n)$	$G(t_n) = I(t_0)\times I(t_n)$

Table A.5: Correlation function values received by the correlator during n acquisition.

The series of G(t) values is typically normalised, such that the value for very large time (as $t \rightarrow \infty$) is $G(\infty) = 1$. For standard light (with Gaussian statistics), this normalisation imposes a theoretically limit of $G(t_0) = 2$ at $t = 0$. However, only carefully optimised optical systems can ever achieve such a high intercept or amplitude.

For a random signal and a large measurement time, all G values would add up to roughly the same number. The signal would then be described as 'uncorrelated', and

the resultant intensity correlation curve would look like random fluctuations about the baseline, similar to intensity correlation curve for H_2O shown in figure A4.3.

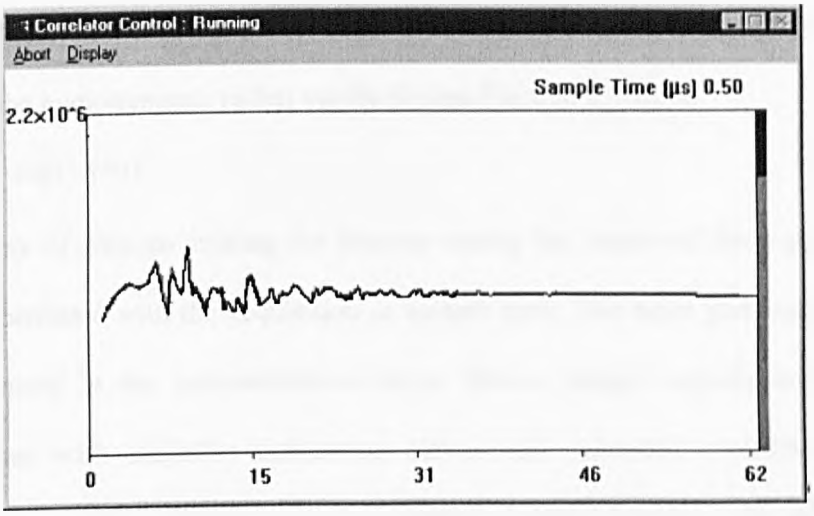

Figure A4.3: Intensity correlation function of an uncorrelated signal.

For light scattered from diffusing molecules however, the intensity correlation curve exhibits an exponential decay, indicating that the signal is correlated.

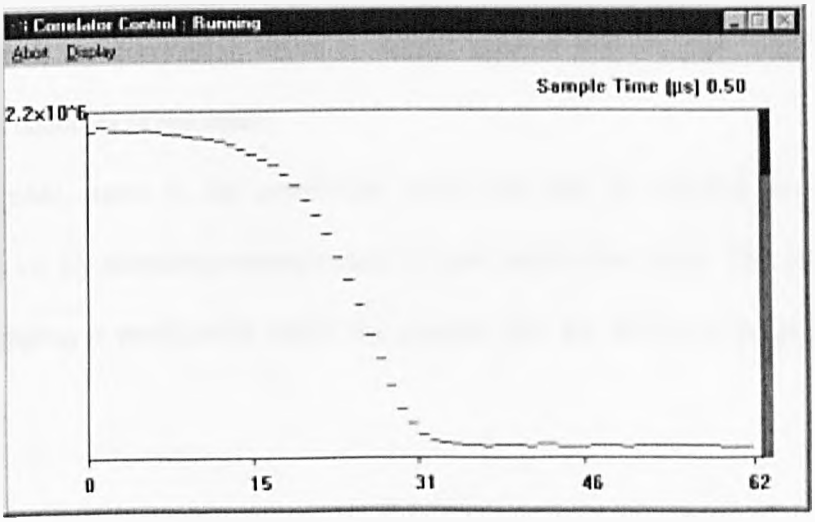

Figure A4.4: Intensity correlation function measured by DLS.

For typical diffusion processes the correlation function has the form of 1 plus an exponential decay function. The decay constant, γ in the following expression, is representative of the diffusional properties of the particle under examination. Hence, evaluation of γ leads to the particle diffusion coefficient, which in turn is used to calculate the hydrodynamic radius via the Stokes Einstein equation.

$$G(\tau) = 1 + \exp(-\gamma * t) \qquad \textbf{eq.A.27}$$

The number of photons striking the detector during the course of the experiment is directly correlated with the acquisition or sample time. The more photons collected, the less noise in the autocorrelation curve. Hence, longer acquisition times are synonymous with smoother correlation curves and enhanced confidence in the experimental results. Because of the correlation with photons collected, longer acquisition times are usually required at low sample concentrations, where the signal to noise intensity ratio is smaller.

On the other hand, the likelihood of a dust event is significantly increased at longer acquisition times. If a dust particle enters the scattering volume during the course of measurement, the correlation curve is shifted upward proportionally, and baseline evaluation becomes problematic.

On the upside, noise in the correlation curve can also be reduced via statistical averaging, i.e. by collecting multiple runs at short acquisition times. This approach to noise averaging is particularly useful for samples that are not clean despite multiple filtrations.

8.4.1.2.Scattering Intensity, Mass and Number.

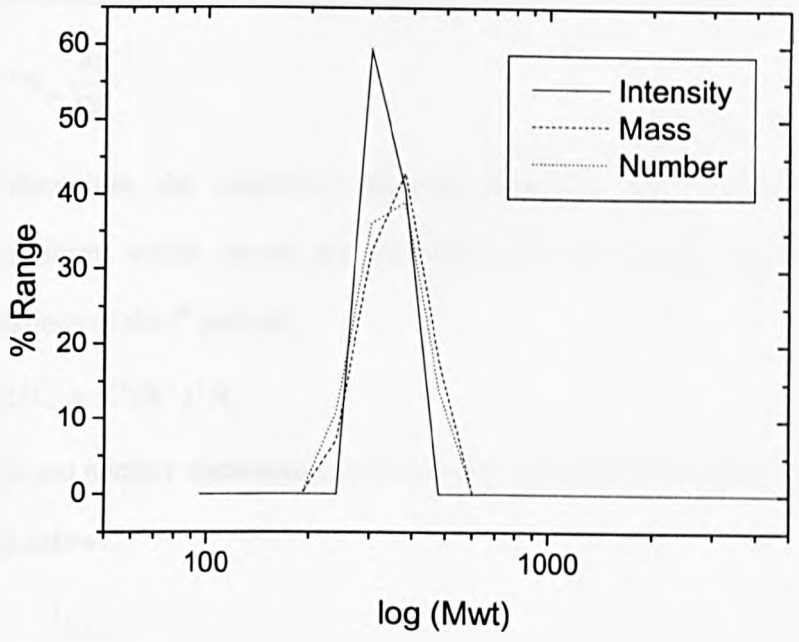

Figure A4.5: Intensity, mass and number distribution of particles measured by DLS.

According to static light scattering theory, the scattering intensity of the i^{th} particle (I_i) in a distribution of particles is proportional to both the molecular weight (M_i) and the concentration as given in the simplified form of the Rayleigh expression shown below (eq.A.29), where C_i is the weight or mass concentration, N_i is the number concentration, and K is a constant.

$$I_i = KM_iC_i = K(M_i)^2N_i \qquad \textbf{eq. A.28}$$

The size or radius (R) of the particle can be estimated from the molecular weight via the partial specific volume (V_p) as shown in the following expression, where N_A is Avogadro's number and x is a shape parameter equal to 3 for spheres and 2 for coils.

$$M_i = R^x N_A \frac{4\pi}{3V_p} \qquad \textbf{eq. A.29}$$

After substitution, the simplified Rayleigh expression can be re-written in the following form, which relates the scattering intensity to the mass and number concentrations of the i^{th} particle.

$$I_i = K'R_i^x C_i = K''(R_i^x)^2 N_i \qquad \textbf{eq. A.30}$$

The mass and number distributions are then calculated from the intensity distribution as shown below.

$$\frac{C_i}{C_i} = \frac{I_i / R_i^x}{\left(I_i / R_i^x\right)} \qquad \textbf{eq. A.31}$$

$$\frac{N_i}{N_i} = \frac{I_i / R_i^{2x}}{\left(I_i / R_i^{2x}\right)} \qquad \textbf{eq. A.32}$$

Chapter 9

References

1)Moad, G.; Solomon, D. H. *The Chemistry of Free Radical Polymerization*; Pergamon: Oxford, 1995.

2)Staudinger, H. *Chem. Ber.* **1920**, *53*, 1073.

3)Peterson, M. D.; Weber, A. G. : USA, 1946; Vol. 2, pp 292.

4)Pavljucenko, V. N.; Kolosova, T. O.; Lovjagina, L. D.; Kerzkovskaja, V. V.; Gromov, E. V.; Vylegzanina, K. A.; Egorova, E. I.; Ivancev, S. S. *Acta Polymerica* **1983**, *34*, 399.

5)Burczyk, A. F.; Odriscoll, K. F.; Rempel, G. L. *J. Polym. Sci.: Polym. Chem.* **1984**, *22*, 3255.

6)Szwarc, M.; Levy, M.; Milkovich, R. *J. Am. Chem. Soc.* **1956**, *78*, 2656.

7)Szwarc, M. *Nature* **1956**, *176*, 1168.

8)Yu, J. M.; Dubois, P.; Jerome, R. *Macromolecules* **1997**, *30*, 6536.

9)Yu, J. M.; Dubois, P.; Jerome, R. *Macromolecules* **1997**, *30*, 4984.

10)Yu, Y. S.; Zhang, L. F.; Eisenberg, A. *Langmuir* **1997**, *13*, 2578.

11)Jin, G. T.; Yang, W. T. *Journal of Polymer Materials* **1994**, *11*, 63.

12)Cazzaniga, L.; Cohen, R. E. *Macromolecules* **1991**, *24*, 5817.

13)Bawn, C. E. H.; Bell, R. M.; Ledwith, A. *Polymer* **1965**, *6*, 95.

14)Dryfuss, M. P.; Dryfuss, P. *Polymer* **1965**, *6*, 93.

15)Vofsi, D.; Tobolski, A. V. *J. Polym. Sci.: Polym. Chem.* **1965**, *3*, 3261.

16)Webster, O. W.; Hertler, W. R.; Sogah, D. Y.; Farnham, W. B.; Rajanbabu, T. V. *J. Am. Chem. Soc.* **1983**, *105*, 5706.

17)Miyamoto, M.; Sawamoto, M.; Higashimura, T. *Macromolecules* **1984**, *17*, 265.

18)Sawamoto, M.; Fujimori, J.; Higashimura, T. *Macromolecules* **1987**, *20*, 916.

19)Faust, R.; Kennedy, J. P. *Polymer Bulletin* **1986**, *15*, 317.

20)Mishra, M. K.; Kennedy, J. P. *J. Macromol. Sci., Chem.* **1987**, *A24*, 933.

21)Mishra, M. K.; Kennedy, J. P. *Polymer Bulletin* **1987**, *17*, 7.

22)Aida, T.; Maekawa, Y.; Asano, S.; Inoue, S. *Macromolecules* **1988**, *21*, 1195.

23)Inoue, S.; Aida, T. *Makromolekulare Chemie-Macromolecular Symposia* **1986**, *6*, 217.

24)Osgan, M.; Teyssie, P. *Polymer Letters* **1967**, *B5*, 789.

25)Szwarc, M.; Van Beylen, M. *Ionic Polymerisation and Living Polymers*; Chapman & Hall: New York, 1993.

26)Seymour, R. B. *J. Macromol. Sci., Chem.* **1981**, *A15*, 815.

27)Minoura, Y.; Ogata, Y. *J. Polym. Sci.: Polym. Chem.* **1969**, *7*, 254.

28)Yong Tan, Y. *Template Polymerization*; Allen, G., Bevington, J. C. and Eastmonds, A. L., Ed.; Pergamon Press: Oxford, 1989; Vol. 3, pp 245, chap.19.

29)Di Silvestro, G.; Sozzani, P. *Polymerisation in Clathrates*; Allen, G., Bevington, J. C. and Eastmonds, A. L., Ed.; Pergamon Press: Oxford, 1989; Vol. 4, pp 303 chap.18.

30)Louis, P. E. J.; Gilbert, R. G.; Napper, D. H.; Teyssie, P.; Fayt, R. *Macromolecules* **1991**, *24*, 5746.

31)Darling, T. R.; Davis, T. P.; Fryd, M.; Gridnev, A. A.; Haddleton, D. M.; Ittel, S. D.; Matheson, R. R.; Moad, G.; Rizzardo, E. *J. Polym. Sci.: Polym. Chem.* **2000**, *38*, 1706.

32)Otsu, T.; Yoshida, M. *Makromolekulare Chemie-Rapid Communications* **1982**, *3*, 127.

33)Kennedy, J. P. *J. Macromol. Sci., Chem.* **1979**, *A13*, 695.

34)Turner, S. R.; Blevins, R. W. *Macromolecules* **1990**, *23*, 1856.

35)Otsu, T.; Yoshida, M.; Kuriyama, A. *Polymer Bulletin* **1982**, *7*, 45.

36)Solomon, D. H.; Rizzardo, E.; Cacioli, E. *Eur. Pat. Appl. EP135280* **1985**, *102*, 221335q.

37)Veregin, R. P. N.; Georges, M. K.; Kazmaier, P. M.; Hamer, G. K. *Macromolecules* **1993**, *26*, 5316.

38)Kato, M.; Kamigaito, M.; Sawamoto, M.; Higashimura, T. *Macromolecules* **1995**, *28*, 1721.

39)Wang, J. S.; Matyjaszewski, K. *J. Am. Chem. Soc.* **1995**, *117*, 5614.

40)Haddleton, D. M.; Crossman, M. C.; Dana, B. H.; Duncalf, D. J.; Heming, A. M.; Kukulj, D.; Shooter, A. J. *Macromolecules* **1999**, *32*, 2110.

41)Percec, V.; Barboiu, B. *Macromolecules* **1995**, *28*, 7970.

42)Uegaki, H.; Kotani, Y.; Kamigaito, M.; Sawamoto, M. *Macromolecules* **1997**, *30*, 2249.

43)Granel, C.; Teyssie, P.; DuBois, P.; Jerome, P. *Macromolecules* **1996**, *29*, 8576.

44)Matyjaszewski, K.; Wei, M.; Xia, J.; McDermott, N. E. *Macromolecules* **1997**, *30*, 8161.

45)Lecomte, P.; Drapier, I.; DuBois, P.; Teyssie, P.; Jerome, R. *Macromolecules* **1997**, *30*, 7631.

46)Moineau, G.; Granel, C.; Dubois, P.; Jerome, R.; Teyssie, P. *Macromolecules* **1998**, *31*, 542.

47)Chiefari, J.; Chong, Y. K.; Ercole, F.; Krstina, J.; Jeffery, J.; Le, T. P. T.; Mayadunne, R. T. A.; Meijs, G. F.; Moad, C. L.; Moad, G.; Rizzardo, E.; Thang, S. H. *Macromolecules* **1998**, *31*, 5559.

48)Le, T. P.; Moad, G.; Rizzardo, E.; Thang, S. H. *Chem. Abstr.* **1998**, *128*, 115390.

49)Le, T. P.; Moad, G.; Rizzardo, E.; Thang, S. H. *PCT Int. Appl. WO 9801478 A1 980115* **1998.**

50)Sawamoto, M.; Kamigaito, M. *Trends in Polymer Science* **1996**, *4*, 371.

51)Matyjaszewski, K.; Gaynor, S.; Greszta, D.; Mardare, D.; Shigemoto, T. *Macromolecular Symposia* **1995**, *98*, 73.

52)Matyjaszewski, K.; Gaynor, S. G.; Greszta, D.; Mardare, D.; Shigemoto, T.; Wang, J. S. *Macromolecular Symposia* **1995**, *95*, 217.

53)Matyjaszewski, K.; Gaynor, S.; Greszta, D.; Mardare, D.; Shigemoto, T. *J. Phy. Org. Chem.* **1995**, *8*, 306.

54)Greszta, D.; Mardare, D.; Matyjaszewski, K. *Macromolecules* **1994**, *27*, 638.

55)Matyjaszewski, K. *Overview: Fundamentals of Controlled/Living Radical Polymerisation*; Matyjaszewski, K., Ed.; ACS: Washington, 1997, pp 2-30.

56)Matyjaszewski, K. *Comparison and Classification of Controlled/Living Radical Polymerisation*; Matyjaszewski, K., Ed.; ACS: Washington, 2000, pp 2-26.

57)Georges, M. K.; Veregin, R. P. N.; Kazmaier, P. M.; Hamer, G. K. *Macromolecules* **1993**, *26*, 2987.

58)Benoit, D.; Grimaldi, S.; Finet, J. P.; Tordo, P.; Fontanille, M.; Gnanou, Y. *ACS Symposium Series*, 1998; Vol. 685.

59)Benoit, D.; Chaplinski, V.; Braslau, R.; Hawker, C. J. *J. Am. Chem. Soc.* **1999**, *121*, 3904.

60)Steenbock, M.; Klapper, M.; Mullen, K.; Bauer, C.; Hubrich, M. *Macromolecules* **1998**, *31*, 5223.

61)Borsig, E.; Lazar, M.; Capla, M.; Florian, S. *Angew. Makromol. Chem.* **1969**, *9*, 89.

62)Chung, T. C.; Janvikul, W.; Lu, H. L. *J. Am. Chem. Soc.* **1996**, *118*, 705.

63)Gridnev, A. A.; Ittel, S. D.; Fryd, M.; Wayland, B. B. *Organometallics* **1993**, *12*, 4871.

64)Davis, T. P.; Kukulj, D.; Haddleton, D. M.; Maloney, D. R. *Trends in Polymer Science* **1995**, *3*, 365.

65)Kharasch, M. S.; Jensen, E. V.; Urry, W. H. *Science* **1945**, *102*, 128.

66)Tatemoto, H. *US Patent 4158678*; Daikin Industries: USA, 1979.

67)Matyjaszewski, K.; Gaynor, S.; Wang, J. S. *Macromolecules* **1995**, *28*, 2093.

68)Mardare, D.; Matyjaszewski, K. *Macromolecules* **1994**, *27*, 645.

69)Gaynor, S.; Greszta, D.; Mardare, D.; Teodorescu, M.; Matyjaszewski, K. *Journal of Macromolecular Science-Pure and Applied Chemistry* **1994**, *A31*, 1561-1578.

70)Greszta, D.; Mardare, D.; Matyjaszewski, K. *Abs. Pap. Am. Chem. Soc.* **1994**, *207*, 80-POLY.

71)Iqbal, J.; Bhatia, B.; Nayyar, N. K. *Chem. Rev.* **1994**, *94*, 519.

72)Lee, G., M.; Weinreb, S. M. *J. Org. Chem.* **1990**, *55*, 1281.

73)Percec, V.; Barboiu, B.; Neumann, A.; Ronda, J. C.; Zhao, M. *Macromolecules* **1996**, *29*, 3665.

74)Moineau, G.; Granel, C.; Dubois, P.; Jerome, R.; Teyssie, P. *Macromolecules* **1998**, *31*, 542.

75)Kotani, Y.; Kamigaito, M.; Sawamoto, M. *Macromolecules* **1999**, *32*, 2420.

76)Kotani, Y.; Kamigaito, M.; Sawamoto, M. *Macromolecules* **2000**, *33*, 6746.

77)Otsu, T. *J. Polym. Sci.: Polym. Chem.* **1968**, *6*, 3075.

78)Tsuji, J.; Sato, K.; Nagashima, H. *Chem. Lett.* **1981**, 1169.

79)Lecomte, P.; Drapier, I.; Dubois, P.; Teyssie, P.; R., J. *Macromolecules* **1997**, *30*, 7631.

80)Uegaki, H.; Kotani, Y.; Kamigaito, M.; Sawamoto, M. *Macromolecules* **1997**, *30*, 2249.

81)Uegaki, H.; Kotani, Y.; Kamigaito, M.; Sawamoto, M. *Macromolecules* **1998**, *31*, 6756.

82)Hayes, T. K.; Villani, R.; Weinreb, S. M. *J. Am. Chem. Soc.* **1988**, *110*, 5533.

83)Matyjaszewski, K.; Wei, M. L.; Xia, J. H.; McDermott, N. E. *Macromolecules* **1997**, *30*, 8161.

84)Ando, T.; Kamigaito, M.; Sawamoto, M. *Macromolecules* **1997**, *30*, 4507.

85)Moineau, G.; Dubois, P.; Jerome, R.; Senninger, T.; Teyssie, P. *Macromolecules* **1998**, *31*, 545.

86)Baumert, M.; Mulhaupt, R. *Macromol. Chem. Rap. Commun.* **1997**, *18*, 787.

87)Braun, D.; Becker, K. H. *Ind. Eng. Chem. Prod. Res. Dev.* **1971**, *10(4)*, 386.

88)Chen, X. P.; Qiu, K. Y. *Macromolecules* **1999**, *32*, 8711.

89)Kotani, Y.; Kamigaito, M.; Sawamoto, M. *Macromolecules* **1999**, *32*, 6877.

90)Kotani, Y.; Kamigaito, M.; Sawamoto, M. *Macromolecules* **2000**, *33*, 3543.

91)Chen, X. P.; Qiu, K. Y. *Chem. Commun.* **2000**, 233.

92)Chen, X. P.; Qiu, K. Y. *Chem. Commun.* **2000**, 1403.

93)Matsumoto, H.; Nakano, T.; Takasu, K.; Nagai, Y. *Tet. lett.* **1973**, *51*, 5147.

94)Matsumoto, H.; Nakano, T.; Takasu, K., Nagai, Y. *J. of Org. Chem.* **1978**, *43*, 1734.

95)Bland, W. J.; Davis, R.; Durrant, J. L. A. *Organometallics* **1985**, *180*, 397.

96)Kotani, Y.; Kamigaito, M.; Sawamoto, M. *Macromolecules* **1998**, *31*, 5582.

97)Senoo, M.; Kotani, Y.; Kamigaito, M.; Sawamoto, M. *Macromolecules* **1999**, *32*, 8005.

98)Ando, T.; Kamigaito, M.; Sawamoto, M. *Macromolecules* **2000**, *33*, 6732.

99)Nishikawa, T.; Kamigaito, M.; Sawamoto, M. *Macromolecules* **1999**, *32*, 2204.

100)Ando, T.; Kamigaito, M.; Sawamoto, M. *Macromolecules* **2000**, *33*, 5825.

101)Takahashi, H.; Ando, T.; Kamigaito, M.; Sawamoto, M. *Macromolecules* **1999**, *32*, 6461.

102)Takahashi, H.; Ando, T.; Kamigaito, M.; Sawamoto, M. *Macromolecules* **1999**, *32*, 3820.

103)Haddleton, D. M.; Duncalf, D. J.; Kukulj, D.; Radigue, A. P. *Macromolecules* **1999**, *32*, 4769.

104)Wang, J. S.; Matyjaszewski, K. *Macromolecules* **1995**, *28*, 7901.

105)Cotton, F. A.; Wilkinson, G.; Gaus, P. L. *Basic Inorganic Chemistry*; Wiley:, 1987.

106)Patten, T. E.; Xia, J.; Abernathy, T.; Matyjaszewski, K. *Science* **1996**, *272*, 866.

107)Grimaud, T.; Matyjasjewski, K. *Macromolecules* **1997**, *30*, 2216.

108)Grubbs, R. B.; Hawker, C. J.; Dao, J.; Frechet, J. M. J. *Angew. Chem., Int. Ed. Engl.* **1997**, *36*, 270.

109)Haddleton, D. M.; Duncalf, D. J.; Kukulj, D.; Crossman, M. C.; Jackson, S. G.; Bon, S. A. F.; Clark, A. J.; Shooter, A. J. *Eur. J. Inorg. Chem.* **1998**, 1799.

110)Wang, X. S.; Malet, F. L. G.; Armes, S. P.; Haddleton, D. M.; Perrier, S. *Macromolecules* **2001**, *34*, 162.

111)Haddleton, D. M.; Duncalf, D. J.; Kukulj, D.; Heming, A. M.; Shooter, A. J.; Clark, A. J. *J. Mater. Chem.* **1998**, *8*, 1525.

112)Xia, J.; Matyjaszewski, K. *Macromolecules* **1997**, *30*, 7697.

113)Queffelec, J.; Gaynor, G. G.; Matyjaszewski, K. *Macromolecules* **2000**, *33*, ASAP.

114)Johnson, R. M.; Ng, C.; Claire, C.; Samson, M.; Fraser, C. L. *Macromolecules* **2000**, *33*, ASAP.

115)Haddleton, D. M.; Jackson, S. G.; Bon, S. A. F. *J. Amer. Chem. Soc.* **2000**, *122*, 1542.

116)Xia, J. H.; Matyjaszewski, K. *Macromolecules* **1997**, *30*, 7692.

117)Zhang, Z. G.; Lin, G. J.; Bell, S. *Macromolecules* **2000**, *33*, 7877.

118)Haddleton, D. M.; Waterson, C. *Macromolecules* **1999**, *32*, *8732*.

119)Haddleton, D. M.; Heming, A. M.; Kukulj, D.; Jackson, S. G. *Abs. Am. Chem. Soc.* **1999**, *217*, 131-PMSE.

120)Haddleton, D. M.; Kukulj, D.; Kelly, E. J.; Waterson, C. *Abs. Am. Chem. Soc.* **1999**, *217*, 202-PMSE.

121)Angot, S.; Murthy, K. S.; Taton, D.; Gnanou, Y. *Macromolecules* **1998**, *31*, 7218.

122)Matyjaszewski, K.; Gaynor, S. G.; Kulfan, A.; Podwika, M. *Macromolecules* **1997**, *30*, 5192.

123)Matyjaszewski, K.; Gaynor, S. G.; Muller, A. H. E. *Macromolecules* **1997**, *30*, 7034.

124)Matyjaszewski, K.; Gaynor, S. G. *Macromolecules* **1997**, *30*, 7042.

125)Percec, V.; Kim, H. J.; Barboiu, B. *Macromolecules* **1997**, *30*, 6702.

126)Percec, V.; Barboiu, B.; Kim, H.-J. *J. Am. Chem. Soc.* **1998**, 305.

127)Qiu, J.; Matyjaszewski, K. *Macromolecules* **1997**, *30*, 5643.

128)Coessens, V.; Pintauer, T.; Matyjaszewski, K. *Prog. Polym. Sci.* **2001**, *26*, 337.

129)Coca, S.; Jasieczek, C. B.; Beers, K. L.; Matyjaszewski, K. *J. Polym. Sci.: Polym. Chem.* **1998**, *36*, 1417-1424.

130)Coca, S.; Matyjaszewski, K. *Abs. Am. Chem. Soc.* **1997**, *213*, 322.

131)Matyjaszewski, K.; Jo, S. M.; Paik, H. J.; Gaynor, S. G. *Macromolecules* **1997**, *30*, 6398.

132)Teodorescu, M.; Matyjaszewski, K. *Macromol. Rapid. Commun.* **2000**, *21*, 190.

133)Coca, S.; Matyjaszewski, K. *Polym. Prepr.* **1996**, *40(2)*, 338.

134)Marsh, A.; Khan, A.; Haddleton, D. M.; Hannon, M. J. *Macromolecules* **1999**, *32*, 8725.

135)Marsh, A.; Khan, A.; Garcia, M.; Haddleton, D. M. *Chem. Commun.* **2000**, 2083.

136)Khan, A.; Haddleton, D. M.; Hannon, M. J.; Kukulj, D.; Marsh, A. *Macromolecules* **1999**, *32*, 6560.

137)Haddleton, D. M.; Clark, A. J.; Crossman, M. C.; Duncalf, D. J.; Heming, A. M.; Morsley, S. R.; Shooter, A. J. *Chem. Commun.* **1997**, 1173.

138)Lourenco, A. *Compt. Rend.* **1859**, *49*, 619.

139)Lourenco, A. *Ann. Chim. Phys.* **1863**, *67*, 257.

140)Wurtz, A. *Compt. Rend.* **1859**, *49*, 813.

141)Wurtz, A. *Ber.* **1877**, *10*, 90.

142)Staudinger, H. *Die Hochmolekularen Organischen Verbindungen*; Springer: Berlin, 1932.

143)Staudinger, H.; Lohman, H. *Ann. Chim.* **1933**, *505*, 41.

144)Smith, K. L.; Van Cleve, R. *Ind. Eng. Chem.* **1958**, *50*, 12.

145)Bailey, F. E.; Powell, G. M.; Smith, K. L. *Ind. Eng. Chem.* **1958**, *50*, 8.

146)Hill, F. N.; Bailey, F. E.; Fitzpatrick, j. T. *Ind. Eng. Chem.* **1958**, *50*, 5.

147)Young, R. J.; Lovell, P. A. *Introduction to Polymers*; 2nd ed.; Chapman & Hall: London, 1991, pp 100-105.

148)Odian, G. ; 3rd ed.; John Wiley & Sons, Inc.: New York, 1991, pp 536-541.

149)Miyazawa, T. *J. Chem. Phys.* **1961**, *35*, 693.

150)Matsuura, H.; Miyazawa, T. *J. Polym. Sci.: Polym. Chem.* **1969**, *7*, 1735.

151)Powell, G. M.; Bailey, F. E. *Kirk-Othmer Encyclopedia of Chemical Technology, Second Supplement*; Standen, A., Ed.; Wiley-Interscience: New York, 1960, pp 597.

152)Bluestone, S.; Mark, J. E.; Flory, P. J. *Macromolecules* **1974**, *7*, 325.

153)Doolittle, A. K. *The Technology of Solvents and Plasticizers*; Willey: New York, 1954, pp 836.

154)Booth, C.; Price, C. *Polymer* **1966**, *7*, 85.

155)Liu, K. J.; Parsons, J. L. *Macromolecules* **1969**, *2*, 529.

156)Rosch, M. *Kolloid-Z* **1956**, *147*, 78.

157)Rastogi, A. K.; St. Pierre, L. E. *J. Coll. Interf. Sci.* **1969**, *31*, 168.

158)Glass, J. E.; Lundberg, R. D.; Bailey, F. E. *J. Coll. Interf. Sci.* **1970**, *33*, 491.

159)Glass, J. E. *J. Phys. Chem.* **1968**, *72*, 4450.

160)Toms, B. A. *Proc. (first) Intern. Congr. on Rheology II*; North Holland Pub. Co.: Amsterdam, 1949; Vol. 135, pp 135.

161)Bailey, F. E.; Koleske, J. V. *Poly(ethylene oxide)*; Academic Press, Inc.: London, 1976.

162)Andrade, J. D.; Hlady, V.; Jeon, S.-I. *Poly(ethylene oxide) and Protein Resistance*; Glass, J. E., Ed.; American Chemical Society: Washington, 1996, pp 51-59.

163)Miller, P. J.; Matyjaszewski, K. *Macromolecules* **1999**, *32*, 8760.

164)Nakagawa, Y.; Miller, P. J.; Matyjaszewski, K. *Polymer* **1998**, *39*, 5163.

165)Matyjaszewski, K.; Miller, P. J.; Fossum, E.; Nakagawa, Y. *Applied Organometallic Chemistry* **1998**, *12*, 667.

166)Chen, X. Y.; Ivan, B.; Kops, J.; Batsberg, W. *Macromol. Chem. Rapid Commun.* **1998**, *19*, 585.

167)Fonagy, T.; Ivan, B.; Szesztay, M. *Macromol. Chem. Rapid Commun.* **1998**, *19*, 479.

168)Waterson, C.; Haddleton, D. M. *Abs. Am. Chem. Soc.* **1999**, *218*, 404-POLY.

169)Jankova, K.; Kops, J.; Chen, X. Y.; Batsberg, W. *Macromol. Chem. Rap. Commun.* **1999**, *20*, 219.

170)Coca, S.; Paik, H. J.; Matyjaszewski, K. *Macromolecules* **1997**, *30*, 6513.

171)Gaynor, S. G.; Matyjaszewski, K. *Macromolecules* **1997**, *30*, 4241.

172)Paik, H. J.; Teodorescu, M.; Xia, J. H.; Matyjaszewski, K. *Macromolecules* **1999**, *32*, 7023.

173)Kajiwara, A.; Matyjaszewski, K. *Macromolecules* **1998**, *31*, 3489.

174)Chen, X. Y.; Gao, B.; Kops, J.; Batsberg, W. *Polymer* **1998**, *39*, 911.

175)Wang, Y. B.; Chen, S.; Huang, J. L. *Macromolecules* **1999**, *32*, 2480.

176)Bednarek, M.; Biedron, T.; Kubisa, P. *Polymer* **2000**, *45*, 664.

177)Bednarek, M.; Biedron, T.; Kubisa, P. *Macromol. Chem. Rap. Commun.* **1999**, *20*, 59.

178)Jankova, K.; Chen, X. Y.; Kops, J.; Batsberg, W. *Macromolecules* **1998**, *31*, 538.

179)Dust, J. M.; Fang, Z. H.; Harris, J. M. *Macromolecules* **1990**, *23*, 3742.

180)Jankova, K.; Kops, J. *J. App. Polym. Sci.* **1994**, *54*, 1027.

181)Haddleton, D. M.; Crossman, M. C.; Dana, B. H.; Duncalf, D. J.; Heming, A. M.; Kukulj, D.; Shooter, A. J. *Macromolecules* **1999**, *32*, 2110.

182)Fukuda, T.; Goto, A.; Ohno, K. *Macromol. Chem. Rap. Commun.* **2000**, *21*, 151.

183)Ohno, K.; Goto, A.; Fukuda, T.; Xia, J. H.; Matyjaszewski, K. *Macromolecules* **1998**, *31*, 2699.

184)Philipsen, H. J. A.; Claessens, H. A.; Bosman, M.; Klumperman, B.; German, A. L. *Chromatographia* **1998**, *48*, 623.

185)Verhelst, V.; Vandereecken, P. *J. Chrom.* **2000**, *871*, 269.

186)Xie, H. Q.; Xie, D. *Progress Polym. Sci.* **1999**, *24*, 275.

187)de Gennes, P.-G. *Macromolecules* **1981**, *14*, 1637.

188)Prokop, R. M.; Hair, M. L.; Neumann, A. W. *Macromolecules* **1996**, *29*, 5902.

189)Richards, R. W.; Rochford, B. R.; Taylor, M. R. *Macromolecules* **1996**, *29*, 1980.

190)Borisov, O. V.; Halperin, A. *Macromolecules* **1999**, *32*, 5097.

191)Tsutsumi, K.; Tsukahara, Y.; Okamoto, Y. *Polym. J.* **1994**, *26*, 1318.

192)Cacioli, P.; Hawthorne, D. G.; Laslett, R. L.; Rizzardo, E.; Solomon, D. H. *J. Macromol. Sci., Chem.* **1986**, *A23*, 839.

193)Tsukahara, Y.; Mizuno, K.; Segawa, A.; Yamashita, Y. *Macromolecules* **1989**, *22*, 1546.

194)Wang, Y. B.; Huang, J. L. *Macromolecules* **1998**, *31*, 4057.

195)Hedrick, J. L.; Trollsas, M.; Hawker, C. J.; Atthoff, B.; Clasesson, H.; Heise, A.; D., M. R.; Mecerreyes, D.; Jerome, R.; Dubois, P. *Macromolecules* **1998**, *31*, 8691.

196)Yamada, K.; Miyazaki, M.; Ohno, K.; Fukuda, T.; Minoda, M. *Macromolecules* **1999**, *32*, 290.

197)Ashford, E. J.; Naldi, V.; ODell, R.; Billingham, N. C.; Armes, S. P. *Chem. Commun.* **1999**, 1285.

198)Robinson, K. L.; Khan, M. A.; de Paz Banez, M. V.; Wang, X. S.; Armes, S. P. *Macromolecules* **2001**, *34*, 3155.

199)Wilkinson, G.; Gillard, R. D.; MacCleverty, J. A. *Comprehensive Coordination Chemistry*; Pergamon Press:; Vol. 5.

200)Hutchinson, R. A.; Beuermann, S.; Paquet, D. A.; McMinn, J. H.; Jackson, C. *Macromolecules* **1998**, *31*, 1542.

201)Fischer, H. *J. Polym. Sci.: Polym. Chem.* **1999**, *37*, 1885.

202)Tsukahara, Y.; Tsutsumi, K.; Yamashita, Y.; Shimada, S. *Macromolecules* **1990**, *23*, 5201.

203)Wang, X.-S.; Lascelles, S. F.; Jackson, R. A.; Armes, S. P. *Chem. Chommun.* **1999**, 1817.

204)Haddleton, D. M.; Kukulj, D.; Duncalf, D. J.; Heming, A. M.; Shooter, A. J. *Macromolecules* **1998**, *31*, 5201.

205)Bailar, J. C.; Emeleus, H. J.; Nyholm, R.; Trotman-Dickenson, A. F. *Comprehensive Inorganic Chemistry*; Pergamon Press:, 1973; Vol. 3.

206)Zhang, Z. B.; Ying, S. K.; Shi, Z. Q. *Polymer* **1999**, *40*, 1341.

207)Banks, R. E. *Organofluorine Chemistry: Principles and Commercial Applications*; Plenum Press:, 1994.

208)Boutevin, B. *J. Polym. Sci.: Polym. Chem.* **2000**, *38*, 3235.

209)Xia, J.; Zhang, X.; Matyjaszewski, K. *Macromolecules* **1999**, *32*, 3531.

210)Pascual, S.; Coutin, B.; Tardi, M.; Polton, A.; Vairon, J.-P. *Macromolecules* **1998**, *32*, 1432.

211)Matyjaszewski, K.; Nakagawa, Y.; Jasieczek, C. B. *Macromolecules* **1998**, *31*, 1535.

212)Williams, D. H.; Fleming, I. *Line broadening and environmental exchange*; 5 ed.; University Press: Cambridge, 1995, pp 102-105.

213)Haddleton, D. M.; A.J., S.; Heming, A. M.; Crossman, M. C.; Duncalf, D. J.; Morsley, S. R. *Atom Transfer Radical Polymerization of Methyl Methacrylate: Effect of Phenols*; Matyjaszewski, K., Ed.; ACS: Washington, 1998, pp 284-295.

214)Haddleton, D. M.; Perrier, S.; Bon, S. A. F. *Macromolecules* **2000**, *33*, 8246.

215)Chambard, G.; Klumperman, B.; German, A. L. *Macromolecules* **2000**, *33*, 4417.

216)Reichardt, C. *Solvents and Solvent Effects in Organic Chemistry*; 2nd ed.; VCH: Weinham, 1988.

217)Reichardt, C. *Chem. Soc. Rev.* **1992**, *21*, 147.

218)Reichardt, C. *Chem. Rev.* **1994**, *94*, 2319.

219)Buncel, E.; Rajagopal, S. *Acc. Chem. Res.* **1990**, *23*, 226.

220)Kosower, E. M. *J. Am. Chem. Soc.* **1958**, *80*, 3253.

221)Marcus, Y. *Chem. Soc. Rev.* **1993**, *22*, 409.

222)Deye, J. F.; Berger, T. A.; Anderson, A. G. *Anal. Chem.* **1990**, *62*, 615.

223)Dutta, A. K.; Kamada, K.; Ohta, K. *J. Photochem. Photobio. A: Chem.* **1996**, *93*, 57.

224)Uusi-Penttilä, M. S.; Richards, R. J.; Torgerson, B. A.; Berglund, K. A. *Ind. Eng. Chem. Res.* **1997**, *36*, 510.

225)Kipkemboi, P. K.; Easteal, A. J. *Aust. J. Chem.* **1994**, *47*, 1771.

226)Deye, J. F.; Berger, T. A. *Anal. Chem.* **1990**, *62*, 1181.

227)Carmichael, A. J.; Seddon, K. R. *J. Phys. Org. Chem.* **2000**, *13*, 591.

228)Matsui, K.; Nozawa, K. *Bull. Chem. Soc. Jpn.* **1997**, *70*, 2331.

229)Choi, M.; Jin, D.; Kim, H.; Kang, T. J.; Jeoung, S. C.; Kim, D. *J. Phys. Chem. B* **1997**, *101*, 8092.

230)Sarkar, N.; Das, K.; Nath, D. N.; Bhattacharyya, K. *Langmuir* **1994**, *10*, 326.

231)White, J.; Kauer, J. S.; Dickinson, T. A.; Walt, D. R. *Anal. Chem.* **1996**, *68*, 2191.

232)Johnson, S. R.; Sutter, J. M.; Engelhardt, H. L.; Jurs, P. C.; White, J.; Kauer, J. S.; Dickinson, T. A.; Walt, D. R. *Anal. Chem.* **1997**, *69*, 4641.

233)Martuscelli, E.; Demma, G. B. *Polymer Blends: Processing, Morphology and Properties*; Martuscelli, E., Palumbo, R. and Kryszewski, M., Ed.; Plenum: New York, 1980, pp 101.

234)Liberman, S. A.; Gomes, A. D.; Macchi, E. M. *J. Polym. Sci.: Polym. Chem.* **1984**, *22*, 2809.

235)Huan, K.; Bes, L.; Haddleton, D. M.; Khoshdel, E. *J. Polym. Sci.: Polym. Chem.* **2001**, *39*, 1833.

236)Borman, C. D.; Jackson, A. T.; Bunn, A.; Cutter, A. L.; Irvine, D. J. *Polymer* **2000**, *41*, 6015.

237)Wu, S. *Polymer Interface & Adhesion*; Marcel Decker: New York, 1982.

238)Evans, D. F.; Wennerstrom, H. *The Colloidal Domain*; 2nd ed.; Wiley-VCH: New York, 1999, pp 45-98.

239)Adamson, A. W. *Physical Chemistry of Surfaces*; 2nd ed.; Wiley&Sons: New York, 1976.

240)Hiemenz, P. C. *Principles of Colloid and Surface Chemistry*; 2nd ed.; J.J.Lagowki, Ed.; Marcel Decker, inc.: New York, 1986, pp 287-352.

241)Johnson, R. E.; Dettre, R. H. *Wetting of Low-Energy Surfaces*; J.C.Berg, Ed.; Marcel Dekker: New York, 1993.

242)Defay, R.; Prigogine, I.; Bellemans, A.; Everett, D. H. *Surface Tension and Absorption*; green & Co. Ltd.:, 1966.

243)Pallas, N. R. *Coll. & Surf.* **1983**, *6*, 221.

244)Schwartz, L. W.; Garoff, S. *Langmuir* **1985**, *1*, 219.

245)Dettre, R. H.; Johnson, R. E. *Coll. Interf. Sci.* **1966**, *21*, 367.

246)Wang, J. H.; Claesson, J. L.; Yasuda, H. *Langmuir* **1994**, *10*, 3887.

247)Evans, D. F.; Wennerstrom, H. *The Colloidal Domain*; 2nd ed.; Wiley-VCH: New York, 1999, pp 153-216.

248)Harkins, W. D.; Jordan, H. F. *J. Am.. Chem. Soc.* **1930**, *52*, 1751.

249)Huh, S.; Mason, C. G. *Coll. & Pol. Sci.* **1975**, *253*, 266.

250)Xu, R. L.; Winnik, M. A.; Riess, G.; Chu, B.; Croucher, M. D. *Macromolecules* **1992**, *25*, 644.

251)Wilhelm, M.; Zhao, C. L.; Wang, Y. C.; Xu, R. L.; Winnik, M. A.; Mura, J. L.; Riess, G.; Croucher, M. D. *Macromolecules* **1991**, *24*, 1033.

252)Xu, R. L.; Winnik, M. A.; Hallett, F. R.; Riess, G.; Croucher, M. D. *Macromolecules* **1991**, *24*, 87.

253)Zhao, C. L.; Winnik, M. A.; Riess, G.; Croucher, M. D. *Langmuir* **1990**, *6*, 514.

254)Hiemenz, P. C. *Principles of Colloid and Surface Chemistry*; 2nd ed.; J.J.Lagowki, Ed.; Marcel Decker, inc.: New York, 1986, pp 223-286.

255)Hiezman, P. C. *Light Scattering by Polymer Solution*; Marcel Decker: New York, 1984; Vol. 10.

256)Phillies, G. D. J. *J. Chem. Phys.* **1988**, *89*, 91.

257)Brown, R. G. W.; Burnett, J. G.; Mansbridge, J.; Moir, C. I. *Applied Optics* **1990**, *29*, 4159.

258)Keller, R. N.; Wycoff, H. D. *Inorg. Synth.* **1947**, *2*, 1.

259)Baehr; Z., D. *Anorg. Allg. Chem.* **1957**, *292*, 119.

260)Deyes, J. F.; Berger, T. A.; Anderson, A. G. *Anal.Chem.* **1990**, *62*, 615.

261)Krause, S.; Iskandar, M.; Iqbal, M. *Macromolecules* **1982**, *115*, 105.

262)Winnik, M. A.; Renliang, X.; Riess, G.; Chu, B.; Croucher, M. D. *Macromolecules* **1992**, *26*, 644.

263)Odian, G. *Principle of Polymerization*; 3rd ed.; Wiley Interscience: New Yprk, 1991.

264)Gilbert, R. G. *Emulsion Polymerization, A mechanistic Approach*; Academic Press: London, 1995.

265)Gallot-Grubisic, Z.; Rempp, P.; Benoit, H. *J. Polym. Sci., Polym. Letters Edn.* **1967**, *5*, 753.

266)Flory, P. J. *Principles of Polymer Chemistry*; Cornell University Press: New York, 1953.

267)Yau, W. W.; Barth, H. G.; Jakson, C. ; T.Provder, E., Ed.; Am. Chem. Soc.: Washington DC, 1992; Vol. 521.

268)Haney, M.; Åmonas, J. E.; Rosen, L. ; T.Provder, E., Ed.; Am. Chem. Soc.: Washington, DC, 1987; Vol. 352.

269)Wyatt, P. J. *Analyt. Chim. Acta* **1993**, *272*, 1.